TTI/NWSC-96/01

Deep Water Single Point Mooring Design

John F. Flory
Henry A. McKenna

Tension Technology International, Inc.

September, 1997

Naval Surface Warfare Center
Carderock Division

REPORT DOCUMENTATION PAGE

Form Approved
OMB No. 0704-0188

REPORT SECURITY CLASSIFICATION UNCLASSIFIED	1b. RESTRICTIVE MARKINGS None
2a. SECURITY CLASSIFICATION AUTHORITY	3. DISTRIBUTION / AVAILABILITY OF REPORT Approved for public release; distribution is unlimited.
2b. DECLASSIFICATION / DOWNGRADING SCHEDULE	
4. PERFORMING ORGANIZATION REPORT NUMBER(S) TTI/NSWC-96/01	5. MONITORING ORGANIZATION REPORT NUMBER(S) NSWCCD-TSS-CR-97-008
6a. NAME OF PERFORMING ORGANIZATION Tension Technology International 6b. OFFICE SYMBOL (if applicable)	7a. NAME OF MONITORING ORGANIZATION Naval Surface Warfare Center, Carderock Division
6c. ADDRESS (City, State, and ZIP Code) 35 Hubbard Road Weston, MA 02193	7b. ADDRESS (City, State, and ZIP Code) 9500 MacArthur Boulevard West Bethesda, MD 20817-5700
8a. NAME OF FUNDING / SPONSORING ORGANIZATION Defense Advanced Research Projects Agency 8b. OFFICE SYMBOL (if applicable) TTO	9. PROCUREMENT INSTRUMENT IDENTIFICATION NUMBER N00167-95-C-0059
8c. ADDRESS (City, State, and ZIP Code) 3701 North Fairfax Drive Arlington, VA 22203-1714	10. SOURCE OF FUNDING NUMBERS PROGRAM ELEMENT NO. 064705D; PROJECT NO.; TASK NO.; WORK UNIT ACCESSION NO.
11. TITLE (Include Security Classification) (U) Deep Water Single Point Mooring Design	
PERSONAL AUTHOR(S) Avery, John F., and Henry A. McKenna	
13a. TYPE OF REPORT Final	13b. TIME COVERED FROM Apr 95 TO Apr 97
14. DATE OF REPORT (Year, Month, Day) 1997, September 10	15. PAGE COUNT
16. SUPPLEMENTARY NOTATION	

17. COSATI CODES			18. SUBJECT TERMS (Continue on reverse if necessary and identify by block number)
FIELD	GROUP	SUB-GROUP	
			offshore basing, deep water mooring, catenary and single anchor leg mooring, CASALM

19. ABSTRACT (Continue on reverse if necessary and identify by block number)

This report presents the results of a feasibility study of single point mooring (SPM) systems for the Mobile Offshore Base, a very large semi-submersible platform, in up to 10,000 ft (3000 m) water depth. The MOB will use the mooring in mild environments. Three moorings were investigated; Single Catenary Leg Mooring (SCLM), Multi-Catenary Anchor Leg Mooring (MCALM), and Catenary and Single Anchor Leg Mooring (CASALM). A force-deflection analysis computer program was written to analyze the CASALM and then adapted for the other moorings. Maximum mooring forces were predicted with the MOB in various sea states.

The SCLM appears to be the most feasible mooring for the MOB. It can moor the MOB in sea state 3 without thruster assist, it is relatively inexpensive, and it is easy to install. The SCLM may consist of only a short chain attached to the MOB, a polyester rope extending down almost to the sea floor, and a length of chain dragging on the sea floor. A vertical uplift anchor might be used to further limit the motions of the MOB.

Continued

DISTRIBUTION / AVAILABILITY OF ABSTRACT ☒ UNCLASSIFIED/UNLIMITED ☐ SAME AS RPT. ☐ DTIC USERS	21. ABSTRACT SECURITY CLASSIFICATION UNCLASSIFIED
22a. NAME OF RESPONSIBLE INDIVIDUAL Keith R. McAllister	22b. TELEPHONE (Include Area Code) (301) 227-5430 22c. OFFICE SYMBOL NSWCCD 293

DD Form 1473, JUN 86 *Previous editions are obsolete.*

19. ABSTRACTT (Continued)

The report includes: Derivation of equations
Mooring computer program, description of program, and user's guide
Information on high holding, vertical uplift resisting anchors
Information on synthetic fiber ropes for deep water mooring

NOTICES

This report was produced under Contract No. N00167-95-C-0059 issued through the Naval Surface Warfare Center, Carderock Division. The Contract Data Requirements List requires that the report be released in the following Contract Line Items Numbers (CDRL):

A003 CASALM Computer Program and Documentation

A004 CALM / CASALM Comparison Report

A005 CASALM Design Report

A006 High Performance Rope Report

The report has been organized into a single document in the following manner:

The main body of the report is the CASALM Design Report (CDRL A005).

The CALM / CASALM Comparison Report (CDRL A004) has been included in the body of the Design Report, primarily in Section 10.

The CASALM Computer Program (on 3.5" disc) and Program User's Guide (hard copy) is included in the Design Report as Appendix A. Appendix B. "Derivation and Explanation of Equations and Methods Used in CALM and CASALM Computer Programs", provides information on the computer program. Appendix C, "Description of the CASALM Computer Program" provides additional information on the program. The source code for the computer program is designated Appendix D and can be found on the computer program disc in a form printable by most word processors; hard copy is not provided. All of the above fulfills the requirements of CDRL A003.

Appendices E and F cover high performance ropes and anchors for deep water mooring and fulfills the requirements of CDRL A006.

EXECUTIVE SUMMARY

This is a feasibility study of single point mooring (SPM) systems for the Mobile Offshore Base (MOB) in water depths up to 10,000 ft (3000 m). The MOB is a very large semi-submersible platform, about 3000 ft (1000 m) long, with a displacement of about 700,000 tons. It will be equipped with thrusters and a dynamic control system. The mooring will be used in mild environments without thrusters, in moderate environments the thrusters will assist, and in severe environments the MOB will leave the mooring.

Three alternative moorings were investigated, a Single Catenary Leg Mooring (SCLM), a Multi Catenary Anchor Leg Mooring (MCALM) (also known is turret mooring), and a Catenary and Single Anchor Leg Mooring (CASALM). The CASALM consists of a riser extending down from the MOB to a weighted junction suspended above the sea floor, and legs extending from this junction to anchors on the sea floor.

A force-deflection analysis computer program was written which describes the complex kinematics of the CASALM with elastic mooring components. A new form of catenary force-deflection equations was derived for use within that program. The program was then adapted to analyze the MCALM and the SCLM. An adaptation of the SPM energy method was used to predict the maximum mooring forces in these systems in various sea states with the MOB.

The study determined that the SCLM and the MCALM could moor the MOB (without thruster assist) in sea state 3 (6.2 ft wave and 19 kt wind), but that the CASALM could only perform this in sea state 2. The MCALM would require a large motor driven turn table on the MOB and a number of very long anchor legs, and therefore it would be expensive. The SCLM has a relatively large swing circle, but it is relatively inexpensive and easy to install..

The SCLM appears to be the most feasible mooring system for the MOB, considering that it is not necessary to maintain a precise moored position . It may not even be necessary to provide an anchor. In this simplest form, the SCLM consists of a short chain attached to the MOB, a long length of polyester rope extending down to a short distance above the sea floor, and a length of chain which serves as a catenary and also drags about on the sea floor.

Appendices to the report contains data on high-holding-capacity anchor technologies and high-strength tension member components for use in deep water moorings. Suction and driven piles and plate anchors provide a moderate uplift capacity. They are now used in relatively deep water and may soon be capable of being installed in this very deep water depth. Chain alone can not be used as the mooring leg in such deep water, and wire rope may also be a problem because of its weight Synthetic fiber rope is lighter in weight and provides elasticity to replace or supplement that of the catenary. Synthetic fiber rope is now used in several deep water oil production system moorings.

CONTENTS

LIST OF FIGURES

LIST OF TABLES

EXECUTIVE SUMMARY

This is a feasibility study of single point mooring (SPM) systems for the Mobile Offshore Base (MOB) in water depths of 10,000 ft (3000 m). The MOB is a very large semi-submersible platform, about 3000 ft (1000 m) long, with a displacement of about 700,000 tons. It will be equipped with thrusters and a dynamic control system. The mooring will be used in mild environments without thrusters, in moderate environments the thrusters will assist, and in severe environments the MOB will leave the mooring.

Three alternative moorings were investigated, a Single Catenary Leg Mooring (SCLM), a Multi Catenary Anchor Leg Mooring (MCALM) (also known is turret mooring), and a Catenary and Single Anchor Leg Mooring (CASALM). The CASALM consists of a riser extending down from the MOB to a weighted junction suspended above the sea floor, and legs extending from this junction to anchors on the sea floor.

A force-deflection analysis computer program was written which describes the complex kinematics of the CASALM with elastic mooring components. A new form of catenary force-deflection equations was derived for use within that program. The program was then adapted to analyze the MCALM and the SCLM. An adaptation of the SPM energy method was used to predict the maximum mooring forces in these systems in various sea states with the MOB.

The study determined that the SCLM and the MCALM could moor the MOB (without thruster assist) in sea state 3 (6.2 ft wave and 19 kt wind), but that the CASALM could only perform this in sea state 2. The MCALM would require a large motor driven turn table on the MOB and a number of very long anchor legs, and therefore it would be expensive. The SCLM has a relatively large swing circle, but it is relatively inexpensive and easy to install..

The SCLM appears to be the most feasible mooring system for the MOB, considering that it is not necessary to maintain a precise moored position . It may not even be necessary to provide an anchor. In this simplest form, the SCLM consists of a short chain attached to the MOB, a long length of polyester rope extending down to a short distance above the sea floor, and a length of chain which serves as a catenary and also drags about on the sea floor.

The CASALM Mooring analysis Computer Program is provided on a disk accompanying this report. The computer program source code is also provided on the disk. Appendices provide the Users Guide for the CASALM and other computer programs and derivations of the new catenary force-deflection equations.

A supplement to the report contains data on high-holding-capacity anchor technologies and high-strength tension member components for use in deep water moorings. Suction and driven piles and plate anchors provide a moderate uplift capacity. They are now used in relatively deep water and may soon be capable of being installed in this very deep water depth. Chain alone can not be used as the mooring leg in such deep water, and wire rope may also be a problem because of its weight Synthetic fiber rope is lighter in weight and provides elasticity to replace or supplement that of the catenary. Synthetic fiber rope is now used in several deep water oil production system moorings.

SECTION 1 - SUMMARY

1.1 Tasks

The objective of this study was to investigate the feasibility of mooring the Mobile Offshore Base in 10,000 ft (3000 m) water depth.

Three alternative Single Point Mooring (SPM) system configurations were examined :

- CASALM (Catenary and Single Anchor Leg Mooring)
- MCALM (Multi-Catenary Anchor Leg Mooring)
- SCLM (Single Catenary Leg Mooring System)

For each of these mooring systems, a number of different design alternatives were examined, including various combinations of synthetic fiber rope, wire rope, and chain, with various pretensions in the anchor legs of the MCALM and CASALM.

There was little prior art on the design of the CASALM. Its unique kinematic combination of mooring components is difficult to analyze. Considerable effort was required developing a mooring analysis computer program which properly accounted for the elastic effects of catenary leg and riser components. That program was then adapted to also analyze the MCALM and the SCLM.

Data was gathered on high-holding-capacity anchor technologies which might be used in very deep water. Data was also gathered on the tension member components which might be used in such deep water moorings, with special emphasis on new high-performance fiber ropes.

The various mooring systems were evaluated on the basis of ability to safely moor the MOB, a very large floating platform, in various sea states. The sea state wave/wind conditions were :

sea state 2	1 ft wave	8.5 kt wind
sea state 3	2.9 ft wave	13.5 kt wind
sea state 4	6.2 ft wave	19 kt wind

The general probability of exceeding sea state 4 is about 40%, and that of exceeding sea state 3 is about 70%. When the limiting sea state is exceeded, the MOB would use thrusters to assist the mooring, and in very high sea states the MOB would cast off from the mooring.

Peak mooring forces were predicted by applying the energy method to the static force-deflection characteristic of each particular mooring system. The predicted sea state limitations are only approximations and should not be used to set operational limitations on the MOB. The results from these analyses can be used to judge the relative ability of the various mooring systems to moor the MOB.

1.2 Findings

The SCLM was found to be the best mooring system for the MOB, especially if the MOB does not need to be maintained in a precise location. Several configurations of the SCLM proved capable of withstanding sea state 4.

In its simplest configuration, the SCLM would consist of a short length of chain attached to the bow of the MOB, a polyester riser extending almost to the sea floor, and a chain or heavy wire ground leg. The ground leg could be permitted to drag along the sea floor without an anchor, unless it is necessary to control the moored position of the MOB. The advantages of this simple, single catenary anchor mooring are: familiar technology, minimum of components, easy to install, and relatively inexpensive.

If more constraint on the mooring position is required, then the end of the SCLM ground leg would be restrained by a suction or driven pile anchor. This would complicate the installation and increase the installed mooring system cost.

The CASALM was found to be not as versatile and capable for this deep water mooring as had been expected. Wide variations of parameters had little effect on its performance, and the CASALM could not be qualified for operation in sea state 4.

The MCALM was found to be an acceptable mooring in sea state 4. However, this required relatively high pretensions in the mooring legs, which would exert high loads on the turntable. Also, very long mooring legs or heavy sinkers would be required to limit anchor uplift.

Available anchoring technology can withstand the high horizontal and vertical mooring forces anticipated in these applications. The suction pile anchor, driven pile anchor, and plate anchor all hold promise. Installation of such anchors in the 10,000 ft (3,000 m) water depth has not yet been accomplished. But the necessary technology and know how can probably be developed and will probably be developed in the near future for deep water oil production.

High strength tension members are now available for withstanding the anticipated high tensions in the anchor legs. Synthetic fiber rope would be preferred in the riser section of the mooring, because of its light weight and elasticity. Wire rope might be used in the riser, but supporting its weight in such deep water is a concern. Chain could not be used in the riser section for this reason. Chain or wire rope could be used in the ground leg to enhance the catenary effect, reduce leg length, and control uplift on anchors.

SECTION 2 INTRODUCTION

2.1 Background

This project was performed in response to ARPA BAA 93-44, "Technology Development in Support of Maritime Platforms, Ships and Boats, Including Modular Systems and Related High Value Components". Item (1f) of that RFP asked for "Deep water, light weight mooring technology capable of single point mooring offshore bases in water depths exceeding 10,000 ft."

The particular offshore base of interest in this study is known as the MOB (Mobile Offshore Base). It consists of a group of semi-submersible modules linked together in series to form a very long logistics support platform. The six module configuration is about 3,000 ft (915 m) long and has a displacement of about 1,500 kip (670 tonne).

Three alternative mooring system configurations were examined in this project: the SCLM (Single Catenary Leg Mooring), the MCALM (Multi-Catenary Anchor Leg Mooring), and the CASALM (Catenary and Single Anchor Leg Mooring),. The MCALM is also know as a turret mooring and would require a large motor driven turntable near the bow of the MOB. The CASALM consists of a riser extending from the MOB down to a weighted junction, from which catenary legs extend to anchors on the sea floor.

The CASALM is relatively untried technology which has exhibited favorable mooring characteristics and also cost advantages on several oil storage and production systems in relatively shallow water where chain catenaries were employed. Calculation of the force-deflection characteristics of the CASALM is complex, and it is even more complicated when the elastic characteristics of the riser and anchor legs are considered.

2.2 Description of Work Accomplished

A force-deflection computer program was written to model the geometry of the CASALM arrangement and include the effects of mooring component elasticities. A new form of the catenary force-deflection equation was derived for use in the program This program was then adapted to conduct similar analyses of the MCALM and the SCLM.

Peak mooring forces for these three mooring systems, with various combinations of design parameters, were predicted in various sea states using the energy method. That method, which is commonly used to estimate peak mooring force in SPMs, superimposes a peak wave energy on the energy stored in the SPM by static wind force. Model test data for a very large tanker was adapted to obtain the wave energy value for the MOB.

Information on anchor systems which might be used in these deep water moorings was gathered and evaluated. Information on the large high-strength chain, wire rope, and synthetic fiber rope which would be required for these mooring systems, was also gathered and evaluated.

A method of installing the CASALM in very deep water was conceived, which utilizes the MOB as the installation platform.

2.3 Organization of this Report

Section 4 briefly describes the available anchor technology which might be applied in deep water moorings. It also describes the state of art of large chains, wire rope and synthetic fiber rope which might be employed in such systems. Emphasis was given to synthetic fiber ropes since that technology is less standardized and less widely known. The high-performance anchor, rope, and chain data gathered for this study are reported in a separate, supplemental report.

Section 5 describes the CASALM. It provides the basic equations used to conduct the force-deflection analysis of that system. It briefly describes the CASALM Analysis Computer Program. The Users Guide for the program is included in Appendix A to this report. The equations used in this program are derived and described in Appendix B. A disk with that program and similar programs for analyzing the MCALM and the SCLM accompanies this report. Section 5 also describes a method for installing the CASALM in deep water, using the MOB as an installation platform.

Section 6 uses data from model tests on the MOB conducted by NSWC to develop wind force and current force coefficients and also steady-state wave force coefficients. It uses data from model tests on a very large tanker moored to an SPM in shallow water to develop a peak wave energy coefficient. Use of the energy method to predict the peak mooring forces on the MOB due to winds and waves is described in Section 6. The available data is not accurate enough to predict the actual peak mooring forces. The data and method are suitable for estimating peak mooring forces for use in comparing the three alternative mooring systems.

Sections 7, 8, and 9 present design analyses of the single catenary mooring, the MCALM, and the CASALM. Various mooring system designs, with different component materials, lengths, and pretensions are analyzed. The energy method is used to predict peak mooring forces for these various mooring systems in several sea states. Potential performances of these mooring system are then compared.

Section 10 summarizes and discusses the results of these analyses. It is concluded that the SCLM is the best mooring for the MOB, considering that the MOB does not need to maintain a precise moored position. If position keeping is not a concern, a simple SCLM with a drag chain and without any anchor would be an inexpensive, easily installed mooring system for the MOB.

Section 11 provides suggestions for use of the techniques presented in this report and makes suggestions for further research to develop the deep water MOB mooring.

SECTION 3 - STATEMENT OF PROBLEM

3.1 Principal Objective

The principal objective of this project was :

> To determine the mooring limits in terms of peak mooring loads applied to the moored MOB, based on state of art of mooring components and SPM system design parameters and techniques.

3.2 Mission Statement

The mission statement was defined as follows :

> To semipermanently moor the MOB in water depths down to 10,000 ft (3,000 m) in various typical abyssal plane soils, with minimized station-keeping fuel consumption.

3.3 Duty Specification

The following duty specification was established for the mooring system :

- Easy to install using conventional vessels and equipment.
- Use conventional, available components to extent possible.
- No requirement for conducting power, fluids, or communications through mooring.
- Portable, reusable in different locations (possibly pre-install some components).
- Components to be salvageable and reusable to extent possible.

3.4 Operating Scenarios

The following operating scenarios were envisioned for this mooring system :

- Maintain the MOB in a generally stationary location for extended time.
- Weathervane into wind and waves to facilitate aviation and alongside-supply operations.
- Remain safely moored in high ocean environment without thrusters (no-assist environment).
- Then use thrusters occasionally to reduce mooring loads (intermittent assist environment).
- Then use thrusters continuously to remain moored (continuous assist environment).
- Then cast off without assistance and sail free until ocean environment subsides.
- After environment subsides, MOB reconnects to SPM with minimum assistance.

SECTION 4 - DEEP WATER ANCHORS AND MOORING ROPES

4.1 Introduction

This section summarizes that information on anchors which is most pertinent to deep water mooring applications. More detailed information on high-performance anchor, rope, and chain technology is provided in a supplemental report.

4.2 Suction Pile Anchors

Suction piles are large metal or concrete cylinders, closed at the top and open on the bottom end. During installation, the suction pile anchor initially penetrates into the sea floor due to its own weight. Water is then evacuated from the interior of the pile by a suction pump, forcing the pile further into the sea floor by the force of external water pressure.

A typical suction anchor for a rating of about 750 kip (400 tonne) horizontal holding capacity would be 15 ft (4.5 m) diameter and 36 ft (11 m) tall. It might weigh about 75 kip (40 tonne) air. The design holding capacity to weight ratio is thus about 10:1. The suction pile anchor is well adapted for the types of soil anticipated in typical deep water mooring applications.

Suction piles are relatively easy to install. They appear to be suitable for installation in 10,000 ft (3,000 m) water depth. They provide good holding capacity in both horizontal and vertical directions. In addition, the suction pile can be recovered and reused, if provision for recovery is made in its design and fabrication.

4.3 Slender Driven Piles

The slender pile is a long cylinder or beam which is driven into the soil by a hammer. In deep water the slender pile is driven by an underwater hydraulic hammer, with fluid supplied either from an electro-hydraulic power pack mounted on the hammer or from a pump on the surface.

Slender piles have been driven in water depths of 4,000 ft (1,200 m). An installation is now being planned for 5,400 ft (1,650 m) water depth. Operators are now planning on installing such piles in water depths of 6,500 ft (2000 m) and are confident of achieving water depths of 10,000 ft (3,000 m).

Deeply driven slender piles are very effective in holding against uplift in the vertical direction. To effectively resist horizontal forces, the mooring leg connection is made at some distance below the sea floor. Large diameter driven piles or piles with supplemented by side plates are necessary to resist high horizontal forces. Piles as large as 7 ft (2 m) diameter have been driven. Horizontal holding capacities as great as 1,100 kip (500 tonne) can thus be achieved.

4.4 Plate Anchors

Plate anchors are flat surfaces which are driven on edge into the sea floor. The mooring line is attached to an offset bracket on the side of the plate. After the pile is driven to the desired depth, the anchor is set is set by pulling vertically on the mooring line. This causes the plate to rotate into a canted position in which the flat surface bears effectively in the soil to resist both vertical and horizontal forces.

The achieved holding capacity depends on the area of the plate and on its structural strength, as well as on the soil properties. Holding capacities of over 1,000 kip (500 tonne) can be achieved.

Plate anchors use the same pile driving equipment as described above for slender pile anchors. For a desired holding capacity, plate anchors would typically be more compact and lighter than comparable pile anchors, thus making transportation and handling easier. However, plate anchor installation requires the extra operation of setting the pile by pulling vertically at high tension.

4.5 High Capacity Drag Embedment Anchors

Conventional embedment anchors have been used for many years in relatively shallow water. Such anchors are simply laid on the ocean floor and dragged horizontally to cause them to dig into the soil. They produce high horizontal holding capacities but only very limited uplift holding capacities.

Recently, improved embedment anchor designs have been developed which promise to produce high resistance to uplift. They are installed much in the same way as conventional embedment anchors. But after they have reached their design burial depth, a trip line is pulled to alter the direction of mooring line pull on the anchor in order to optimize the resistance to uplift.

It would be difficult to install any drag embedment anchors in deep water. First the anchor must be placed horizontally on the sea floor and facing in the proper orientation. Then a substantial horizontal force must be exerted to drag the anchor into the soil. It would be difficult to monitor the depth of anchor embedment.

It would be very difficult to assure positioning of the drag embedment anchor at a relatively precise radial distance form the center of the mooring. The CASALM junction probably can not be provided with means for adjusting the lengths of individual anchor legs, and thus it would be important to place each anchor point at a relatively precise position if four or more anchor legs are employed on the CASALM.

4.6 Chain

Anchor chain is a well developed commodity product. Its quality is specified and controlled by various classification societies. It is available in various grades, with standardized strength characteristics.

Stud link chain is commonly used as ship-board mooring chain. The stud serves to hold the link open and to prevent it from distorting under high tension, which is important when the chain must be handled over a pocketed windlass. The stud also serves to prevent the chain from tangling when it is stored in a chain locker.

Studless chain has recently been introduced for use in semi-permanent offshore moorings, where handling and storage are not considerations. . This chain without studs is somewhat stronger and also somewhat more elastic than conventional chain.

Chain is commonly used as mooring legs on offshore production platforms and other vessels in relatively shallow water. Here it functions as a catenary to produce the restoring force.

It is impractical to use chain in this manner in very deep water. The weight of suspended chain consumes a large proportion of the chain's strength. In 10,000 ft (3,000 m) water depth, the weight of suspended chain is over two-thirds of the chain strength. That is greater than the proof load normally applied to test chain. Even at a modest catenary scope of 1.2 (ratio of suspended chain length to water depth), the catenary tension would exceed the break strength of the chain.

In deep water the chain catenary hangs essentially straight down unless considerable extra pretension is applied. And in this vertical position the catenary restoring effect is very ineffective.

In deep water moorings, chain may be used in the ground leg, that portion of the anchor leg which usually lies on the ground. Here it can provide a catenary effect, depressing the anchor leg, reducing the overall scope of line, and reducing uplift on the anchor point. Chain also resists abrasion against the sea floor. In the CASALM chain might be used as the entire anchor leg extending up to the junction point.

Chain does not produce a torque effect when tensioned. Thus it is preferable over wire for use in series with synthetic fiber rope, where torque balance problems are a concern.

4.7 Wire Rope

Wire rope is also generally a commodity product. The conventional wire rope constructions used on ship winches and in lifting operations are covered in various national and industry standards. API has standards for the types of wire rope normally used on offshore exploration and production vessels. Special forms of wire rope, for example bridge strand, are used in some mooring applications.

In intermediate water depth mooring applications, wire rope is commonly employed in a catenary mode instead of chain. But wire rope catenaries also have water depth limitations. In 10,000 ft (3,000 m) water depth, about 20% of the strength of the wire rope is taken up in supporting the suspended weight of the wire. In this water depth, a substantial pretension must be exerted to create the catenary effect. Thus wire rope is generally impractical for use throughout the entire anchor leg in very deep water. Wire rope might be used in the anchor legs and riser of a CASALM.

As with chain, wire rope can be used on and near the sea floor to provide weight to reduce the required length of anchor leg, reduce uplift on the anchor, and resist abrasion.

Care must be taken when wire rope is used in series with synthetic fiber rope, or even when two different types of wire rope are used in series. Wire rope tends to unlay when tension is applied. This effect produces a torque which causes the wire to rotate if both ends are not restrained. Unless the other fiber or wire rope has the same torque characteristics, this torque effect will cause one of the ropes to unlay and the other to tighten lay, and this action can weaken or destroy the ropes.

4.8 Synthetic Fiber Ropes

The three principal synthetic fiber rope making materials of possible use in deep water moorings are polyester, aramid, and HMPE (high modulus polyethylene).

Polyester ropes have been used in marine applications for many years without problems. Unlike nylon, polyester does not lose strength, has good abrasion resistance, and provides good cyclic load life when wet. The quality of the polyester yarn used in rope making is very important. Yarn with a high-quality marine finish should be used to assure achieving the potential strength and cyclic load life of the polyester rope.

Polyester rope provides a substantial amount of elasticity. Thus when used as an anchor leg, it serves more as a spring than as a catenary.

Very large polyester ropes are available or can be made which meet the strength requirements of deep water mooring applications. A 10 in. (250 mm) diameter polyester parallel-strand rope would have a break strength of about 3,300 kip (1,500 tonne). Such rope can now be made in lengths up to about 4,250 ft (1,300 m). The parallel-strand rope making technique can be scaled up to make larger or longer ropes.

Aramid fiber rope has been used in small marine moorings for about 20 years with no problems. Difficulties have been experienced in using very large aramid ropes; the cause of these problems has now been identified as axial compression fatigue. There is now a better understanding of this problem and it can probably be avoided by proper attention to termination design and operating procedures.

In large sizes, aramid fiber rope is about twice as strong as the same diameter of polyester fiber rope. A 6 in. (152 mm) diameter parallel strand aramid rope has a break strength of about 2,600 kips (1,200 tonne).

Aramid fiber has a higher elastic modulus than polyester. An aramid fiber rope of a given strength would be about 2.5 times stiffer (in axial tension) than a polyester rope of the same size. Thus aramid fiber rope would be favored where the overall length of a mooring system component is critical, for example in the riser leg of a CASALM; polyester fiber rope would be preferred where higher elasticity was important.

HMPE fiber was introduced to rope making about ten years ago. It has been used without problems as ship board mooring lines for several years and also has been used successfully in other marine applications.

HMPE fiber rope is nearly the same strength as aramid fiber rope of the same size. The elastic moduli of aramid and HMPE ropes are essentially the same.

HMPE fiber is lighter than water, that is, it will float in sea water and has positive buoyancy when submerged. In air, the weight of a given quantity of HMPE rope would be about two-thirds that of the same quantity of polyester or aramid rope. Since HMPE rope is about twice as strong as a polyester rope of the same size, an HMPE rope would weigh about a third as much as a polyester rope of the same strength. This can be a consideration in shipping and handling.

HMPE fiber ropes will experience creep, that is a progressive increase in length when maintained at moderate tension. Under high tension, this creep can lead to failure of the rope.

Polyester ropes are generally much less expensive than aramid or HMPE ropes ov the same strengths. This is an important consideration in view of the large quantities of fiber rope that might be involved in a deep water mooring. Table 4-1 lists approximate properties of large parallel strand polyester ropes.

Table 4.1 Polyester Parallel Strand Rope, approximate properties

Diameter		Dry Weight		Weight in Water		Break Strength		Modulus	
in.	mm	lb/ft	kg/m	lb/ft	kg/m	kip	kg	lb/in/in x 10^6	kg/mm/mm -x 10^6
3	76	3.1	4.6	0.8	1.2	448	203	5	2.3
4	102	5.4	8.0	1.4	2.1	719	326	8	3.6
5	127	8.5	12.7	2.2	3.3	1036	470	12	5.4
6	152	12.2	18.2	3.2	4.8	1398	634	16	7.3
7	178	16.7	24.9	4.3	6.4	1800	817	21	9.5
8	203	21.8	32.5	5.6	8.3	2240	1016	27	12
9	229	27.5	41.0	7.1	10.6	2718	1233	33	15
10	254	34.0	50.7	8.8	13.1	3230	1466	40	18

SECTION 5 - DESCRIPTION OF CASALM
(Catenary and Single Anchor Leg Mooring)

5.1 Introduction

One of the objectives of this project was to further develop the concept of the CASALM for possible use in mooring the MOB in very deep water. This included writing a static force-deflection analysis which properly models the kinematics of the CASALM and incorporates the elastic characteristics of its mooring components. This also included investigating methods for installing the CASALM in very deep water.

This Section describes the CASALM and its components in some detail. It gives a brief explanation of the static analysis of the CASALM and of the CASALM Analysis Computer Program. That program is briefly described here and is covered in more detail in Appendix C. This Section also describes a method of installing the CASALM in deep water from the MOB.

5.2 Description of the CASALM

CASALM is an acronym for Catenary and Single Anchor Leg Mooring. It consists of a buoy on the sea surface, a riser extending down from the buoy to a weighted junction suspended above the sea floor, and catenary anchor legs extending radially from the junction to anchors on the sea floor. The CASALM is shown in Figure 5-1.

When used for mooring the MOB in deep water, it is envisioned that the MOB vessel itself will serve as the buoy. The junction is suspended beneath the MOB by a vertical riser leg.

The top or the riser would be fastened at or near the bow of the MOB to promote weather-vaning. A length of chain may be provided at the top of the riser to facilitate installation. This chain could be pulled in though a pocketted windlass or a linear traction winch in order to lift the junction. The chain could then be restrained against high mooring loads by means of a chain stopper device.

Most of the length of riser would be made up of synthetic fiber rope or possibly wire rope. Chain could not be used as the riser in water depths approaching 10,000 ft (3,000 m), because the weight of suspended chain would be excessive. The riser length would be chosen to suspend the junction at a chosen elevation above the sea floor. Thus in 10,000 ft of water, a typical riser length would be about 9,000 ft (2,750 m). This riser could be made up of several sections of rope joined by plate shackles or other suitable connection means. The riser would be connected to the junction by a short length of chain to avoid abrasion.

An inline tension swivel joint might be incorporated into the riser. However this should not be necessary in a deep water mooring, especially considering that the MOB is equipped with thrusters. The very long riser will be able to accommodate many numbers of turns without

causing problems. The torque induced by turns in this very long riser would not be sufficient to rotate a swivel. Instead, a count should be maintained of the number of times the MOB rotates about the mooring, and then the MOB thrusters could be periodically employed to "unwind" the riser.

The junction may be a thick-walled pressure vessel which is filled with pressurized air or gas in order to reduce its weight during lowering and installation and to prevent its collapse at extreme water depth. The pressurized gas within the junction may be also used to provide power to drive the anchor piles. After the anchor piles are set and the junction is raised to its mooring position, the junction might be filled with barite drilling mud or other suitable heavy ballast material to produce the desired weight.

The anchor legs would be connected around the peripheral of the junction. If fiber rope is used in the anchor legs, a short length of chain may be provided to alleviate abrasion at these connections.

Most of the length of each anchor leg would preferably be polyester rope, in order to provide the desired elasticity. Wire or chain might be used, relying in this case on the catenary effect instead of the rope elasticity. The anchor leg would be connected to the anchor pile through a short length of chain or wire rope in order to resist abrasion on the sea floor.

5.3 Static Analysis of the CASALM

Figure 5-2 illustrates a static analysis of the CASALM system in elevation and plan views. The nomenclature used in the figure and in the following equations is given in Table 5-1.

In the undeflected position, the riser hangs straight down, the junction is directly under the buoy, and the catenary anchor legs extend in a symmetrical pattern from that junction to anchor points on the sea floor. In this analysis it is assumed that all of the anchor points are in the same water depth and that all of the catenary anchor legs are identical as to segment length and weight.

When a horizontal force F is applied to the buoy, it deflects to the side, and the same horizontal force is applied to the junction. This causes the riser to tilt to an angle ρ. The riser length is designated by R. The horizontal deflection of the top of the riser with relation to the junction is then :

$$D_r = R(\sin \rho) \qquad 5\text{-}1$$

The junction elevation above the sea floor is designated by E_j. As the riser tilts, the junction is lifted by a distance :

$$E_{jR} = R(1 - \cos \rho) \qquad 5\text{-}2$$

This horizontal force also causes the junction to deflect horizontally with respect to the ground, through a distance D_j. Thus the total horizontal deflection of the top of the riser, called the buoy, from its initial position is :

$$D_b = D_j + D_r \qquad 5\text{-}3$$

The horizontal deflection of the junction causes the top of each of the catenary anchor legs to deflect. The azimuth angle of the leg from the direction of junction deflection is γ. The top horizontal deflection of a particular anchor leg, designated by the subscript n is :

$$d_n = D_j \cos \gamma \qquad 5\text{-}5$$

The horizontal force which this deflection produces in that particular anchor leg is then determined by the applicable catenary equations and also the elasticity equations for the constituent tension members.

The sum of these horizontal forces in the anchor legs acting on the junction must be in equilibrium with the applied horizontal force F. For anchor leg n, the top total (tangential) force is designated as f_n and the top angle from the horizontal as Θ. Then by summing the horizontal forces on the junction :

$$F = \Sigma\ f_n \sin \gamma_n \cos \theta_n \qquad 5\text{-}6$$

The vertical forces acting on the junction must also be in equilibrium. The vertical force in the riser is the horizontal force times the tangent of the riser angle. This must equal the sum of the vertical forces applied by the anchor legs, such that :

$$F \tan \rho = \Sigma f_n \sin \theta_n \qquad 5\text{-}6$$

The above equations, together with the appropriate force-deflection equations for catenaries and elastic tension members, are sufficient to solve the CASALM force-deflection characteristics. However, the interdependencies of these various equations complicate the solution.

The riser angle ρ can be found from Equation 5-6 as :

$$\rho = \arctan\left(\frac{F}{\Sigma\ f_n \sin \theta_n} \right) \qquad 5\text{-}7$$

But the solution of this equation requires knowledge of f_n and Θ_n for each catenary leg. The particular shape of and forces in each catenary leg depend upon the elevation and offset of its upper end. These offsets are functions of E_{jR}, the increase in junction elevation due to riser tilt, and D_j, the horizontal deflection of the riser due to the applied force Both E_{jR} and D_j depend upon the riser angle, as given in Equations 5-1, 5-2 and 5-3. Thus a trial and error solution must be accomplished.

If the elasticity of the riser is considered, then the stretch of the riser ΔR created by the increase in vertical force must now be considered. This necessitates recalculating the riser deflection and the junction deflection. The change in riser deflection due to a change in its length is :

$$\Delta D_r = \Delta R \sin \rho \qquad 5\text{-}9$$

The change in junction deflection which results in a change in riser length is :

$$\Delta E_{jR} = \Delta R(1 - \cos \rho) \qquad 5\text{-}10$$

5.4 Other CASALM Design Considerations

Figure 5-3 illustrates the mooring arrangement and input and output parameters featured in the CASALM Mooring Analysis Computer Program.

The riser can have elasticity. However, allowing the riser to elongate in response to applied load makes the CASALM analysis much more complicated. The CASALM computer program does account for riser elasticity.

The anchor legs do not necessarily need to perform as catenaries. Instead, they may perform as elastic springs, for example synthetic fiber rope. The CASALM computer program accommodates as many as three segments in each anchor leg; each of these segments can have a distinct unit weight and a distinct elasticity, and concentrated weights (sinkers) can be placed on the connections between these segments.

In the analysis performed by the CASALM computer program, the top of the riser remains at a constant elevation above the sea floor, as though attached to the hull of the moored vessel. In the more general case, the buoy at the top of the riser might be underwater or might be pulled under water by the forces. Also, the moored vessel may be attached to the buoy by a tension member such as a hawser. That hawser may be elastic such that its length changes with applied force. And the angle of that hawser may also change as the buoy elevation decreases. In addition, it may be necessary to account for tilt of the buoy. Each of these factors further complicate the CASALM analysis, and thus they are beyond the scope of this investigation and of the computer program.

5.5 Installation of the CASALM

The steps of installing the CASALM are showing schematically in Figure 5-4 and in a scale elevation view in Figure 5-5. The components of the CASALM can be preassembled while lying alongside or under the platform. This arrangement is indicated by Step 1.

The riser line is reeved through the mooring point and through a large traction winch near the bow of the MOB. The riser line may be stored on a large winch or may be coiled inside a suitable large drum in the manner used for cable laying.

In preparation for installation, the junction is positioned near or under the traction winch and temporarily secured to the platform. The riser line is then secured to the top of the junction.

For a CASALM in a water depth of about 10,000 ft (3,000 m), each anchor leg would typically be about 1,500 ft to 3,000 ft (500 to 1,000 m) long, shorter than the length of the platform. Thus It would be convenient to arrange these anchor legs alongside the platform during preparations for deployment. The several anchor legs may first be fastened to their respective connection points on the junction.

In preparation for deployment, the several anchor piles are temporarily secured along the sides of the platform. All of the anchor piles might be arranged in this manner on one side of the platform, or half of them might be thus arranged on each side of the platform at suitable distances back from the junction. In further preparation, the designated anchor leg is to the side of each anchor pile.

Anchor tending winches are provided on each side of the platform near the stern. An anchor tending line from each of these winches extends to and is attached to its respective anchor pile. The piles can be bundled together to better control them as the system is lowered.

After the CASALM assembly is rigged as described above, the junction is released from the platform and lowered by the traction winch. This step is indicated by Step 2 in Figure 5-4.

After the junction and mooring legs clear the bottom of the platform, the anchor piles are released. Other winches (not shown) might be used to control their initial rate of descent, until the anchor legs and the anchor tending lines become taut.

During the lowering process, the junction is suspended by the riser leg from the mooring point, the bundled anchor piles are suspended by the anchor tending lines from the respective tending winches, and the junction and the bundled anchor piles are interconnected by the anchor legs.

Tension is maintained on the pile tending lines to assure that these anchor piles remain above and away from the junction, and to prevent the various lines from rotating and tangling as the assembly is lowered to the bottom.. It may be necessary to use anchor handling boats to apply sufficient radial tension during the lowering operation.

Lowering proceeds in this manner until the junction rests (temporarily) on the sea floor. The point at which the junction touches the ocean floor defines the center of the mooring. A moderate tension is maintained on the riser leg to prevent it from contacting with the anchor tending lines and to prevent the junction from settling too far into the sea floor under its own weight.

While the junction rests on the ocean floor in this position, each of the anchor piles is set at a distance from that position. This is Step 3 in Figure 5.4.

One anchor pile is set at a time. The tending line is pulled in a designated radial direction from the junction to apply tension to the respective anchor leg. The tending line is then paid out until the anchor pile touches bottom. The distance from the mooring center to the anchor pile is predetermined by the lightly tensioned length of the anchor line. Maintaining outward tension on the anchor leg assures that the anchor pile is positioned at that predetermined distance and that its anchor line connection point faces toward the mooring center.

After each anchor pile is positioned in this manner, it is set or driven into the ocean floor. This action might be performed by suction, by jetting, by driving, or by vibration, as described in Appendix A.

The thrusters on the MOB can used to pivot it around the mooring point. In this manner, all of the anchor piles can be positioned and driven in sequence with positioning and control from the platform.

Alternatively, each anchor pile can be drawn into position by a supply boat or other vessel pulling on the tending line.

After all anchor piles are set as described above, the junction is pulled off the ocean floor by the traction winch. Step 4 in Figure 5.4 shows this operation.

If synthetic fiber anchor lines are employed, then the elasticity of these lines will allow the junction to lift a moderate distance, even though the lines are originally taut to the anchor piles.

An arrangement can be made to temporarily shorten the anchor legs in order maintain the anchor piles at a short distance from the junction during the lowering and driving operation and then to release an additional length of line in order to provide a longer a longer anchor leg. Corrosive links or tension break-away links could be used for this purpose.

After the junction has been raised to the desired elevation, additional ballast can be added. This might be done by lowering barite into the junction through high-pressure hoses from the surface.

As the anchor piles may not immediately achieve their full holding capacity, it may be necessary for the platform to continue to use its thrusters to augment station keeping for some period of time.

TABLE 5-1 NOMENCLATURE OF THE CASALM

Term		Definition
Riser Angle	ρ	Tilt angle of riser from vertical
Leg Top Angle	Θ	Angle at top of anchor leg from horizontal
Anchor Angle	α	Angle at bottom of anchor leg at anchor point
Ground-Leg Angle	Y	Angle between anchor legs in horizontal plane
First Ground-Leg Angle	Y_1	Angle from direction of force application to closest anchor leg.
Riser Length	R	Length of riser.
Applied Force	F	Horizontal force on top of riser, called buoy.
Junction Elevation	E_j	Elevation of junction point above ground.
Elevation Change due to Riser Tilt	E_{jR}	Change in junction elevation due to tilt of riser.
Elevation Change due to Riser Stretch	ΔE_{jR}	Change in junction elevation due to stretch of riser
Buoy Deflection	D_b	Horizontal deflection of top of riser (buoy) due to applied force.
Junction Deflection	D_j	Horizontal deflection of junction.
Junction Deflection Change due to Riser Stretch	ΔD_j	
Riser Deflection	D_r	Horizontal deflection of riser top from junction.
Riser Deflection Change due to Riser Stretch	ΔD_r	
Anchor Leg Top Deflection	D_n	Horizontal deflection of anchor leg n resulting from junction deflection.

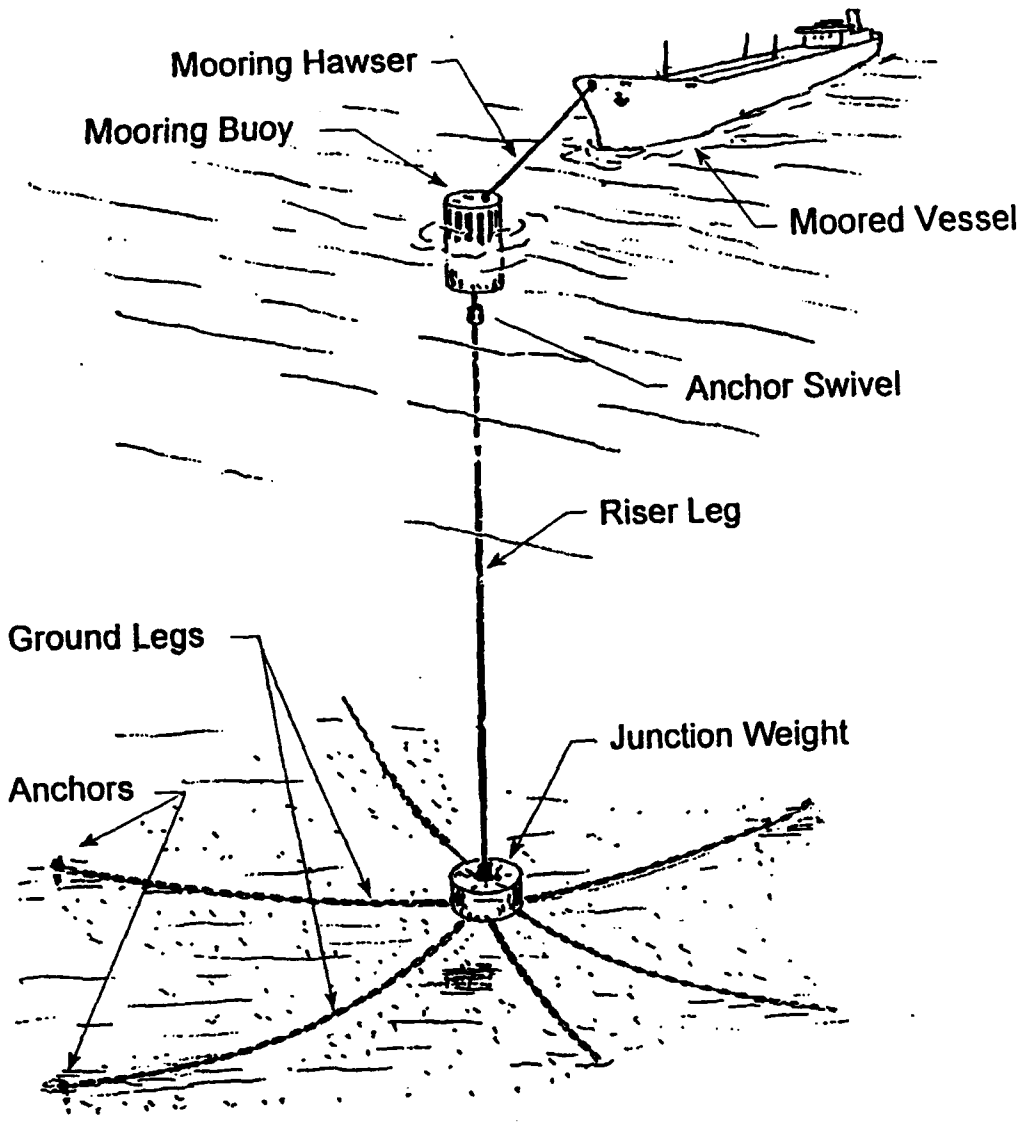

Figure 5-1 The CASALM (Catenary and Single Anchor Leg Mooring)

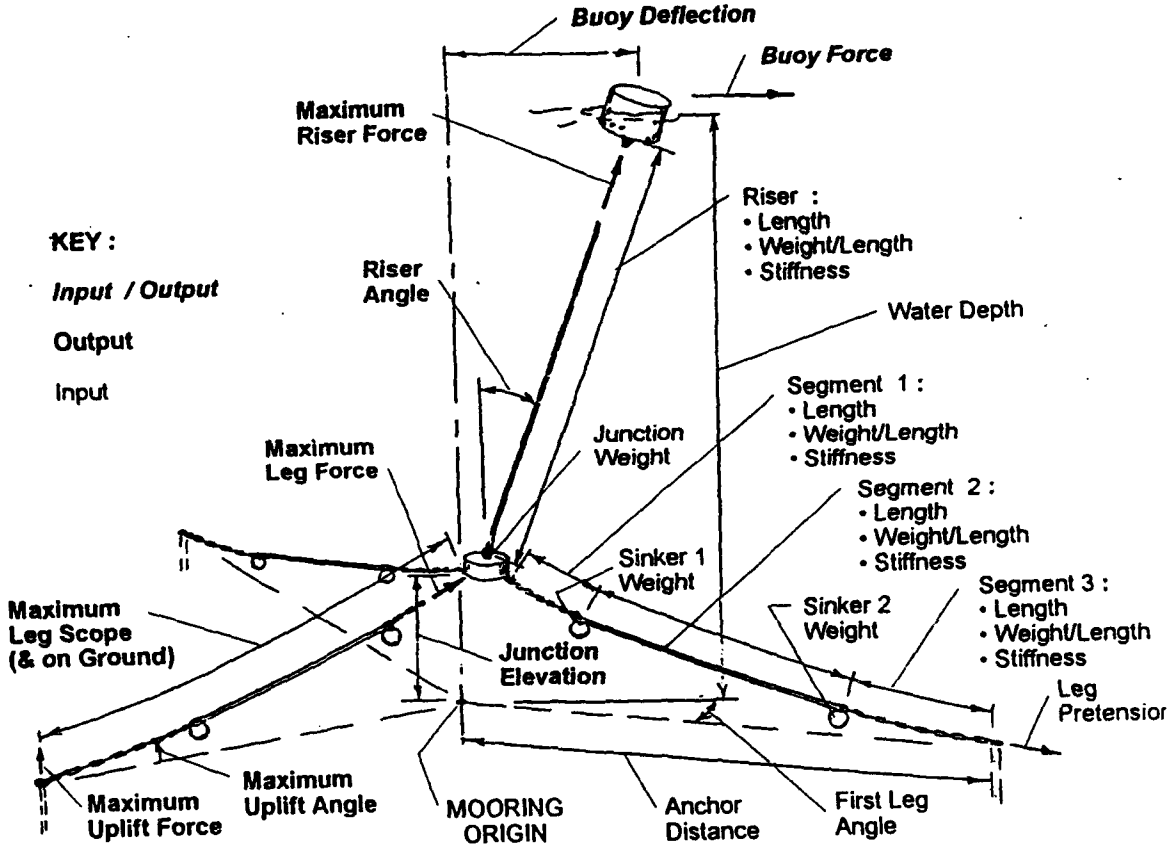

Figure 5-2 Parameters Used In CASALM Analysis Computer Program

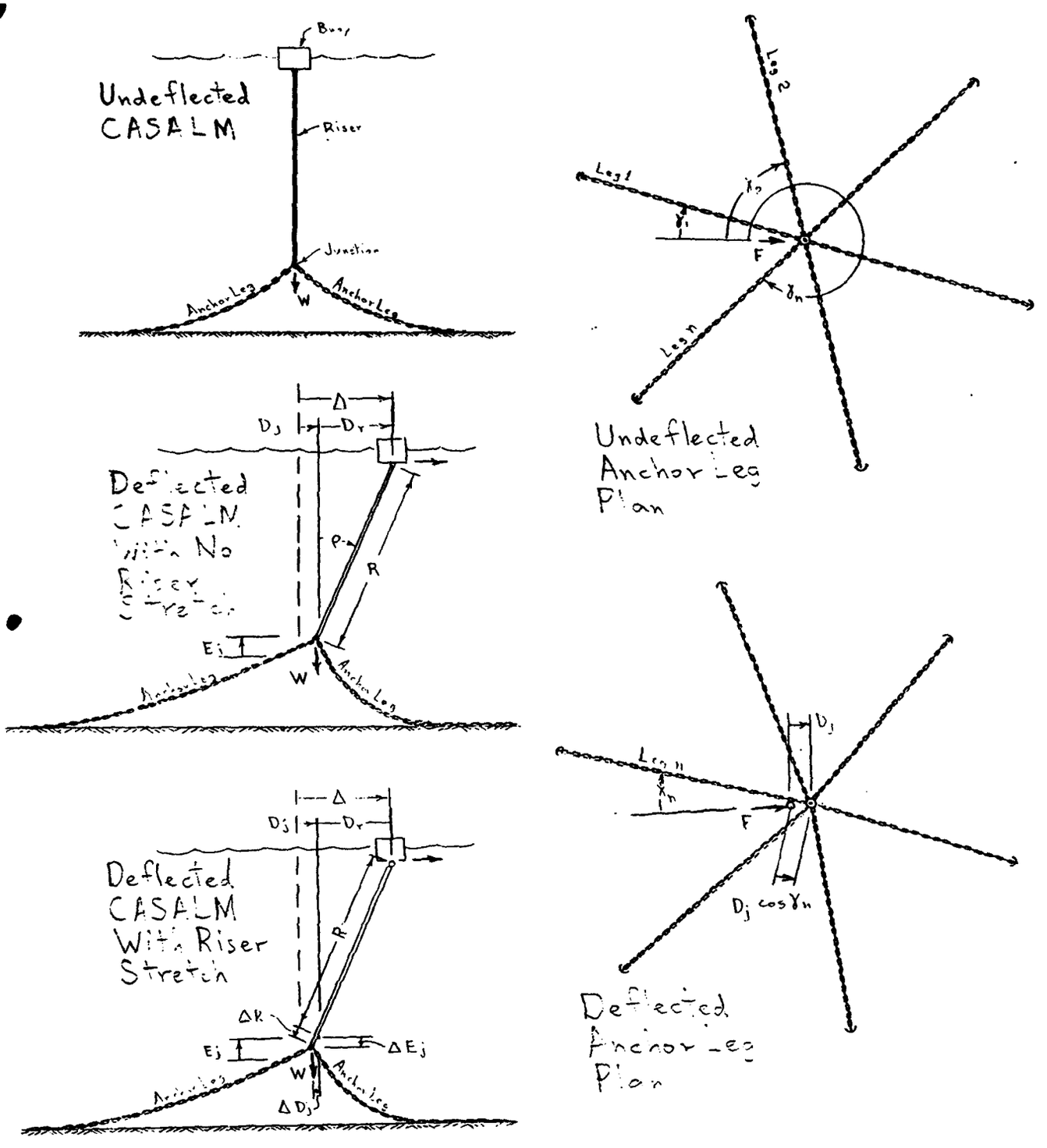

Figure 5-3 Static Analysis of the CASALM

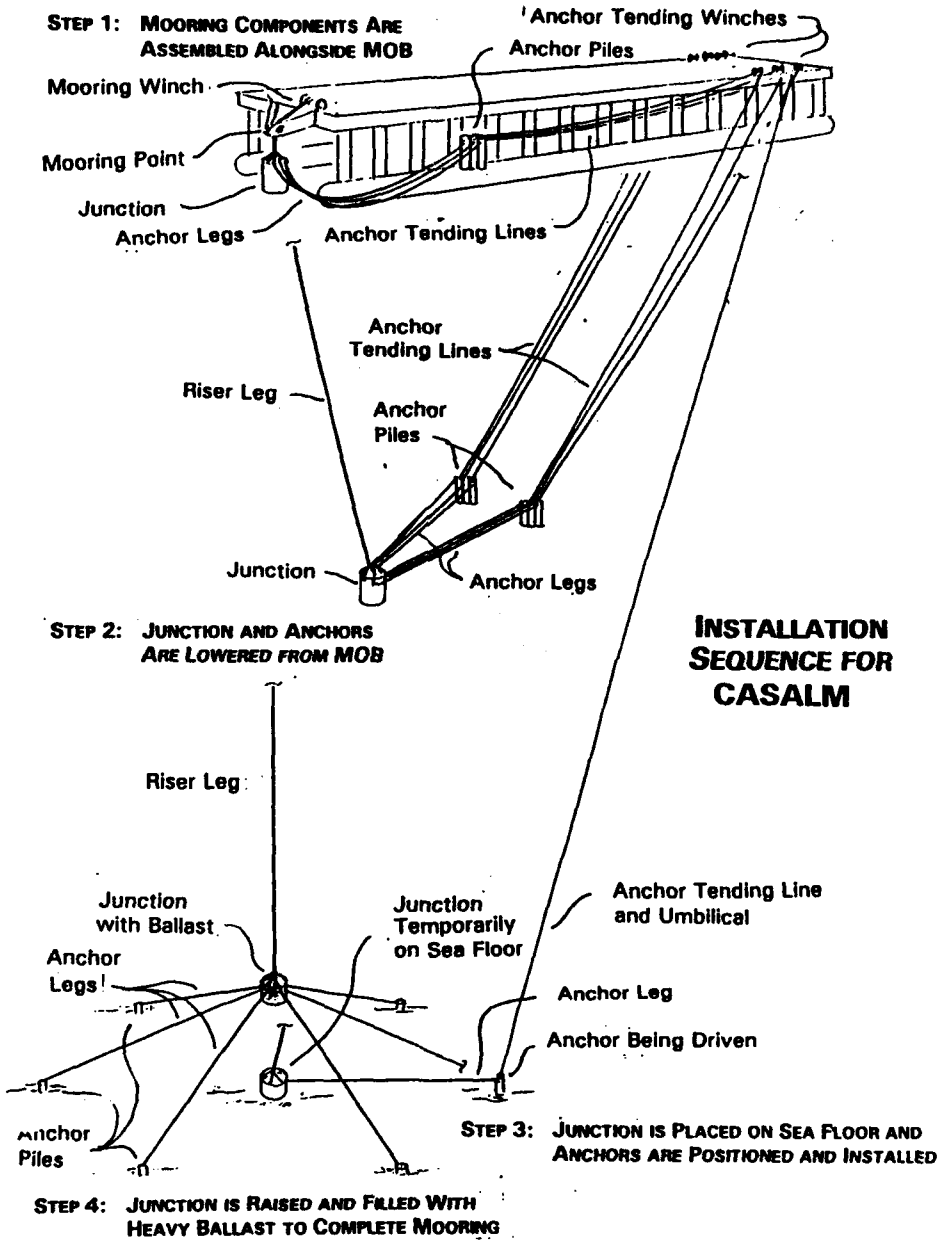

Figure 5-4 Installation Sequence For the CASALM

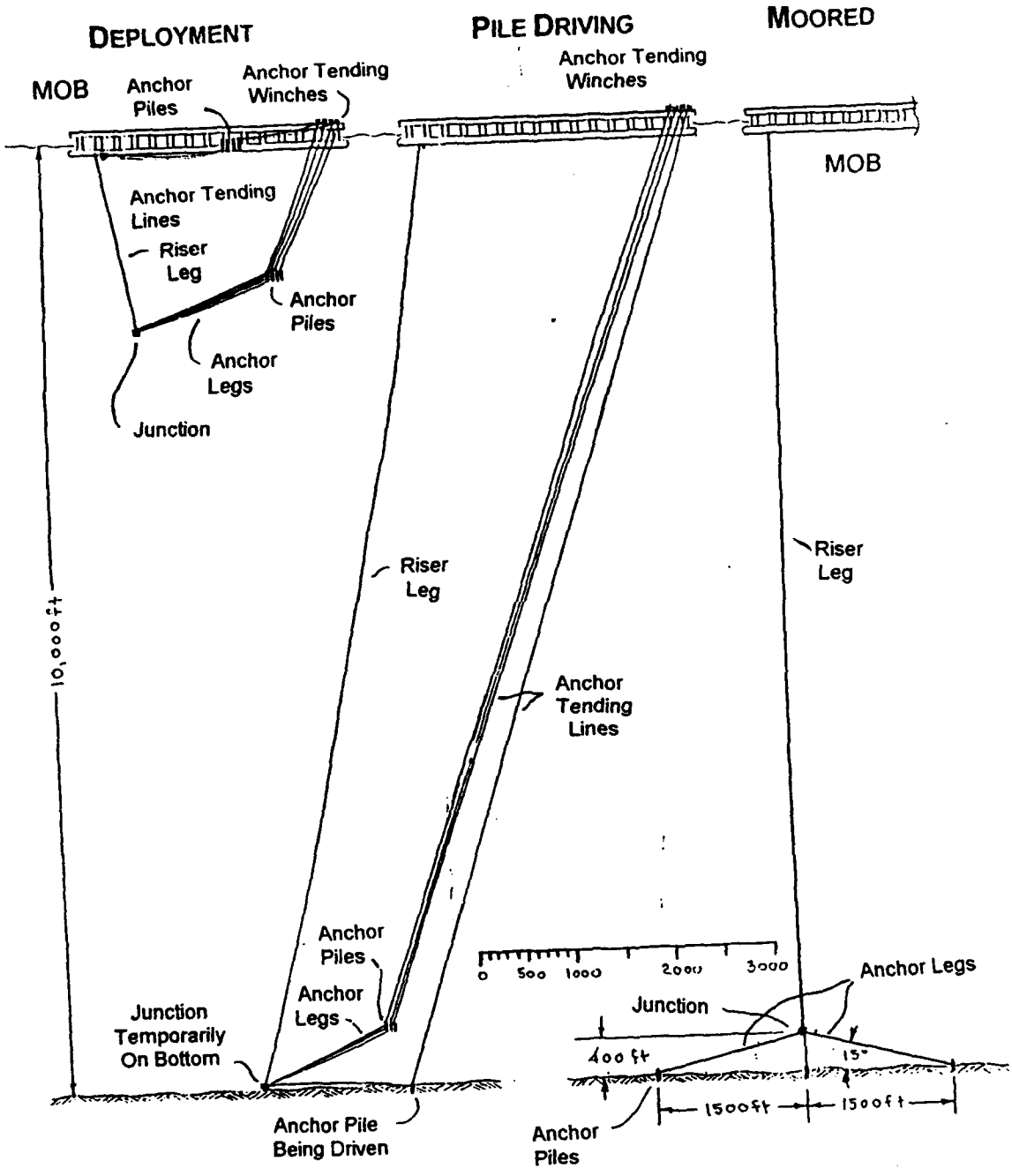

Figure 5-5 Elevation View of CASALM

SECTION 6 - ENVIRONMENTAL FORCES ON MOB

6.1 Introduction

The estimates of wind, current, and wave forces and also wave energies discussed in this Section are used to conduct mooring analyses on the three alternative mooring systems in the following Sections.

The MOB (Mobile Offshore Base) is essentially a group of semi-submersible modules linked together in series to form a very long logistics support platform. The six-module configuration is about 3,000 ft (915 m) long and about 300 ft (92 m) wide. In the "operational draft" condition, 100 ft (30 M) draft, its total displacement is approximately 1,500 kip (670 tonne). In the 85 ft "survival draft" condition, the total displacement is approximately 1,360 kip (620 tonne).

The MOB will be provided with thrusters to accomplish dynamic positioning. The prime function of the mooring system will be to securely moor the MOB in mild to moderate conditions and to supplement the thrusters in more severe conditions. One objective of this study was to determine the approximate limiting environment in which the mooring system alone could provide sufficient restraint without the need for thrusters.

6.2 Basis for Wind, Current, and Wave Forces

The estimated forces on the MOB due to wind, current, and waves are adapted from the NSWC report "Measured and Predicted Hydrostatic Response of a Mobile Offshore Base (MOB)".[1] These forces have not been verified by the authors of this report.

It would be simple to compare the various mooring systems based on superposition of the wave force and wind force values from the NSWC MOB report. However, the resulting mooring force would be the same in all cases, because that superposition method does not account for differences in the energy absorbing capabilities of the various mooring systems. Also, the wave forces in the NSWC MOB report represent steady state conditions, but they do not represent the "slowing varying wave drift forces" which are recognized as being the principal source of high loads on SPMs.

The wave energy is adapted from model tests on very large tankers conducted in the planning of the Louisiana Offshore Oil Port.[2] This estimate of energy is only a rough approximation of the wave energy which might act on the MOB. It is used here to illustrate the use of the wave energy analysis technique and to compare the relative performance of alternative mooring configurations.

The results achieved by using the wave energy method on the MOB mooring in deep water are only rough approximations of the peak mooring forces which might be experienced in any given environment, because the vessel, the mooring system, and the water depth upon which the method parameters are based are much different. These results should not be relied upon to

establish actually operating limit conditions for the MOB at any of the mooring systems investigated here.

The predicted peak mooring results can be used for comparing alternative mooring systems. Even here, some allowance should be made for the overall deflection of the mooring system. Experience from model testing indicates that lower peak forces will be experienced on SPMs which allow relatively little freedom of movement of the vessel than on SPMs which allow much freedom of movement. That effect is not reflected in the force-prediction energy method employed here.

6.3 Bow-On Wave and Wind Forces

Table 6-1 summarizes the estimated wave and forces on the MOB in given sea states, comprised of waves and corresponding winds, approaching the moored vessel directly from the bow.

Wave drift forces at various sea states were taken from Figure 17 "Mean Surge Drift Force on the MOB at the Operational Draft versus Sea State" of the NSWC MOB report. These forces were plotted against the corresponding significant wave heights, and a straight line was drawn through these data. The fact that a straight line was the best representation of these wave drift force data is surprising, because such data generally fits a curve which is nearly a function of the square of wave height. From that line, the wave drift force was found to be $C_{wv0°} = 3.3$ kip/ft. The bow-on wave drift force on the MOB can thus be estimated from the equation :

$$\text{Wave Force, bow-on (kip)} = 3.3 \times H_s$$

where :

H_s = Significant Wave Height, ft.

The wind drag forces given in the NSWC MOB report were calculated using an API procedure. The surge force at various angles, produced by a 24.5 kt wind, is depicted in Figure 14 "Surge Force on the MOB at the Operational Draft in Sea State 5 with a 24.5 Knot Wind and a 1 Knot Current". That value at 0° is 300 kip. The wind drag was assumed to be a function of the square of wind velocity. Thus the underlying bow-on wind force coefficient is 0.5 kip/kt^2. The wind force at other velocities can then be found from :

$$\text{Wind Force, bow-on (kip)} = 0.5 \times V_w^2$$

where :

V_w = Wind Velocity, kt

6.4 Wave and Wind Forces at 30° off Bow

Table 6-2 summarizes the estimated forces on the MOB when given sea states approach the moored vessel at an angle of 30° off the bow. As explained below, these resulting forces are not in line with the approaching seas and wind at 30°, but instead they are at almost 90° off the bow.

The first order wave drift force at 30° off the bow was estimated from Figure 18 "Mean Sway Drift Force on the MOB at the Operational Draft versus Sea State" of the NSWC MOB report. From that figure, the sway force at each sea state was taken and then divided by the corresponding wave height to determine a wave force coefficient. These derived wave force coefficients for sea states 5 through >8 were then averaged to determine a coefficient $C_{wv30°}$ =26 kip/ft. Note that this wave force coefficient, like that for bow-on surge force, is proportional to wave height instead of to the square of wave height, which is unusual. The equation for wave force is then :

$$\text{Wave Force at 30° (kip)} = 26 \times H_s$$

(The corresponding mean surge drift forces, given in Figure 17 of the NSWC MOB report, are much smaller than the sway forces used above. The effect of vectorial adding these two forces would be insignificant.)

Wind force at 30° off the bow was estimated from Figure 14 "Surge Force on the MOB at the Operational Draft in Sea State 5 with a 24.5 Knot Wind and a 1 Knot Current" and Figure 15 "Sway Force on the MOB at the Operational Draft in Sea State 5 with a 24.5 Knot Wind and a 1 Knot Current" of the NSWC MOB report. Those figures show that the wind surge force at 30° is about 500 kip and the wind sway force is about 300 kip. Adding these forces vectorial gives a total resultant wind force of 360 kip. From this wind drag force in a 24.5 kt wind, the wind (quadratic) drag coefficient is derived as $C_{wd30°}$ = 1 kip/kt^2. The corresponding equation for wind force is then :

$$\text{Wind Force at 30° (kip)} = 1 \times V_w^2$$

Note that with an attack angle of 30°, the resultant wind force is at about 30° off the bow, but the resulting wave force is at almost 90° off the bow. Note also that the first order wave forces are generally much less than the wind forces. Accordingly, the resulting combined force will be nearly 90° off the bow. Accordingly, the force totals are approximate, based only on adding the sway component of wave force to the wind force.

6.5 Bow-On Current Drag Force

Figure 29 "Drag for the Mobile Offshore Base at the Operational Draft Towing Forward" in the referenced NSWC MOB report was used to estimate a suitable current drag coefficient. The data in that figure appears to fit a quadratic drag equation. The corresponding bow-on current drag coefficient is $C_{c0°}$ = 13.3 kip/(ft/sec)^2. Thus the bow-on current drag equation is :

$$\text{Current Force, bow-on (kip)} = 13.3 \times V_c^2$$

where :

V_c = Current Velocity, ft/sec

This equation is expressed in terms of ft/sec instead of knots because in the CASALM design analyses, this current force is used to represent fluid drag on the moving vessel instead of a directly applied force.

6.6 Peak Forces Due to Waves Produced by Dynamic Effects

The peak mooring forces produced by a vessel moored at an SPM can not be estimated by the simple superimposing of quasi-static wind, wave, and current forces on the vessel. That simple analysis method might be suitable for a vessel moored alongside a pier or relatively tightly constrained at a spread mooring. But at SPMs the peak forces are produced by dynamics as the vessel moves freely about.

It is generally not practical to conduct a full dynamic analysis of the response of a vessel moored at an SPM. The moored vessel has considerable freedom of movement in the horizontal plane, not only in surge but also sway. The vessel's pitch and heave can also have an influence on peak mooring loads in some circumstances.

Consider the response of the moored vessel in surge only. Here the vessel responds much like a mass suspended on a "spring" under the influence of gravity. The mass is that of the vessel, together with its added mass, a function of the water which moves with the vessel. In this case, the "spring" is the force-deflection characteristic of the SPM. But this SPM force-displacement characteristic is generally very non-linear. And if the vessel is moored to the SPM by a bow hawser, the spring exerts no force when the vessel rides up on the mooring point.

The vessel mass is very large, and the "spring" is relatively soft, at least for small deflections. Thus the natural period of this system is very long, and the moored vessel moves about at periods much longer than the wave period. The forcing function for this long-period vessel response is principally wave drift force, which (simplisticly) is proportional to the square of the envelope of the wave height-time history.

Wave height in the ocean is very irregular over time. Over one sample interval of time, say 10 minutes, the average wave heigth may be relatively low, for example 5 ft. but over the next 19 minute interval of time , the average wave height may be higher, for example 7 ft.

The forces on the vessel are roughly proportional to the square of wave height. These forces will be much higher during those periods of high waves. In the above example, the wave forces experienced during the 7 ft wave interval of time might be twice those wave forces experienced over the 5 ft wave interval of time.

The long term variation of wave height, and thus of wave forces, are very important to the prediction of peak mooring forces at an SPM. This is sometimes called the "slowly varying wave drift force". Also, the period between successive intervals of high wave heights is much more important than the first-order wave period in causing vessel excitation at an SPM.

A vessel moored at an SPM will tend to drift forward during an interval of low waves and then drift backward during an interval of high waves. The peak force imposed by the vessel on the mooring in response to this dynamic response of the vessel may be substantially higher than would be experienced if these same high waves were always present. Detailed information on the shape of the vessel hull and the wave height-time history are necessary to properly incorporate this drift force phenomena into a dynamic analysis, even in only the surge mode.

In a similar manner, the moored vessel responds in a long period irregular pattern to variations in wind velocity and direction. In some circumstances, even variations in current can impose a dynamic effect on the vessel moored at a single point mooring. Many instances are know in which a moored tanker broke away from an SPM due to a "sudden" change in wind or current velocity or direction.

At an SPM, the moored vessel also has considerable freedom to move in sway, and yaw in the horizontal plane. The vessel's pitch, and heave may also have a significant influence on peak mooring loads. And coupling between these various modes of vessel response further complicate the dynamic analysis.

Several computer programs are now available which can perform a realistic and generally accurate dynamic response analysis of a vessel moored at an SPM. However, these programs are very expensive, and they require much knowledge and preparation to set up and run a particular analysis. Thus they are not generally practical for everyday use.

6.7 The Energy Method For Predicting Forces at SPMs

The peak mooring forces experienced at an SPM depend not only on the environment, but also on the energy absorbing "spring" characteristics of that mooring. Recognizing this, Flory developed the energy theory as a method of predicting mooring forces at SPMs.[3,4] The use of the energy method in the design of SPMs is also described in the U.S. Navy "Fleet Moorings" Design Manual 26.5.[5]

The basic concept is that the energy absorbed by the mooring system is the same for a given vessel size in a given environment when comparing different mooring systems having similar characteristics. That energy is approximately proportional to the square of wave height and to the square root of ship size. The energy theory can be used (within limits) to predict mooring forces with other vessel sizes in other wave heights and also for other similar mooring systems, if the mooring force for one set of conditions are known.

The energy absorbed in a mooring system at a given deflection is essentially equal to the area

under the force-deflection curve up to that particular deflection.

A simplified adaptation of the energy method is used in this study. That method is described as follows :

1. The force-deflection curve for the mooring system is calculated

2. The static force due to wind and current is applied to that force-deflection curve to determine the energy stored in the mooring system up to that force, $E_{Wind\&Current}$.

3. The energy corresponding to the wave induced forces is determined, E_{Wave}.

4. That wave energy is added to the wind and current energy to determine the energy corresponding to the peak forces, $E_{Wind\&Current} + E_{Wave} = E_{Peak}$.

5. The peak force is then determined by applying the peak energy E_{Peak} to the force-deflection curve.

The use of this method is illustrated in Figure 6.1.

6.8 Basis For the Wave Energy Prediction

There is no directly applicable data for predicting the peak wave-induced mooring forces on the MOB moored at an SPM in very deep water. Many model tests have been conducted on smaller tanker shaped vessels moored at SPMs in relatively shallow water, but these are generally not available and not applicable.

A few tests were conducted on a model of a 700,000 dwt oil tanker moored to a Single Anchor Leg Mooring (SALM) type of SPM in approximately 125 ft (31 m) water depth as part of the mooring system evaluation process for the Louisiana Offshore Oil Port (LOOP). Those tests were conducted in significant wave heights of 4, 12 and 15 ft (1.2, 3.7 and 4.6 m) with wind and current. Based on those data, the following empirical equation has been developed to estimate the wave energy for this size of vessel :

$$E_{Wave} = 28{,}000 \times H_s^{\,2}$$

where:

E_{Wave}	=	Energy stored corresponding to peak forces due to waves, kip ft
H_s	=	Significant wave height, ft.

That equation was then used to calculate Table 6.3. An example of the application of this technique is included in Section 9.

It must be noted that this relationship is only a rough approximation, based on a vessel of similar size but of dissimilar shaped moored at a different type of SPM in shallow water. This significant wave force relationship is used here only as a demonstration of the wave energy technique and for the purpose of comparing alternative mooring systems. Much additional data would be needed in order to apply this technique in the actual design of such a mooring system.

6.9 Discussion

As cautioned above, the peak forces predicted by this method for the MOB moored at the systems considered in this study are only approximations. They are probably not accurate predictions of the peak forces which might be experienced in any given sea state and on any given mooring.

These peak forces can be used to make comparisons between the performance of different mooring systems. Even here, caution should be used, because the method used here does not account for the overall deflection of the vessel on the mooring as it effect the freedom of vessel movements and the resulting peak dynamic loads.

The accuracy of this technique when applied to the MOB moored in deep water can be improved when better actual data becomes available. Such data might be obtained from model testing or from dynamic computer simulation.

References:

1. Jones, H., J. O'Dea, W. McCreight, and L. Motter, "Measured and Predicted Hydrostatic Response of a Mobile Offshore Base (MOB)", Hydrodynamics Directorate Research and Development Report CRDKNSWC-HD-0279-02, Carderock Division, Naval Surface Warfare Center, Bethesda, MD, January, 1995

2. "LOOP/SeaDock SPM Model Test Program", Test Study III, Operational Study, Netherlands Ship Model Basin, May, 1975.

3. Flory, J.F., S.P. Woehleke and Capt. J.R. Sherrard USCG, "Hawser System Design for Single Point Moorings", ***Offshore Technology Conference Proceedings***, Offshore Technology Conference, Richardson, TX, May, 1978.

4. Flory, J.F., et.al, ***Guidelines For Deepwater Port Single Point Mooring Design***, US Coast Guard Report No. C.G.-D.49-77, US Department of Transportation, Washington, DC, Sept., 1977.

5. *Fleet Moorings, Basic Criteria and Planning Guidelines*, Design Manual 26.5, Naval Facilities Engineering Command, Alexandria, VA, June, 1985.

TABLE 6.1 BOW-ON WAVE AND WIND FORCES ON MOB

Sea State	Probability	Significant Wave Height ft	Mean Wind Speed kt	Wave "Drift" Force kip	Wind Drag Force kip
1	"0	0.1	3	0.3	4.8
2	7.2	1.0	8.5	3.3	38.5
3	22.4	2.9	13.5	9.6	97.0
4	28.7	6.2	19.0	20.5	192.0
5	15.5	10.7	24.5	35.3	320.0
6	18.7	16.4	37.5	54.0	750.0
7	6.1	24.6	51.5	81.0	1410.0
8	1.2	37.7	59.5	125.0	1890.0
>8	1.2	45.9	63.0	150.0	2100.0

TABLE 6-2 30° OFF BOW WIND AND CURRENT FORCES ON MOB

Sea State	Probability	Significant Wave Height ft.	Mean Wind Speed kt	Wave "Drift" Force kip	Wind Drag Force kip
1	~0	0.1	3	2.6	9.0
2	7.2	1.0	8.5	26.0	72.2
3	22.4	2.9	13.5	75.4	182.0
4	28.7	6.2	19.0	161.0	361.0
5	15.5	10.7	24.5	278.2	600.0
6	18.7	16.4	37.5	426.0	1400.0
7	6.1	24.6	51.5	640.0	2650.0
8	1.2	37.7	59.5	980.0	2950.0
>8	1.2	45.9	63.0	1200.0	3310.0

TABLE 6.3 ESTIMATED WIND FORCE AND WAVE ENERGY ON MOBILE OFFSHORE BASE

Sea State	Probability	Mean Wind Speed kt	Bow-On Wind Drag kip	30° Off Bow Wind Drag kip	Significant Wave Height ft	Peak-Force Wave Energy kip ft
1	~0	3	4.8	9	0.1	280
2	7.2	8.5	38.5	72.2	1.0	28,000
3	22.4	13.5	97	182	2.9	235,480
4	28.7	19.0	192	361	6.2	1,076,320
5	15.5	24.5	320	600	10.7	3,205,720
6	18.7	37.5	750	1,400	16.4	7,530,880
7	6.1	51.5	1,410	2,650	24.6	16,944,480
8	1.2	59.5	1,890	2,950	37.7	39,796,120
>8	1.2	63.0	2,100	3,310	45.9	58,990,680

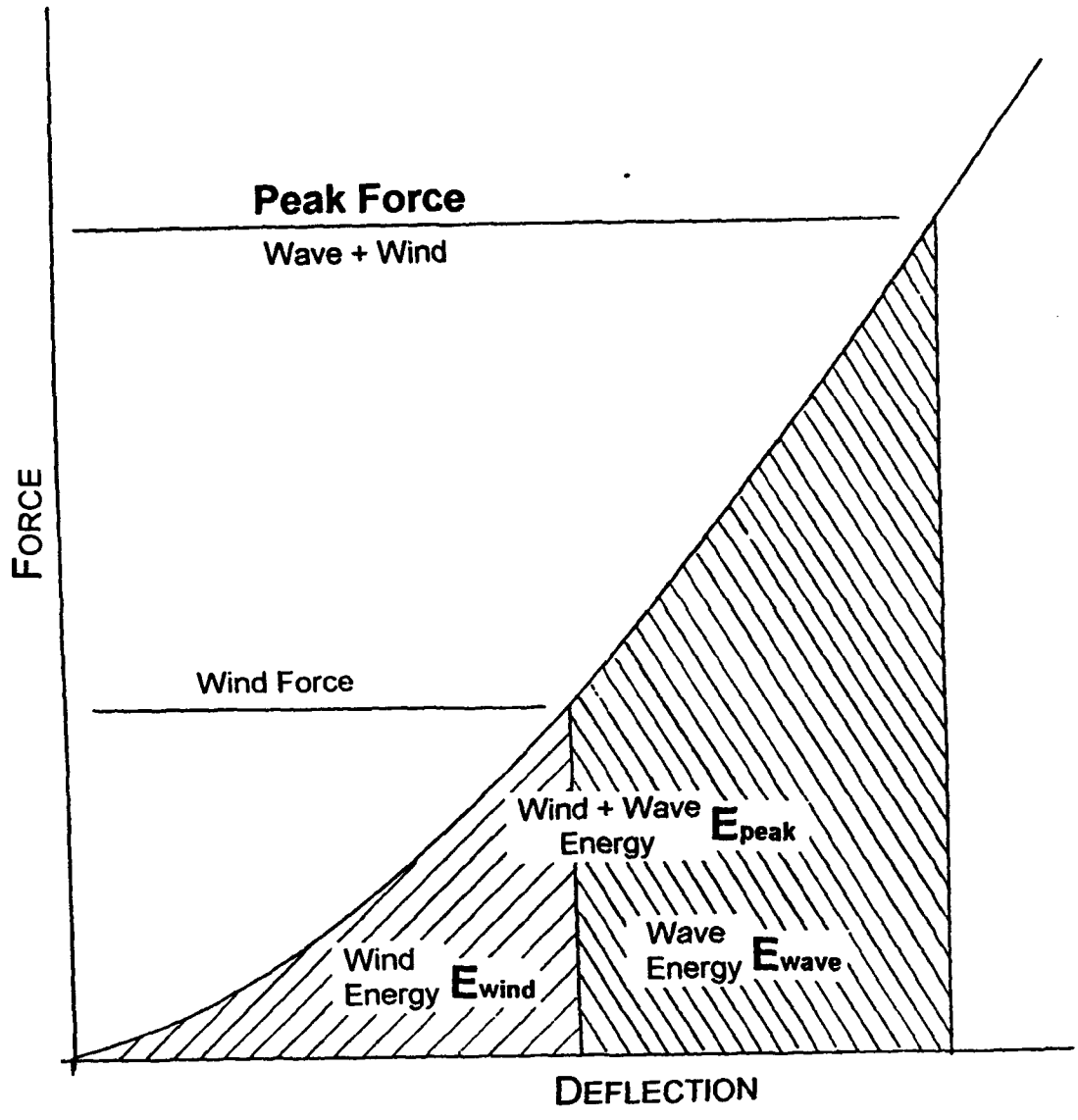

Figure 6-1 Application of the Energy Method for Predicting Peak Forces

SECTION 7 - ANALYSIS OF SINGLE CATENARY LEG MOORING

7.1 Introduction

The simplest mooring system which can be envisioned for the MOB is a single catenary leg extending down to an anchor point on the sea floor. Several alternative single catenary moorings are analyzed here:

- Polyester "Catenary" with short chain ends
- Wire Catenary with short chain ends
- Polyester Riser / Wire Catenary
- Polyester Riser / Chain Catenary
- Polyester Riser / Sinker / Chain Ground

The results of these analyses are summarized in Table 7.1. The force-deflection curves are illustrated in Figure 7.1

7.2 Description of the Catenary Analysis Program

A principal component of both the CASALM and the MCALM Analysis Computer Programs is the subroutine SEGMTCAT, which analyzes the force-deflection characteristics of a multi-segment catenary anchor leg with and without uplift on the anchor point. A separate Catenary Analysis Computer Program was prepared which utilizes that subroutine. It operates in the same manner as the other programs.

In the Catenary Analysis Computer Program (and the subroutine SEGMTCAT), the anchor leg is comprised of three segments. Each segment is described by unit weight, break strength, and elastic modulus. Sinkers can be incorporated at the junctions between the segments. Uplift can be applied to the anchor point.

The measurement of deflection is directly related to the undeflected position of the catenary, in which the anchor leg hangs straight down and touches the sea floor directly beneath its top point. The program assumes that the portion of the anchor leg which lies on the sea floor in this undeflected position lies in a straight path, under no tension and with no slack, to the anchor point.

This differs from the coordinate system commonly used in catenary analysis, by which the position of the top of the catenary is measured from the lowest point on the catenary curve, a point which moves as force is applied to that catenary.

7.3 Description of the Mooring System Components

Synthetic fiber ropes are attractive for use in deep water moorings because of their light weight. A synthetic fiber rope catenary mooring is not a true catenary; most of the force-deflection characteristics of this system are a direct function of the elastic modulus of the polyester rope instead of the catenary effect of its weight. Nevertheless, the term catenary is used here to describe these moorings.

Polyester rope has elasticity characteristics which are desirable for use as anchor legs in a deep water mooring. Note however that the polyester rope functions more as an elastic spring than as a catenary. Polyester is well suited for cyclic load service in water. The polyester rope used in this analysis was a 7 in. (178 mm) diameter with a break strength of 2,700 kip (1,220 tonne). Its unit weight in sea water is 4 lb/ft (6 kg/m). The elastic modulus is 33,400 kip/ft/ft (15,150 tonne/m/m).

A 5 inch (130 mm) chain is used in these analyses It has a break strength of 2,590 kip (1,175 tonne), a unit weight of 206 lb/ft (307 kg/m), and an elastic modulus of 28,600 kip/ft/ft (13,000 tonne/m/m).

The wire used in these analyses is a 5 in. (130 m) diameter steel wire rope with a break strength of 2,140 kip (970 tonne). It has a unit weight of 42 lb/ft (62 kg/m) in sea water. A typical modulus for a steel wire rope of this size is 171,000 kip/ft/ft (77,600 tonne/m/m).

7.4 Analysis of Polyester Rope Single Leg Catenary Mooring

The polyester single catenary mooring system analyzed here incorporated a short, 200 ft (650 m) length of stud link chain at the upper end of the anchor leg to facilitate attachment to the MOB. It incorporated a 1,000 ft (300 m) length of stud link chain at the bottom end to attach to the anchor point. The anchor point was arbitrarily positioned at a horizontal distance of 30,000 ft (9150 m) from the top of the catenary in the undeflected position.

The deflection permitted by the polyester SCLM may be excessive. At very low horizontal force there is almost no restoring force. This polyester mooring deflects to 5,000 ft (1,500 m) from its undeflected position under an applied horizontal force of just 25 kip 11 tonne). It does not begin to provide substantial restoring force until it deflects beyond about 8,000 ft (2,400 m).

In sea state 2 (1 ft wave and 8.5 kt wind) and also in sea state 3 (2.9 ft wave and 13.5 kt wind) the leg tensions in this polyester single catenary mooring are tolerable, and there is no anchor uplift. However, at sea state 3 (6.2 ft wave and 19 kt wind) the anchor leg tension is relatively high, about 70% of the break strength of the polyester rope. The anchor uplift of 420 kip (190 tonne) in sea state 3 may not tolerable.

7.5 Analysis of Wire Rope SCLM

The wire single catenary mooring analyzed here incorporated the same 200 ft (60 m) short section of chain at the upper end as was used in the above polyester case. In the undeflected position, the tension of the suspended wire and chain is 433 kip (195 tonne).

The force-deflection characteristics of this wire single catenary mooring are much better than the polyester case. A horizontal force of 25 kip (11 tonne) produces a deflection or only 1,600 ft (490 m), as compared to the above 5,000 ft (1,500 m) deflection in the above all-polyester system.

The predicted peak horizontal force in sea state 2 is essentially the same in both systems, but because of the weight of the wire, the peak anchor leg tension is much higher in the wire system. In sea state 3, the peak horizontal force is less in the wire system, although the peak leg tension is still higher.

With the wire single catenary system in sea state 4, the predicted peak horizontal force is significantly less, and the peak anchor leg force is also less. The predicted 1,897 kip (860 tonne) peak force is over 80% of the break strength of the 5 in. wire used in this analysis. Larger wire could be employed, but this would in turn increase the pretension requirements and increase the peak forces.

In sea state 4, there is no uplift on the anchor leg for this wire single catenary system. Only about 12,000 ft (3,600 m) of wire was lifted from the sea floor. Thus the length of wire in this system could have been much shorter. (Note that the elastic effect of the length of any component which remains on the ground is not considered in these analyses.)

7.6 Analysis of Polyester Riser on Wire Single Catenary Mooring

The principal disadvantage of the wire single catenary system is the heavy weight of suspended wire, especially in the undeflected position. Synthetic fiber rope could be used as a riser to eliminate most of that initial pretension.

In this analysis, a 100 ft (30 m) length of chain is attached between the top of the polyester riser and the MOB to facilitate hook-up and to prevent abrasion. A 9,800 ft (2,990 m) length of polyester rope is used as the riser, so that the rope does not touch the sea floor in the undeflected position.

This arrangement produces an attractive force-deflection characteristic, as shown in Figure 7.1 and described in Table 7.1. Under a very low applied horizontal force, this polyester/wire single catenary system deflects much more than the all-wire system but much less than the all-polyester system. A horizontal force of 25 kip (11 tonne) produces a deflection of about 3,250 ft (990 m).

The change in slope of this mooring system is gradual. It does not have the relatively abrupt change exhibited in the all-polyester system (at about 8,000 ft, 2,440 m deflection) .

In sea state 2, the predicted peak horizontal force on this polyester/wire single catenary mooring is 96 kip (44 tonne). This produces a peak force of 214 kip (97 tonne) in the anchor leg.

In sea state 3, the peak horizontal force is 211 kip (96 tonne), and the corresponding peak anchor leg force is 375 kip (170 tonne). Note that, although the horizontal force is greater in this system than in the two cases discussed above, the peak anchor leg force is less.

The polyester riser on the wire catenary leg mooring system experiences a peak horizontal force of 1,456 kip (660 tonne) in the sea state 4 environment. This produces a predicted peak anchor leg force of 1,682 kip (763 tonne). This value is about 63% of the break strength of the polyester rope, which is a tolerable occasional peak force on that type of rope in this particular mooring application. At this force, about 20,000 ft (6,000 m) of wire was lifted off the sea floor, and the deflection was about 8,500 ft (2,590 tonne).

7.7 Analysis of Polyester Riser on Chain Single Catenary Mooring

Chain may be preferable for use as the ground leg in conjunction with a polyester riser in a deep water single catenary mooring. Chain provides a greater unit weight. Also, chain is not apt to create torque problems when used in series with a synthetic fiber rope.

The mooring arrangement analyzed here is the same as in the preceding case, except that chain is used instead of wire rope as the ground leg. This creates an even more attractive force-deflection curve.

A horizontal force of 25 kip (11 tonne) produces a deflection of less than 2,200 ft (670 m). The predicted peak horizontal force in sea state 2 is 99 kip (40 tonne). This produces a peak tension in the polyester riser of 305 kip (140 tonne). The peak horizontal force in sea state 3 is 346 kip (157 tonne), with a corresponding riser tension of 689 kip (313 tonne). These riser tensions are greater than those experienced in these sea states with wire, because of the weight of chain which is lifted off the sea floor.

In sea state 4, the predicted peak horizontal force in this polyester/chain single catenary mooring is 1,274 kip (578 tonne). The corresponding peak riser tension is 1,834 kip (832 tonne). That value is almost 70% of the break strength of the polyester rope, probably an acceptable value for occasional peak loads.

At a horizontal force of 1,000 kip (450 tonne), the system deflects by about 6,600 ft (2,000 m). An 8,000 ft (2,400 m) length of chain will prevent uplift on the anchor point, substantially less than the 20,000 ft (6,000 m) length of wire required to prevent uplift on the anchor in the preceding case.

7.8 Analysis of Polyester Riser with Sinker and Chain SCLM

Sinkers are frequently used in catenary moorings to reduce the length of ground leg which is necessary to prevent or limit uplift on the anchor point. Sinkers can also impart more desirable force-deflection characteristics to the mooring.

The mooring system in this analysis is identical to the polyester riser with chain ground leg system of the preceding analysis, except that a 100 kip (45 tonne) sinker is placed at the junction between the polyester rope and the chain. The 100 ft (30 m) length of chain at the top of the riser was retained, and the unstretched length of the riser remained at 9,800 ft (2,990 m). Thus this sinker exerts a 74 kip (34 tonne) pretension in the riser in the undeflected position. The use of the sinker reduced the length of ground leg which was required to prevent uplift on the anchor slightly to approximately 7,500 ft (2,290 m).

The use of such a sinker makes only a slight change in the force-deflection curve, as can be seen in Figure 7.1. The deflection in response to a 25 kip (11 tonne) horizontal force is about 14,300 ft 4360 m). A 1,000 kip (450 tonne) force produces a deflection of approximately 6,450 ft (1,970 m).

In the sea state 2 environment, the peak horizontal force is estimated to be 95 kip (43 tonne). Because of the weight of the lifted sinker and chain, this produces a peak riser force of 348 kip (158 tonne). The sea state 3 environment exerts a peak horizontal force of 348 kip (158 tonne), and the corresponding peak riser force is 736 kip (334 tonne). The peak horizontal forces are essentially the same with this sinker added to the system, but the peak riser forces are somewhat higher.

The sea state 4 environment exerts an estimated peak horizontal force of 1238 kip (562 tonne). And this produces a peak riser force of 1,830 kip (830 tonne). This apparent anomaly as compared with the preceding case may be explained by the more efficient energy absorbing qualities of this single catenary mooring with sinker at the greater deflections.

7.9 Discussion

The SCLM experiences tolerable mooring forces in sea state 3 (2.9 ft wave and 8.5 kt wind). In some configurations, for example those employing a length of heavy wire or chain on the ground, it may experience tolerable mooring forces even in sea state 4 (6.9 ft waves and 19 kt winds).

These predictions of mooring forces are only rough approximations. They are based on an empirical technique derived from peak mooring forces measured in model tests on a vessel of similar size but moored by a much different type of SPM and in much shallower water. These and the other predictions of mooring forces in later Sections should not be used to establish actually operating limits for the MOB at these moorings, but they can be used to make comparisons of the probably relative performance on these moorings.

The above cited mooring deflections at the SCLM do not take into account the great freedom of vessel movement permitted at such a mooring. For example, in sea state 4 the polyester riser on wire SCLM deflected about 8,500 ft (2,600 m) from its undeflected position, but in this process

it lifted about 20,000 ft (6,000 m) of wire from the sea floor. With an anchor point placed at 20,000 ft back from the undeflected position, the moored vessel would then have moved to a position over 5 miles (over 8.5 km) away from the anchor point. And the effective swing circle is over 10 miles (17 km) in diameter.

In other words, the moored vessel is permitted to move over a distance about five times the water depth. This may not be a problem when mooring the MOB, but it would be excessive in some other applications.

The SCLM can apply horizontal force to the anchor point from any direction. This may not be a major problem with suction or driven piles, but it would produce problems with plate anchors and drag anchors, which only resist pull out in one direction. This problem would be overcome by positioning three or more such anchors in a pattern facing the center of a circle, and with ground legs from these anchors to a common connection junction to which the single catenary leg is then connected. What has been described is essentially a slack riser CASALM. That option will be discussed further in Section 9.

The very long length of ground leg employed in these deep water SCLMs will be tensioned to the point where it pulled out straight out from the anchor point only under relatively high mooring forces. When the direction of mooring force application changes, this long ground leg will then be dragged along the sea floor to a new position. This action of dragging the ground leg will effectively serve as a means of dissipating mooring energy. That effect can not be accounted for in these analyses.

For the MOB mooring requirements, it might be practical to use an SCLM with a polyester rier and a long length of drag chain or heavy wire ground leg on the sea floor but no anchor in the sea floor. When the mooring force becomes so great that most of the chain or wire is lifted off the sea floor, the rest of that ground leg is simply dragged along the sea floor until the mooring force decreases. This dragging catenary arrangement would eliminate the need for providing and driving anchors and also for assuring that the mooring force is applied in the proper direction to anchors.

With this dragging catenary system, if the predominant forcing environment was from one direction and the MOB was to remain on station for a long time, then the accumulated drag distance might become a problem. The MOB thrusters could be used to assure that it did not drift into an unsafe position, for example into a platform or into very shallow or deep water. But it might be necessary to occasionally pick up the entire drag catenary assemble and reposition it.

TABLE 7-1 SCLMs

Leg :	Polyester (chain ends)	Wire (chain top)	Polyester/ Wire	Polyester/ Chain	Polyester / Sinker/Chain
Up. Seg. Lng.	200	200	100	100	100
Md. Seg. Lng.	38,794	20,000	9,800	9,800	9,800
Lw. Seg.Lng.	1,000	0	23,000	8,000	7,500
Sinker Wgt.					100
Deflection :	Horiz.Force	Horiz.Force	Horiz.Force	Horiz.Force	Horiz.Force
0	0	0	0	0	0
1,000	1.3	12	2	5	15
2,000	3.8	36	8	21	43
3,000	7.8	74	20	64	100
4,000	14	135	47	166	215
5,000	25	237	104	367	432
6,000	45	421	229	722	792
7,000	87	790	492	1,253	1,324
8,000	183	1,556	1,032	1,916	
9,000	421		1,927		
10,000	1,038				
Sea State 2 :					
Horiz. Force	90	88	96	99	95
Leg Tension	164	520	214	305	348
Anchor Uplift	0	0			
Sea State 3 :					
Horiz. Force	500	316	211	346	348
Leg Tension	570	745	375	689	736
Anchor Uplift	20	0			
Sea State 4 :					
Horiz. Force	1,740	1,370	1,456	1,274	1,238
Leg Tension	1,880	1,787	1,682	1,834	1,830
Anchor Uplift	420	0	0	0	0

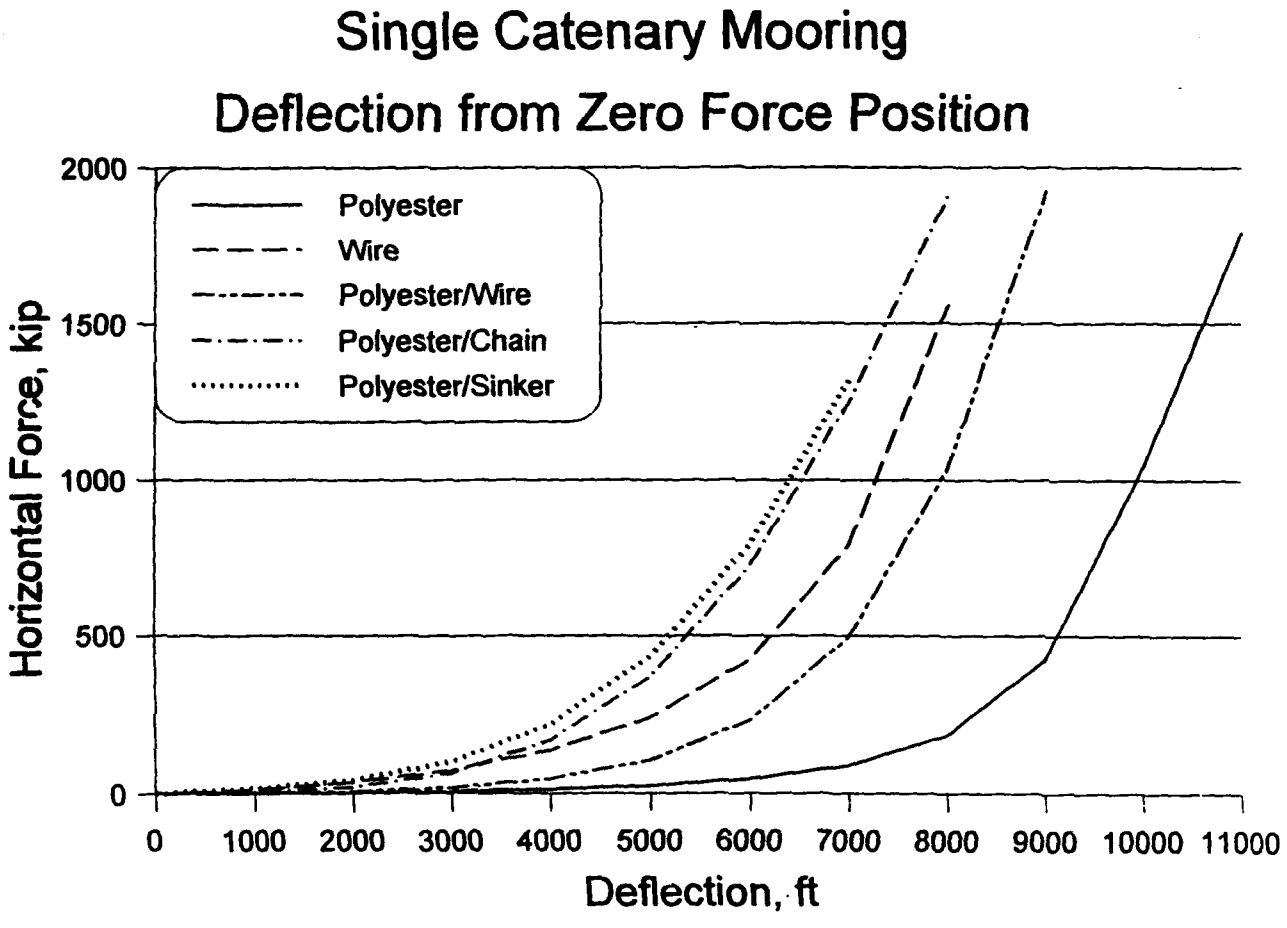

Figure 7-1 CASALM Force / Deflection Curves

SECTION 8 - ANALYSIS OF THE MCALM
(Multi-Catenary Anchor Leg Mooring)

8.1 Introduction

One option for mooring the MOB is an adaption of the turret mooring, which is now used to moor offshore exploration and production vessels. The turret mooring consists of a turntable mounted within or on the vessel hull to which a number of catenary anchor mooring legs are attached. These catenary anchor legs extend out to anchor points as a considerable distance from the center of the mooring. The system is referred to here as the MCALM (Multi Catenary Anchor Leg Mooring).

This turntable must be relatively large. It must withstand the full vertical and horizontal mooring forces. It must incorporate the means of securing and possibly adjusting the mooring legs. In the MOB, this turntable would not need to incorporate drilling equipment or subsea production communication means.

It would be necessary to provide some means of driving this turntable in order to allow the MOB to rotate about the mooring without imposing high strains on the moorings. Otherwise the torque created by the mooring legs might not be sufficient to rotate the turntable.

Several alternative MCALM systems are explored in this Section :

- All-Polyester Anchor Legs
- Polyester with Chain Anchor Legs
- Aramid with Chain Anchor Legs
- Wire Anchor Legs.

8.2 Description of the MCALM Analysis Program

A MCALM Analysis Computer Program was developed along with the CASALM Analysis Computer Program. This MCALM program is essentially the CASALM program without the riser feature. It operates in the same way as the CASALM program and incorporates most of its features.

In the MCALM Analysis Computer Program, the anchor legs attach directly to the buoy (instead of to a junction point). This buoy point remains at a fixed elevation above the sea floor. Each anchor leg consists of three segments. There is no riser leg.

8.3 All-Polyester Anchor Leg Analysis

The MCALM with an all-polyester anchor leg was analyzed at several pretensions. A 7 in. (178 mm) diameter polyester rope was modelled. This rope has the same characteristics as that described in the preceding section. The anchor points were positioned at 30,000 ft (10,000 m) from the center of the mooring. The anchor leg length was varied to produce the desired pretension.

The results at pretensions of 50, 100, 150, and 200 kip (23, 45, 68, and 90 tonne) are summarized in Table 8-1. The force-deflection curves are given in Figure 8-1.

At 50 kip (23 tonne) pretension, the anchor legs hang almost straight down. The resulting MCALM is very soft, deflecting 3,400 ft (1,000 m) at an applied horizontal force of 100 kip (45 tonne) and 5,500 ft (1,700 m) at 500 kip (225 tonne) horizontal force. This mooring system is probably too elastic to be viable. The other pretensions produce more reasonable force-deflection characteristics.

The energy method analysis indicates that with proper pretension, such an all-polyester MCALM would be tenable in sea state 4. In that environment, the 100 kip (45 tonne) pretension MCALM experiences a peak horizontal force of 1728 kip (784 m). This produces a peak force of 1607 kip (739 tonne) in the anchor leg, about 60% of the break strength. Frequent loads of this magnitude would deteriorate the rope, but an occasional load of this magnitude could probably be tolerated. The peak anchor uplift force of 386 kip (175 m) may be excessive.

Although the force-deflection characteristics for the all-polyester MCALM with these pretensions differ widely, there is essentially no difference in the peak anchor leg forces in the sea state 4 (6.9 ft waves and 19 kt wind) environment. This is not so in the sea-state 2 (1 ft waves and 8.5 kt wind) environment, in which the peak anchor leg tension at 200 kip (90 tonne) pretension is more than double that at the 50 kip (23 tonne) pretension.

8.4 MCALM Analyses, Polyester/Chain Anchor Legs

Using polyester throughout such an anchor leg configuration may not be practical. It will be necessary to provide chain near the anchor to resist abrasion and to control uplift. It will probably also be necessary to use chain at the upper end in order to provide a means of pretensioning the system.

In the following analyses, each leg was provided with 1,000 ft (300 m) of 5 in. (127 mm) stud link chain at the anchor end and with 200 ft (60 m) of 6 in. (153 mm) stud link chain at the buoy end. This stud link chain had a unit weight of 206 lb/ft (306 kg/m), which combined with the suspended weight of the synthetic rope portion of the leg, produced a minimum pretension of approximately 80 kip (36 tonne) with no offset of the catenary (hanging straight down).

As in the preceding case, the anchors are positioned at 30,000 ft (10,000 m) from the center of the mooring. The length of the polyester segment was varied to produce the desired pretension.

The results at pretensions of 100, 125, 150, and 175 kip (45, 57, 68, and 79 tonne) are summarized in Table 8-2. The force-deflection curves are shown in Figure 8-2.

The presence of these chains in the anchor leg greatly altered the force-deflection characteristics for any given pretension, but the general shape of the force-deflection curves did not change substantially.

At any given pretension, the all-polyester MCALM was significantly stiffer. For example, on the all-polyester mooring with 100 kip (45 tonne) pretension, a horizontal force of 1200 kip (545 tonne) produced a deflection of about 3100 ft (950 m), but with the chain, this force produced a deflection of 5000 ft (1500 m).

The force-deflection characteristics of the all-polyester system at 150 kip (68 tonne) pretension is very similar to that of the polyester/chain system at 175 kip (80 tonne). Using the peak forces predicted by the energy method, the dynamic response appears also to be similar. In the all-polyester system with 150 kip (68 tonne) pretension, the peak horizontal forces in sea states 2, 3 and 4 are 140, 536, and 1864 kip (64, 243, and 846 tonne) respectively, while in the 175 kip (79 tonne) pretension polyester/chain system, these forces are 138, 538, and 1830 kip (63, 244, and 839 tonne) respectively.

8.5 Aramid Anchor Leg MCALM

Other materials and combinations of materials could be used in the MCALM anchor legs. In addition to the two combinations discussed above, the use of aramid rope with chain, wire rope with chain, and all-wire were explored. The results are summarized in Table 8-3. The various force-deflection curves are shown in Figure 8-3.

Aramid rope is much stiffer than polyester rope when compared on an equivalent strength basis. Aramid rope is stronger on a size-comparison basis than polyester rope. Aramid rope is heavier than the same size polyester rope when immersed in sea water.

The aramid/chain MCALM which was analyzed consisted of the same ground and top chain sections as were used above in the polyester/chain systems with the same 30,000 ft (10,000 m) anchor distance. The length of aramid rope between the chains was adjusted to obtain 100 kip (45 tonne) pretension.

This stiffer aramid rope produces a mooring system with a less linear force-deflection curve. As might be expected, the aramid/chain anchor leg force deflection curve is stiffer that that of the polyester/chain system with the same pretension in each.

A horizontal force of 100 kip (45 tonne) produced a deflection of about 1,300 ft (400 m) in the aramid/chain system but produced a deflection of about 2200 ft (670 m) in the polyester/chain system. At a horizontal force of 1,000 kip (454 tonne), the deflections were about 2,950 ft (900 m) for the aramid/chain system and about 4,750 ft (1,450 m) for the polyester/chain system. Beyond this point, the aramid/chain system is very stiff.

Application of the energy method indicates that the aramid/chain system would be less viable in high sea states. In sea state 2, the peak anchor leg tensions in the two systems are about the same, even though the horizontal force on the aramid/chain system is greater. In sea state 3, the peak leg tension in the aramid/chain MCALM is 786 kip (356 tonne?), twice as great as that in the polyester/aramid MCALM. The aramid/chain MCALM is untenable in sea state 3.

8.6 Wire/Chain Anchor Leg MCALM

In this case, a 5 in. (127 mm) diameter wire is used as the riser section of the anchor leg. This wire has a break strength of 2,140 kip (970 tonne), a unit weight of 206 lb/ft (306 kg/m) and an elastic modulus of 171,000 kip/ft/ft (78,000 tonne/m/m). The total length of this wire was 35,900 ft (10,950 m). The same size and lengths of end chain were used as in the previous case. As before, the anchor point was at 30,000 ft (10,000 m) from the center of the mooring.

This arrangement produced a pretension of 500 kip (225 tonne) in each anchor leg. The associated vertical force in each leg is about 495 kip. Note that the total downward vertical force on the mooring turntable for this 6-wire case is thus almost 3,000 kip (1,350 tonne) in the undeflected position and will be higher when the mooring is deflected. *This might not be a* feasible mooring system for that reason.

The force-deflection curve produced by this wire/chain MCALM arrangement which provides reasonable restoring forces at low deflections and changes only slightly in slope at increasing deflections. A horizontal force of 100 kip (45 tonne) deflects the mooring only 750 ft, and a horizontal force of 1,000 kip (450 tonne) deflects the mooring about 3,700 ft (1,130 m).

Sea state 4 exerts a predicted peak horizontal force of only 1,242 kip (564 tonne) on this mooring system. The resulting peak force in the most highly loaded anchor leg is only 1,423 kip (647 tonne), less than two-thirds of the break strength of the wire. Almost all of the wire and chain was lifted of the sea floor at this peak force.

8.7 All-Wire Anchor Leg MCALM

A 5 in. (127 mm) diameter wire was considered here. This is the same wire as that considered in the preceding section. The total length of wire in each leg was 36, 500 (11,125 m), and end chains were not employed. This all-wire mooring produces a tension of 400 kip (180 tonne) when it is suspended in 10,000 ft (3,000 m) of water (not accounting for the effect of wire stretch).

When the stated length of wire is installed with an anchor point at 30,000 ft (10,000 m) from the mooring center, the resulting pretension is 500 kip (225 tonne), as in the preceding case. And as before, this required pretension is probably excessive for use with the envisioned turret mooring.

This all-wire mooring system created a force-deflection curve which was very similar to but a little stiffer than the wire-chain MCALM system. When a 100 kip (45 tonne) horizontal force is applied, the deflection is about 540 ft (165 m). The system deflects about 3,500 ft (1,070 m) under an applied horizontal force of 1,000 kip (450 tonne).

In sea state 4, the peak anchor leg tension is essentially the same as that for the wire/chain case, even though the predicted peak horizontal force is slightly higher. At this peak force of 1,306 kip (592 tonne), almost all of the 30,000 ft (10,000 m) length of wire was lifted off the sea floor.

8.8 Discussion

A number of the MCALM configurations which were analyzed here may be able to safely moor the MOB in sea state 4 (6.9 ft waves and 19 kt wind) without thruster assist. As shown in Table 8-3, all of the cases except the aramid/chain case achieve peak leg tensions of less than about 60% of the break strength of the respective mooring components.

The wire/chain and the all-wire cases apply no uplift on the anchor point. However, in these cases almost all of the most highly loaded anchor leg was lifted off the sea floor at the peak force produced in sea state 4. The length of these lines might be decreased, allowing an uplift on the anchor.

The six anchor legs of the all-wire case require almost 220,000 ft (67,000 m) of ˜ in. (127 mm) wire, with a total weight of about 8,750 kip (3,970 tonne). For the all polyester case, the total length of the six legs was 200,700 ft (61,200 m), with a total weight of ₄bout 800 kip (365 tonne). The lengths of chain used in the other cases would reduce these lengths and weights. But the top and bottom chains in the six legs had a total length of 7,200 ft (2,200 m) and a weight of 1,400 kip (670 tonne).

The turntable required for this MCALM arrangement on the MOB would be a costly item. It is probably feasible to provide such a turntable for the polyester anchor leg cases, based on the technology developed for similar turret mooring systems employed on offshore exploration and production vessels.

The total vertical force exerted on the mooring turntable by the MCALM systems which employ wire catenaries may be excessive. It would be difficult and very expensive to provide a turntable system which could withstand such high forces.

This MCALM mooring system thus may be feasible, but it may also be very expensive.

TABLE 8-1a MCALM, VARIATION OF ANCHOR LEG PRETENSIONS, ALL-POLYESTER CATENARY LEGS

Leg :					
Length, ft	36,500	33,460	32,591	32,100	
Pretension	50	100	150	200	
Deflection :	Horiz.Force	Horiz.Force	Horiz.Force	Horiz.Force	Horiz.Force
0	0	0	0	0	
500	9	60	125	211	
1000	19	129	281	589	
1500	30	218	601	1168	
2000	42	356	1096	1820	
2500	58	669	1664	2513	
3000	79	1137	2296	3219	
3500	107	1621	2965		
4000	148	2147			
4500	210	2708			
5000	300				
5500	498				
6000	854				
6500	1251				
7000	1689				
7500	2128				
8000	2568				

TABLE 8-1b MCALM, VARIATION OF ANCHOR LEG PRETENSIONS, ALL-POLYESTER CATENARY LEGS

Leg :					
Length, ft	36,500	33,460	32,591	32,100	
Pretension	50	100	150	200	
Sea State 2 :					
Horiz. Force	89	114	140	172	
Leg Tension	107		209	275	
Anchor Uplift	0	0	0	15	
Sea State 3 :					
Horiz. Force	364	431	536	644	
Leg Tension	359	390	495	612	
Anchor Uplift	19	43	79	117	
Sea State 4 :					
Horiz. Force	1607	1728	1864	1996	
Leg Tension	1602	1607	1620	1611	
Anchor Uplift	341	386	404	409	

TABLE 8-2 MCALM, VARIATION OF ANCHOR LEG PRETENSIONS, POLYESTER/CHAIN CATENARY LEGS

Leg :					
Md. Seg. Lng.		34,000		31,900	
Pretension		100	125	150	175
Deflection :	Horiz.Force	Horiz.Force	Horiz.Force	Horiz.Force	Horiz.Force
0	0	0	0	0	0
500		19	48	82	118
1000		39	102	176	263
1500		62	170	312	562
2000		92	267	606	1010
2500		132	467	1040	1566
3000		190	838	1550	2179
3500		273	1284	2094	2828
4000		453	1768	2721	
4500		791	2272		
5000		1200			
5500		1643			
6000		2105			
Sea State 2 :					
Horiz. Force		93	108	123	138
Leg Tension		146		200	
Anchor Uplift		0		0	
Sea State 3 :					
Horiz. Force		378	423	473	538
Leg Tension		377		448	
Anchor Uplift		0		0	
Sea State 4 :					
Horiz. Force		1621	1687	1746	1830
Leg Tension		1589		1589	
Anchor Uplift		153		188	

TABLE 8-3 MCALM, VARIOUS CATENARY ANCHOR LEGS

Leg :	All-Polyester	Polyester/ Chain	Aramid/ Chain	Wire/ Chain	All-Wire
Md. Seg. Lng.	33460	34,000	32,700	35,920	35620
Pretension	100	100	100	500	500
Deflection :	Horiz.Force	Horiz.Force	Horiz.Force	Horiz.Force	Horiz.Force
0	0	0	0	0	0
500	60	19	33	67	92
1000	129	39	70	138	188
1500	218	62	119	215	295
2000	356	92	193	302	419
2500	669	132	420	407	572
3000	1137	190	1061	537	770
3500	1621	273	1829	703	1037
4000	2147	453		936	1399
4500	2708	791		1251	1903
5000		1200		1709	
5500		1643			
6000		2105			
Sea State 2 :					
Horiz. Force	114	93	102	114	124
Leg Tension	153	146	146	545	540
Anchor Uplift	0	0	0	0	0
Sea State 3 :					
Horiz. Force	431	378	609	345	374
Leg Tension	390	377	611	678	685
Anchor Uplift	43	0	0	0	0
Sea State 4 :					
Horiz. Force	1728	1621	2177	1242	1306
Leg Tension	1607	1589	2169	1423	1425
Anchor Uplift	386	153	360	0	0

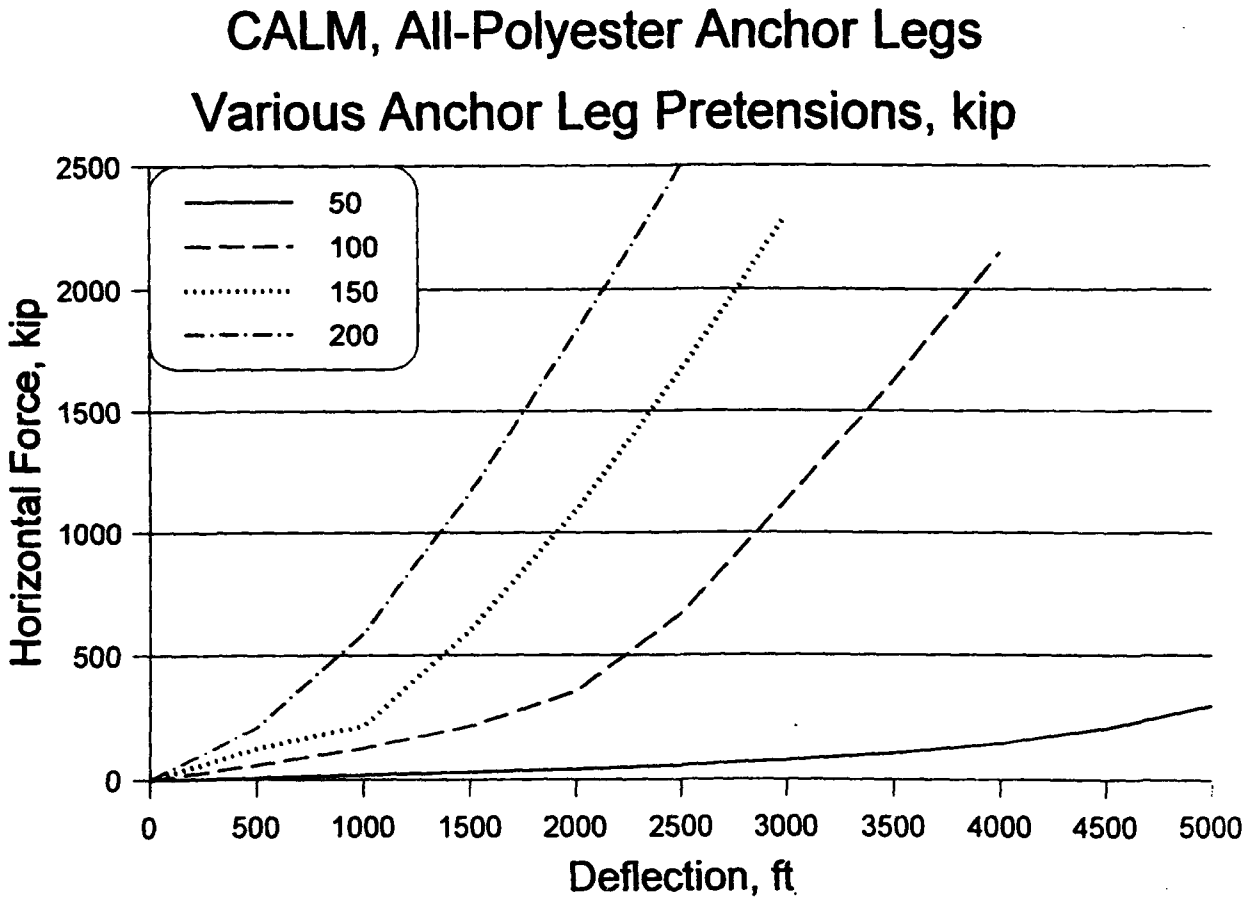

Figure 8-1 All-Polyester MCALM

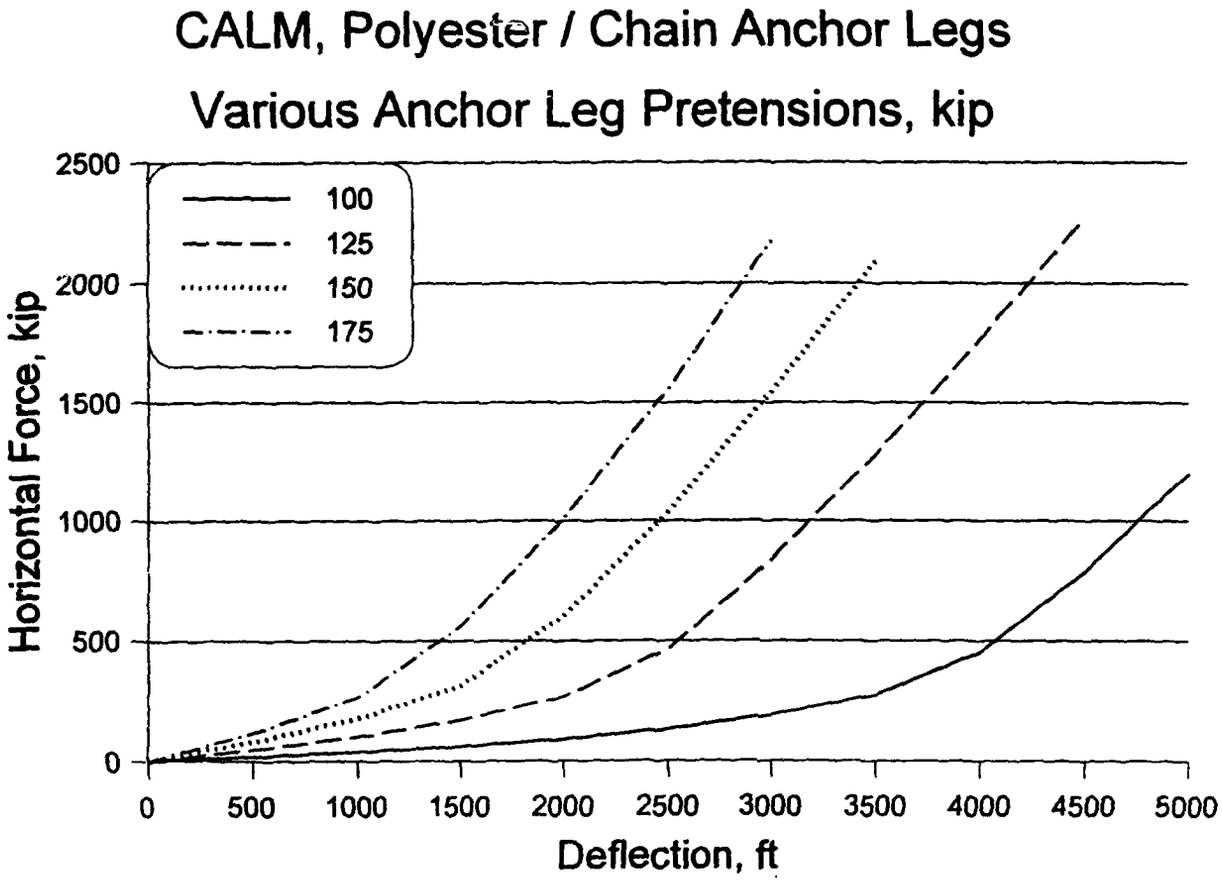

Figure 8-2 Polyester/Chain MCALM

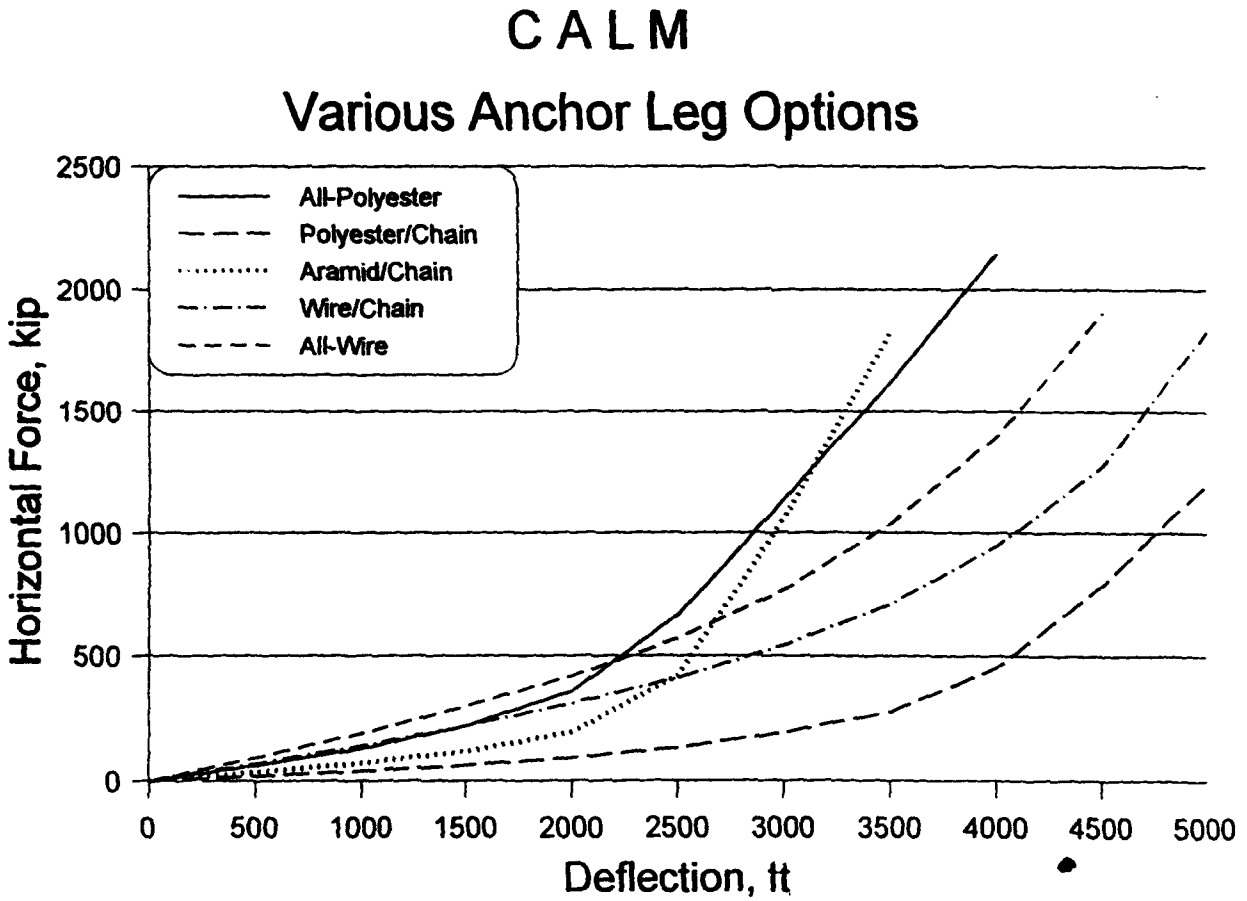

Figure 8-3 Comparison of Various MCALMs

SECTION 9 - ANALYSIS OF THE CASALM
(Catenary and Single Anchor Leg Mooring)

9.1 Introduction

A number of CASALM systems are analyzed and examined in this Section. The analyses were conducted using the CASALM Analysis Computer program. The CASALM system and the program are described in Section 5. The parameters used in these examples are not necessarily suitable or optimum for an actual CASALM system design.

The characteristics of the mooring line components are taken from the tables in Section 4. The peak mooring forces in various sea states are calculated. The mooring forces and wave energies are taken from Table 6-3.

9.2 Example of CASALM Analysis

The data used in this example can be called up in the CASALM Analysis Computer Program by clicking the ***Use Demo Data*** button. This case is used to illustrate the use of the program in the CASALM Program Users Guide.

Table 9-1 lists the data for this example case, together with explanations for the bases for the various data. These data are used here to perform an energy method prediction of peak mooring force.

In order to perform each of these analyses in a short time, only one mooring leg segment comprised entirely of synthetic rope was employed in these analyses. The program can handle two additional segments, for example lengths of chain at the top and the bottom of the anchor leg. But the program takes much longer to reach a solution when all three segments are employed, and the program may fail to converge in some extreme cases. The results are not significantly different unless very long lengths of chain are used.

To create the base case, click the ***Plot Energy Data*** button. Enter ***100*** as Defl. Increment and ***5000*** as Max. Deflection. Then click the ***Display Data*** button. Calculation of the Deflection-Energy Table may take several minutes, depending on the processor speed of the computer. A yellow message box appears on the screen, indicating the deflection being presently calculated. Calculation of successive deflections continues until the strength of one of the mooring components, and when this occurs an appropriate message appears. Strike ***Enter*** and the Deflection-Energy Table appears.

This table may be printed by clicking the ***Print Data*** button. That print-out is included here as Table 9-2. A Deflection vs. Energy Graph can be viewed by clicking on ***Show Data***.

The Force-Deflection Table for this case can be viewed by clicking on the ***Force*** key and then clicking ***Display Data*** on that screen. A print-out of that table is reproduced here as Table 9-3.

The riser break strength of 3,800 kip (1,725 tonne) is exceeded beyond a buoy deflection of 4,400 ft (1,340 m). As shown in Table 9-3, at this deflection the force in the most highly loaded anchor leg is 2,041 kip (926 tonne), and the anchor uplift is 692 kip (314 tonne). Table 9-2 shows that the energy stored in the system at this deflection is 1,503,674 kip ft (208,000 tonne m).

9.3 Example Calculation of Peak Mooring Forces

The steps in calculating the peak horizontal force in the CASALM due to winds and waves are shown in Table 9-4.

For Sea State 2, with an 8.5 kt wind at 30° off the bow, the force on the MOB is 72 kip (33 tonne). Place the cursor in the Force cell and enter ***72***. Application of this horizontal force deflects the example CASALM to a point where **47,727** kip ft of energy is stored, as displayed in the Energy cell.

The significant wave height for this Sea State 2 is 2.9 ft, and the corresponding wave energy is 28,000 kip ft. Enter the sum of the wind energy and the wave energy, ***75727*** kip ft, in the Energy cell. The corresponding peak horizontal force in the example CASALM due to wind and waves is then displayed in the Force cell, **130** kip.

To calculate the other forces in the example CASALM at this peak force, ***Return*** to the main data screen. Enter the peak force ***130*** kip, and the deflection and other forces will be calculated and displayed. In this case the Buoy Deflection is ***2258*** ft. The Max Riser Force is **570** kip, 15% of the riser strength, and the Max Leg Force is **312** kip, only 12% of the anchor leg strength. All of these results are listed in Table 9-4.

The results for similar calculations for Sea States 3 and 4 are also given in Table 9-1. In Sea State 3, the predicted peak horizontal mooring force is **498** kip, the peak riser force is **1518** kip, and the peak anchor leg force is **907** kip. The uplift on the anchor is **252** kip. These are believed to be acceptable values.

In Sea State 4, the peak energy is 1,796,668 kip ft. Table 9-2 indicates that this exceeds the energy capacity of this example CASALM system. When an attempt is made to calculate the force corresponding to this force, the program displays an appropriate warning message.

9-4 Effect of Varying Junction Elevation With Constant Riser Pretension

The junction elevation used in the above example was 500 ft (150 m) above the sea floor, in 10,000 ft (3,000 m) water depth. What is the effect of varying this junction elevation while maintaining the same undeflected riser tension?

Table 9-5 summarizes the results for a series of case with junction elevations of 100, 200, 300, 400, and 500 ft (30, 60, 90, and 120 m). These data are plotted in Figure 9-1.

As the junction elevation is raised, the deflection of the CASALM at any applied horizontal force decreases. This effect is not sufficient to substantially affect the energy absorbing capacity of the CASALM. At higher junction elevations, the peak horizontal force required to store any given amount of wind and wave generated energy increases slightly.

Note that in this example case, the length of the anchor legs was adjusted to maintain the same riser leg pretension. Thus the anchor leg pretension is very high at the low junction elevation.

9.5 Effect of Varying Junction Elevation With Constant Leg Length

A CASALM system is installed with a given junction weight and with pre-set anchor leg lengths. The suggested method of installation is to set the junction on the ocean floor, deploy the anchor legs, and then lift up on the riser to apply pretension to the legs. What is the effect of lifting up on the riser with constant junction weight and anchor leg length?

It is not surprising that the force-deflection characteristic of this system becomes stiffer as the junction elevation increases. Table 9-7 show a CASALM with a 100 kip (45 tonne) junction weight and a 3,015 ft (920 m) anchor leg length, in 10,000 ft (3,000 m) water depth with an anchor distance of 3,000 ft (915 m). Figure 9-2 shows the force-deflection characteristics for these three cases.

At a junction elevation of 100 ft (30 ft), the riser pretension is 150 kip (68 tonne) and the anchor leg pretension is only 4 kip (2 tonne). (Note that the riser's weight also contributes to its pretension.) When the junction is raised to 200 ft (60 m), the anchor leg pretension increases to 27 kip (12 m). And when the junction is raised to 300 ft (91 m), this pretension increases to 68 kip (31 tonne).

9.6 Effect of Increasing Junction Weight With Constant Riser and Leg Lengths

The junction weight on a CASALM serves as a pendulum weight, tending to restore the riser to the vertical when its top is displaced. It might be possible to increase or decrease the junction weight, even after the CASALM is installed. What is the effect of varying the junction weight with a constant riser length and constant anchor leg lengths?

The effect of varying the junction weight is surprisingly slight, as shown in Figure 9-3 and Table 9-7. Here the junction weight was varied from 0 to 300 kip (136 tonne). Anchor leg length was not varied. The pretension in the zero junction weight case is 102 kip (46 tonne), representing the sum of vertical pulls of the pretensioned anchor legs.

As the junction weight increases, the junction elevation decreases slightly, from 511 to 478 ft (156 to 146 m) because of stretch in the riser. And as a result of this decrease in junction

elevation, the anchor leg pretension decreases from 29 to 24 kip (13 to 11 tonne). This illustrates the complex relationships between the parameters within the CASALM system.

However, the horizontal force to produce various deflections changes very little over this range of junction weights. The mooring force required to produce a 1,000 ft (300 m) deflection changed from 11 to 40 kip (5 to 18 kip). But the mooring force required to produce a 4,000 ft deflection (1,220 m) changes from 1,090 to 1,152 kip (495 to 523 tonne), an increase of only 62 kip (28 tonne).

This large change in junction weight had very little effect on the predicted peak mooring forces.

9.7 Discussion

The predicted mooring forces in sea state 3 (2.9 ft wave and 13.5 kt wind) are acceptable in all of the above cases, but they are not acceptable in sea state 4 (6.2 ft wave and 19 kt wind). In either sea state, there was little difference in peak mooring forces over large variations of CASALM system design parameters. This indicates that the CASALM performance is relatively insensitive to changes in these design parameter.

The CASALM did not prove to be an acceptable MOB in sea state 4 (6.9 ft wave and 19 kt wind) in any of the configurations investigated here. This indicates that the potential performance of the CASALM as a deep water mooring system is not as good as that of the MCALM or of the SCLM.

In the discussion at the end of Section 7, it was suggested that the simple catenary leg mooring could be improved by employing three or more anchors facing inward, with ground legs extending from these anchors to a central junction, and with the catenary anchor leg attached to that junction. The system which was described is an adaptation of the CASALM, in which the riser is initially slack instead of tensioned in the undeflected position.

This slack-riser CASALM arrangement helps assure that mooring forces are applied in the optimum direction on each anchor. Another feature of this arrangement is that those anchors which are opposite and at right angles to the direction of mooring force application all serve to hold the junction point down. This feature is illustrated in Figure 9-5.

The attractiveness of this alternative system was discovered too late in this study to permit analyses to be made of that slack riser CASALM arrangement.

The present CASALM Mooring Analysis Computer Program is not capable of analyzing the slack-riser case, in which the junction is initially on the sea floor. The program could be modified to analyze such a case, but this might not be an easy task, especially if the catenary effect in the riser is to be included.

TABLE 9-1 EXPLANATION OF VALUES USED IN DEFAULT EXAMPLE

Parameter	value	units	significance
Water Depth	10,000	ft	ARPA criteria
Riser Length	9,000	ft	typical
Riser Strength	2,600,000	lb	6 in. aramid rope
Riser Weight/Length	4.0	lb/ft	6 in. aramid rope
Riser Stiffness	80,000,000	lb/ft/ft	6 in. aramid rope
Junction Weight	100,000	lb	typical
Number of Anchor Legs	6		typical
First Leg Angle	0	degrees	force in line with anchor leg
Anchor Distance	3,000		typical
Segment 1	lower anchor leg segment, connects to anchor		
Segment 2	middle anchor leg segment, provides elasticity		
Segment 2 Weight/Length	4	lb/ft	9 in. polyester rope
Segment 2 Strength	2,600,000	lb	9 in. polyester rope
Segment 2 Length	2550	ft	typical
Segment 2 Stiffness	33,000,000	lb/ft/ft	9 in. polyester rope
Sinker 2 Weight	0		no sinker
Segment 3	upper anchor leg segment, connects to junction		

TABLE 9-2 CASALM EXAMPLE CASE, DEFLECTION VS. FORCE TABLE

CASALM Mooring Force Calculation, performed at 20:29 March 18, 1997

Water Depth = 10,000 ft
Anchor Distance = 3,000 ft
Junction Elevation = 100 ft
No. of Anchor Legs = 6

Component	Length ft	Strength kip	Weigth/Length kip/ft	Stiffness kip/ft/ft
Riser	9,878	3,800	.004	82,000
Segment 1				
Segment 2	2,993	2,690	.004	33,000
Segment 3				

Riser Weight = 40 kip
Junction Weight = 100 kip
Sinker 1 Weight = kip
Sinker 2 Weight = kip

Buoy Deflct ft	Buoy Force kip	Riser Force kip	Riser Angle deg.	Junctn Elevatn ft	Anchor Leg Tension kip	Anchor Uplift kip	Min. Leg on Ground ft
0	0	200	.0	100	127	0	470
100	1	200	.4	101	128	0	460
200	4	201	1.3	103	128	0	441
300	7	201	2.1	107	128	0	410
400	8	202	2.5	109	129	0	354
500	9	204	2.9	113	129	0	299
600	12	205	3.7	120	131	0	219
700	15	207	4.4	130	131	0	142
800	16	210	4.8	134	131	0	56
900	18	212	5.5	145	134		0
1,000	21	216	6.2	157	139	1	0
1,100	24	221	6.8	168	144	2	0
1,200	26	227	7.3	179	152	3	0
1,300	29	233	7.8	190	160	4	0
1,400	29	241	7.5	183	168	5	0
1,500	34	251	8.5	206	181	7	0
1,600	37	261	8.8	213	192	9	0
1,700	47	276	10.6	266	213	11	0
1,800	53	287	11.3	286	224	13	0
1,900	58	305	11.7	297	240	16	0
2,000	58	323	11.0	271	261	20	0
2,100	73	349	12.9	337	288	24	0
2,200	79	375	12.8	331	315	29	0
2,300	89	399	13.6	357	336	33	0
2,400	94	432	13.3	340	368	39	0
2,500	115	471	14.8	402	400	46	0
2,600	131	514	15.4	423	438	54	0
2,700	152	565	16.2	455	475	62	0
2,800	173	620	16.8	478	518	72	0
2,900	199	680	17.6	511	572	84	0
3,000	220	751	17.6	503	615	96	0
3,100	252	822	18.3	534	669	109	0
3,200	283	904	18.7	546	724	124	0
3,300	325	990	19.6	588	778	139	0
3,400	367	1,086	20.2	611	843	157	0
3,500	398	1,183	20.1	593	909	176	0

TABLE 9-3 CASALM EXAMPLE CASE, DEFLECTION VS. ENERGY

CASALM Mooring Energy Calculation, performed at 20:29 March 18, 1997

Water Depth = 10,000 ft Junction Elevation = 100 ft
Anchor Distance = 3,000 ft No. of Anchor Legs = 6

Component	Length ft	Strength kip	Weigth/Length kip/ft	Stiffness kip/ft/ft
Riser	9,878	3,800	.004	82,000
Segment 1			.	
Segment 2	2,993	2,690	.004	33,000
Segment 3			.	

Riser Weight = 40 kip Junction Weight = 100 kip
Sinker 1 Weight = kip Sinker 2 Weight = kip

Horizontal Deflection ft	Horizontal Buoy Force kip	Data Energy ft-kip	Mooring Energy ft-kip
100	1	66	66
200	4	263	330
300	7	527	857
400	8	726	1,583
500	9	858	2,441
600	12	1,056	3,497
700	15	1,320	4,816
800	16	1,518	6,334
900	18	1,714	8,048
1,000	21	1,975	10,022
1,100	24	2,237	12,259
1,200	26	2,499	14,758
1,300	29	2,761	17,519
1,400	29	2,891	20,410
1,500	34	3,154	23,564
1,600	37	3,548	27,112
1,700	47	4,203	31,315
1,800	53	4,989	36,305
1,900	58	5,514	41,819
2,000	58	5,776	47,595
2,100	73	6,563	54,157
2,200	79	7,611	61,769
2,300	89	8,397	70,166
2,400	94	9,183	79,349
2,500	115	10,494	89,843
2,600	131	12,329	102,172
2,700	152	14,163	116,335
2,800	173	16,259	132,594
2,900	199	18,617	151,211
3,000	220	20,975	172,186
3,100	252	23,594	195,779
3,200	283	26,737	222,517
3,300	325	30,405	252,922
3,400	367	34,596	287,518
3,500	398	38,263	325,782

TABLE 9-4 CASALM EXAMPLE CASE

Parameter	Units				
Sea State		0	2	3	4
Wind	kt	0	8.5 kt @ 30°	13.5 kt @ 30°	19 kt @ 30°
Waves, $H_{1/3}$	ft	0	1.0 ft	2.9 ft	6.2 ft
Applied Wind Force	kip	0	72	182	361
Wind Deflection	ft	0	1943	2454	
Wind Energy	ft-kip	0	47726	112,218	239,668
Wave Energy	ft-kip	0	28,000	235,000	1,557,000
Peak Energy	ft-kip	0	75,726	347,218	1,796,668
Peak Horizontal Force	kip	0	130	498	X
Peak Vessel Deflection	ft	0	2,258	3,225	
Riser Angle	degree	0	13.7	19.4	
Junction Elevation	ft	500	728	895	
Peak Riser Tension	kip	200	570	1,518	
Peak Leg Tension	kip	28	312	907	
Peak Uplift Force on Anchor	kip	0	0	252	

Table 9-5 VARIATION OF JUNCTION ELEVATION WITH CONSTANT RISER PRETENSION

Riser :					
Length, ft	9878	9778	9678	9578	9479
Pretension, kip	200	200	200	200	200
Leg :					
Length, ft	2993	3006	3020	3039	3063
Pretension	127	63	45	34	28
Junction :					
Weight	100	100	100	100	100
Elevation	100	200	300	400	500
Deflection :	Horiz.Force	Horiz.Force	Horiz.Force	Horiz.Force	Horiz.Force
0	0	0	0	0	0
500	9	11	11	10	9
1000	21	21	22	22	21
1500	34	37	42	42	37
2000	58	73	79	84	84
2500	115	136	157	189	199
3000	220	252	304	356	388
3500	398	472	545	629	681
4000	702	796	901	1016	1111
4500	1121	1278	1425	1582	
5000	1739				
Sea State 2 :					
Horiz. Force	99	109	114	114	130
Riser Tension	427	477	510	522	570
Leg Tension	357	354	340	310	312
Sea State 3 :					
Horiz. Force	467	472	466	459	498
Riser Force	1314	1366	1387	1404	1518
Leg Tension	996	978	938	900	907

Table 9-6 VARIATION OF JUNCTION ELEVATION WITH CONSTANT LEG LENGTH

Riser :					
Length, ft	9884		9780		9677
Pretension, kip	150		178		210
Leg :					
Length, ft	3015	3015	3015	3015	3015
Pretension	4		27		68
Junction :					
Weight	100	100	100	100	100
Elevation	100	150	200	250	300
Deflection :	Horiz.Force	Horiz.Force	Horiz.Force	Horiz.Force	Horiz.Force
0	0	0	0	0	0
500	7		8		11
1000	15		18		24
1500	22		32		47
2000	41		52		84
2500	68		115		178
3000	157		231		325
3500	335		451		566
4000	597		765		932
4500	1027		1215		1456
5000	1613				
Sea State 2 :					
Horiz. Force	120		113		104
Riser Tension	443		468		494
Leg Tension	301		317		339
Sea State 3 :					
Horiz. Force	489		484		462
Riser Tension	1314		1364		1338
Leg Tension	915		948		959

Table 9-7 VARIATION OF JUNCTION WEIGHT WITH CONSTANT RISER AND LEG LENGTHS

Riser :					
Length, ft	9479	9479	9479	9479	9479
Pretension, kip	102	151	200	297	395
Leg :					
Length, ft	3063	3063	3063	3063	3063
Pretension	29	29	28	26	24
Junction :					
Weight	0	50	100	200	300
Elevation	511	505	500	488	478
Deflection :	Horiz.Force	Horiz.Force	Horiz.Force	Horiz.Force	Horiz.Force
0	0	0	0	0	0
500	5	7	9	15	20
1000	11	15	21	31	40
1500	21	28	37	50	63
2000	73	73	84	105	115
2500	178	189	199	199	231
3000	356	377	388	409	419
3500	66	671	681	702	723
4000	1090	1100	1111	1131	1152
Sea State 2 :					
Horiz. Force	122	118	130	104	106
Riser Tension	526	521	570	499	545
Leg Tension	345	312	312	193	160
Sea State 3 :					
Horiz. Force	495	493	498	472	465
Riser Tension	1493	1506	1518	1482	1482
Leg Tension	941	919	907	840	784

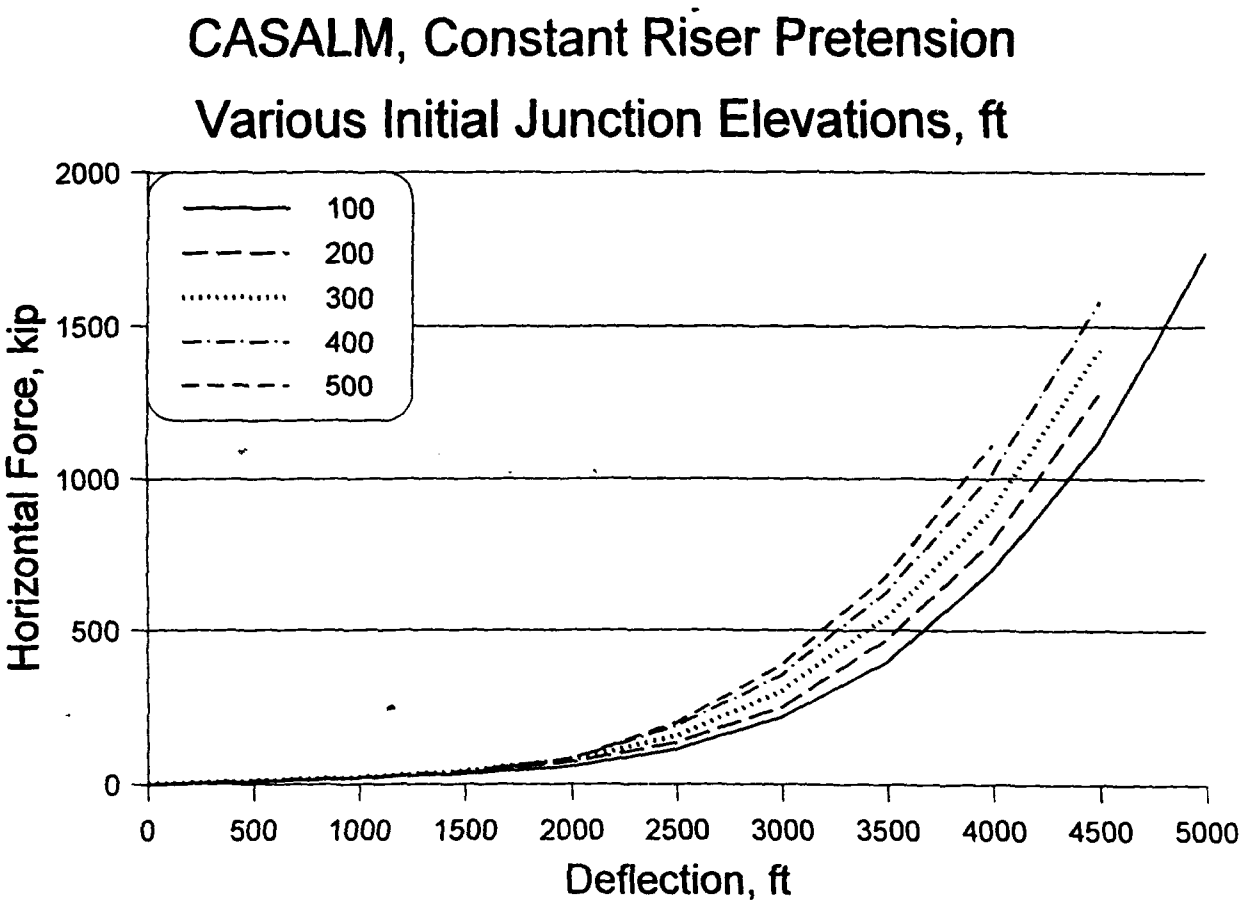

Figure 9-1 Effect of Varying Junction Elevation With Constant Riser Tension

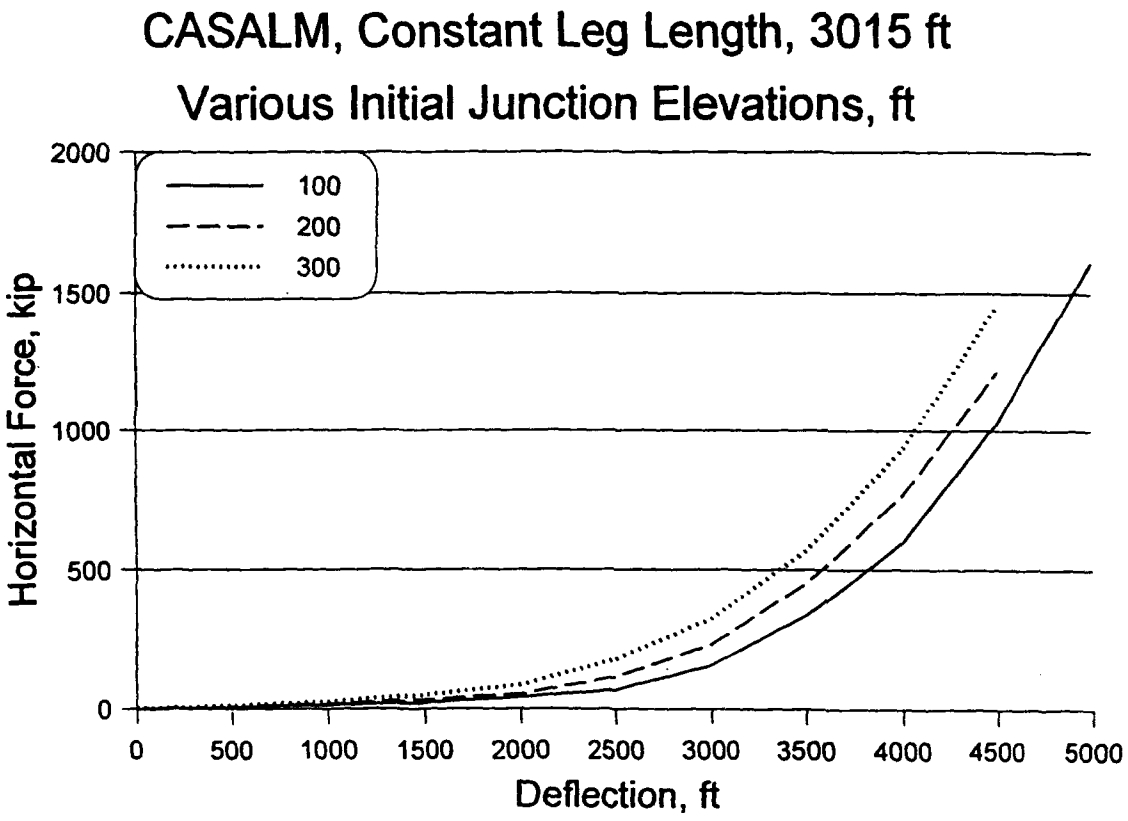

Figure 9-2 Effect of Varying Junction Elevation with Constant Leg Length

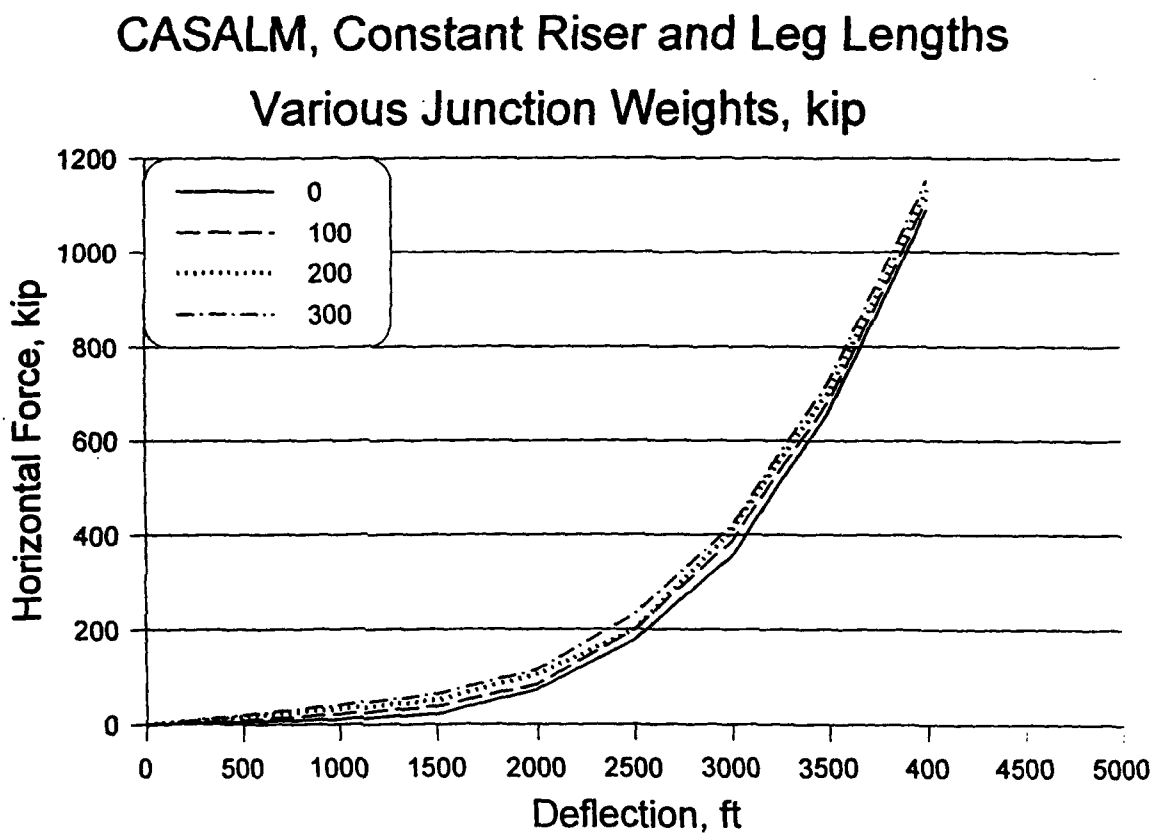

Figure 9-3 Effect of Varying Junction Weight with Constant Lengths

SECTION 10 - DISCUSSION

10.1 Introduction

This section summarizes the major findings of the preceding three Sections, which presented results of analyses of the following three types of SPMs :

- CASALM (Catenary and Single Anchor Leg Mooring)
- MCALM (Catenary Anchor Leg Mooring)
- SCLM (Single Catenary Leg Mooring)

Typical force-deflection curves for these systems are shown in Figure 10-1. Pertinent information and performance data are summarized in Table 10-1.

10.2 Bases for Comparisons

These systems are judged on the bases of their abilities to safely moor the MOB without thruster assist in various ocean environments, particularly sea state 3 (2.9 ft waves and 13.5 kt wind) and sea state 4 (6.2 ft waves and 28.7 kt wind).

Peak mooring forces and tensions in these environments were predicted made by an adaptation the energy method, using mooring force data from other dissimilar mooring situations. These predictions were made only for the purpose of determining the relative performances of the several mooring systems and of the many alternate possible embodiments of those systems. If one design was predicted to safely moor the MOB only in sea state 3 and a second design was predicted to safely moor it in sea state 4, then that second system is probably more capable than the first.

But because only limited and dissimilar actual SPM mooring force data was available for performing these analyses, the sea state limitations predicted here should not be used to judge the actual limitations on any of these moorings. These mooring systems might actually be capable of safely mooring the MOB in even higher environments.

The same types and sizes of mooring components were used in all of the analyses. For example, wherever polyester rope was used, it was a 9 in. (230 mm) diameter polyester rope with a break strength of 2,700 kip (1,220 tonne). Thus even though other, higher strength components may be available or become available in the future, the relative comparisons of these mooring systems will probably not change significantly.

10.3 The CASALM

The performance of the CASALM was not as good as had been expected. Based on the analyses conducted here, it is an acceptable mooring for the MOB in sea state 3. But in sea state 4 the

predicted peak tension in the riser exceeded the break strength of a 9 in. (230 mm) diameter polyester rope, which indicates that the CASALM is probably not a viable mooring in that higher environment.

The principal problem with the CASALM is that its geometry restricts the angle at which the riser can withstand the applied horizontal force. In the examples analyzed here, the riser inclined to 25° or more, But even at that angle, the peak tension in the riser was almost 2.4 times the peak horizontal force. Altering the junction elevation, the junction weight, and other parameters did little to alleviate this situation.

The CASALM otherwise exhibits good mooring system properties. The peak horizontal deflection in sea state 3 was about the same as that of the MCALM with 100 kip pretension and about two-thirds that of the SCLM. The swing circle was about half that of the SCLM. The length of mooring leg materials used in the CASALM is much less than that for the MCALM. The connection of the CASALM to the MOB would be very simple and much less costly that for the MCALM.

10.4 The MCALM

The MCALM configuration discussed here consists of six polyester rope anchor legs connected to chain ground legs. The higher pretension, 125 kip (57 tonne), created a better force deflection curve than did the 100 kip (45 tonne) pretension case. In these examples, the length of the polyester rope extended to within a few hundred feet of the interface with the chain ground leg in the pretensioned condition. For the 125 kip pretension case this required a total length of over 200,000 ft (70,000 m) of polyester rope.

The predicted peak mooring forces for both of these MCALMs were acceptable. In sea state 3 the peak forces were significantly less for the 125 kip pretension system than for the 100 kip pretension, but in sea state 4 the peak forces were essentially the same in both systems, reflecting the effect of the non-linear force-deflection curve. With the MCALM, the peak horizontal mooring force is distributed among two or three anchor legs, instead of being carried by only one anchor leg as with the CASALM and the SCLM.

Although the MCALM exhibits favorable mooring performance with the MOB in this deep water application, it is probably not a good candidate for this situation.

First it will require a large, motor operated turntable on the MOB to attach and support the anchor legs. The total vertical load of the pretensioned legs will be substantial. And the peak forces experiences in the mooring environment will result in even higher load. A surface buoy might serve as the attachment point for the catenary anchor legs, much in the same manner as with the CALM type SPM used to moor large oil tankers in shallow water. However, such a buoy would need to be very large, with a displacement of possibly 1,000 kip (450 tonne) to support the anchor leg pretensions and to remain upright and on the surface under high mooring loads. Such a large buoy would probably still require a turntable to track the swings of

the moored vessel. And a bow hawser or yoke arrangement would be required between the buoy and the MOB.

Installation of the MCALM in deep water will require placing possibly six anchors at widely distributed points on the deep ocean floor. Unlike with the CASALM or the SCLM, this will necessitate repositioning the surface vessels involved in this anchor point installation. The MCALM in this water depth requires large quantities of mooring rope and chain for the six ground legs.

Thus the MCALM will probably be a very expensive alternative for mooring the MOB in very deep water.

10.5 The SCLM

The SCLM is the simplest of the moorings considered here to design and install. As the name implies, it consist of a single catenary leg, consisting of a riser of synthetic or wire rope, possibly with chain at the top to facilitate connection to the MOB and with chain at the bottom to connect to the anchor and to alleviate abrasion on the sea floor. In the system considered here for mooring in 10,000 ft (3,000 m) water depth, the length of the polyester rope riser was 9,800. There was a 100 ft (30 m) chain at the top. A 30,000 (9,100 m) length of chain ground leg was used in the analysis, but only several thousand ft of this chain lifted off the ground. This indicates that the length of chain in the ground leg can be relatively short.

The peak horizontal forces on the SCLM are the lowest of those systems considered here. This reflects the relatively shallow slope of the force-deflection curve.

The SCLM exhibited very reasonable peak predicted forces in sea state 3. The peak tension in the riser is only about a quarter of the break strength of the polyester rope used in this analysis. Even in sea state 4 these forces are probably acceptable. The peak riser tension in that sea state, 1,820 kip (825 tonne) is about two-thirds of the polyester rope break strength.

The SCLM has a very large swing circle, compared to the other mooring systems considered here. The swing circle is defined here as the total diameter of freedom of movement about the center of the mooring. In the SCLM the MOB is free to swing completely around the anchor position instead of just around the undeflected catenary top position. Thus the length of ground leg which is lifted from the ground must be added to the deflection of the mooring top in determining the swing circle.

For the SCLM, this swing circle in sea state 3 is about 15,000 ft (4,600 m), and in sea state 4 it is about 27,000 ft (8,200 m). Expressed another way, in sea state 3 the ratio of swing circle to water depth is about 1.5, and in sea state 4 this ratio is about 2.7. This large swing circle would be excessive in some applications, but it will probably not be a problem when mooring the MOB.

If the MOB moored position can be allowed to move, it is not necessary to anchor the SCLM

ground leg. Otherwise, the anchor leg can be anchored, preferably by a suction or driven pile which can tolerate force from any direction. If the direction of force application on the anchor is a problem, three or more suitable directional anchors could be arranged in an inward facing pattern, and chain or wire could be connect between these anchors to a central junction to which the ground leg is attached. This is essentially an adaptation of the CASALM

10.6 The SCLM Is the Most Promising Mooring For The MOB

Based on the above analyses, the SCLM is the most promise mooring system for the MOB, considering the duty statement given in Section 3. Specifically, if it is not necessary that the MOB maintain a precise station, but can be allowed to move about in a large swing circle around the center of the mooring, then the MOB is an acceptable mooring. And if further movement of that mooring center can be tolerated, then the SCLM does not even need an anchor set in the sea floor.

The SCLM is the least complicated and least expensive of the alternatives considered here. It can consist only of a short length of chain or wire attached to the MOB bow, a length of polyester rope extending almost to the sea floor, and a suitable length of chain or heavy wire as a ground leg which is allowed to drag about on the sea floor. A suction or driven pile can be used to anchor the ground leg if it is necessary to prevent the MOB moored position from moving about.

TABLE 10-1 COMPARISON OF ALTERNATE DEEP WATER MOORING SYSTEMS

System >	CASALM	MCALM	MCALM	SCLM
description	100 kip Junction wt. 100 ft. Junction elv.	Polyester / Chain 100 kip pretension	Polyester / Chain 125 kip pretension	Polyester Riser Chain Ground Leg
Length of Riser, ft	9,800	-	-	9,800
Total Length of Ground Legs	18,000 (polyester)	153,000 (polyester)	204,000 (polyeter)	6,500 (chain)
Pretension, kip	200	100	125	80
In Sea State 3 :				
Peak Horiz. Force, kip	467	378	423	361
Peak Riser Tension, kip	990	377	410	689
Peak Leg Tension, kip	1,314	-	-	
Horiz. Deflection, ft	3,600	3,900	2,400	5,000
Swing Circle, ft	7,200	7,800	4,800	15,000
In Sea State 4 :				
Peak Horiz. Force, kip	x	1,621	1,687	1,274
Peak Riser Tension, kip	x	1,589	1,595	1,820
Peak Leg Tension. kip	x			
Horiz. Deflection, ft	x	5,500	3,900	7,000
Swing Circle, ft.	x	11,000	7,800	27,000

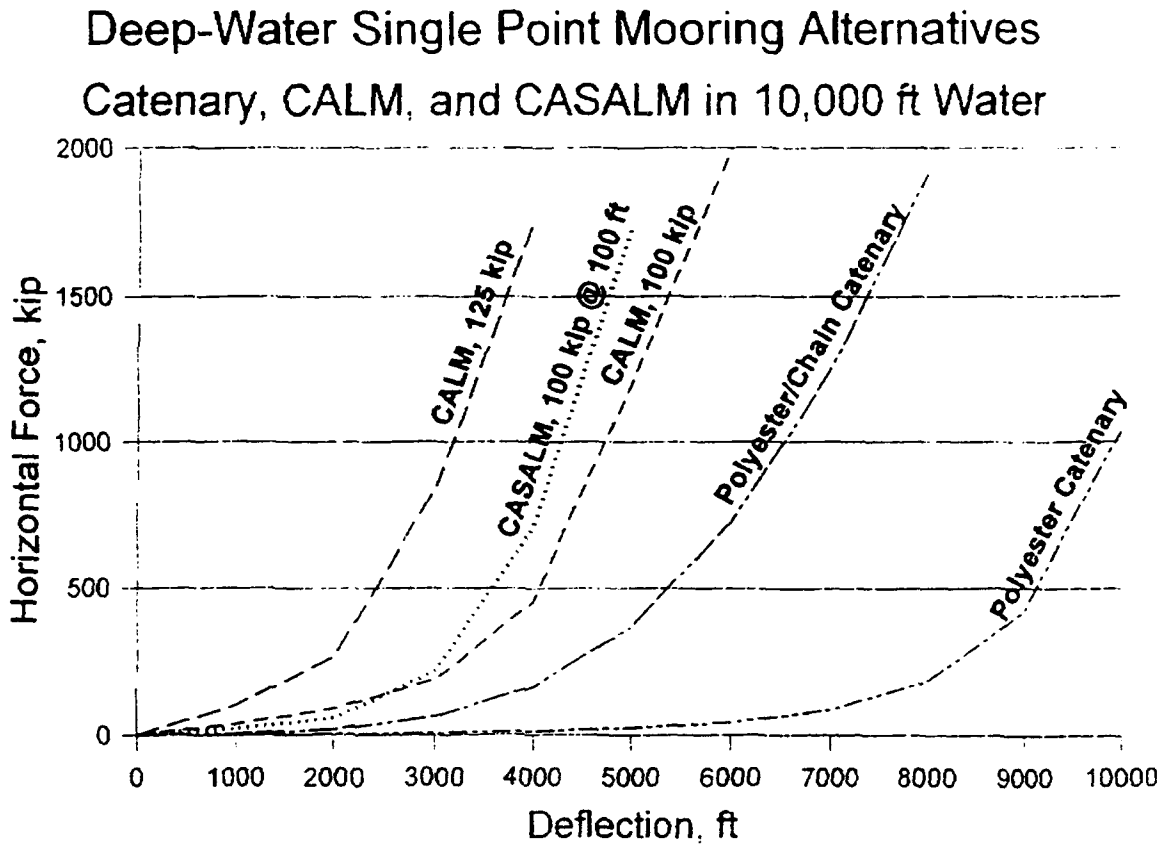

Figure 10-1 Force-Deflection Curves For Deep Water Mooring Systems

SECTION 11 - RECOMMENDATIONS FOR FURTHER WORK

11.1 Introduction

This Section provides brief recommendations for additional research studies to develop mooring system designs for the MOB. These include small-scale model testing to determine the second-order wave drift and drag coefficients for the MOB, dynamic analyses of deep water mooring systems using those coefficients, and large-scale offshore testing of the SCLM drag mooring concept. It also makes recommendations for adapting the CASALM computer program to analyze the Fleet Mooring and for using the new catenary force-deflection equations in other computer programs and calculations.

11.2 Further Development of Force-Deflection Computer Programs

The Catenary, CALM and CASALM force-deflection computer programs were written to compare the mooring performances of the respective mooring systems for this research project. They are not fully "debugged" and are not yet finished products. Other programs exist which can analyze the Catenary and CALM systems. But the CASALM program is probably unique in its abilities to properly model the kinematics of this complex mooring system taking into account the stretch of the various components.

The CASALM is essentially the same as the Fleet Mooring now used in many Navy installations. In the Fleet Mooring the moored vessel is moored to a small buoy by an elastic hawser or a chain catenary, while in the CASALM the buoy is integrated into the moored vessel. In the Fleet Mooring, the buoy can be pulled under the water surface, and the connection between the vessel and the buoy can extend either as an elastic element or as a catenary.

The computer program now used to analyze the Fleet Mooring does not properly model the kinematics of that system. In that program, the junction is treated simply as a clump weight on a single catenary leg, instead of properly accounting for the uplift effect of the other catenary legs. The CASALM program now properly accounts for that effect

The CASALM program could be enhanced to include the effects of buoy submergence and hawser extension in order to fully model the Fleet Mooring. Inclusion of buoy submergence and hawser extension would further complicate the computation procedures, which now take into account the effects of riser and anchor leg stretch and up to three segments in each anchor leg. Those features were important for the deep water mooring analysis, but they could be modified or deleted from a Fleet Mooring program to simplify the program and reduce computation time.

In developing the computer programs, new catenary force-deflection equations were derived which directly relate catenary top deflection to the undeflected position of the catenary. These equations greatly simplify the catenary force-deflection portion of the program. They are documented in an Appendix to this report.

These new catenary equations should be considered for use in other catenary programs and calculations. They are easier to use than the traditional catenary equations. They much more efficient in computer programs th.». finite difference solutions

11.3 Dynamic Computer Analysis of Deep Water Moorings

The static analyses conducted in this study provide only approximations of the mooring system performance. The vessel moored at an SPM can move about in "unpredictable" manners, and in these deep water mooring systems that movement can be very large. The dynamic forces which result from such vessel movements induce high forces in the mooring system. The energy method was used in this study to predict these dynamic forces. But as stated earlier, the data used in those analyses was not appropriate, and thus the predicted forces are probably not correct.

Dynamic computer programs are available for modelling the response of a vessel moored at an SPM. The author is familiar with the TERMSYM II program, developed by MARIN, Waginengen, the Netherlands. That program generally accounts for all of the important parameters and effects and has given good correlation with model test results and full scale SPM performance. Other similar programs may also be available, but their qualifications and verification should be carefully evaluated before they are used for this purpose.

Such a dynamic computer program could be used to conduct a more thorough evaluation of the MOB with the SCLM and possibly other deep water mooring systems. This would yield good predictions of vessel movements and mooring forces.

11.4 Small Model Testing of MOB

It would not practical to conduct meaningful model tests of the deep water mooring systems in conventional hydrodynamic model test basins. The water depth in the model basin is the principal limitation. Wind and waves should be imposed from different directions. The model basin must have a large area to accommodate the very large swing circle, especially for the SCLM. Even with a water depth of 10 ft (3 m), the scale for testing a mooring is 10,000 ft of water is 1:1000.

Model testing might be conducted to determine the second-order wave drive and drag coefficients of the MOB. These data would then be useful input to a dynamic analysis computer program, as suggested above.

11.5 Large Model Testing ot Deep Water Moorings

The SCLM drag mooring appears to be the best means of mooring the MOB, considering that the MOB does not need to be maintained at a precise location. It would be relatively easy to conduct a large model test of the drag catenary mooring in a suitable offshore environment to demonstrate the technique and gather further data.

A barge or other suitable vessel could be moored in relatively deep water by a suitable synthetic rope riser and a suitable chain or heavy wire ground leg without an anchor. The vessel size, water depth, and sea floor soil conditions, as well as the expected wind, wave and current environments, would be selected to model the MOB mooring situation to the extent possible. The characteristics of the mooring components would be suitably scaled. For example, mooring a 300 ft (100 m) long barge in 1000 ft (300 m) of water would constitute a model scale of 1:10.

The mooring system should be instrumented to record tension and inclination at the upper end of the riser, which would be a short length of chain attached to the end of the synthetic rope. The position of the moored vessel would be monitored and recorded using GPS. Its heading would also be recorded. The wind, wave, and current environments should also be recorded.

This deep water mooring experiment should be conducted for an adequate length of time in order to determine the response in a variety of environments. It would not be necessary to have personnel on the moored vessel other than for the purposes of maintaining the instrumentation.

After collecting the data, the recorded wave, wind, and current as well as the resulting mooring forces would be analyzed by appropriate scaling factors to predict the performance of the MOB mooring.

APPENDIX A

CASALM ANALYSIS COMPUTER PROGRAM

USERS GUIDE

A-1. INTRODUCTION

CASALM is an acronym for "Combined Catenary and Single Anchor Leg Mooring." This type of single point mooring system is shown in Figure A-1.

A-1.1 Description of the CASALM Mooring System

The CASALM consists of a large buoy on the sea surface, a riser extending down from the buoy to a weighted junction suspended above the sea floor, and catenary anchor legs extending radially from the junction to anchors on the sea floor.

When a force deflects the buoy to the side, the riser tilts and lifts the junction. As the junction is lifted, both the horizontal and vertical forces in the anchor legs increase. Both the junction weight and the vertical anchor leg forces act on the bottom of the tilted riser to produce a pendulum restoring force. Mooring restoring force is also produced by the horizontal forces in the deflected anchor legs acting on the junction.

The anchor legs do not necessarily need to perform as catenaries. Alternatively, they may be synthetic fiber ropes, serving as elastic springs.

A-1.2 About the CASALM Mooring Analysis Computer Program

The CASALM program was written by Tension Technology International as part of the project to develop "deep water, light weight mooring technology capable of single point mooring offshore bases in water depths exceeding 10,000 ft.", ARPA Program NWSC-96-1. This was performed under Contract No. N00167-95-C-00590, administered by the Navy Surface Warfare Center, Carderock Division.

It was necessary to develop a unique program to analyze the complex kinematic features of the CASALM with elastic tension components. The CASALM program along with the CALM and Catenary subprograms were written to compare the mooring performances of the respective mooring systems. They have been verified against other calculation methods. But they are not fully "debugged" and are not yet finished products. The programs have not been checked out with all possible combinations of parameters.

The calculation methods used in these programs are documented in Appendix B. A new form of catenary force-deflection equation was derived in developing these programs. That new catenary force-deflection equation may be useful to other catenary solutions..

The CASALM program involves many iteration and "trial and error" steps to reach a solution. Thus the calculation may take a long time, especially on older, slower PCs. In some cases the program may failed to reach a solution. In some cases the solutions of two almost identical cases may be somewhat different, possibly because in one case a "trial and error" reached a solution "from the left" and in the other it reached a solution "from the right". The CALM and the Catenary programs should not have these problems, and should be useful for very rapid solutions to problems. The reasonableness of solutions should be examined, especially in critical applications.

A-1.3 Versions of the Mooring Analysis Computer Program

The CASALM Analysis Computer Program calculates the force-deflection characteristics and other properties of the CASALM. The program is written for Microsoft Windows 3.1. It will also run in Microsoft Windows 95 and IBM OS/2.

The program is complied in two different versions: CASALM-1 and CASALM-3. Figures A-2 and A-3 show the main data input/output screens for these two programs. The CASALM-3 version accommodates three segments in each anchor leg. The CASALM-1 version has only one segment in each anchor leg. It is easier to use and runs faster than CASALM-3 and is adequate for most analyses. This Users Guide describes the three-segment feature of CASALM-3, but otherwise it is also applicable to version 1.

One of the subroutines of the CASALM program calculates the force-deflection characteristics of a multi-leg catenary anchor leg mooring (CASALM). A separate CALM Analysis Computer Program has been compiled which features that subroutine. Another subroutine calculates the force-deflection characteristics of a three-segment catenary leg. A separate Catenary Analysis Computer Program has been compiles with that subroutine. Figures A-4 and A-5 show the main screens for those programs. The pertinent portions of this Users Guide apply to those separate programs.

A-1.4 Overview of the CASALM Analysis Computer Program

Figure A-2 shows the Main Screen of the CASALM 3 program, with example data displayed. Figure A-6 illustrates the various input and output parameters of the CASALM-3 Mooring Analysis Computer Program.

All anchor legs are identical. Each anchor leg can consist of up to three distinct segments (in CASALM-3). The segments can differ in weight, strength, and tension stiffness. Sinker weights can be placed at the connections between the segments. All anchor points are at the same water depth.

The anchor legs are arranged symmetrically about the junction (in the undeflected position), such that they are separated by identical angles. The angle between the direction from which force is applied and the nearest anchor leg is one of the input parameters. The angles of all other legs are then calculated from this force origin direction.

The input data which describe the CASALM system are listed on the left of the main screen. The Buoy Deflection, Buoy Force and other output data are listed on the right of the screen. Command buttons which perform additional analyses and other functions appear at the lower right of the screen.

An abbreviated display of these instructions can be displayed at any time by clicking on the **Show Instructions** button in the top center of the screen. The first time these instructions are called up, there will be a long pause as they are read from the hard disk, but the instructions will appear quickly during subsequent call-ups. Click on **Hide Instructions** to return to the program. Clicking on the **Notes** button will provide a brief description of the particular version of the CASALM program.

A-2. About the Program and This Users Guide

2.1 Conventions Used In This Users Guide

In this Users Guide, the names of data entry cell labels are printed as Unbold Block Letters. On the program screens, these labels appear to the left of the data entry cell to which they apply. When such a label is referred to in this guide, the text actually refers to the data entry cell to the right of that label.

On the data screen, optional data entry cells are labeled in *italics*. Accordingly the optional data entry cell label names are printed here in *Unbold Italic Block Letters*.

Data which is entered from the keyboard is printed in this Users Guide in ***Bold Italic Block Letters***. In the following instructions, striking the ***Enter*** (or ***Return***) key will be implicit after any instructions to type input data.

The labels on buttons which carry out commands are also printed here in ***Bold Italic Block Letters,*** because they are another means of data input. These command buttons are "pressed" by clicking with the mouse (moving the cursor over the command button with the mouse and pressing the left mouse button).

Each command button also has a "hot-key" letter, indicated by an underline in its label. When this Users Guide instructs you to click on a command button, you may instead execute that command by simultaneously pressing the ***Alt*** key and the underlined "hot-key" letter.

For example, to exit the program, you may move the cursor to the ***Exit*** button at the upper right corner of the screen and "click" to exit from the CASALM program. Or alternatively

you may hold down the ***Alt*** key while pressing ***x***. The instructions for such a command may be given here simply as ***Alt-x*** or whatever other underlined letter key is to be pressed. That alternative will be implicit in any instructions to "click" (or similar) on a command button.

Data output display cells will be referred to here by the label in the cell which precedes them. For example, Riser Angle designates the output cell to the right of that phrase.

Output data which appears in a data display cell while running the following examples are given here in **Bold Block Letters**.

A-2.2 Conventions Used on the CASALM Data Screens

On the CASALM computer program screens, data input cells are normally displayed with a white or a cream background. Data input focus can be switched to an adjacent data input cells by use of the mouse and cursor or the ***Up*** and ***Down Arrow*** keys.

The cell which has data input focus (default cell) is indicated by a dotted-red (or pink) background, and a blinking vertical cursor bar appears within that cell. As soon as any data is entered or changed in that cell, its background changes to orange (or red/yellow stripes) which indicates that the data which appears within that cell has not yet been entered into the program. And when that data is input to the program, for example by striking the ***Enter*** key, the cell background color is restored.

During data input on the left side of the screen, when either the ***Enter*** key or the ***Down Arrow*** (on cursor control pad) is pressed, the entered data is accepted, and the input focus jumps to the next cell in the sequence. The normal data entry sequence (after specifying units) begins with the Water Depth cell at the upper left of the screen and proceeds down the left column of CASALM system design data.

If the ***Up Arrow*** key is pressed, the entered data is accepted and the input focus jumps to the previous cell in the sequence. This is useful for correcting previous entries.

If the ***Page Down*** key is pressed, the entered data is accepted, all input data is checked, and the input focus then jumps to the Buoy Deflection cell. This short cut is useful after you have changed one or several parameters.

After all data has been entered and checked by the program (as explained below), data input focus is on the Buoy Deflection cell at the upper right corner of the screen. Focus can be switched between that cell and the Buoy Force cell by using either the ***Down Arrow*** or the ***Up Arrow*** key. Data input focus can be returned to Water Depth, at the top of the CASALM system parameter column at any time by pressing the ***Page Up*** key.

With focus on a particular cell, hitting the ***Escape*** key before hitting the ***Enter*** or applicable ***Arrow*** or ***Page*** key will restore the previous data in that cell. This can be used to abort the entry of bad data.

A-2.3 Program Execution Message Boxes

After data input, the program checks data for completeness and consistency. If it detects a problem, an appropriate message will appear, prompting you to enter missing data or to re-enter data which is inconsistent with the configuration of the CASALM system. Click on the ***OK*** button or hit ***Enter***, and the data entry focus will transfer to an appropriate data entry cell.

The program may produce a solution which causes over tension in the riser or in an anchor leg segment. It may make several recalculation attempts to correct that condition. But if it is unsuccessful, it then accepts the over tension condition and continues with calculations. After completing its calculations, the program will then display a message indicating which mooring component was over tensioned.

A-2.4 Use of Units Within the CASALM Program

The CASALM computer program is "dimension neutral". With one exception*, it carries out all calculations using dimensionless equations.

The user may choose any consistent set of length and force/weight units for entry in the program. The units which are designated for input are then also used for output.

The same units must be used for both force and weight. In the traditional English system these units may be ft (feet) for length and lb (pounds), kip (kilo pound) or any of the various tons for both force and weight. In the traditional metric system these units may be m (meters) for length and kg (kilograms) for both force and weight. Or an appropriate designation may be used for metric ton (1000 kg).

This simple means of designating units conflicts with the SI system, which distinguishes between force and weight. In the SI system, the basic force unit is the newton (n), and the basic unit of mass is the kilogram. The newton is related to the kilogram by Newton's equation $F = m \times a$, where the acceleration of gravity in the SI (and metric) system is 9.8066 m/sec^2. Thus the relationship between the newton force and the kilogram mass is 1 n = 1 kg / 9.8066.

The newton is too small to be practical for CASALM design and analysis. The kilonewton (kn) may be practical. The meganewton (Mn), which is one million newtons, may be more practical. For SI analyses, It is suggested that this CASALM analysis program be run with either kg or Mg (Megagram or metric ton) as both weight (mass) and force units. Then

---

* The user must enter the acceleration of gravity on the Dynamic Simulation Data Screen.

convert the force outputs to a convenient multiple of newtons, using the following relationships:

1 kn = 1 kg x 102
1 kn = 1 Mg x 0.102
1 Mn = 1 Mg x 102

A-3. Entering Data Into the CASALM Program

Figure A-7 shows the main CASALM data input/output screen as it appears at start-up, with no data entered. When the CASALM program starts, input is focused on the Length Unit input cell near the upper left of the screen. That cell then has a dotted-red background, and a blinking cursor appears in that cell.

A particular set of input data will be used here to demonstrate the CASALM program. The demonstration begins with manual entry of some of those data. The complete set of default input data may be selected at any time by clicking on the ***Use Demo Data*** button near the bottom right of the screen or by pressing ***Alt-U***.

A-3.1 Designating Units

As an example of data input, place the data-input focus on the cell to the right of the label Length Unit, type ***ft*** and hit ***Enter***. The program accepts this input, and ft automatically appears beside all appropriate data input and display cells.

The data input focus then changes to the cell beside Force-Weight Un. (unit). Here type ***kip*** The data input focus jumps to the Water Depth data cell, near the upper left corner of the screen, and lb appears in all appropriate cells.

Any other consistent set of length and force-weight units could be entered, as discussed above.

A-3.2 Describing CASALM Components

The properties of the various components of the CASALM system are input on the left side of the screen. If you have entered unit designations as described above, the data input focus is now on the cell following Water Depth, as indicated by a dotted-red background.

Type ***10000*** in that cell (and hit *Return*). The background of that cell changes back to white, indicating that the data has been accepted. The background of the cell immediately beneath it, Riser Length, changes to dotted-red, indicating that it is now the data input focus.

Don't enter data with commas. For example, the program will not recognize 10,000 as a valid entry.

To continue with the example, enter ***9456*** in the Riser Length cell. The program will not recognize the case in which riser length equals zero, even though this may appear to be a means of calculating a CALM. If riser length is very close to water depth, the program may have difficulty converging on answers.

Type ***3800*** in the Riser Strength cell. Numbers can be entered in engineering notation. For example, this number could alternatively be entered as ***38e2*** for 38×10^2.

A-3.3 Optional Data Need Not be Entered

Certain input data are required to properly run the program, and other input data are optional. On the data entry screen, the captions for optional data are given in *italics*.

For example, Riser Length and Riser Strength are required. *Riser Wt/Lgth* (riser weight per unit length) and *Riser Stiffness* are optional. To skip entering any data for *Riser Wt/Lgth*, simply hit ***Enter*** , ***Down Arrow***, or ***Tab*** while focus is on that cell.

If riser weight per unit length is not entered, the program assumes that the riser is neutrally buoyant, but **NA** (not applicable) appears in that data cell after the data check. The CASALM program uses the value of riser weight only to determine the difference between tensions at the top and bottom of the riser. The program does not treat the CASALM riser as a catenary. Instead it assumes that the riser remains straight. This causes very little error in practical CASALM system calculations.

If riser stiffness is not entered, infinite stiffness is assumed, and **NA** appears in that data cell. Then the riser length remains constant and does not stretch due to tension.

It is not necessary to enter *Junction Weight*. However, one of the features of the CASALM system is the ability to concentrate supplementary weight at the junction instead of distributing it as sinkers among the various anchor legs.

All weights and unit weights entered in to the program should be expressed as weight in water, accounting for the weight of the displaced water. Thus for example, the weight of steel, 490 lb/ft^2, should be adjusted for the weight of displaced sea water, 64 lb/ft^2, so that its weight in water is 426 lb/ft^2. Accordingly the total weight in air of any solid steel object should be multiplied by 0.87 to convert to the weight in water.

To continue with this example, enter ***0.004*** in the *Riser Wt/Lgth* cell, ***82000*** in the *Riser Stiffness* cell and ***1000*** in the *Junction Weight* cell.

A-3.4 Anchor Leg Data Input

The maximum number of anchor legs which can be analyzed in the CASALM program (as now compiled) is eight. The minimum number of anchor legs is two, provided that they are in line with the applied force, as explained below under Review of Original Anchor Leg Data. For this example, enter ***6***.

The anchor legs are equally spaced around the junction point at the center of the mooring. Thus the program automatically calculates the angle between legs, which for this example case is 60°. It is necessary to define the angle between these legs and the direction from which the force is applied. The First Leg Angle is defined as that angle between the force origin direction and the closest anchor leg. A negative angle may be specified if appropriate. For this example, enter a First Leg Angle of ***0***, meaning that the force is applied in line with an anchor leg.

The program requires data for at least one anchor leg segment, but it does not require that data be entered for all three segments. Defining a unit weight for a particular segment designates that it exists. Each such defined-weight segment must also have a defined length and a defined strength. But if a unit weight is not defined for a segment, the program ignores that segment, even though other data are input for it.

The component unit weights account for buoyancy in water. If an anchor leg segment is neutrally buoyant, designate its unit weight as ***0*** to indicate to the program that it exists. Otherwise the program will ignore its existence and display **NA** in that cell. As noted above, it is not necessary to define a unit weight for the riser.

Figure A-8 shows the Main Screen with all of the example CASALM system data entered. To follow this example, you may continue to enter these data. Or you may elect to have the program enter these default data by typing ***Alt-U*** or clicking on ***Use Default Data***.

A-4. Data Checks and Data Revision

Any of the following acts will signal the program that data input is completed: Hitting ***Enter***, ***Tab***, or ***Down Arrow*** while data focus is on *Lwr. 3 Stiffness*; hitting ***Page-Down*** while data focus in on any data input cell; or by moving the cursor to either the Buoy Deflection or Buoy Force cell, entering data, and then hitting ***Enter***.

A-4.1 Program Performs Input Data Checks

After all data describing the CASALM system are entered, the program checks the data for completeness and correctness. If an error is detected, the program displays an appropriate message. These messages were discussed above.

A-4.1 Adjusting Catenary Leg Pretension and Junction Elevation

After the data is checked and accepted, the resulting Leg Pretension is shown near the bottom right of the screen. In this example case that value is **100 kip**. If a particular anchor leg pretension value is desired, revise the various pertinent input values to obtain that value.

The (junction) Jnctn Elevation appears in the middle of the right column after the input data are checked. If a value for riser stiffness was entered, the Jnctn Elevation may be greater than Water Depth minus Riser Length. In this example case it is **490 ft**. The junction elevation has changed because the riser has stretched due to the junction weight and the weight of the anchor legs. If a particular Junction Elevation is desired, adjust the Riser Length in order to achieve that elevation.

Until a deflection or force is applied to the buoy, the Max Leg Force is the same as the Leg Pretension. The Max Leg Scope is the length of anchor leg which is lifted of the ground in the most highly loaded leg, and the Min Leg on Gnd is the length remaining on the ground in that leg. For this example case, for the undeflected position, the Max Leg Scope is **2601 ft** and the Min Leg on Gnd is **449 ft**. Note that the sum of these two lengths is greater than the total untensioned lengths of the anchor leg segments.

A-4.2 Viewing Original Anchor Leg Configuration

A complete description of the original anchor leg configuration, with no buoy deflection, can be viewed by clicking on the ***Review Original Leg*** button or by typing ***Alt-O***. This data display screen is shown in Figure A-9. All of the legs are equally tensioned in this undeflected buoy condition.

The Horizontal Deflection from Zero-Load Position, **347 ft**, is the deflection of the top of an individual anchor leg from its undeflected position (hanging straight down) to its point of connection with the junction.

The **100 kip** Top Pretension is that tension at the top of the catenary anchor leg which produced this Horizontal Deflection. It is the highest tension in the anchor leg, unless negative values for sinker weight and segment unit weight have been entered. The CASALM may not produce correct answers if a negative value is entered for the weight per unit length of a catenary segment or sinker weight.

The Top Angle is the angle at the top of the anchor leg from the horizontal. A top angle of 90° would indicate that the anchor leg is hanging straight down. In this example case the Top Angle is **36.6 degrees**. The **81 kip** Horizontal Force and the **60 kip** Top Vertical Force could be calculated from the Top Pretension and the Top Angle, but all values are displayed for convenience.

The Upper Tensioned Length, **201 ft**, is the length of the upper segment under the applied pretension. If a stiffness was not defined for that segment, then this length will be the same as the segment length entered on the main data input screen.

The Middle and Lower Maximum Tensions are the maximum tensions in the middle and the lower anchor leg segments respectively. These tensions may be much less than the maximum tension in the upper segment, because the upper segment is tensioned by its own weight as well as by the weights of the sinkers and segments beneath it. In this example, the upper segment is heavy anchor chain, while the middle segment is light weight synthetic rope.

The Middle Maximum Tension for this example case is **83 kip**. The Middle Tensioned Length is **2356 ft**. Note that this is 56 ft longer than the untensioned length of this polyester segment. The Lower Maximum Tension for this example case is **81 kip**. The Lower Tensioned Length is **45 ft** indicating that only a portion of this ground leg is lifted.

Conditions and Notes indicates **Low Seg Tangent**, which means that the lower segment is tangent to the ground. Other conditions which might be displayed are discussed in section 6.3.

One of the special properties of a catenary system is that the horizontal force is the same at all points along the catenary. Thus the horizontal force at the top of the catenary, at any point along the catenary, and also at the point where the catenary is tangent to the sea floor is **81 kip**. In the anchor tangent and uplift cases this horizontal force is also applied to the anchor. If sea-floor friction is ignored, that horizontal force is applied to the anchor in all cases.

The Total Tensioned Scope is the total length of all segments in an anchor leg that are lifted off the sea floor. The Origin to Gnd. or Anchor is the horizontal distance from the center of the mooring (in the undeflected position) to either the point at which the anchor leg is tangent with the sea floor (or lifts up on a sinker on the sea floor) or the anchor (in the case of anchor uplift).

The Anchor Uplift Angle is measured from the horizontal. The Anchor Uplift Force could be calculated from the horizontal force and this angle, but it is displayed here because it may be an important criterion in judging the suitability of a mooring system design. In this example case, these values are zero, because the catenary is tangent with the sea floor beyond the anchor point.

The Upper and Lower Sinker Elevations are the respective elevations of the two sinkers above the sea floor. From these anchor leg data, together with the junction elevation and the origin to ground distance, the original anchor leg configuration can be sketched.

The values displayed on this "Original Anchor Leg Parameters" screen remain unchanged when force or deflection is applied to the buoy. Thus these parameters of the anchor leg in the undeflected position can be reviewed at any time by striking ***Alt-O***.

A-4.3 Revising Input Data

With data input focus on either the Buoy Deflection or Buoy Force cell, you may return to the Water Depth data entry cell at the top left of the screen by striking ***Page Up***. You may then scroll down that CASALM system parameter column or use the mouse to move the cursor to the cell in which you wish to revise data.

You can revise input data at any time. Move the cursor to that particular data input cell, click the left mouse button to give focus to that cell, and then enter data. When you click on or scroll to a data entry cell, its background will change to dotted-red. As soon as you begin entering data, that background will change to orange. When revising data, the program does not delete or overwrite existing data in a cell, so you will need to manually delete the previous data. As soon as you hit the enter key, the revised data is accepted, and the data entry focus jumps to the next cell.

The CASALM program does not check the data entry each time that you revise a data input cell. It only checks data when one of the events described at the beginning of this section takes place.

The CASALM program does not automatically recalculate the Deflection-Force relationship after you revise input data, even after the input focus returns to the Buoy Deflection data entry cell. Instead, you must again hit ***Enter*** with the input focus on either the Buoy Deflection or the Buoy Force cell in order to recalculate the system forces and deflections.

A-5. Calculating Force-Deflection Results

A-5.1 Calculating Force For Given Deflection

After the program checks the data, input focus is set on the Buoy Deflection cell at the upper right of the screen. You may toggle between this data entry cell and the Buoy Force cell by using the ***Up Arrow*** or ***Down Arrow*** key.

When focus is on the Buoy Deflection cell, that cell has a red-dotted background. As soon as you begin entering data, the cell background changes to orange. When you hit the ***Enter*** key, calculation begins.

While the program is performing calculations, the cursor changes to a rotation double-arrow / hour glass. The program beeps at the completion of calculation, the cursor bar or arrow returns, and the cell which has data-entry focus returns to a red-dotted background.

As an example, enter ***3000*** as Buoy Deflection. After calculating, the program displays **511 kip** as the Buoy Force. The screen then appears as in Figure A-10. A horizontal force of 511 kip on the buoy will cause it to deflect 2000 ft, or 20% of the water depth.

A-5.2 Other Main Screen Output Data

Various other output data are displayed on the right side of the Main Data Screen.

Riser Angle is measured from the vertical. In this example case it is **18.2 degrees**.

The Max Riser Force in this example is **1653 kip**. This is about 40% percent of the input strength of the riser. If a positive riser weight per unit length is entered, this force is at the top, but if a negative riser weight per unit length (buoyant condition) is entered, the maximum riser force is at the bottom of the riser.

The Jnctn Elevation in this example is **842 ft**. This indicates that the junction has lifted 352 ft above its original elevation of 490 ft.

The Max Leg Force in this example case is **881 kip**. This is about 33% of the input strength of any of the segments. The Max Leg Scope is the length of anchor leg which has been lifted off the ground. In this case, that value is **3132 ft**.

The Min Leg on Gnd in this case is lift Force is **0** indicating that there is uplift on the anchor of the most highly loaded anchor led. The MaxUplift Force is **130 kip**, and the Max Uplift Angle is **8.9 degrees**. These values are for the most highly loaded anchor leg.

A-5.3 Calculating Deflection For Given Force

Now hit ***Up Arrow*** or ***Down Arrow*** (or use the mouse) to move the data-input focus to the Buoy Force cell, and that cell turns dotted-red. Hit ***Enter*** to accept the present value ***511*** as input.

The program will generally take longer to calculate buoy force than buoy deflection. After the program generates a solution, it displays the data. Figure A-11 shows the result of this example calculation, in which Buoy Deflection is **3019 ft**. This is in very good agreement with the previously calculated value. In general, as much as a 1% variation from the reciprocal calculation answer is not unreasonable, considering the complexities of the calculations.

The reciprocal answers do not agree precisely with each other because the CASALM program uses different methods to calculate Buoy Force and Buoy Deflection. Thus checking an answer against its reciprocal is a way of verifying the answer. But the two answers may differ by several percent due to various factors, such as round-off errors and the permitted

tolerances in various convergence routines. In the rare case where the program may fail to converge to an answer, the reciprocal answer can be found by trial and error.

Please use the ***Up Arrow*** to return to the Buoy Deflection cell and enter the value ***3000*** again. This will recalculate the basic example case used here, in order to correspond with the following explanations.

A-6. RESULTS FOR VIDUAL ANCHOR LEGS

The Main Screen displays only some output for the most highly loaded anchor leg. It is sometimes helpful to review the forces in each of the individual anchor legs, for example, either to check if other legs are applying uplift on anchors or to review forces in anchor leg segments.

A-6.1 Displaying Anchor Leg Configuration

The data for all anchor legs can be viewed by typing ***Alt-A*** or by clicking on the ***Summary All Legs*** button. Figure A-12 shows those data for this example case.

To later return from this Anchor Leg Data Display Screen, click the cursor on the minimize box in its upper right-hand corner, or click the cursor anywhere on that portion of the Main Screen which is visible above it. If ick on the close screen box in the upper left-hand corner, these values will be lost, a nchor leg data screen will display **NA** until this or another case is recalculated.

A-6.2 Orientation of Anchor Legs

The anchor legs are distributed at equal angles around the mooring point. The orientation of the anchor legs is defined by the First Leg Angle as entered on the main data-entry screen. This First Leg Angle is the angle between the direction from which the force is applied and the direction of the anchor leg which is closest to that force direction.

In the Catenary Anchor Legs Screen, the Vector Angle defines the angle of each leg with relation to this force origin direction. In this example, the First Leg Angle entry was *0*, meaning that the force was in line with an anchor leg. Thus in this example case, in which there are six legs, the other legs are distributed at angles of 60°, 120°, etc.

If the force is not applied in line with an anchor leg, enter the angle between the direction from which the force is applied and the anchor leg which is closest to that force direction. The program makes no distinction between clockwise and counter clockwise directions. But if the first leg angle is measured clockwise from that direction of force application, then the other anchor leg angles should be interpreted as clockwise, and vice versa.

The program will run with as few as two anchor legs, if they are in line with the force application direction. The program assumes that each anchor leg remains in its original plane. Thus it cannot correctly handle the case of two anchor legs which are not essentially in line with the force application direction.

With three anchor legs, it is important to define the force origin direction in relation to that leg which is closest to that direction. The force-deflection calculation results can be significantly different when the force origin direction is in line with one leg than when the force origin direction is at 60° to a leg (midway between two legs).

A CASALM with four anchor legs is not as sensitive to the relationship between the anchor legs and the force origin direction. However for critical analyses, the cases of 0°and 45° should both be checked. Systems with six or more anchor legs are not very sensitive to the direction of force application.

A-6.3 Individual Anchor Leg Data

The Horizontal Deflection of each anchor leg is defined as its offset from its undeflected position, in which that particular leg hangs straight down with no applied horizontal force. Anchor Leg 1, the most highly loaded leg, is deflected the most, **802** (ft). This should not be compared directly with the original deflection (395 ft) for this leg. This value now pertains to the catenary top deflection from its slack position at the present junction elevation, which is much higher than the original elevation. The elevation of the top of all anchor legs changes with the junction elevation, and this changes the apparent slack position of each leg.

Note that much of the buoy deflection is accommodated by tilting and stretching of the riser. In this case, most of the 3000 ft buoy deflection was accommodated by riser tilt, and only about 140 ft of deflection was provided by offset of the junction point.

The Horizontal Force, Top Tension, Top Vertical Force and Top Angle are as described above for the Initial Anchor Leg Parameters Section. Also, the Middle Seg. Tension and the Lower Seg. Tension are as described above.

The Conditions note applies to the contact of the catenary on the sea floor for each leg. **Low Seg** would indicates that the first (lower) segment is tangent to the sea floor at some point. **Mid Seg** would indicate that the middle segment of that leg is tangent to the sea floor, etc. **Sinker 1** would indicate that the lower (first) sinker remains on the sea floor and that the adjacent (middle) anchor leg is tangent to the sea floor at that point or applies uplift to that sinker, etc. The **Anchor** condition indicates that the anchor leg is tangent to or applies uplift on the anchor.

The Total Scope is the total length of anchor leg that is lifted off the sea floor. The Origin to Gnd./Anchor is the horizontal distance from the center of the mooring (in the

unloaded position) to either the point at which the anchor leg is tangent with the sea floor (or lifts up on a sinker on the sea floor) or to the anchor (in the case of anchor uplift).

In this example case, uplift is applied to all anchors. The meanings of the Anchor Uplift Angle and the Anchor Uplift Force are self evident. Recall that in the original position, the lower segment was tangent to the ground in all legs.

A-7. VIEWING FORCE-DEFLECTION TABLE AND GRAPH

The CASALM Analysis Computer Program can display and print a table or graph of the forces corresponding to a range of deflection values.

A-7.1 Displaying the Force-Deflection Screen

To access the Force-Deflection data screen, click the cursor on the ***Plot Force Data*** button or press ***Alt-F***. When this screen is first displayed, the data input focus is on the Deflection Increment cell. This screen is shown in Figure A-13.

You can return to the main data display screen at any time by clicking on ***Return*** or by typing ***Alt-R***. Alternatively, you can proceed directly to calculating and viewing the Deflection vs. Energy characteristics of the CASALM system (discussed in Section 8) under analysis by clicking on ***Energy***.

As an example calculation, enter ***100*** for deflection increment. The data input focus changes to Maximum Deflection. Here enter ***3300***. This calculation of 33 steps may take some time.

A-7.2 The Force-Deflection Data Table

After entering the deflection data on the Force-Deflection Screen, click the cursor on the ***Display Data*** button. The program will begin calculating a table of deflection vs. force for the input data. During calculations, the deflection step which is being calculated is displayed in a yellow box in the center of the screen..

After results for all deflections are calculated, the table of Buoy Deflection vs. Buoy Force is displayed, as shown in Figure A-14. The anchor leg and anchor point data in this table are for the most highly loaded anchor leg. Note that the leg lifts completely off the ground and begins applying uplift on the anchor at a buoy deflection of between 2,100 and 2.200 ft.

That table can be sent to a printer by clicking on ***Print Data***. Figure A-15 is that print-out for the present example. The printed table provides a record of all the CASALM design parameters used in the analysis.

A-7.3 The Force-Deflection Data Graph

A graph of this data can be displayed by clicking on ***Show Graph***. Figure A-16 shows an example of that graph screen.

For each value of deflection, the graph shows the applied horizontal force to the buoy, the maximum force in the riser, the maximum force in the most highly loaded anchor leg, and the uplift on the anchor in that leg.

The graph plot can be printed out by clicking on ***Plot Graph***. The printed graph is shown here as Figure A-17. These data are the same as for the screen display.

The date and time at which the calculation was performed is given on each printed table and graph, so that the various printed data for the same analysis case can be associated later. This is important because the printed graph does not list the CASALM system parameters.

A-8. The Deflection-Mooring Energy Screen

Mooring energy is the total energy stored in the CASALM system up to any defined horizontal deflection of the buoy. Thus it is the area under the force-deflection curve.

The Deflection-Energy characteristic of the CASALM, and of any single point mooring system, is an important design considerations. In general, a mooring system which stores a greater amount of energy at relatively small deflections will experience lower peak dynamic peak mooring loads. If the mooring absorbs little energy at small deflections and then becomes very stiff at large deflections, the moving vessel can inflict very high mooring forces.

A-8.1 Displaying the Deflection-Mooring Energy Screen

From the Main Screen, click the cursor on the ***Plot Energy Data*** button or enter ***Alt-E***. The Deflection-Mooring Energy Screen is similar to the Force-Deflection Screen. This screen is shown in Figure A-18 When this screen is first displayed, the data input focus is on the Deflection Increment cell.

To return to the main data display screen, click on ***Return*** or type ***Alt-R***. Alternatively, you can proceed to the Force-Deflection Data Screen by clicking on ***Force***.

If the Force-Deflection calculation was previously performed and the CASALM system description has not changed, then the default values for Deflection Increment and Maximum Deflection shown on the Deflection-Mooring Energy Screen are the same as used in that earlier calculation. If you do not change these default input data, then the energy graph and table will be displayed without recalculating data.

If the default input data does not appear or it has been altered, enter ***100*** for Deflection Increment and ***3300*** for Maximum Deflection in order to continue with the example.

A-8.2 Calculation Mooring Energy Table

Click on the ***Display Data*** button to bring up the Mooring Energy Data Table. This table shows Horizontal Deflection, Horizontal Buoy Force, Delta Energy, and Potential Energy. That table for the example case is shown in A-19. The data can be printed out, as shown in Figure A-20.

The Delta Energy is the amount of energy stored in the mooring system from the previous deflection to the present (row designation) deflection calculation. It can be used to interpolate between total energies at defined deflections. The Potential Energy is the sum of these delta energies at the particular deflection.

A-8.3 Displaying the Mooring Energy Graph

A graph of Deflection vs. Mooring Energy is shown when the ***Show Graph*** button is clicked. Figure A-21 is that graph for the example case. The graph can be printed as shown in Figure A-22.

This Deflection-Mooring Energy graph is essentially an integration of the area under the Force-Deflection graph. It gives a visual representation of the effectiveness of the mooring system in storing energy.

The Deflection- Mooring Energy Graph and Table can be printed by the steps described above for the Force-Deflection Graph and Table.

A-9. Mooring System Dynamic Simulation

This feature of the CASALM mooring analysis simulates the action of the moored vessel being pushed back on the mooring system by a change in applied forces, thus producing dynamic mooring loads. It is accessed by clicking on the ***Calculate Dynamics*** button on the Main Data Screen.

A-9.1 Principals of Dynamic Simulation

Figure A-23 illustrates the principals used in this dynamic simulation. A moored vessel starts at an Initial Deflection relative to the mooring center with an Initial Velocity. In response to an Applied Force the Vessel Mass accelerates. But the acceleration of the vessel is retarded by Drag in proportion to the square of its velocity. The vessel motion is also retarded by the restoring force of the mooring.

The Initial Deflection is the point from which the simulation begins. This Initial Deflection is referenced from the center of the mooring system, at which there is no applied force to the buoy. The Initial Deflection can be a negative value, indicating that the vessel motion begins at a position ahead of the no-force position. The vessel can be given an Initial Velocity and an Initial Acceleration at this initial position, but these values are better left as zero unless good estimates can be made for them.

A-9.2 Increment and Limit Data for Dynamic Simulation

Click on the ***Dynamic Simulation*** button on the Main Screen to bring up the Dynamic Simulation Screen. Figure A-24 shows this screen with example input data.

If a Force-Deflection or Deflection-Mooring Energy calculation has been carried out, and the mooring system parameters have not been changed, then default values for Deflection Increment and Maximum Deflection are displayed when this Dynamic Simulation Screen is first displayed. In any case, the data entry focus is on the Deflection Increment cell. The default values can be accepted by simply hitting ***Enter***.

The Deflection Increment establishes the mooring deflection increment between successive calculations. This increment can influence the calculated results. But if the increment is too small, the calculations will take a long time. Because this simulation is only an approximation of the true mooring system dynamics, any enhancement in accuracy achieved by using a very small increment may be illusionary.

It is recommended that the Deflection Increment be chosen so that at least ten increments are calculated before the dynamic simulation ends. The same increment should be used when performing dynamic simulations for alternate mooring systems which are to be compared.

The Maximum Deflection is a calculation cut-off point which may optionally be used to prevent the program from attempting to calculate at extreme deflections which are unreasonable or pose calculation problems. Once chosen, this input value may be increased during program calculation.

A-9.4 Other Input Data for Dynamic Simulation

The other default values used in this example can be called to the screen by clicking on ***Use Demo Data***. In this example, the initial values are set to zero; that is the vessel begins at the center of the mooring with no velocity.

The Vessel Weight is preferably its total displacement in water, entered as weight instead of mass. If there is no initial deflection and no initial velocity, this weight value does not have a major effect on the maximum forces which are calculated by the Dynamic Simulation. Thus any extra precision, such as accounting for added mass is not important, as long as the same

Vessel Weight is used for all comparable calculations. For the example given here, enter ***1500000000*** (lbs) (or ***1.5e9***) as weight. This is the approximate mass of the Floating Offshore Base (MOB).

The Gravity Acceleration must be consistent with the weight and length units used throughout the program. In the ft-lb system, the acceleration of gravity is 32.2 ft/sec^2. In the metric and SI systems, the acceleration of gravity is 9.82 m/sec^2

The Applied Force is applied as a constant throughout the dynamic calculation. It is suggested that this be the force exerted on the vessel by a realistic wave drift force and its corresponding wind velocity. Approximate values for the bow-on wave drift force and the bow-on wind drag force may be used here. The calculation is sensitive to this term, but because of the nature of the simulation, extreme precision is not warranted.

For this simulation, enter ***106.6*** (kip) for the Applied Force. This is the approximate bow-on force due to Sea State 3 (2.9 ft significant wave height, 13.5 kt wind) on the MOB.

The Drag Coefficient is used by the program to apply a quadratic drag proportional to the square of the vessel's velocity during each step of the simulation. If the bow-on current force on the vessel is known at a particular velocity, an appropriate drag coefficient can be derived from that data. For the MOB, enter ***13.3*** (kip/ft^2) for this Drag Coefficient.

A-9.5 Performing the Dynamic Simulation

To initiate the dynamic simulation, click on the ***Calculate*** button or enter ***Alt-C***. The details of the Dynamic Simulation are given in an appendix.

For each increment of deflection, the program calculates the acceleration and velocity resulting from the applied force, the mooring restoring force, and the resisting drag. At first both Acceleration and Velocity values are positive. When the restoring force of the mooring exceeds the applied force, the Acceleration values becomes negative, and the values of Velocity begins to decrease.

Figure A-24 shows the Dynamic Simulation Screen during the example calculation. At this point in the calculation, the Max. Deflection was **1300** ft. The Max. Force at this point was **85** kip. The vessel's Acceleration was **-.00017** ft/sec/sec, indicating it was beginning to decelearate at this point. Its Velocity at this point was **1.6** ft/sec, just past the peak velocity.

The dynamic simulation proceeds until the Velocity becomes negative. At this point, the system reaches its maximum deflection, and the vessel begins moving back toward the mooring point. The program estimates the maximum deflection by interpolating between the deflections corresponding to the last positive and first negative values of velocity. It then

calculates the maximum force in the mooring system corresponding to that deflection. These values are then displayed.

For this example case the Maximum Deflection is **2242 ft**, and the corresponding Maximum Force is **237 kip**. This is the horizontal force exerted by the vessel on the mooring at this maximum deflection point. This result is shown in Figure A-25.

When you return to the Main Data Screen (type ***Alt-R*** or click on the ***Return*** command button), the results of the dynamic analysis are shown on that screen. You can then see the corresponding forces in the various mooring components

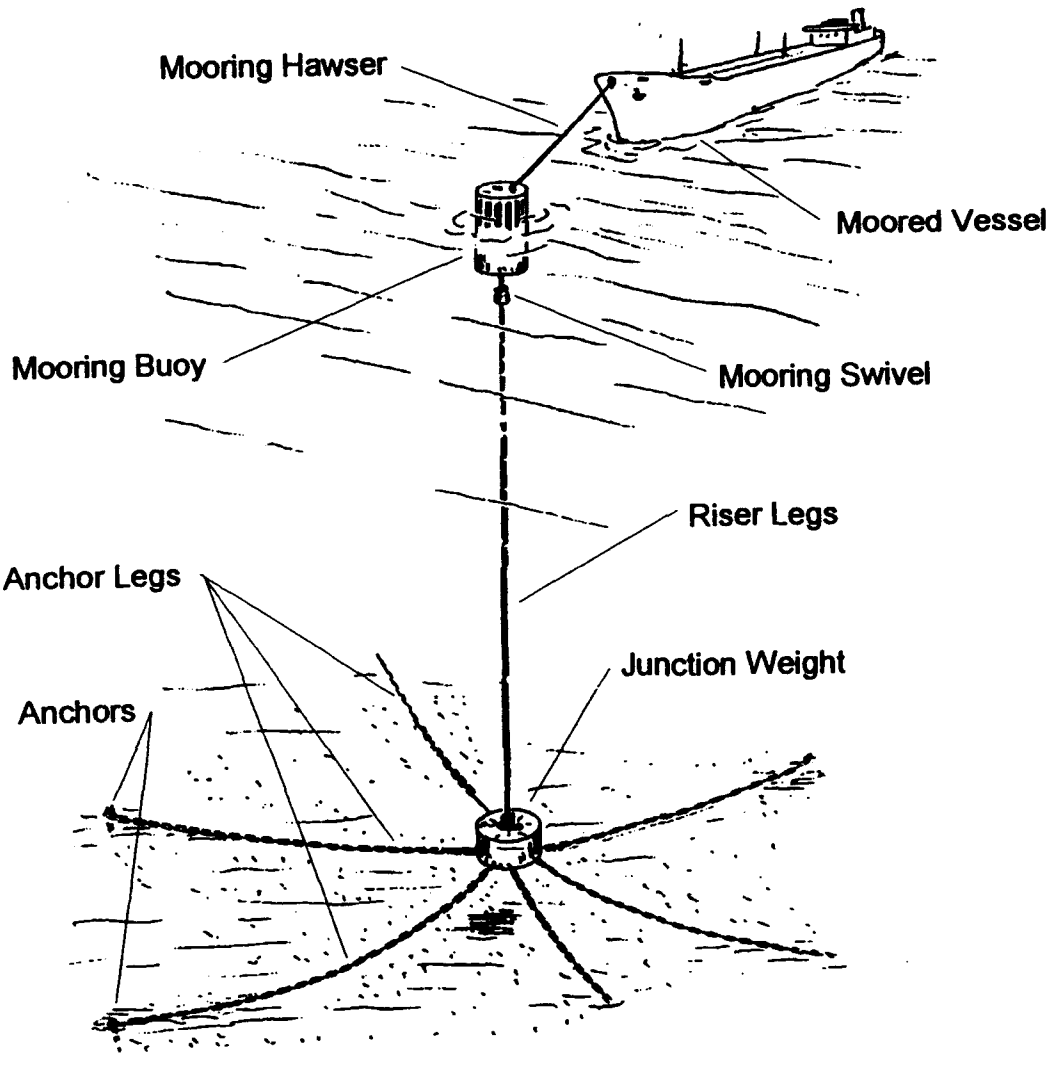

Figure A-1 Arrangement of Catenary and Single Anchor Leg Mooring System

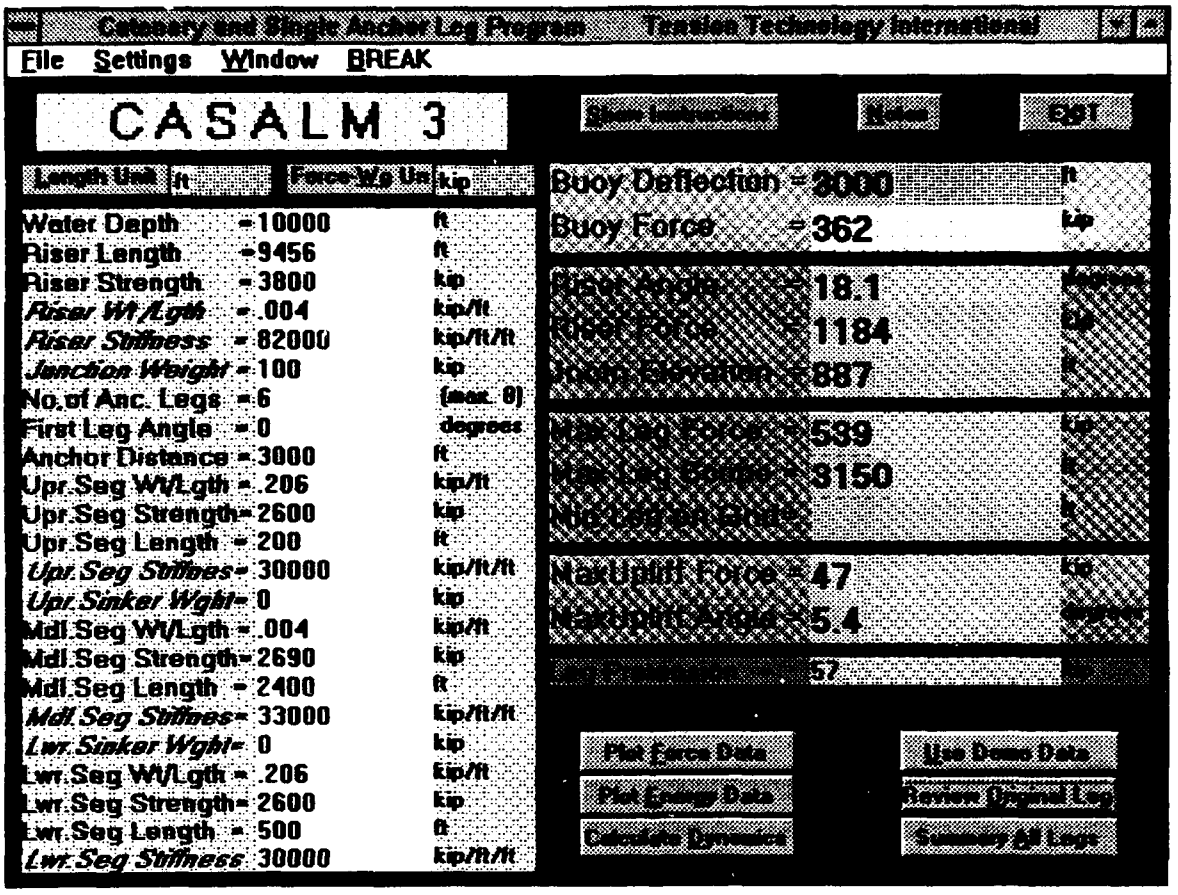

Figure A-2 CASALM-3 Program Main Data Input/Output Screen

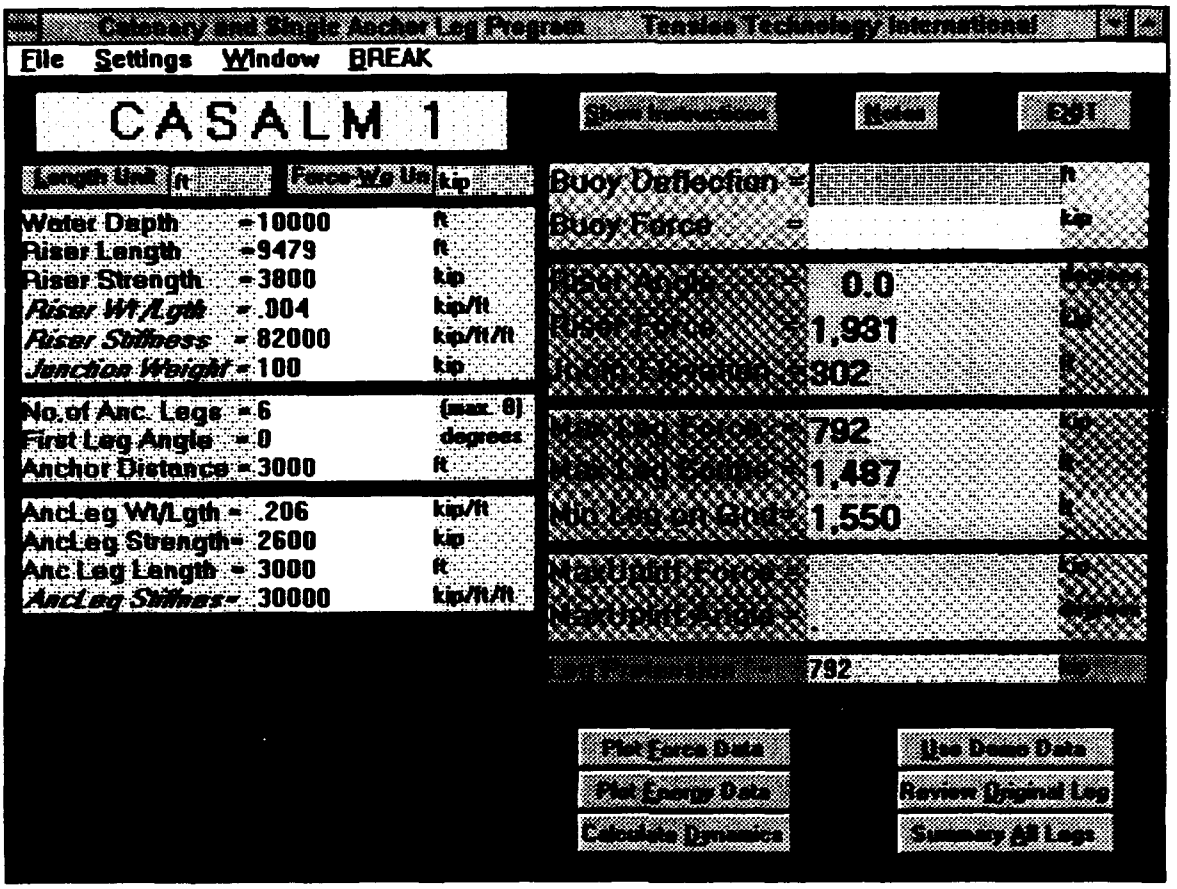

Figure A-3 CASALM-1 Program Main Data Input/Output Screen

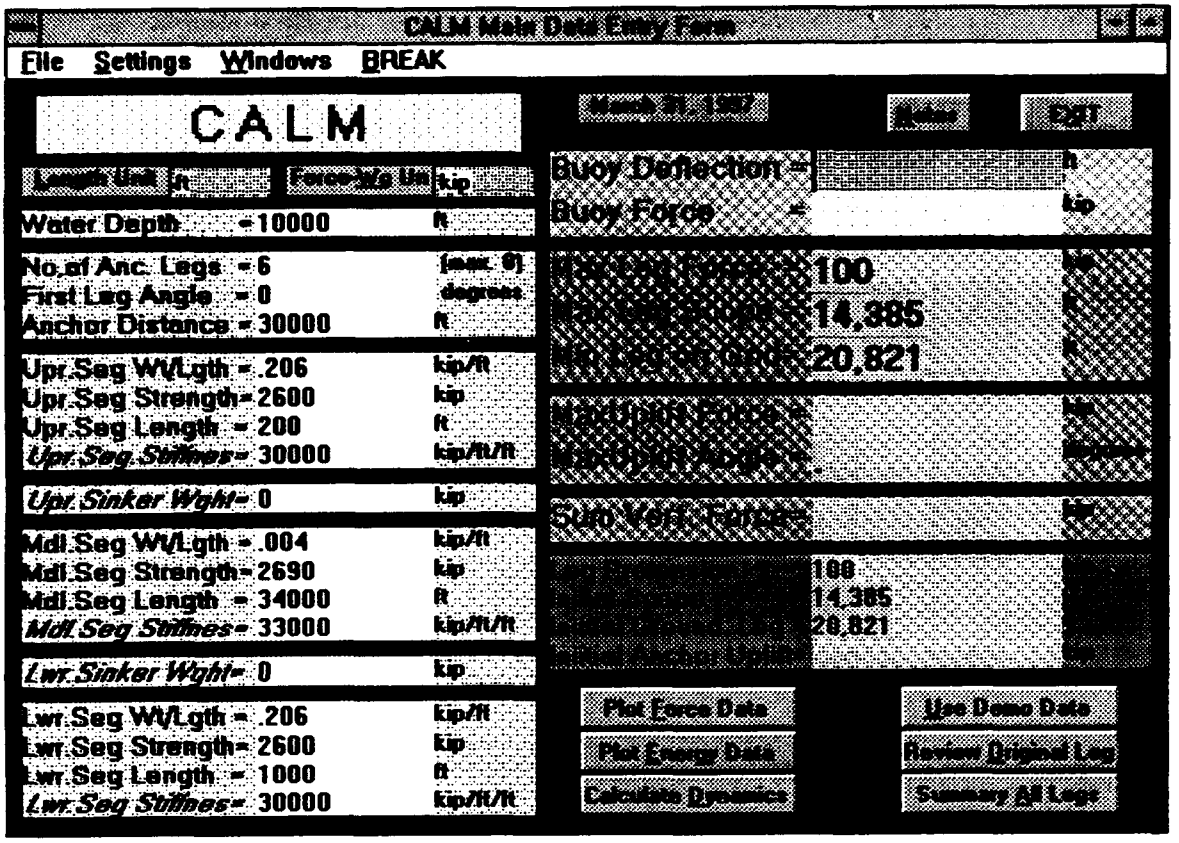

Figure A-4 CALM Program Main Data Input/Output Screen

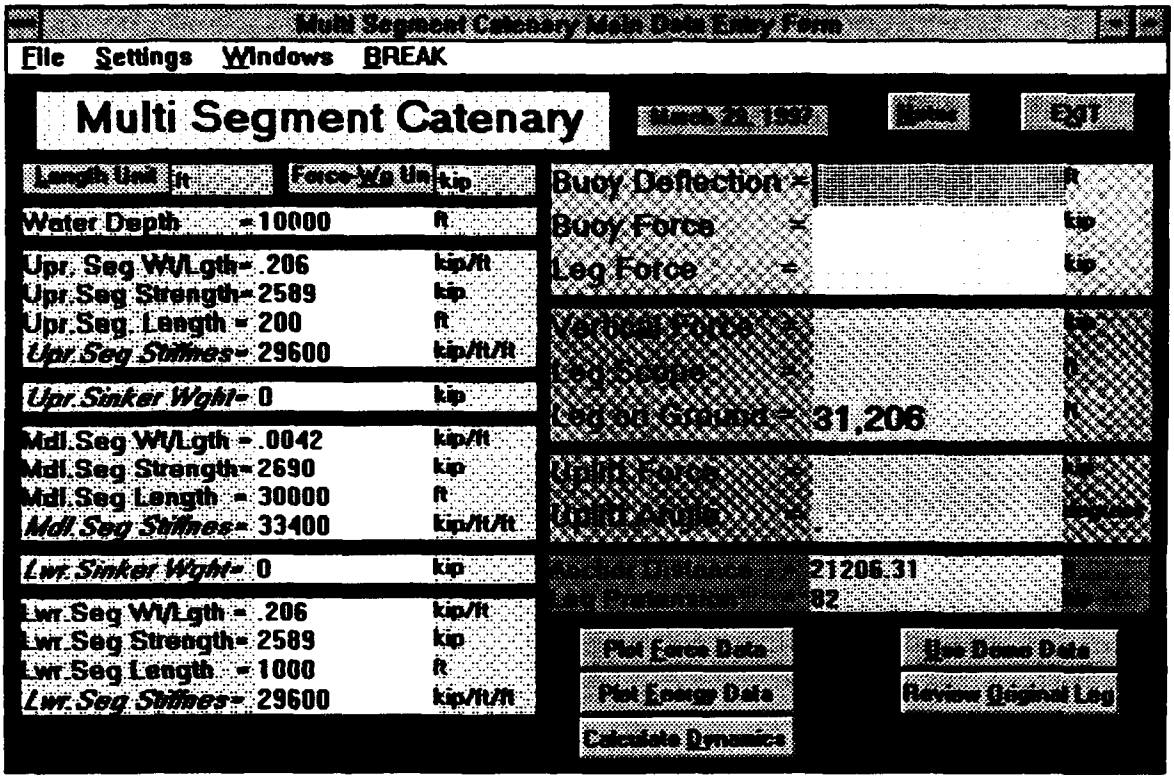

Figure A-5 Catenary Program Main Data Input/Output Screen

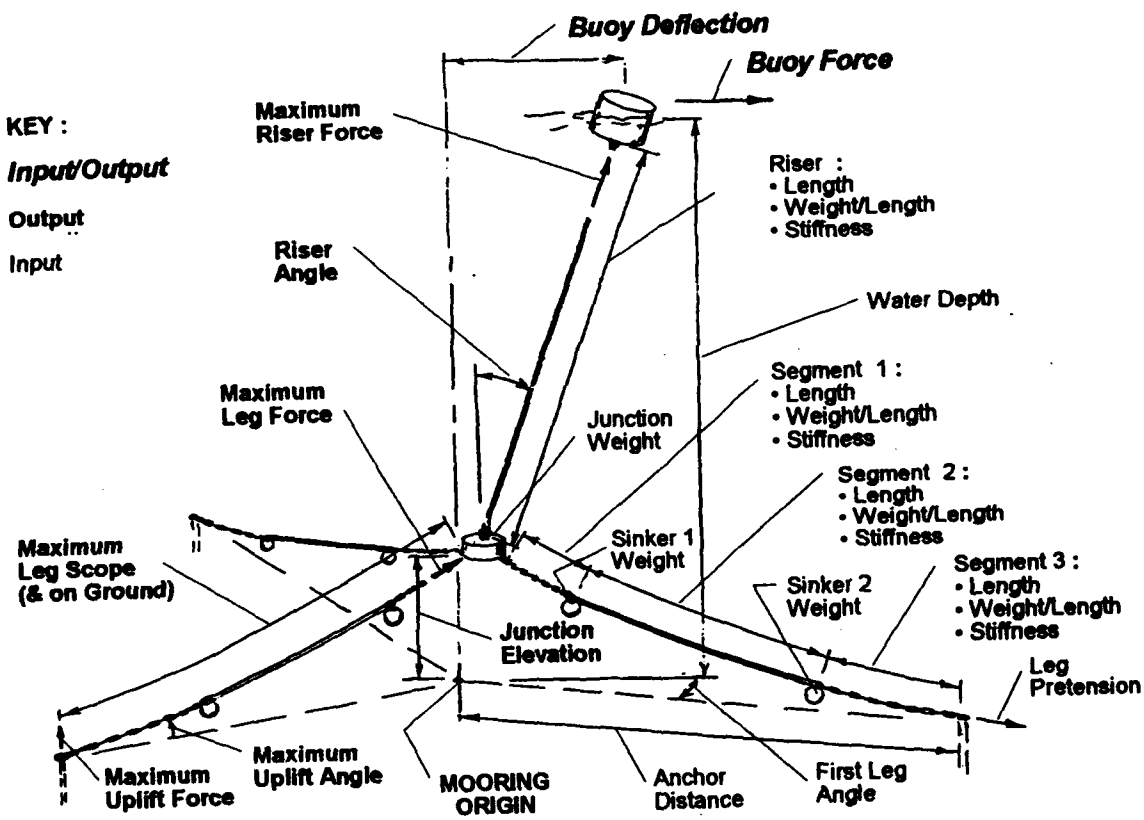

Figure A-6 Input and Output Parameters of CASALM Program

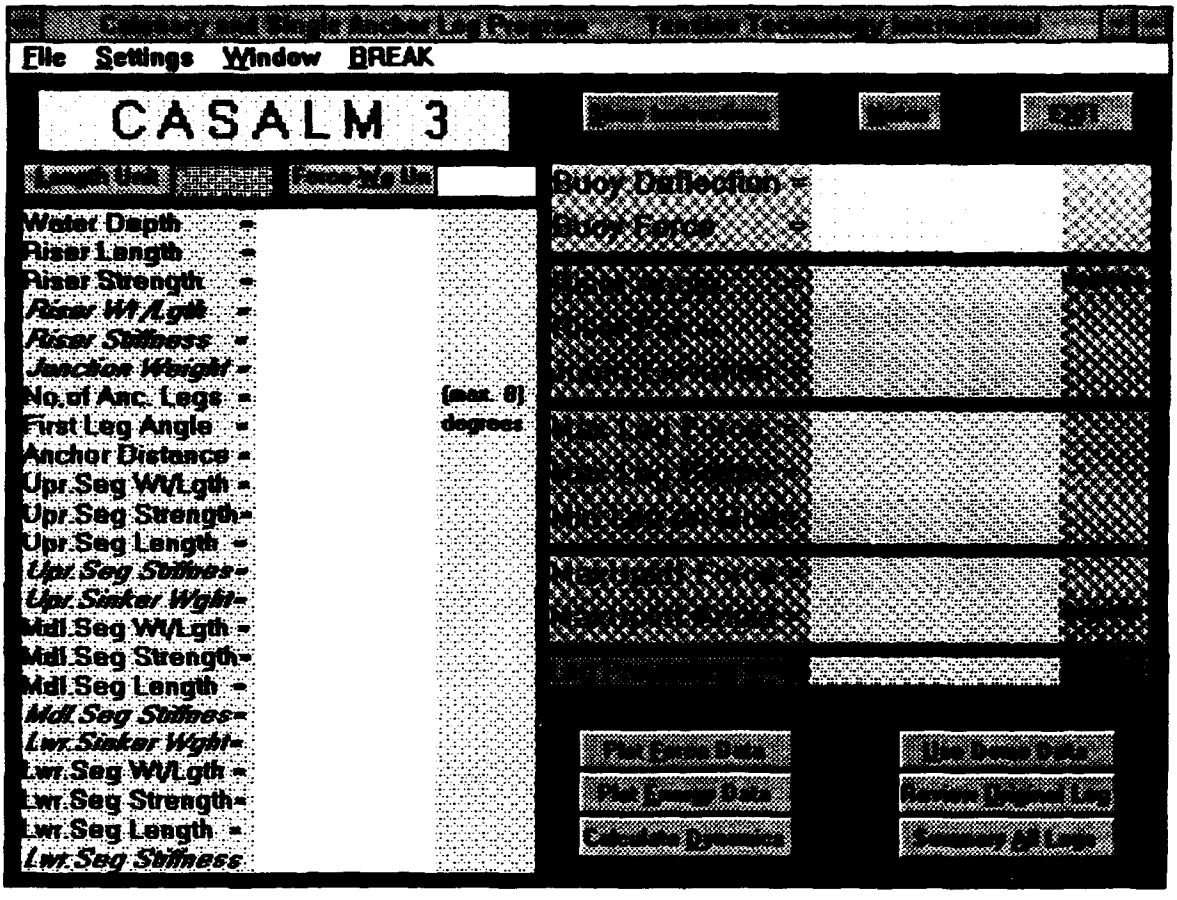

Figure A-7 CASALM Main Screen as it appears at strart-up

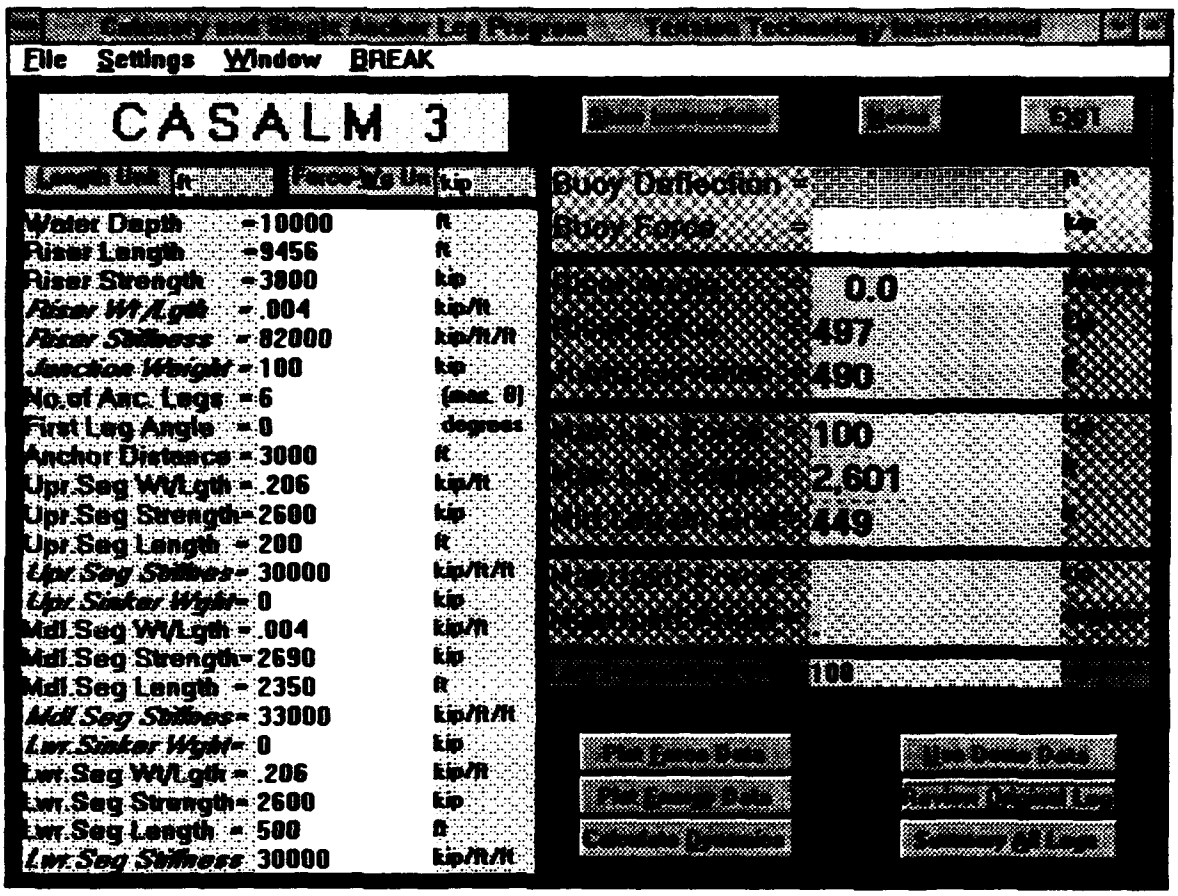

Figure A-8 Main Screen with example data entered

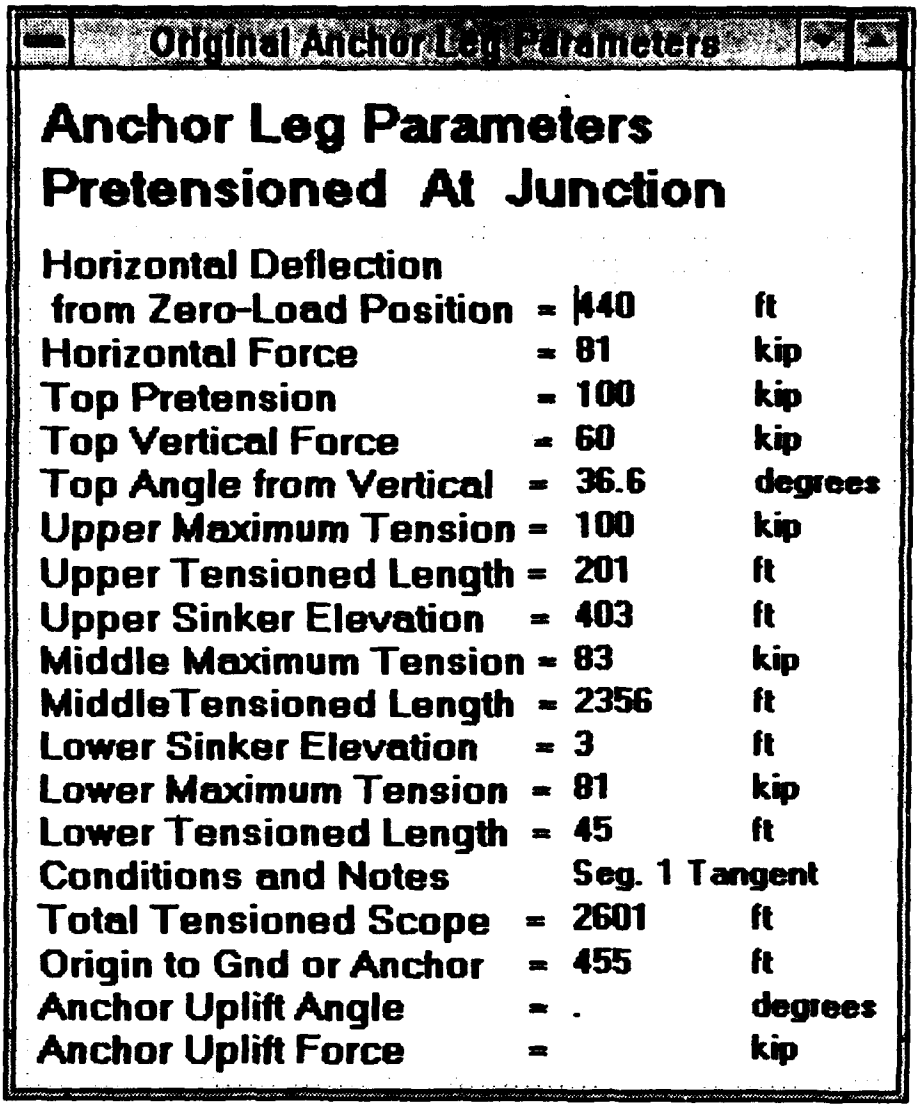

Figure A-9 Original Anchor Leg Data Screen

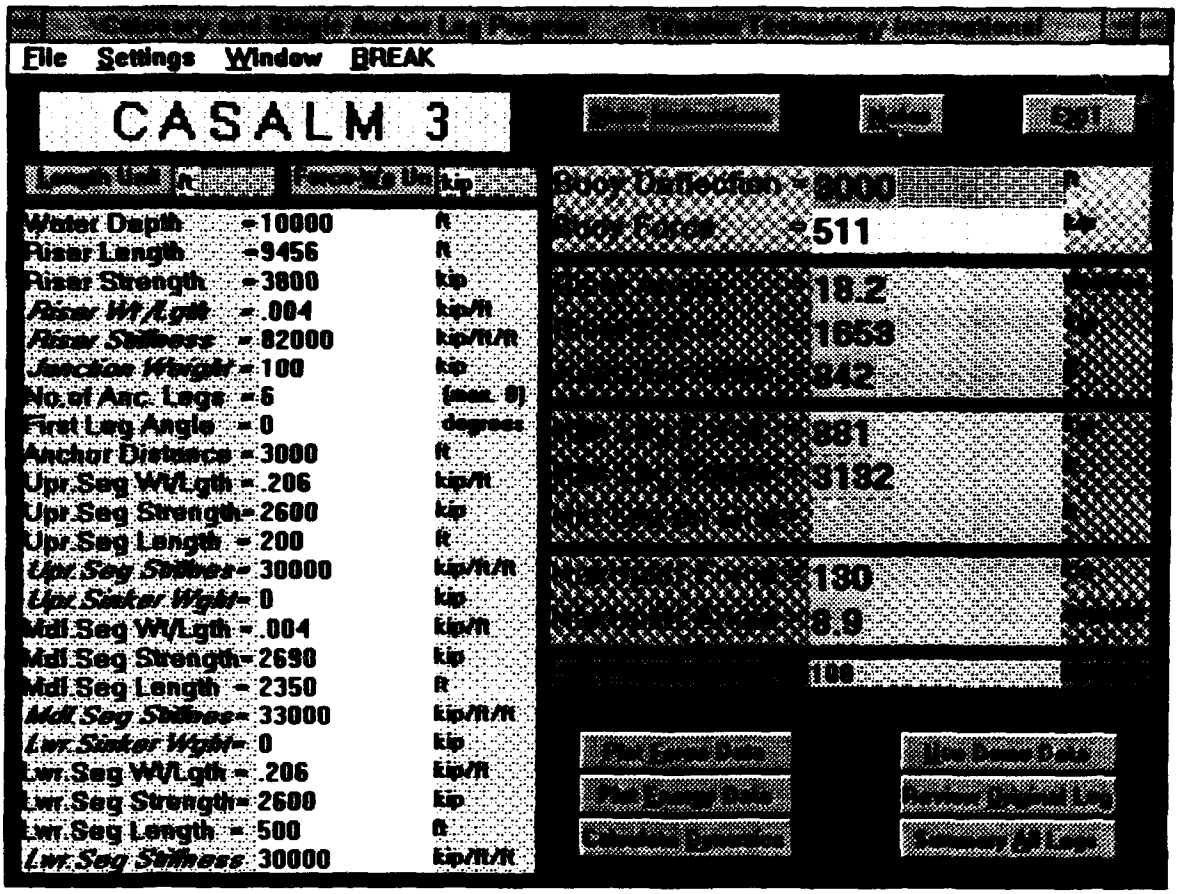

Figure A-10 Main Screen with solution to example Buoy Deflection input

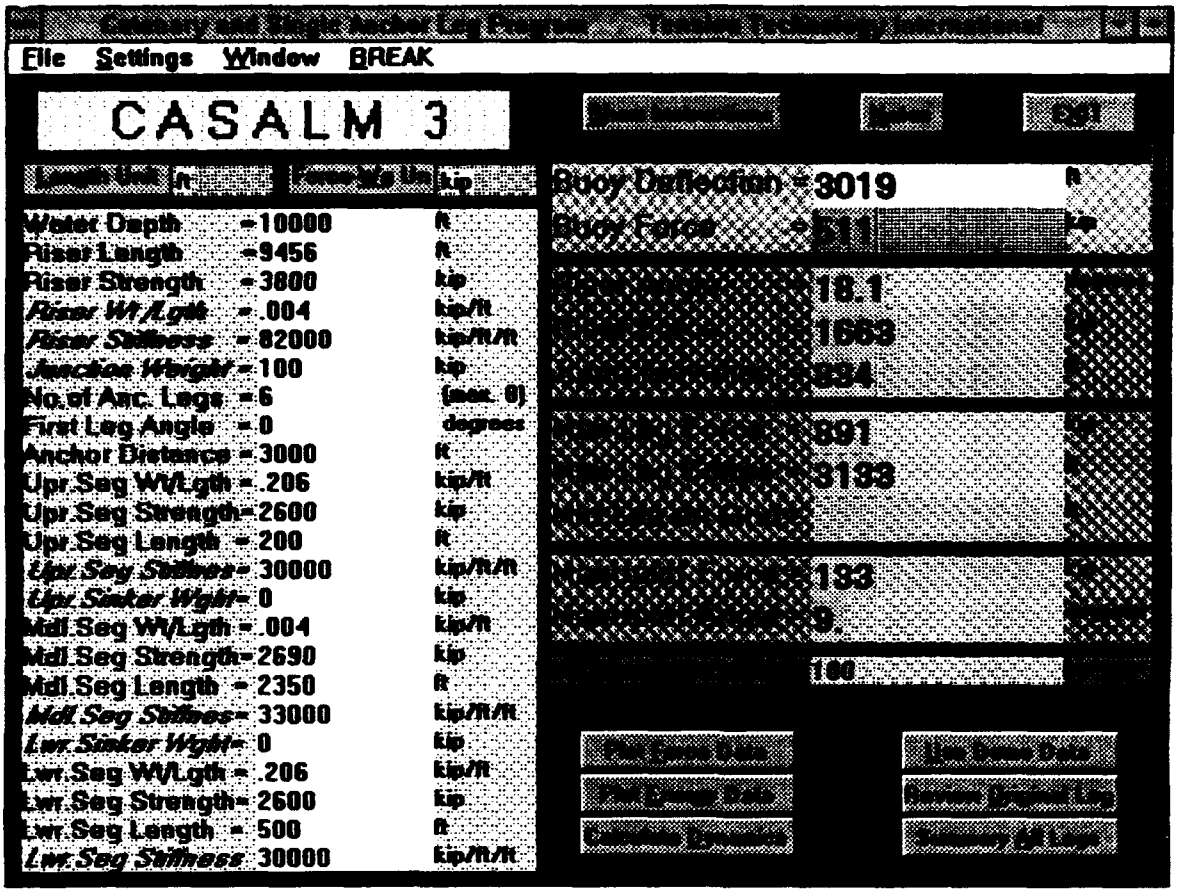

Figure A-11 Main Screen with solution to example inverse Buoy Force input

Catenary Anchor Legs

Anchor Leg	No. 1	No. 2	No. 3	No. 4	No. 5	No. 6
Vector Angle	.	60.	120.	180.	240.	300.
Horizontal Deflection	802	793	775	765	775	793
Horizontal Force	844	755	588	500	588	755
Top Tension	891	800	627	536	627	800
Top Vertical Force	267	263	218	194	218	263
Top Angle	18.8	19.2	20.3	21.2	20.3	19.2
Middle Segment	879	787	614	522	614	787
Lower Segment	876	785	612	520	612	785
Conditions	Anchor	Anchor	Anchor	Anchor	Anchor	Anchor
Total Scope	3133	3124	3108	3099	3108	3124
Origin to Gnd./Anchor						
Anchor Uplift Angle	9.	8.2	6.2	4.6	6.2	8.2
Anchor Uplift Force	133	110	64	40	64	110

Figure A-12 Anchor Leg Data Summary Screen

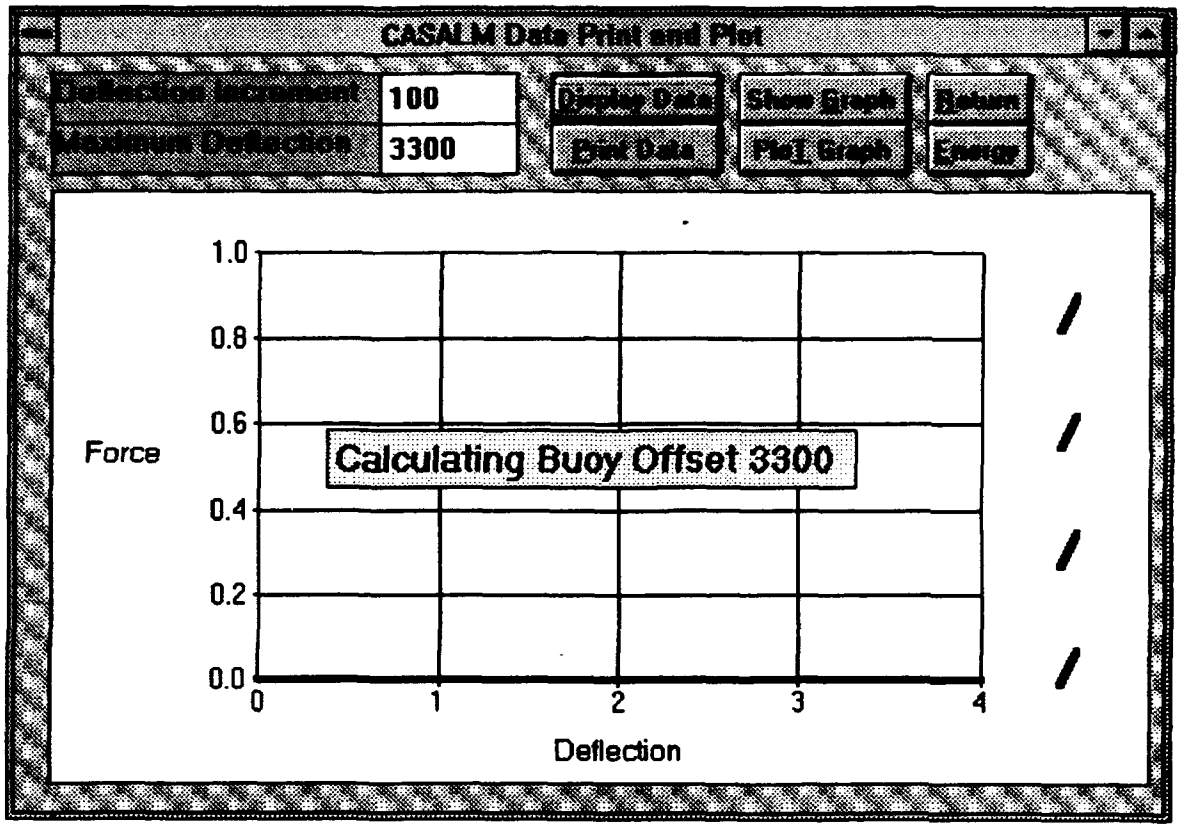

Figure A-13 Force-Deflection Calculation Screen

Data Display

CASALM Forces 16:30 August 29, 1997

Buoy Deflctn ft	Buoy Force kip	Riser Force kip	Riser Angle deg.	Jnctn Elevtn ft	Anc. Leg Tension kip	Anc. Pt. Uplift kip	Leg on Gnd ft
0	0	497	0	490	100	0	449
100	6	498	.7	490	103	0	452
200	12	499	1.4	492	106	0	449
300	16	502	1.8	494	109	0	446
400	21	506	2.3	497	112	0	442
500	28	510	3.1	503	118	0	436
600	32	518	3.5	507	125	0	427
700	38	527	4.1	514	131	0	421
800	46	539	4.9	524	141	0	409
900	46	550	4.8	521	151	0	397
1,000	56	570	5.6	533	166	0	379
1,100	60	584	5.9	536	177	0	368
1,200	75	606	7.1	558	197	0	344
1,300	85	631	7.7	569	217	0	319
1,400	95	660	8.2	579	238	0	294
1,500	110	696	9.0	597	264	0	263
1,600	115	718	9.1	595	279	0	243
1,700	135	758	10.1	621	310	0	205
1,800	149	799	10.6	633	341	0	165
1,900	164	847	11.0	641	372	0	124
2,000	184	896	11.6	659	404	0	82
2,100	199	945	11.9	664	435	0	39
2,200	228	1,000	12.9	697	476	3	0
2,300	248	1,059	13.2	705	518	15	0
2,400	272	1,127	13.6	714	559	28	0
2,500	297	1,198	13.9	721	601	41	0
2,600	336	1,275	14.8	752	653	56	0
2,700	375	1,359	15.4	776	714	75	0
2,800	414	1,451	15.9	792	756	89	0
2,900	463	1,542	16.7	826	819	109	0
3,000	511	1,653	17.2	842	881	130	0
3,100	560	1,773	17.5	849	954	154	0
3,200	618	1,889	18.1	874	1,026	179	0
3,300	677	2,016	18.6	888	1,099	205	0

Figure A-14 Force-Deflection Data Table Screen

CASALM Mooring Force Calculation, performed at 16:30 August 29, 1997

Water Depth = 10,000 ft Junction Elevation = 490 ft
Anchor Distance = 3,000 ft No. of Anchor Legs = 6

Component	Length ft	Strength kip	Weigth/Length kip/ft	Stiffness kip/ft/ft
Riser	9,456	3,800	.004	82,000
Segment 1	500	2,600	.206	30,000
Segment 2	2,350	2,690	.004	33,000
Segment 3	200		.206	30,000

Riser Weight = 38 kip Junction Weight = 100 kip
Sinker 1 Weight = kip Sinker 2 Weight = kip

Buoy Deflct ft	Buoy Force kip	Riser Force kip	Riser Angle deg.	Junctn Elevatn ft	Anchor Leg Tension kip	Anchor Uplift kip	Min. Leg on Ground ft
0	0	497	.0	490	100	0	449
100	6	498	.8	490	103	0	452
200	12	499	1.5	492	106	0	449
300	16	502	1.9	494	109	0	446
400	21	506	2.4	497	112	0	442
500	28	510	3.2	503	118	0	436
600	32	518	3.6	507	125	0	427
700	38	527	4.3	514	131	0	421
800	46	539	5.1	524	141	0	409
900	46	550	4.9	521	151	0	397
1,000	56	570	5.8	533	166	0	379
1,100	60	584	6.2	536	177	0	368
1,200	75	606	7.4	558	197	0	344
1,300	85	631	8.0	569	217	0	319
1,400	95	660	8.5	579	238	0	294
1,500	110	696	9.4	597	264	0	263
1,600	115	718	9.4	595	279	0	243
1,700	135	758	10.5	621	310	0	205
1,800	149	799	11.0	633	341	0	165
1,900	164	847	11.4	641	372	0	124
2,000	184	896	12.1	659	404	0	82
2,100	199	945	12.4	664	435	0	39
2,200	228	1,000	13.5	697	476	3	0
2,300	248	1,059	13.8	705	518	15	0
2,400	272	1,127	14.2	714	559	28	0
2,500	297	1,198	14.6	721	601	41	0
2,600	336	1,275	15.5	752	653	56	0
2,700	375	1,359	16.2	776	714	75	0
2,800	414	1,451	16.8	792	756	89	0
2,900	463	1,542	17.7	826	819	109	0
3,000	511	1,653	18.2	842	881	130	0
3,100	560	1,773	18.6	849	954	154	0
3,200	618	1,889	19.3	874	1,026	179	0
3,300	677	2,016	19.8	888	1,099	205	0

Figure A-15 Force-Deflection Data Table Print Out

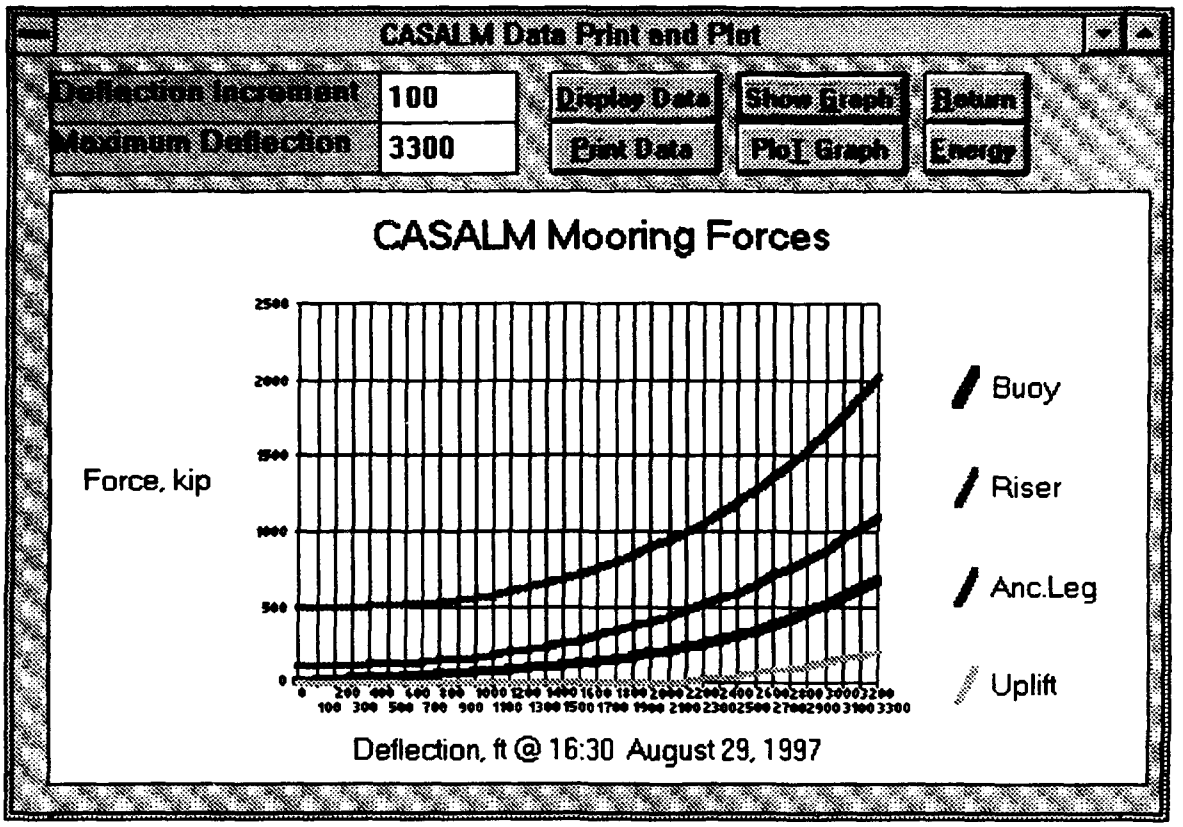

Figure A-16 Force Deflection Curve Screen

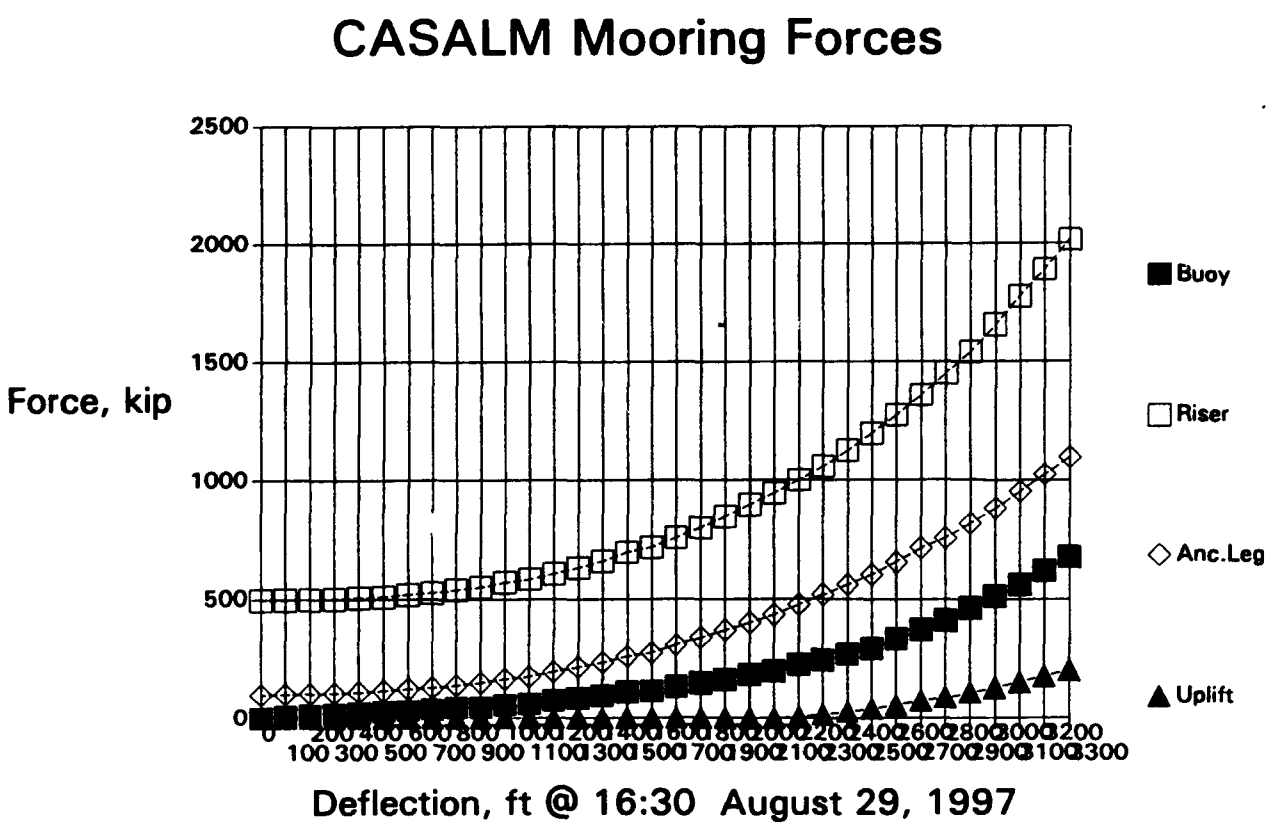

Figure A-17 Force-Deflection Curve Print-Out

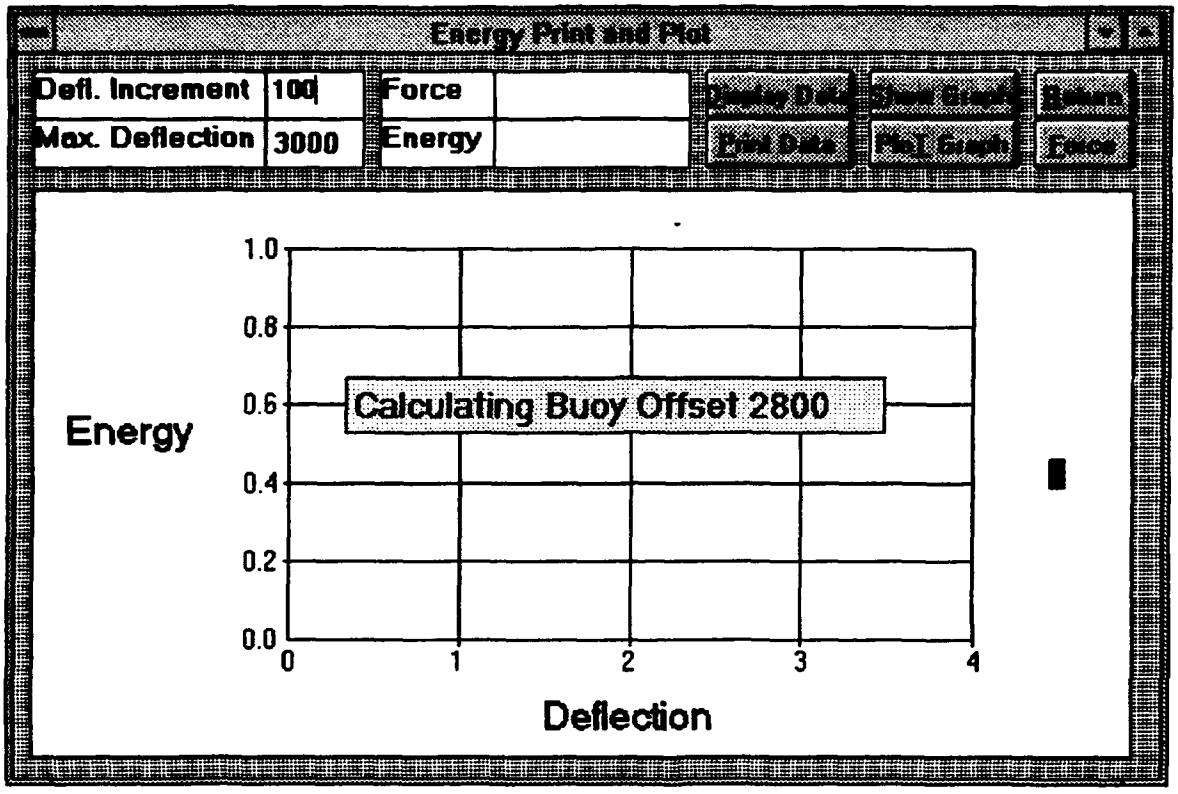

Figure A-18 Mooring Energy Calculation Screen

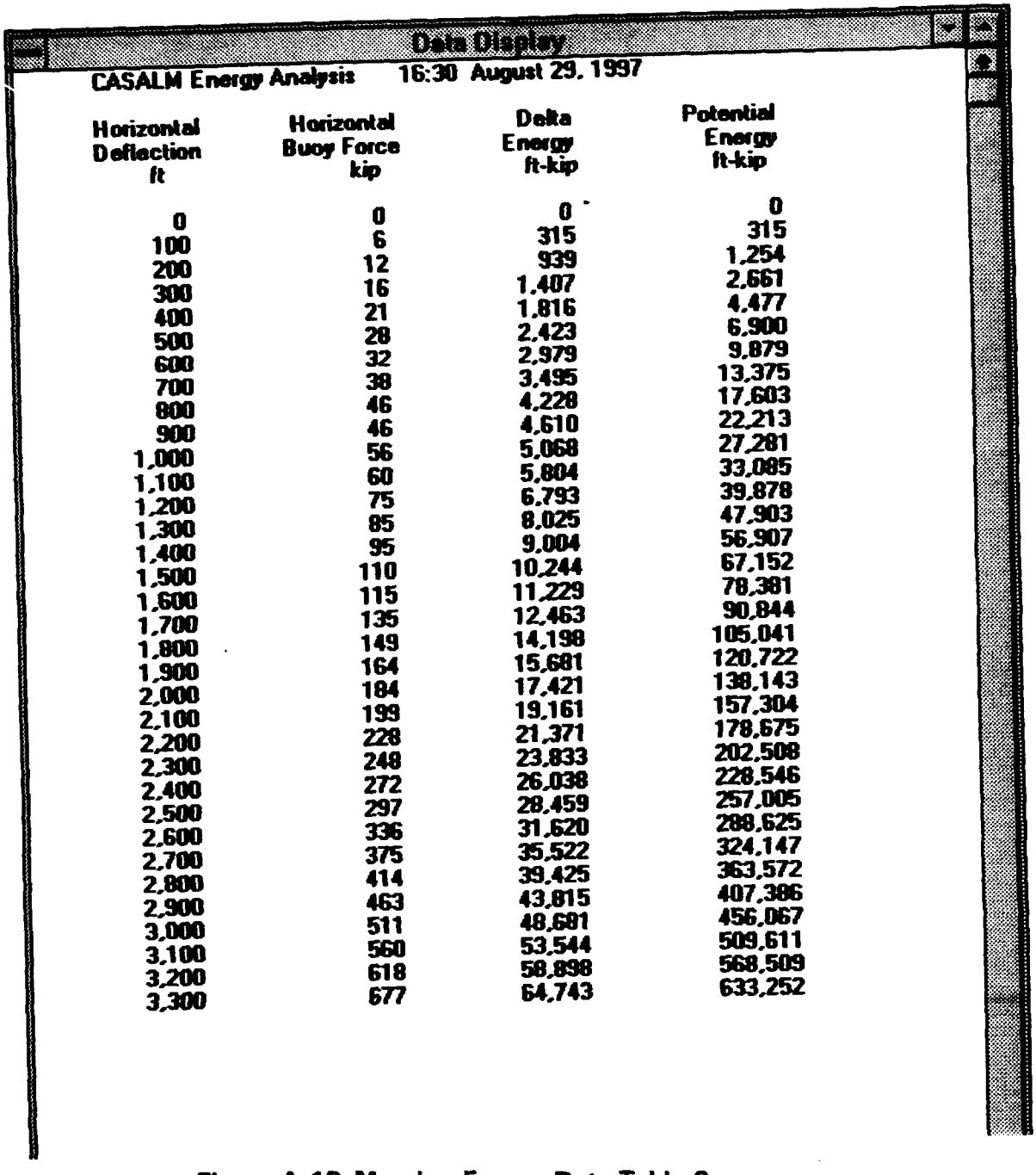

Data Display

CASALM Energy Analysis 16:30 August 29, 1997

Horizontal Deflection ft	Horizontal Buoy Force kip	Delta Energy ft-kip	Potential Energy ft-kip
0	0	0	0
100	6	315	315
200	12	939	1,254
300	16	1,407	2,661
400	21	1,816	4,477
500	28	2,423	6,900
600	32	2,979	9,879
700	38	3,495	13,375
800	46	4,228	17,603
900	46	4,610	22,213
1,000	56	5,068	27,281
1,100	60	5,804	33,085
1,200	75	6,793	39,878
1,300	85	8,025	47,903
1,400	95	9,004	56,907
1,500	110	10,244	67,152
1,600	115	11,229	78,381
1,700	135	12,463	90,844
1,800	149	14,198	105,041
1,900	164	15,681	120,722
2,000	184	17,421	138,143
2,100	199	19,161	157,304
2,200	228	21,371	178,675
2,300	248	23,833	202,508
2,400	272	26,038	228,546
2,500	297	28,459	257,005
2,600	336	31,620	288,625
2,700	375	35,522	324,147
2,800	414	39,425	363,572
2,900	463	43,815	407,386
3,000	511	48,681	456,067
3,100	560	53,544	509,611
3,200	618	58,898	568,509
3,300	677	64,743	633,252

Figure A-19 Mooring Energy Data Table Screen

CASALM Mooring Energy Calculation, performed at 16:30 August 29, 1997

Water Depth = 10,000 ft Junction Elevation = 490 ft
Anchor Distance = 3,000 ft No. of Anchor Legs = 6

Component	Length ft	Strength kip	Weigth/Length kip/ft	Stiffness kip/ft/ft
Riser	9,456	3,800	.004	82,000
Segment 1	500	2,600	.206	30,000
Segment 2	2,350	2,690	.004	33,000
Segment 3	200		.206	30,000

Riser Weight = 38 kip Junction Weight = 100 kip
Sinker 1 Weight = kip Sinker 2 Weight = kip

Horizontal Deflection ft	Horizontal Buoy Force kip	Delta Energy ft-kip	Mooring Energy ft-kip
100	6	315	315
200	12	939	1,254
300	16	1,407	2,661
400	21	1,816	4,477
500	28	2,423	6,900
600	32	2,979	9,879
700	38	3,495	13,375
800	46	4,228	17,603
900	46	4,610	22,213
1,000	56	5,068	27,281
1,100	60	5,804	33,085
1,200	75	6,793	39,878
1,300	85	8,025	47,903
1,400	95	9,004	56,907
1,500	110	10,244	67,152
1,600	115	11,229	78,381
1,700	135	12,463	90,844
1,800	149	14,198	105,041
1,900	164	15,681	120,722
2,000	184	17,421	138,143
2,100	199	19,161	157,304
2,200	228	21,371	178,675
2,300	248	23,833	202,508
2,400	272	26,038	228,546
2,500	297	28,459	257,005
2,600	336	31,620	288,625
2,700	375	35,522	324,147
2,800	414	39,425	363,572
2,900	463	43,815	407,386
3,000	511	48,681	456,067
3,100	560	53,544	509,611
3,200	618	58,898	568,509
3,300	677	64,743	633,252

Figure A-20 Mooring Energy Data Table Print-Out

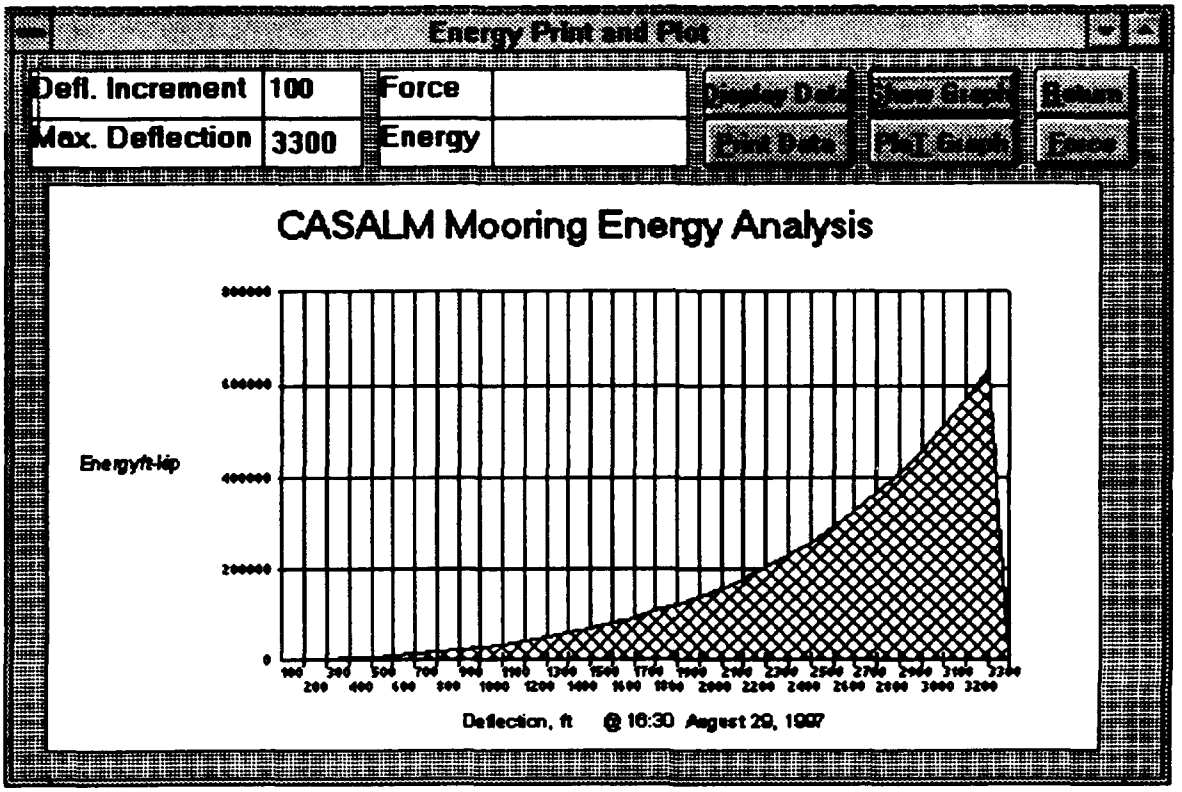

Figure A-21 Mooring Energy Curve Screen

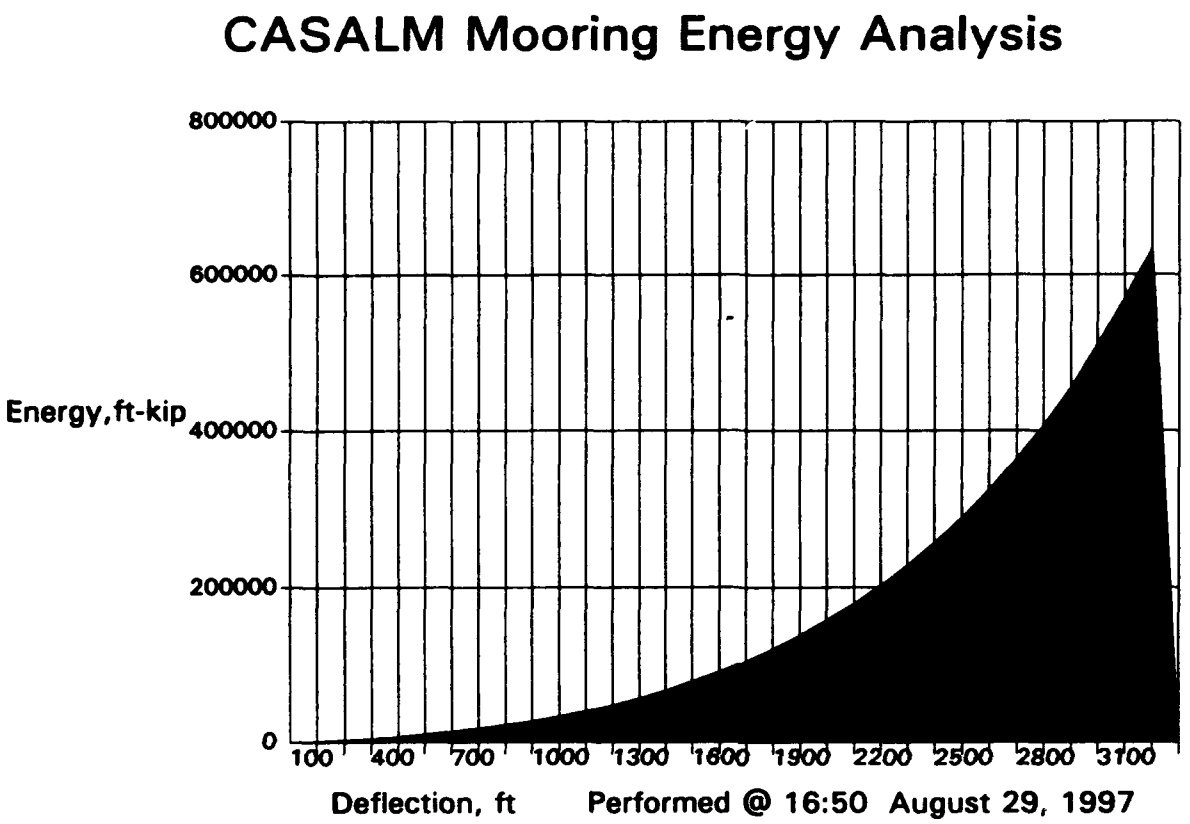

Figure A-22 Mooring Energy Curve Print-Out

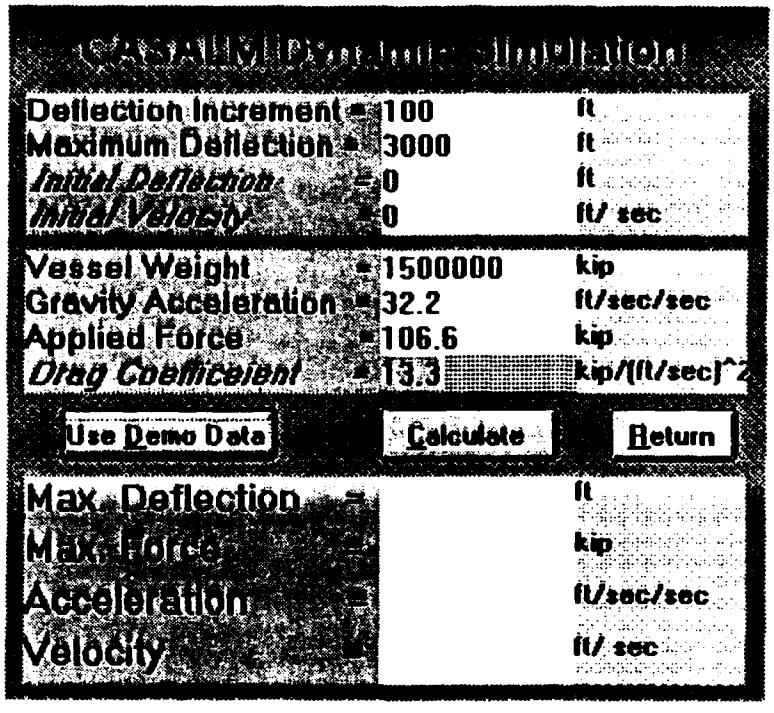

Figure A-23 Dynamic Simulation Calculation Screen

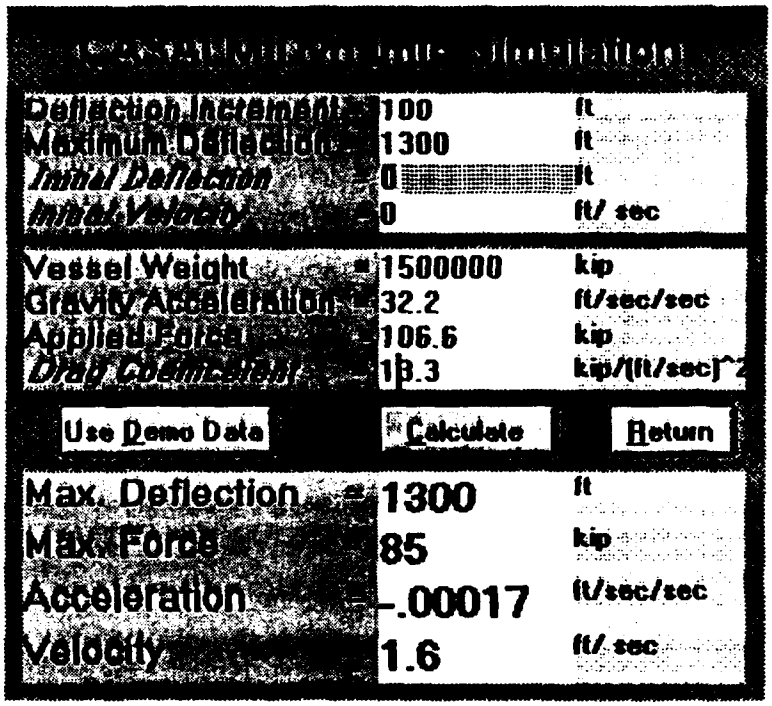

Figure A-24 Dynamic Simulation Screen during calculation

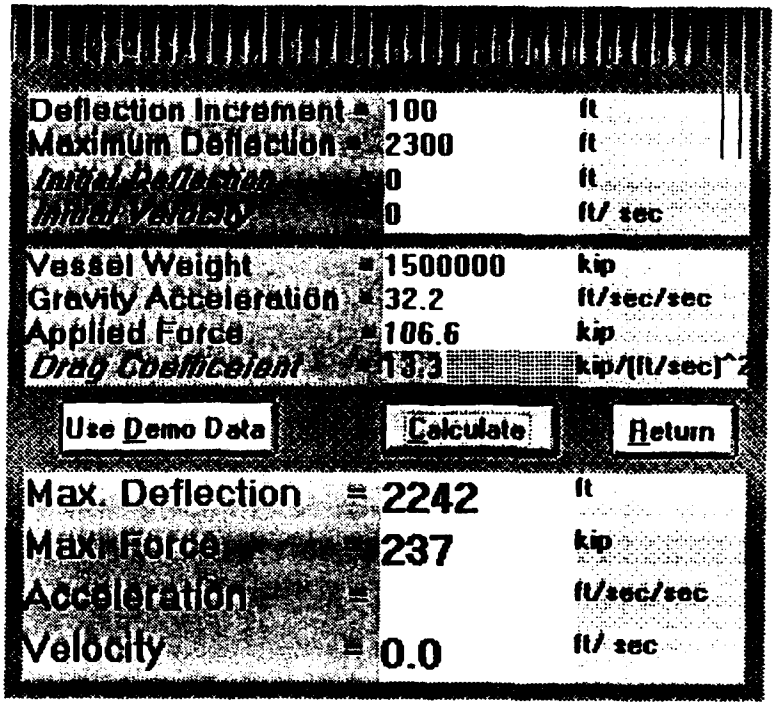

Figure A-25 Dynamic Simulation Screen with solution

APPENDIX B

DERIVATION AND EXPLANATION OF EQUATIONS AND METHODS USED IN CALM AND CASALM COMPUTER PROGRAMS

This Appendix documents the equations and methods used in the CALM and the CASALM computer programs. These programs use a novel method and new equations to calculate the deflection-force characteristics of the catenary anchor leg.

Some previous catenary anchor leg analysis programs have used the traditional catenary equations, which are discussed in the beginning of this memorandum. The traditional catenary equations are cumbersome for performing force-deflection analysis, principally because they reference deflection to the catenary generation point. The generation point is the origin which is used in the equations to describe, or mathematically "generate", the catenary curve shape. The catenary generation point is not stationary; its horizontal and vertical positions change as the catenary deflects. This greatly complicates the process of describing the deflection of a cantenary anchor leg from its slack position, especially when there is uplift on the anchor point.

The new form of catenary equation references the catenary deflection to a stationary point corresponding to the slack or undeflected position of the catenary anchor leg. It features only one principal equation, which directly relates applied force to deflection. It avoids the complexities of calculating the scope of the catenary and the position of the catenary generation point. It avoids the use of hyperbolic functions. This greatly simplifies the analysis of a catenary anchor leg.

Other previous catenary anchor leg analysis programs have used a finite difference calculation method, in which the catenary is treated as a large number of rigid, weighted components or links joined together in series and hanging under the influence of gravity. The finite difference calculation method seeks a solution for the configuration or catenary shape which balances the forces at each junction. This method of solution requires many calculation steps. It is efficient if the various links have different properties, such as weight or elasticity, but it is not efficient if most or all of the links are identical.

The calculation method used in the CALM and CASALM programs does use this finite difference calculation method to account for as many as five components - three catenary segments and two sinkers at the junctions. But it treats each of the catenary segments as a single component, having catenary properties as described by the new catenary equations. This greatly reduces calculation time.

These two programs directly account for the elastic characteristics of the lines making up the catenary segments. This somewhat complicates the solution of the CALM system. This greatly

complicates the solution of the CASALM, because of the interaction between the length of the riser and the elevation of the junction between that riser and the catenary anchor legs.

This elastic component solution of the CASALM system would probably be very difficult to accomplish in a computer program which employed the finite difference method. Such a program would take a very long time to converge on an answer; it would probably be unstable and either not converge or converge on a wrong answer converge in many cases. Even the present CASALM computer program sometimes takes a long time to converge on an answer and does not achieve convergence in some cases.

The CASALM computer program is completely documented in a separate memorandum. The code for the program is provided as a separate volume.

B-1 Introduction

This memorandum first derives the new equation for the case in which the catenary anchor leg is tangent to the sea floor. The traditional catenary equations are introduced in this first secion. The new equation for the case in which the catenary anchor leg applies uplift on an anchor or other component is then derived. This case is developed to address solving multiple catenary segments connection in series with weights concentrated at the connections.

The memorandum then describes the solution of the CALM, in which a number of catenary anchor legs come together at a junction. Finally, it describes the steps in solving the CASALM, in which the junction point is suspended by a single anchor leg from the surface.

B-1.1 Nomenclature

The nomenclature is summarized in Table 1. The first time a term is used, it appears in *italics*. Some of these terms differ from those used in the traditional method of catenary analysis.

The catenary is the shape of a weighted flexible line suspended between two points under the influence of gravity.

The physical catenary material is called *chain*, although the catenary may be comprised of any other flexible tension member, for example rope or cable. The chain has a *unit weight* (weight per unit length) w.

A *horizontal force* is applied to the *top* of the catenary. The subscript t designates variables associated with the top of the catenary. Thus the horizontal force at the catenary top is designated as H_t.

The *ground* is the surface on which the unlifted portion of chain rests. The *scope* is the distance along the catenary between any two points. The scope or length of chain which is lifted off the ground is designated by S.

B-1.2 New Catenary Coordinate System

In this first case, the catenary is tangent to the ground, such that no uplift is applied at the bottom of the chain. The unlifted portion of the catenary rests on a horizontal surface called the *ground plane*. The point at which the catenary touches the ground plane is the *ground point*.

The *base point* is the lowest point on the catenary curve, designated here by the subscript b. In this ground tangent catenary case, the base point is on the ground plane and is coincident with the ground point. Later in the uplift case, the base point will be beneath the ground plane.

Elevation refers to a vertical measurement above the base point and is designated by E. The top of the catenary is assumed to move only horizontally. Thus the elevation of the top above the base point E_t is a constant. For the ground tangent catenary case in a typical marine mooring analysis, this is the water depth.

In the *undeflected position*, with no horizontal force, the catenary hangs straight down and touches the ground plane at a point directly beneath the catenary top. This undeflected position is illustrated in Figure 1. The principal advantage of the method of catenary analysis presented here is that the defection of the top of the catenary is referenced directly to this undeflected catenary position.

Deflection refers to a horizontal measurement from the undeflected catenary position. When horizontal force is applied to the top of the catenary, it deflects from the undeflected position through a distance D_t in the direction of that force. This deflected catenary position is shown in Figure 2.

As the top deflects, additional catenary chain is lifted off the ground plane, and the base point deflects in the direction opposite the applied force. This *base deflection* is designated by D_b.

B-1.3 Traditional Catenary Coordinate System

The mathematic equations traditionally used to describe the shape of the catenary curve are based on a different coordinate system than that used here. The origin of that coordinate system is here called the catenary *generation point*. This traditional catenary coordinate system is shown in Figure 3.

The generation point is located at a distance C directly below the base point. This distance C is here called the *catenary parameter*. It appears in several important catenary equations, but otherwise the catenary parameter has no physical significance.

In the undeflected catenary position the generation point corresponds to both the base point and the ground point. Thus $C = 0$ in the undeflected position.

The traditional catenary coordinate system, with its origin at the generation point, has the disadvantage that the location of this generation point changes as force is applied. The generation point depresses below the ground plane, and it also moves away from the undeflected catenary position. Calculation of the actual deflection of the top of the catenary are greatly complicated by these movements of the generation point in the traditional catenary coordinate system.

B-1.4 Relationships Between Traditional and New Coordinate Systems

In the traditional coordinate system, the vertical distance of a point on the catenary above the generation point is designated by Y. Here that vertical dimension property is called *height* to distinguish it from elevation, which is measured from the ground plane. The height of the catenary top above the generation point is then Y_t. It generally has no direct physical significance.

Since the catenary top is at an elevation E_t above the base point, and the catenary generation point is at a distance C below that base point :

$$Y_t = C + E_t \tag{1}$$

Here we will use the term ***distance*** to refer to horizontal measurements from the catenary generation point. In the traditional catenary coordinate system, the horizontal distance from the catenary generation point to a point on the catenary is designated by X. In this new catenary coordinate system, that distance of the catenary top from the generation point is the sum of top deflection and base deflection :

$$X_t = D_t + D_b \tag{2}$$

B-2 THE TRADITIONAL CATENARY EQUATIONS

The following traditional catenary equations are taken from the Navy Fleet Moorings Design Manual DM 26.5.* These equations have been adapted to the catenary coordinate system and terminology introduced here. For general reference, some equations are presented in several different but equivalent forms.

B-2.1 Catenary Force Relationships

Using the nomenclature introduced above, the forces on and within the catenary can be calculated by the following equations.

---

* Naval Facilities Engineering Command, *Fleet Moorings, Basic Criteria and Planning Guidelines*, Design Manual 26.5, June, 1985, page 135 +.

One of the important properties of the catenary is that the horizontal force is related to the catenary parameter :

$$\begin{aligned} H &= wC \\ &= T\cos\theta \end{aligned}$$

$$\begin{aligned} C &= \frac{H}{w} \\ &= \frac{T}{w}\cos\theta \end{aligned} \tag{3}$$

The horizontal force applied to the catenary top is H. Because no other horizontal forces are applied to the catenary, the horizontal force H is the same at any point along the catenary. The horizontal force at the top is thus the same as that at the base point, $H_t = H_b$.

Another important property of the catenary is that the tangential force can be related to the height of the catenary :

$$\begin{aligned} T &= wY \\ &= w(C+E_t) \\ &= w\left(\frac{H}{w}+E_t\right) \\ &= H + E_t w \end{aligned}$$

$$Y = \frac{T}{w} \tag{4}$$

Since the unit weight of the catenary line is w, the total weight of the catenary is wS. Because the sum of vertical forces must balance, the vertical force at the top of the catenary is :

$$\begin{aligned} V &= wS \\ &= T\sin\theta \\ &= (H+E_t w)\sin\theta \end{aligned}$$

$$\begin{aligned} S &= \frac{V}{w} \\ &= \frac{T}{w}\sin\theta \\ &= \left(\frac{H}{w}+E_t\right)\sin\theta \end{aligned} \tag{5}$$

The total or tangential force T at any point in the catenary can be determined by vector addition of the horizontal and vertical force components :

$$T = \sqrt{H^2 + V^2} \tag{6}$$

B-2.2 Traditional Catenary Shape Equations

Using the nomenclature introduced above, the catenary shape can be calculated with the following equations :

$$Y^2 = S^2 + C^2$$

$$\begin{aligned} S &= \sqrt{Y^2 - C^2} \\ &= \sqrt{(C + E_t)^2 - C^2} \\ &= \sqrt{2CE_t + E_t^2} \end{aligned} \tag{7}$$

$$\begin{aligned} Y &= C \cosh \frac{X}{C} \\ &= C \cosh\left(\frac{D_t + D_b}{C}\right) \end{aligned} \tag{8}$$

$$\begin{aligned} S &= C \sinh \frac{X}{C} \\ &= C \sinh\left(\frac{D_t + D_b}{C}\right) \end{aligned} \tag{9}$$

B-2.3 Catenary Angle Equations

The angle of the slope of the catenary at any point from horizontal is designated as θ. It can be found from any of the following equations:

$$\begin{aligned} \theta &= \arctan \frac{V}{H} \\ &= \arctan\left(w \frac{S}{H}\right) \end{aligned} \tag{10}$$

$$\begin{aligned} \theta &= \arccos \frac{H}{T} \\ &= \arccos\left(\frac{H}{H + E_t w}\right) \end{aligned} \tag{11}$$

$$\theta = \arcsin \frac{V}{T}$$
$$= \arcsin\left(\frac{wS}{H+E_t w}\right) \quad (12)$$

B-2.4 Traditional Force-Deflection Solution of the Catenary

The available catenary equations, given above, do not provide a direct relationship between the force H on the catenary and the resulting horizontal deflection D_t of the top from the catenary undeflected position.

An equation of the form $H = f(X)$ can not be derived, because equations (8) and (9) which involve X are transcendental; that is, the dependent parameter C appears on both sides of the hyperbolic trigonometric function. This type of equation can not be solved directly, but it can be solved by trial-and-error methods.

The relationship $X = f(H)$ can be solved through the use of a series of equations, as will be demonstrated later. That calculation procedure is cumbersome, because X relates to the catenary generation point which is not in a fixed position. Like the base point, the catenary generation point moves from the undeflected position when force is applied. This complicates the analysis of catenary mooring systems.

B-3 New Catenary Force-Deflection Solution

By defining the catenary origin at the undeflected position of the catenary, a new set of catenary equations can be developed which greatly simplify the analysis of catenary mooring systems.

The catenary undeflected origin position is shown in Figure 1. With no horizontal force applied to the chain, it hangs straight down and touches the ground at a point immediately beneath its top. This undeflected ground point is used as the origin for the following catenary equations.

The vertical force at the top in this undeflected position is equal to the unit weight of chain times the top elevation or water depth :

$$V_b = E_t w \quad (13)$$

Figure 2 shows the catenary shape after application of a horizontal force. When the top of the catenary deflects, the chain scope increases as chain is lifted off the ground plane. The change in

scope is equal to this additional length of lifted chain. As a result, the base point deflects along the ground by D_b. (It is assumed that there is no slack in the chain which lies on the ground.)

Thus for any given horizontal deflection D_t of the catenary top from the origin, the scope of chain between the base point and the catenary top is :

$$S = D_b + E_t \tag{14}$$

B-3.1 Non-Dimensionalized Equations

For convenience, the following catenary dimensions and forces are non-dimensionalized. All dimensions are divided by the catenary top elevation E_t, which is the water depth.

All forces are divided by $E_t w$, which is the weight of a length of chain corresponding to the water depth or catenary top elevation in the undeflected position. Thus for example, the horizontal force parameter becomes $H / E_t w$.

With knowledge of the horizontal force H on the catenary, the tangent force at the top of the catenary can be directly determined by the following adaptation of Equation (4) :

$$\frac{T_t}{E_t w} = \frac{H}{E_t w} + 1 \tag{15}$$

From this equation and Equation (11), the slope at the top of the catenary is found :

$$\theta_t = \arccos \frac{H}{T_t}$$

$$= \arccos \left(\frac{H}{H + E_t w} \right) \tag{16}$$

T he vertical force V_t at the top of the catenary can then be obtained from the preceding and Equation (5) :

$$\frac{V_t}{E_t w} = \frac{H + E_t w}{E_t w} \sin\theta_t$$

$$= \left(\frac{H}{E_t w} + 1 \right) \sin\theta_t$$

$$= \frac{H}{E_t w} \left(\frac{1}{\frac{H}{H + E_t w}} \right) \sin\theta_t$$

$$= \frac{H}{E_t w} \frac{\sin\theta_t}{\cos\Theta_t}$$

$$= \frac{H}{E_t w} \frac{1}{\tan\theta_t} \qquad (17)$$

When the vertical force is known, the catenary scope can be determined by Equation (5). Adapting that equation to the non-dimensional equation form, it becomes :

$$\frac{S}{E_t} = \frac{V_t}{E_t w} \qquad (18)$$

Using Equations (2) and (14), the horizontal deflection of the top from the zero-deflection position can then be expressed as :

$$\frac{D_t}{E_t} = 1 + \frac{X_t}{E_t} - \frac{S}{E_t} \qquad (19)$$

B-4 THE NEW CATENARY EQUATION : BOTTOM TANGENT CASE

The above set of equations could be used to solve for the relationship $D_t = f(H)$. But the relationship can be conveniently expressed by a single equation as follows.

The inverse hyperbolic sine can be expressed as a natural log function:

$$\text{arcsinh}\, k = \ln\left(k + \sqrt{k^2 + 1}\right) \qquad (20)$$

Using this equation to transform Equation (9), it becomes :

$$D_t + D_b = C\, \text{arcsinh}\frac{S}{C}$$

$$= C \ln\left\{ \frac{S}{C} + \sqrt{\left(\frac{S}{C}\right)^2 + 1} \right\} \qquad (21)$$

Substituting Equations (14) for D_b and (3) for C in the above equation and then rearranging, it becomes :

$$D_t = E_t - S + \frac{H}{w} \ln\left\{\frac{Sw}{H} + \sqrt{\left(\frac{Sw}{H}\right)^2 + 1}\right\} \tag{22}$$

The equation is made non-dimensional by dividing all terms by E_t:

$$\frac{D_t}{E_t} = 1 - \frac{S}{E_t} + \frac{H}{wE_t} \ln\left\{\frac{Sw}{H} + \sqrt{\left(\frac{Sw}{H}\right)^2 + 1}\right\} \tag{23}$$

A new variable Q is defined as the ratio of the applied horizontal force to the initial vertical force in the undeflected position (water depth times unit weight of chain).

$$Q = \frac{H}{wE_t} \tag{24}$$

Note that Q has a simple physical significance. It is the ratio of the applied horizontal force to the weight of suspended chain in the particular water depth (vertical tension) in the undeflected catenary position.

Equation (7) is rearranged, substituting Equation (4) for C, and introducing the term Q, to achieve :

$$S^2 = 2CE_t + E_t^2$$

$$\frac{S^2}{E_t^2} = \frac{2H}{wE_t} + 1$$

$$= 2Q + 1$$

$$\frac{S}{E_t} = \sqrt{2Q + 1} \tag{25}$$

Substituting these into Equation (23), it can then expressed as :

$$\frac{D_t}{E_t} = 1 - \sqrt{2Q+1} + Q \ln\left\{1 + \frac{1}{Q} + \frac{\sqrt{2Q+1}}{Q}\right\} \tag{26}$$

This equation can readily be used in a spreadsheet or a computer program and can be preprogrammed into some pocket calculators.

Because the variable H appears both outside and inside the ln term, it is not possible to invert Equation (25) to directly solve for $H = f(D_t)$. However, it is relatively convenient to use the above equation to solve for that relationship by trial and error.

B-4.2 Verification Calculations

The use of this new form of catenary equation is demonstrated in Table 2. Here the new method is compared with the traditional method.

In the demonstration, the catenary anchor leg consists of a 100 mm stud link chain with a unit weight of 219 kg/m in a water depth of 183 m. A horizontal force of 200000 kg is applied to this anchor leg. What is the horizontal deflection of the catenary top due to this horizontal force?

Solving this problem using the above traditional catenary equations involves seven calculation steps. It requires calculating the catenary parameter C, the vertical and tangent forces at the top of the catenary, the scope of the catenary S, and the distance D_b through which the base point deflects from the undeflected catenary in the process of calculating the top horizontal deflection D_t The traditional method also involves the inverse hyperbolic sine (arcsinh) function, which is not available on many calculators and spread sheets.

Solving this catenary problem by the new method introduced here involves only two steps (only one step if equation (23) is used). It employees the natural log (ln) function, which is much more accessible than the inverse hyperbolic sine function. The second step involves a long equation, but this can readily be programmed on a spread sheet or in a computer program.

The principal advantage of this new method is that it directly relates the applied force to the deflection at the top of the catenary. It does not require calculating the parameters C, S and D_b, and the algebraic "bookkeeping" involved in their use.

B-5 The Bottom Uplift Case

The preceding section addressed the case in which the length of chain extending to the anchor is sufficient that the catenary does not exert an upward force on the anchor. Thus the catenary is tangent with the ground at its lowest point. The case in which the catenary applies an uplift force to an anchor or other component is now addressed.

When a catenary anchor leg exerts an upward force on an anchor, the catenary intersects the ground at an angle α at this anchor point. This case of an uplifted catenary is shown in Figure 4. The ground is defined as the horizontal plane through the anchor point. The subscript a refers to forces and dimensions associated with this anchor point and its plane.

Figure 1 shows this catenary at the zero-deflection position, defining the origin for deflection measurements. The catenary is analyzed as a conventional catenary until its tangent point on the ground reaches the anchor, the position shown in Figure 5. Additional horizontal force on the top of the catenary then exerts an uplift force V_a on the anchor, as show in Figure 6.

That portion of the catenary extending from the anchor to the top is called the *real catenary*. The properties of an imaginary catenary extending below the anchor are also of concern in this case. This portion of the catenary beneath the anchor point is called the *phantom catenary*.

This uplift case is very difficult to analyze using the traditional catenary equations. The analysis can be greatly simplified by referencing horizontal deflections to the origin defined by the vertical chain in the zero-deflection position, as was done above for the plane catenary case.

In this zero deflection position, the chain touches the ground directly beneath its top and then extends horizontally along the ground to the anchor point. It is assumed that there is no slack in the chain which rests on the ground. The length of chain on the ground between this origin and the anchor is D_a. The distance from the base to the top of the catenary is E_t.

The total length of chain from the catenary top to the anchor is called L_{at}. Thus

$$L_{at} = E_t + D_a \tag{27}$$

Unlike the corresponding values D_g and S for the ordinary catenary case, which changed as horizontal force was applied, these values D_a and L_{at} are constants for the uplift catenary case. This simplifies the derivations and the analyses.

B-5.1 The Uplifted Catenary Deflection-Force Equation

Equation 5-90 from Navy Mooring Manual DM 26.5 deals with this case. Rewriting that equation to correspond to the present notation, it becomes :

$$\frac{2H}{w} \sinh \frac{D_a + D_t}{2H/w} = \sqrt{L_{at}^2 - E_t^2} \tag{28}$$

This equation can be altered to the following forms.

$$\frac{D_a + D_t}{2H/w} = \operatorname{arcsinh}\left\{ \frac{w}{2H} \sqrt{(D_a + E_t)^2 - E_t^2} \right\} \tag{29}$$

$$D_a + D_t = \frac{2H}{w} \operatorname{arcsinh}\left\{ \frac{w}{2H} \sqrt{D_a^2 + 2D_aE_t} \right\} \tag{30}$$

The equation can be non-dimensionalized by dividing through by E_t and manipulated to :

$$\frac{D_t}{E_t} = \frac{2H}{wE_t} \operatorname{arcsinh}\left\{ \frac{wE_t}{2H} \sqrt{\left(\frac{D_a}{E_t}\right)^2 + \frac{2D_a}{E_t}} \right\} - \frac{D_a}{E_t} \tag{31}$$

Equation (30) appears cumbersome, but in its non-dimensionalized form it involves only two independent variables H/wE_t and D_a/E_t. For convenience new composite variables A and B are introduced.

$$A = \frac{2H}{wE_t} \tag{32}$$

$$B = \left(\frac{D_a}{E_t}\right)^2 + \frac{2D_a}{E_t} \tag{33}$$

Equation (31) then becomes :

$$\frac{D_t}{E_t} = A \operatorname{arcsinh}\left\{\frac{1}{A}\sqrt{B}\right\} - \frac{D_a}{E_t} \tag{34}$$

Equation (31) can be transformed by the natural log substitution, Equation (20), to become :

$$\frac{D_t}{E_t} = A \ln\left[\frac{1}{A}\left\{\sqrt{B} + \sqrt{B+A^2}\ \right\}\right] - \frac{D_a}{E_t} \tag{35}$$

Any of these Equations (31), (34) or (35) can be used to directly solve for D_t, the horizontal deflection of the catenary top from its original zero-deflection position when a horizontal force H is applied to it. The term D_a / E_t is simply the ration between the length of chain which lies on the ground in the undeflected position to the water depth

Equation (35) involves the ln function, found in most calculators and computer programming languages, instead of the troublesome arcsinh function. Thus it may be preferred.

Because the applied force H or the term A which involves that force appears on both sides of the **arcsinh** or **ln** terms respectively, it is not possible to invert any of these equations to directly solve for the relationship $H = f(D_t)$. However, these equations provide convenient means of solving for that relationship by trial and error methods.

These equations only apply when $S > L_{at}$, that is when uplift force is applied to the anchor point. Otherwise there is no vertical force on the anchor, and the earlier Equations (24) and (26) still apply.

B-5.2 Solution for Vertical Uplift Force

Since the horizontal force is the same throughout the chain,

$$T_a = \sqrt{H^2 + V_a^2} \tag{36}$$

But solving for the vertical force V_a at the anchor requires some knowledge of the parameters of the phantom catenary beneath the anchor point.

Equations (5-90) through (5-92) from Navy Mooring Manual DM 26.5 provide help in solving this difficult problem. These equations relate the dimensions of and the forces in the phantom catenary to a point on the real catenary horizontally midway between the top and the anchor, as illustrated in Figure 7. Equation (28) was the adaptation of DM 26.5 equation (5-90).

The horizontal distance X_m from the catenary base point (and generation point) to this real catenary horizontal midpoint is given by DM 26.5 equation (5-91) adapted here as :

$$X_m = C \operatorname{arctanh} \frac{E_t}{S_{at}} \tag{37}$$

where S_{at} is the scope along the real catenary between the anchor and its top.

The horizontal distance from the anchor to the top of the real catenary X_{at} is:

$$X_{at} = 2C \operatorname{arcsinh} \left\{ \frac{\sqrt{S_{at}^2 - E_t^2}}{2C} \right\} \tag{38}$$

The horizontal projection of the phantom catenary (distance from the base point to the anchor point) is provided by DM 26.5 equation (5-92) adapted here as :

$$X_{ba} = X_m - \frac{X_{at}}{2} \tag{39}$$

The catenary parameter, given by Equation (3), is the same for the real and the phantom catenaries. Knowing X_{ba}, the horizontal extension of the phantom catenary, the scope of the phantom catenary from its base point or tangent point b to the base plane to the anchor point a at the bottom of the real catenary can then be found by Equation (9).

$$S_{ba} = C \sinh \frac{X_{ba}}{C} \tag{40}$$

And thus the uplift vertical force V_a at the bottom of the real catenary by Equation (5) is:

$$\begin{aligned} V_a &= w S_{ba} \\ &= w C \sinh \frac{X_{ab}}{C} \end{aligned} \tag{41}$$

The height Y_{ba} of the anchor plane above the phantom catenary base plane is found by Equation (8) as:

$$Y_{ba} = C \cosh \frac{X_{ba}}{C} \tag{42}$$

And the tangential or tension force T_a at the anchor can be calculated from Equations (4) and (8):

$$\begin{aligned} T_a &= w Y_{ba} \\ &= w C \cosh \frac{X_{ab}}{C} \end{aligned} \tag{43}$$

The tangential force T_t at the top of the catenary can now be found:

$$T_t = T_a + w E_t \tag{44}$$

B-6 Multi -Segment and Sinker Catenaries

The cases of catenaries comprised of multiple segments of chains having different unit weights and multiple segments connected by sinker weights pose special problems. But the above equations for uplift on an anchor can facilitate the solution of such problems.

The general case, with two segments connected at a junction is shown in Figure 8. An upper chain segment S_{ij} and a lower chain segment S_{jg} are joined at junction point j. Where necessary, variables pertaining to the upper segment will be designated by prime; for example the vertical force at the bottom of the upper segment (at the junction point) is designated as V'_j

Unfortunately, the elevation of this junction point is not fixed. Thus the case must be solved by trial-and-error. A trial value for the elevation of the junction above the ground E_j is established. Knowing the horizontal force H, the deflection of the junction D_{jg} can be calculated by Equation (24) or (26). The vertical force V_j beneath the junction can be found from Equations (18) and (19).

If a junction weight W_j is present, it is added in order to obtain the vertical force V_j above the junction.

$$V'_j = V_j + W_j \tag{45}$$

The upper segment is then treated as an anchor-uplift case. The effective top elevation of this upper segment case is :

$$E_{jt} = E_t + E_j \tag{46}$$

The vertical force at the top of the catenary is :

$$V_t = V'_j + w S_{jt} \tag{47}$$

Because the scope of the real portion of this upper segment is known, the anchor deflection D_a' associated with it can be found.

$$D'_a = S_{tj} - E_{tj} \tag{48}$$

With this value, the deflection D_{tj} of the top segment can be calculated by Equation (35).

The total horizontal projection of the two catenary segments can then be found from .

$$D_{gt} = D_{aj} + D_{jt} \tag{49}$$

The lifted scope of the lower segment S_{gj} can be found from Equation (5). Then, knowing the length of the lower segment L_{aj}, the deflection of the top of the catenary from the zero-deflection postion can be determined.

$$D_t = L_{aj} + L_{jt} - S_{aj} - S_{jt} \tag{50}$$

The above calculation scheme can also be used when the two segments have different unit weights, $w \neq w'$.

If there are three or more segments, then the elevations of both junctions must be found. That case can not be solved directly. However, it can be solved by trial and error, using a trial value for the elevation of the upper segment.

B-7 Solving the Catenary Anchor Leg Mooring System

The CALM (catenary anchor leg mooring) system consists of several catenary anchor legs joined together at a single point in a balanced pattern. The simplest such system consists of two catenary anchor legs on opposite sides of the junction point. When the system consists of three or more catenary anchor legs, it is the familiar Catenary Anchor Leg Mooring (CALM) type of single point mooring.

B-7.1 Opposed 2 Catenary Anchor Leg Case

The simplest catenary anchor leg mooring system consists of two catenary anchor legs acting in opposition to each other. It will be used here to illustrate the method of superpositioning the catenary anchor leg force-deflection curves.

Figure 9A shows a single catenary anchor leg with its anchor to the left, and Figure 9B shows its force-deflection curve. This will be called the left anchor leg. Figure 9C shows a single catenary anchor leg with its anchor to the right, and Figure 9D shows its force-deflection curve. This will be called the right anchor leg. The two catenary systems are identical as to unit weight, length ,and depth., and thus their force deflection characteristics are identical.

Figure 10A shows these two catenary anchor legs joined together at a junction point. In joining the two catenary systems together, the initial deflection of the left anchor leg is D_{Li} and

the initial deflection of the right anchor leg is D_{Ri}. In the absence of any other force on the junction point, the initial forces exerted by these catenary anchor legs are equal and opposite, $F_{Ri} = F_{Li}$, and thus $D_{Li} = D_{Ri}$. Figure 10B shows the superpostion of the two anchor leg force-deflection curves in this position in which there is no horizontal force on the junction.

Now let a force F_J be exerted on the junction point, to move it to the right through a deflection D_J, as shown in Figure 11A. The deflection of the left anchor leg is :

$$D_L = D_{Li} + D_J \tag{51}$$

And the deflection in the right anchor leg is :

$$D_R = D_{Ri} - D_J \tag{52}$$

B-7.2 Force-Deflection Curve for the Opposed Anchor Leg System

The force-deflection curve of the opposed catenary anchor leg system, achieved by superposition of the force-deflection curves of the left and right anchor legs, is shown in Figure 11B. The force on the junction at any deflected position is the difference between the forces in the left and the right anchor legs at that position.

The preferred method of solving for the opposed catenary case is to know the junction deflection D_J, and with knowledge of the initial deflections of the anchor legs, to solve for the corresponding anchor leg deflections. Then determine the corresponding forces F_L and F_R and use these to determine the force applied to the junction F_J.

The force in the left leg increases and the force in the right leg decreases, such that

$$F_J = F_L - F_R \tag{53}$$

Because of the non-linear nature of the catenary force-deflection curve, it is not possible to simply solve for F_J by Equation (53). That equation can be solved by using a trial value for F_L or F_R. If F_J is know and the objective is to find the corresponding value of D_J, this may preferably done by using trial values for D_J.

B-7.3 Opposed Multi Catenary Anchor Leg System

Figure 12 shows a plan view in which a number of catenary anchor legs connected together at a junction point. In this initial, undeflected junction position, the forces imposed by the various anchor legs are in balance at the junction.

A force is imposed on this multi catenary anchor leg system from the left. The anchor legs are numbered in a clockwise direction from this force-application direction. The respective anchor leg azimuth angles are designated γ_1 through γ_n from the direction of force application

Figure 13 shows this multi catenary anchor leg system with the junction deflected through a distance D_J by an imposed force F_J.

Thus the deflection of the top of a selected catenary anchor anchor n in its original plane due to junction deflection D_J is :

$$D_n = D_{ni} + D_J \cos \gamma_n \tag{54}$$

The horizontal force F_n in a selected catenary anchor leg n can be found from the force-deflection characteristics for that particular catenary anchor leg.

The horizontal force which produces the deflection can be found by vector summing the forces in all of the catenary anchor legs :

$$F_J = F_1 \cos \gamma_1 + F_2 \cos \gamma_2 + \ldots + F_n \cos \gamma_n \tag{55}$$

The total vertical force exerted on the junction point by all of the catenary anchor legs can also be found by simple summation :

$$F_{VJ} = F_{V1} + F_{V2} + \ldots + F_{Vn} \tag{56}$$

B-8 Solving the Combined Catenary and Single Anchor Leg Mooring

The combined catenary and single anchor leg mooring (CASALM) consists of a single anchor leg or riser connected from a buoy or a vessel at the sea surface down to a weighted junction point suspended above the sea floor and of catenary anchor legs extending from the junction to anchors on the sea floor. An elevation view of CASALM arrangement is shown in Figure 14.

Figure 15 shows this CASALM in a deflected position. As the top point or buoy is deflected to the side, the riser tilts and lifts up on the junction point. The deflection of the junction point is less than that of the top point. But the deflection and increased elevation of the junction point increases the forces in all of the anchor legs.

B-8.1 Force-Deflection Analysis of the Inelastic CASALM

In the undeflected position, the riser hangs straight down, the junction is directly under the buoy, and the catenary anchor legs extend in a symmetrical pattern about that junction to anchor points on the sea floor. In this analysis, all of the anchor points are in the same water depth and all of the catenary anchor legs are identical.

When a horizontal force F is applied to the buoy, it deflects to the side a distance Δ and the same force is transmitted to the junction. This causes the riser to tilt to an angle ρ. The riser length is designated by R. The horizontal deflection D_R of the top of the riser with relation to its bottom point (the junction) is then :

$$D_R = R \sin \rho \tag{57}$$

The junction elevation above the sea floor is designated by E_J. As the riser tilts, the junction is lifted by a distance

$$E_J = R\,(1 - \cos \rho) \tag{58}$$

This horizontal force also causes the junction to deflect horizontally with respect to the sea floor through a distance D_J. Thus the total horizontal deflection of the top of the riser, called the buoy, from its initial position is :

$$D_B = D_J + D_R \tag{59}$$

The horizontal deflection of the junction causes the top of each of the catenary anchor legs to deflect. The horizontal deflection of an anchor leg designated by the subscript n is :

$$D_n = D_j \cos \gamma_n \tag{60}$$

The horizontal force in that particular anchor leg is then determined by the applicable catenary equations.

The sum of horizontal forces in the anchor legs acting on the junction must be in equilibrium with the applied horizontal force F. For anchor leg n, designate the top total (tangential force as f_n and the top angle from the horizontal as θ. Then by summing the horizontal forces on the junction :

$$F = \Sigma f_n \sin \gamma_n \cos \Theta_n \tag{61}$$

The vertical forces acting on the junction must also be in equilibrium. The vertical force in the riser is the horizontal force times the tangent of the riser angle. This must equal the sum of the vertical forces applied by the anchor legs, such that :

$$F \tan \Phi = \Sigma f_n \sin \Theta_n \tag{62}$$

The above equations are sufficient to solve the non-elastic CASALM force-deflection characteristics. However, the interdependencies of these variables complicate the solution.

The riser angle ρ can be found by inverting Equation (62) :

$$\Phi = \arctan\left(\frac{F}{\Sigma f_n \sin \Theta_n}\right) \tag{63}$$

But the solution of this equation requires knowledge of both f_n and θ_n for each catenary anchor leg. The particular shape of and forces in each catenary leg depend upon knowledge of the position of its upper end, that is the junction point. The junction position is described by E_J and D_J. But E_J and D_J both depend upon the riser angle, as given in Equations (59), (60), and (61). Thus a trial and error solution must be accomplished.

B-8.2 Force-Deflection Analysis of the Elastic CASALM

If the riser and/or the catenary anchor legs are elastic, then the solution of the CASALM can be much more complicated. The force-deflection characteristics of each element of the system must be considered.

Figure 16 shows the effect of stretch of the riser due to the increased tension caused by the deflection of its top. The change in riser length is ΔR. This change in riser length allows the deflection of the junction point to regress by a distance ΔD_J. And it allows the junction elevation to depress by a distance ΔE_J.

These changes in the junction point position necessitate recalculation of the forces in the anchor legs. And this results in a decrease in both the horizontal and vertical forces exerted on the junction. As a result, the tension in the riser decreases.

Thus a trial and error solution involving not only the forces exerted on the displaced junction point by the anchor legs but also the change in length of the riser must be accomplished.

August 20, 1997

TABLE 1 DEFINITIONS OF TERMINOLOGY AND VARIABLES

TERM		DEFINITION
anchor leg azimuth angle	γ_n	angle from direction of force application to anchor leg n of CALM in plan view
anchor point	a	the point at which a segment is anchored to the ground
anchor to top distance	X_{at}	distance between anchor point and top of catenary
base deflection	D_b	the deflection of the base point from the undeflected position
base point	b	the lowest point on the complete catenary curve (subscript)
base to anchor distance	X_{ba}	distance from catenary generation point to anchor point
base to anchor scope	S_{ba}	scope of phantom anchor leg from base to anchor point
bottom vertical force	V_{mb}	the vertical force on the bottom of the segment extending between points m and n
buoy deflection	D_b	deflection of CASALM buoy (total CASALM deflection)
CALM junction deflection	ΔD	Deflection of junction (CALM)
CASALM deflection	Δ	deflection of riser top or buoy of CASALM
catenary parameter	C	catenary parameter, the vertical distance from the generation point to the base point
catenary system top elevation	E_t	elevation of top of upper segment above ground plane of a multi-segment catenary system
catenary system top elevation	E_t	elevation of top of upper segment above ground plane of a multi-segment catenary system
chain		the physical catenary material, may be chain, rope, cable, or other similar material
deflection	D	horizontal distance of a point on the catenary from the origin
distance	X	horizontal distance of a point on the catenary from the generation point
elevation	E	vertical distance of a plane or point from the ground plane
generation point		the point from which the catenary shape is mathematically "generated"
ground deflection	D_g	the horizontal measurement from the undeflected position to the ground point
ground	g	the surface upon which the unlifted chain rests (subscript)
ground deflection	D_g	the horizontal measurement from the undeflected position to the ground point

TERM		DEFINITION
ground plane		the horizontal plane through the point at which the catenary touches the ground
ground point		the point at which the catenary touches the ground
ground tangent case		the case in which the catenary is tangent to the ground
height	Y	the vertical distance of a point on the catenary above the generation point
horizontal force	H	horizontal force on the catenary (same at all points)
horizontal length	X_{mn}	the horizontal projected length of the scope of the segment between points m and n
imaginary tangent point	i	the point at which the imaginary portion of a segment is tangent with the imaginary base plane
initial leg force	F_{LI}	initial force in left (or right) opposed anchor leg
initial leg deflection	D_{ni}	initial deflection of nth leg of CALM
initial leg deflection	D_{LI}	initial deflection of left (or right) opposed anchor leg
junction deflection	D_j	deflection of CASALM junction point due to riser tilt
junction regression	ΔD_j	change in CASALM junction point deflection due to riser stretch
junction depression	ΔE_j	change in junction elevation due to stretch of riser
junction elevation	E_j	change in height of CASALM junction due to riser tilt
junction force	F_J	horizontal force applied to junction
junction lift	Δ_j	change in CASALM junction elevation due to riser tilt
junction weight	W_j	sinker weight at junction between two catenary segments
leg deflection	D_L	deflection of left (or right) opposed anchor leg
leg deflection	D_n	deflection of anchor leg n of CALM
length	l_{mn}	length of segment extending from point m to point n
lower segment		the segment extending from point 0 to point 1
middle segment		the segment extending from point 1 to point 2
midpoint distance	X_m	distance from catenary generation point to horizontal midpoint of real catenary
origin		the position of the undeflected catenary
phantom catenary		the continuation of a catenary beyond the bottom of the catenary segment extending to its tangent point with a horizontal plane
point force	P_m	the force (weight or buoyancy) concentrated at the connection point m
real catenary		that portion of a catenary segment which extends from its bottom to its top
riser angle	ρ	angle of tilted CASALM riser from vertical

TERM		DEFINITION
riser deflection	D_R	horizontal projection of tilted CASALM riser length
riser length	R	length of CASALM riser
riser stretch	ΔR	change in riser length due to its elasticity and tension
scope	S	distance along the catenary between two points
segment		a flexible tension member extending between two end points.
segment catenary parameter	C_{mn}	the vertical distance from the generation point to the base point for the segment between points m and n
segment length	L	length of chain (lifted and unlifted, in a catenary segment
slope	Θ	angle from the horizontal of the catenary at a point
tension, tangential force	T	the tension or tangential force in the catenary at a point
top	t	the upper end of the chain (subscript)
top deflection	D_t	the horizontal distance from the origin to the top
top elevation	E_t	the vertical distance of the top above the ground plane
top height	Y_t	the vertical distance of the top above the generation point
top vertical force	V_{mt}	the vertical force on the top of the segment extending between points m and n
undeflected position		the position of the catenary with no applied horizontal force
upper segment		the segment extending from point 2 to point 3
variable A	A	$2H/(wE_t)$
variable B	B	$(D_e/E_t)^2 + 2D/E_t$
variable Q	Q	ratio of applied horizontal force to product of water depth and unit chain weight, $H/(wE_t)$
vertical distance	Y_{mn}	the vertical projected length of the scope of the segment between points m and n
vertical force	V	vertical force on the catenary at a point
vertical junction force	F_{VJ}	sum of vertical anchor leg forces on junction of CALM
weight	w	unit weight of chain
weight (unit)	w_{mn}	weight per unit length of segment extending from point m to point n
zero-load point	z	the point at which the system of catenary touches the ground with no applied horizontal force

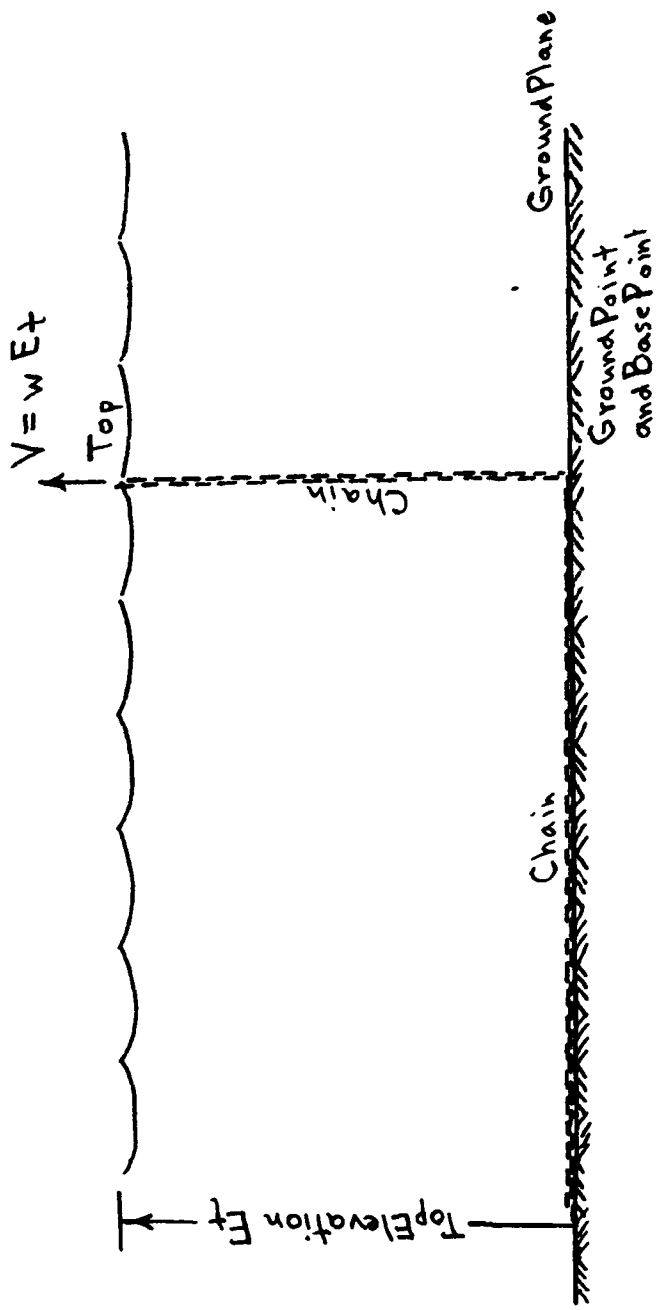

Figure 1. Undeflected position of catenary anchor leg, showing origin of new catenary equation coordinate system.

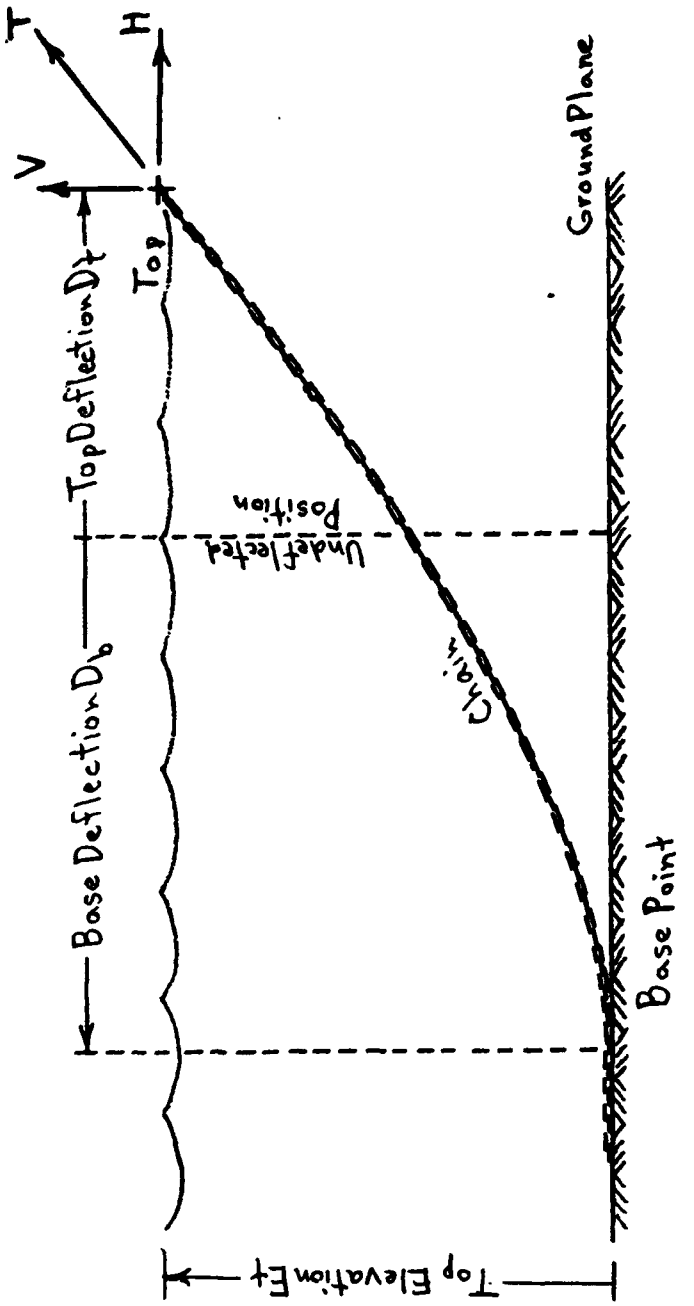

Figure 2. Deflected position of tangent catenary anchor leg, showing new catenary equation coordinate system.

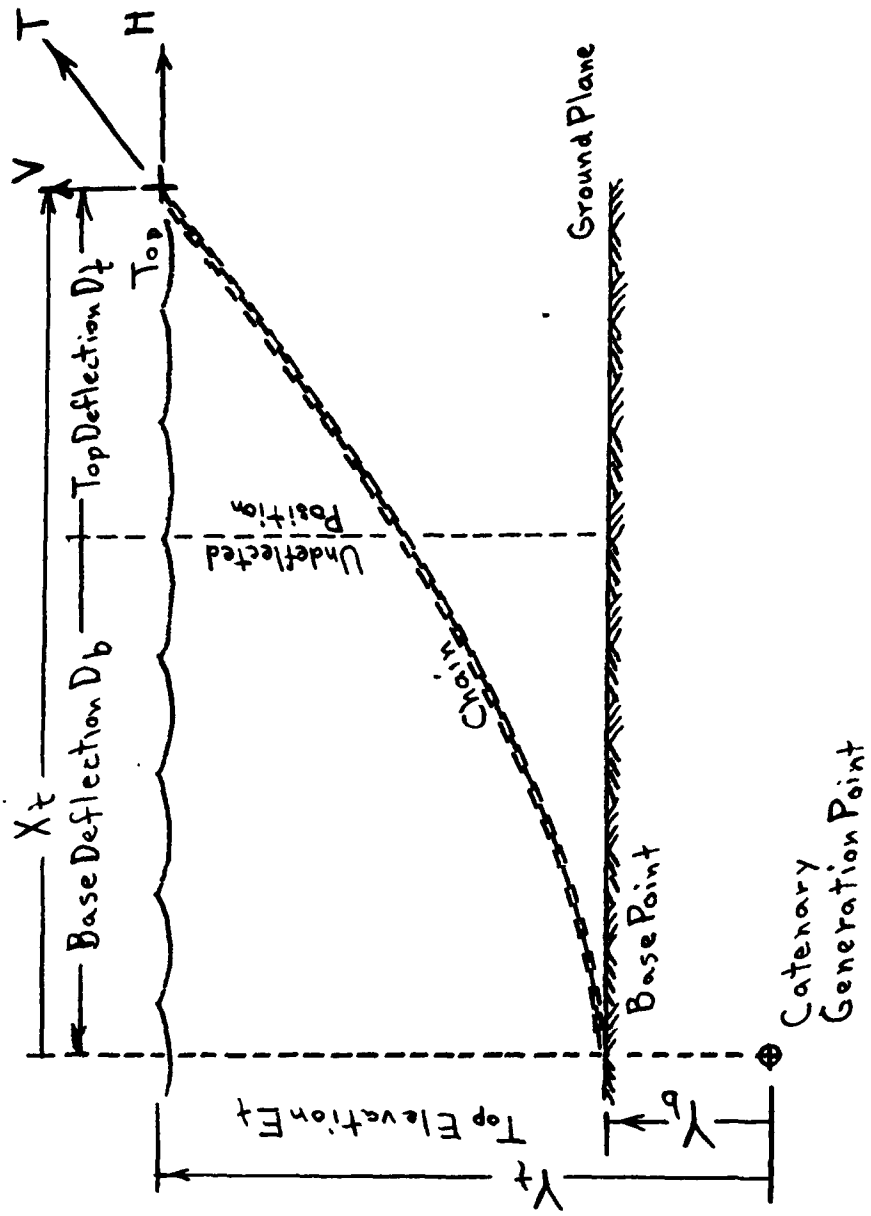

Figure 3. Deflected position of tangent catenary anchor leg, showing traditional catenary equation coordinate system.

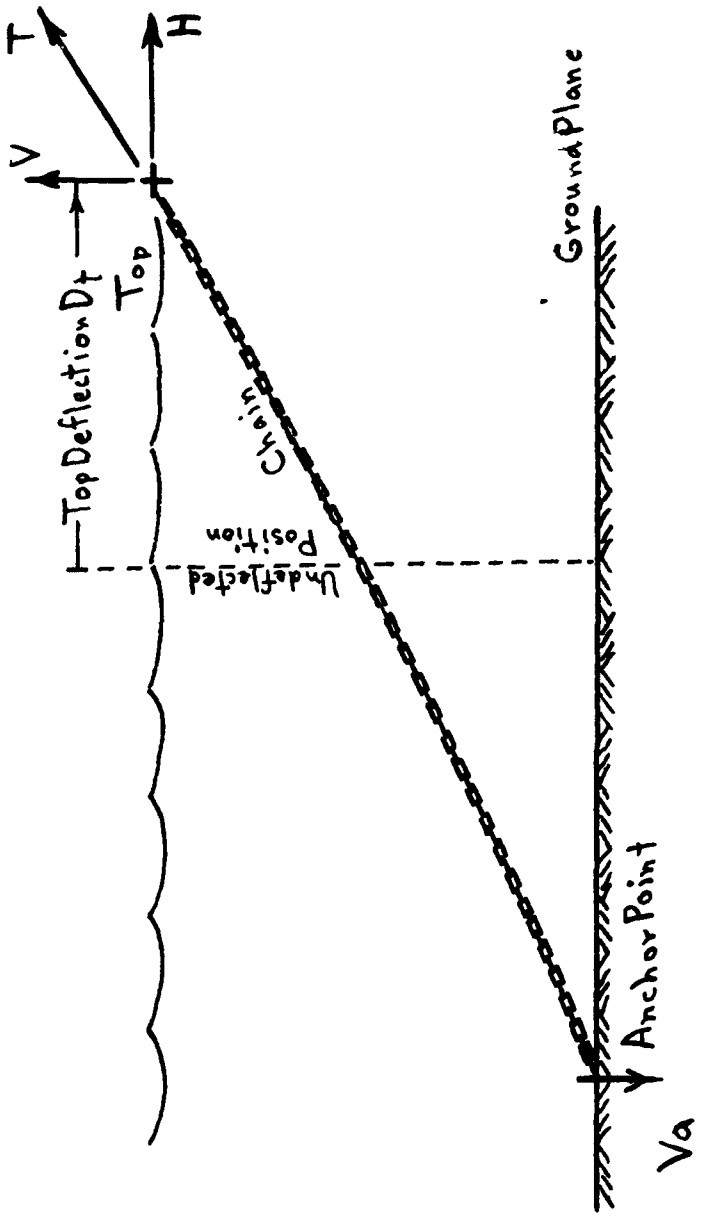

Figure 4. Deflected uplift catenary anchor leg.

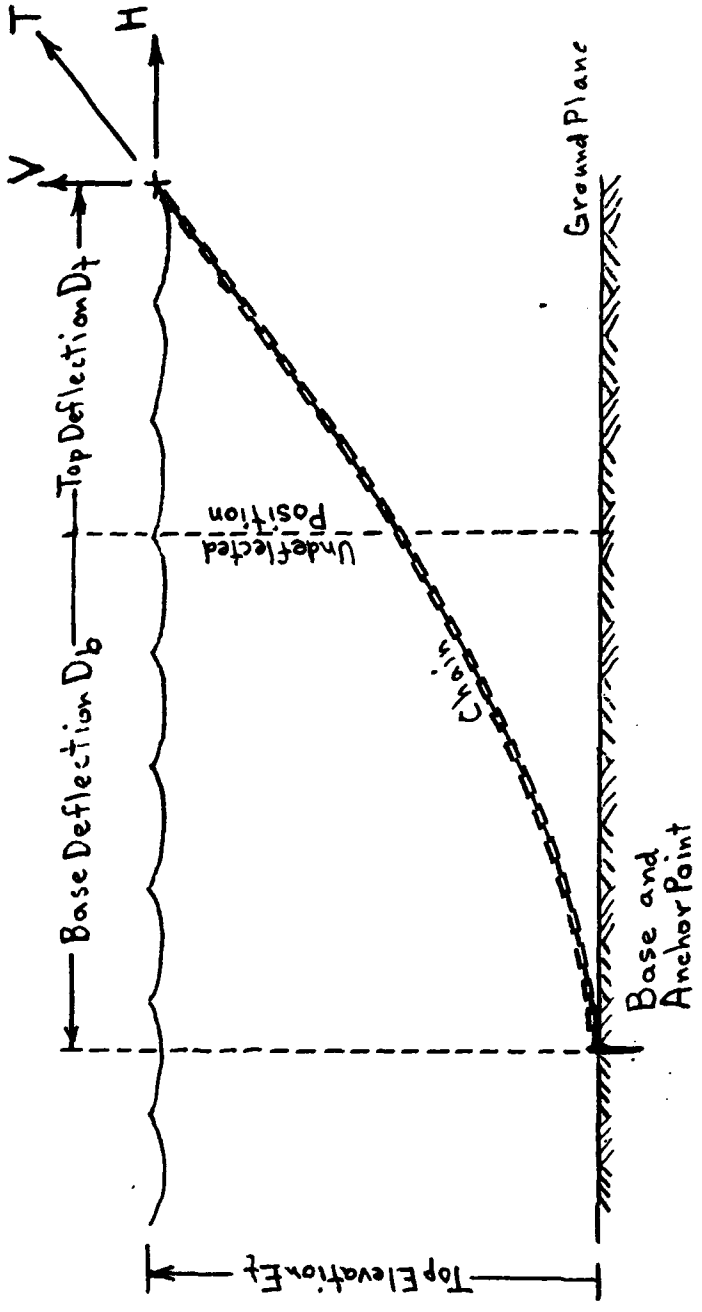

Figure 5. Deflected uplift catenary anchor leg at anchor point tangent position.

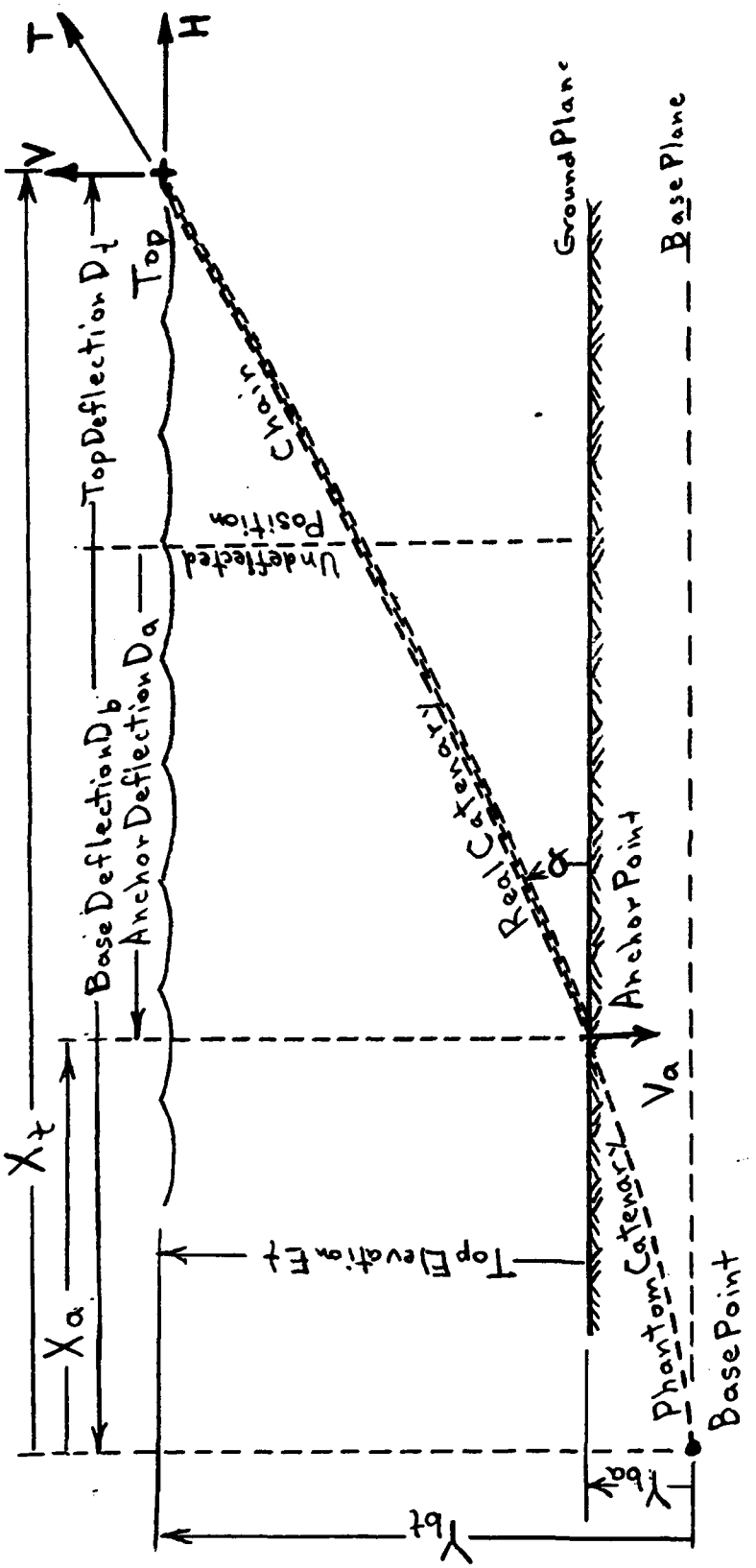

Figure 6. Deflected uplift catenary anchor leg imposing uplift on anchor leg, with base point beneath the ground plane.

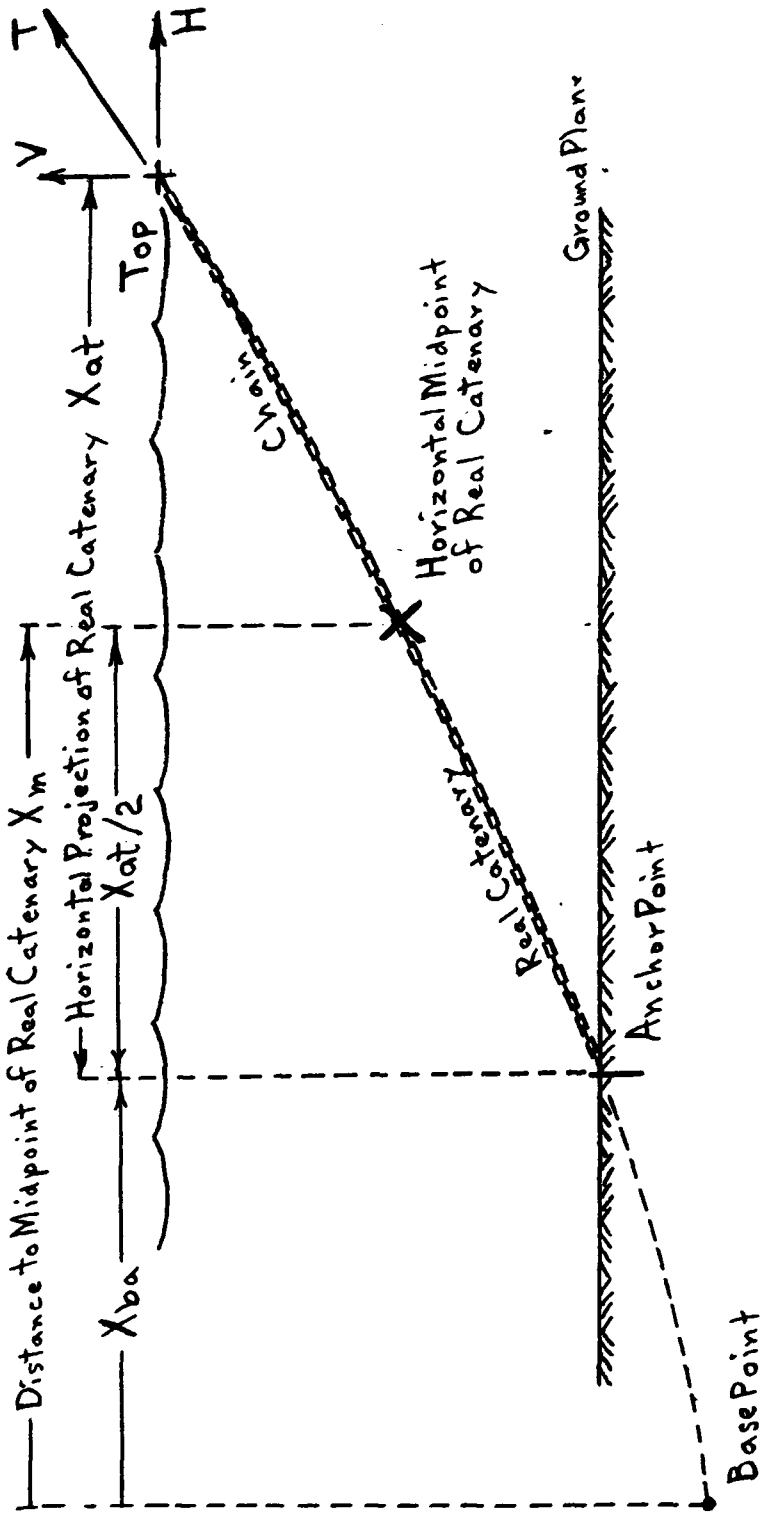

Figure 7. Distance from base point to the horizontal midpoint of catenary of real catenary and to the anchor point.

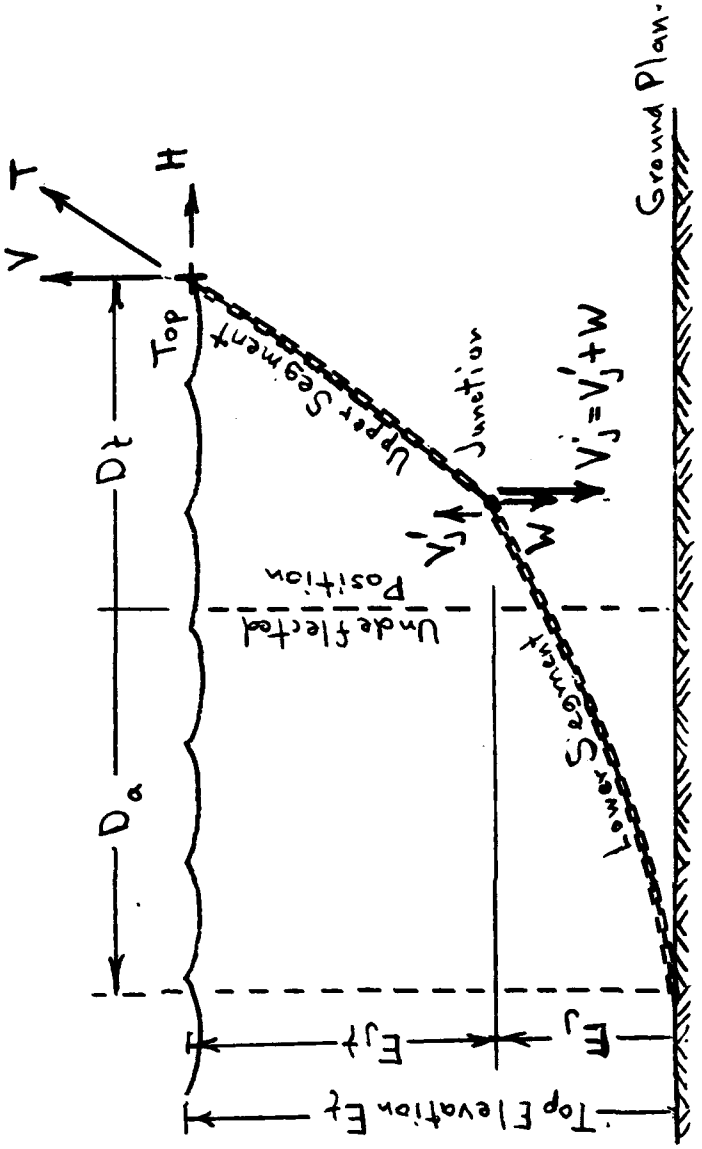

Figure 8. Solving multiple catenary segments in series.

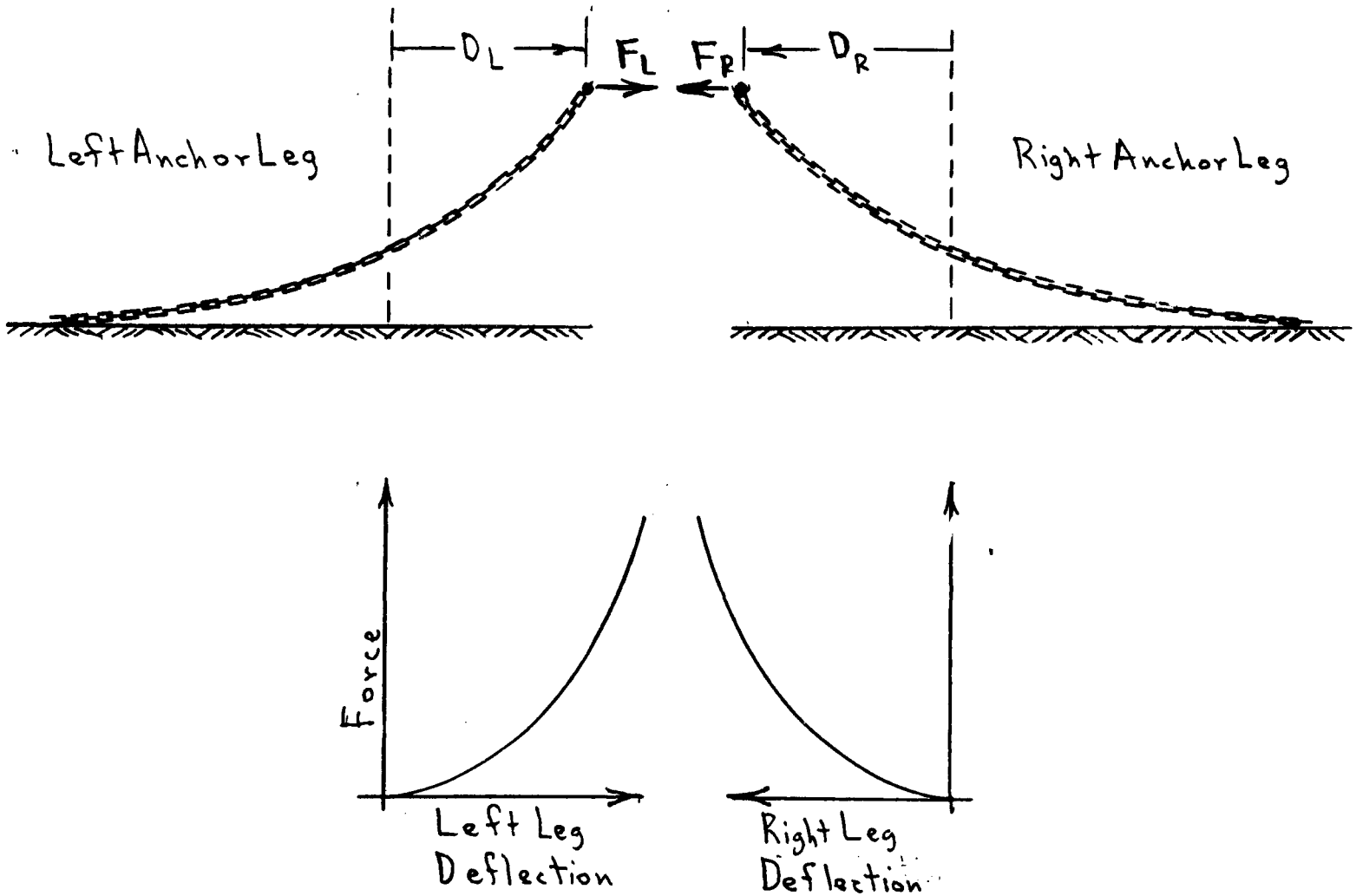

Figure 9. Opposed catenary anchor legs, left and right with force-deflection curves.

Fig 10

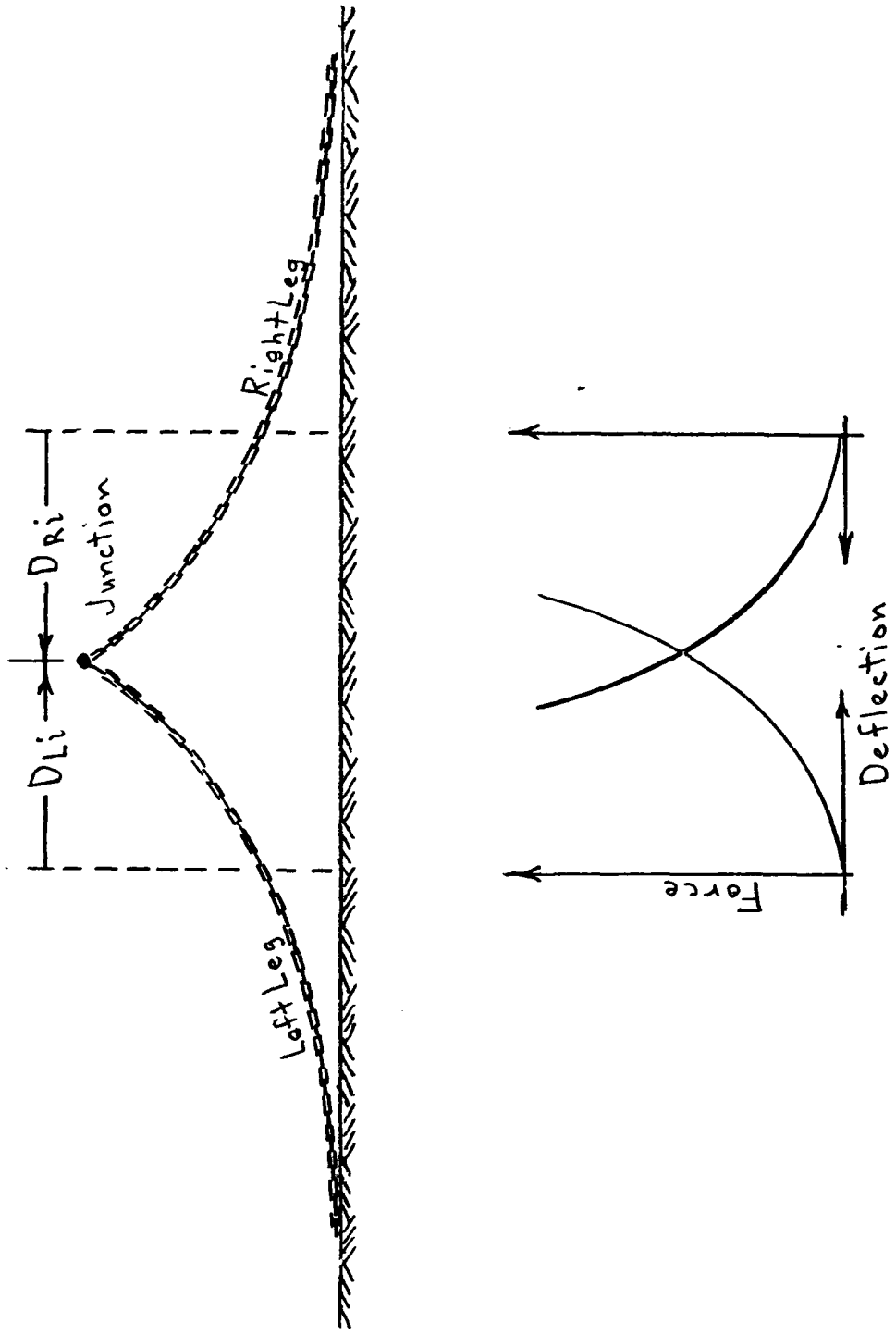

Figure 10. Opposed catenary anchor legs joined together at a junction.

Fig 12

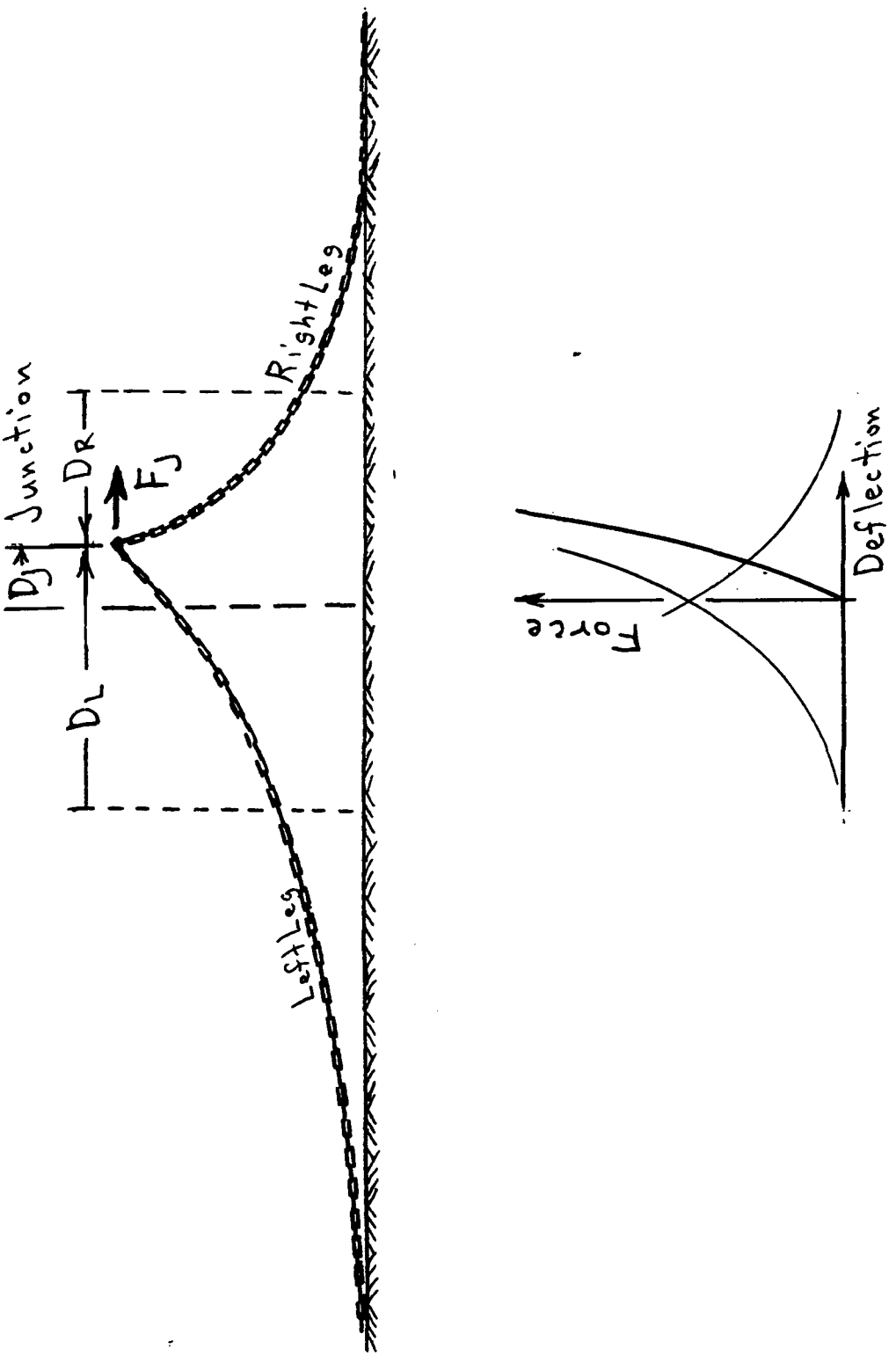

Figure 11. Opposed catenary anchor legs joined together with deflected junction showing superpositioning of force-deflection curves.

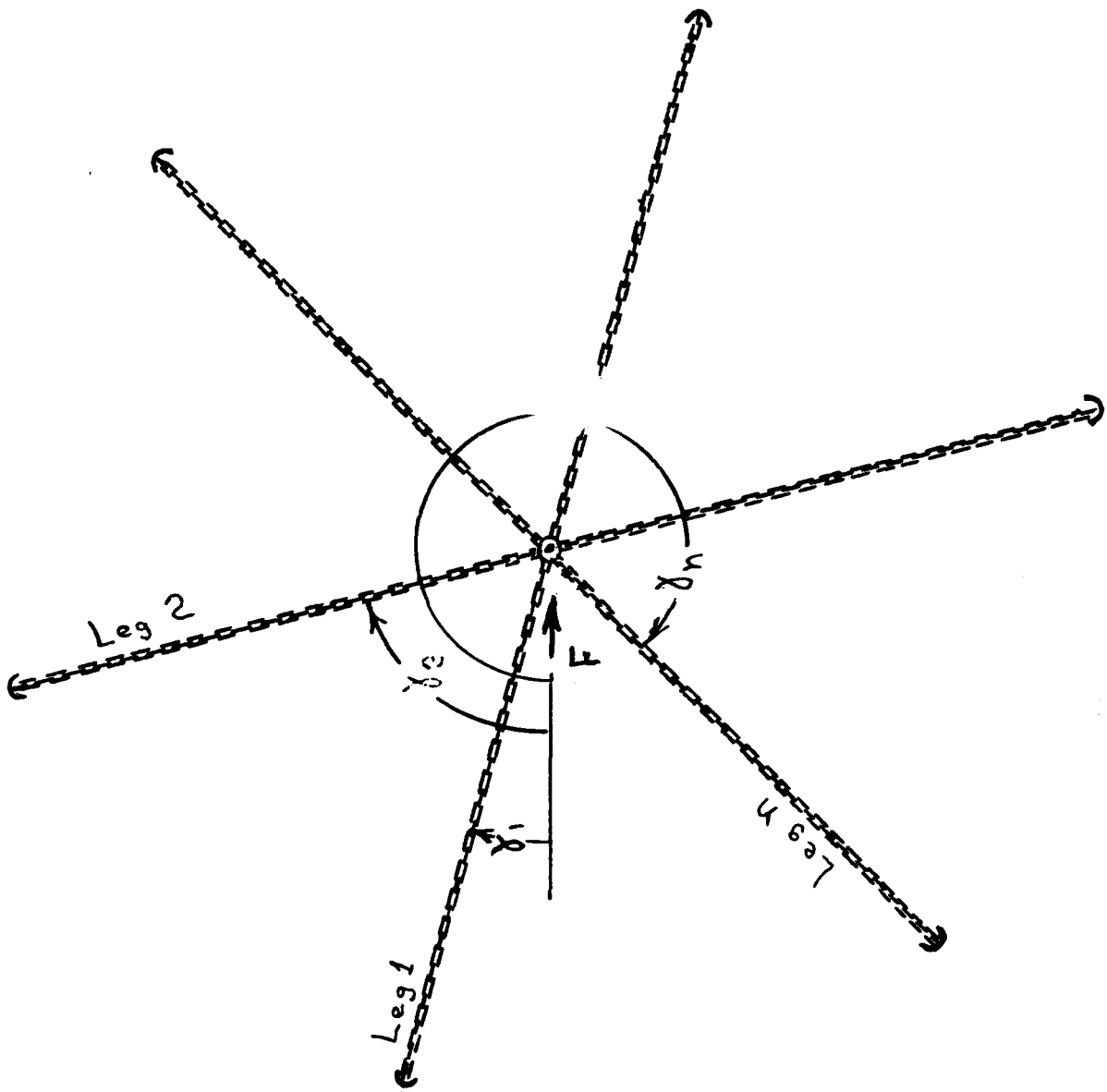

Figure 12. Plan view of multiple catenary anchor legs joined together at a junction.

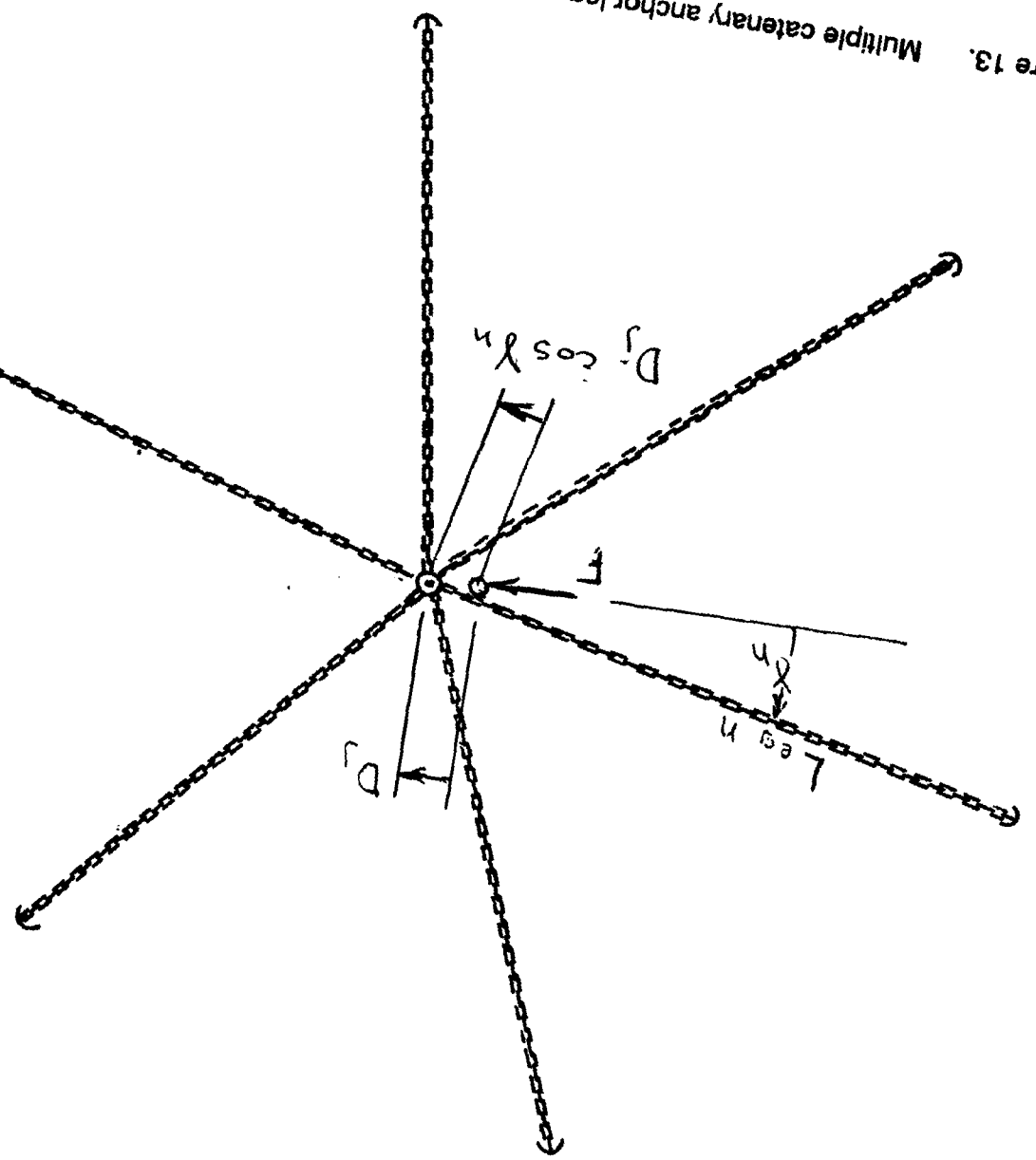

Figure 13. Multiple catenary anchor legs with deflected junction.

Fig 13

Fig 15

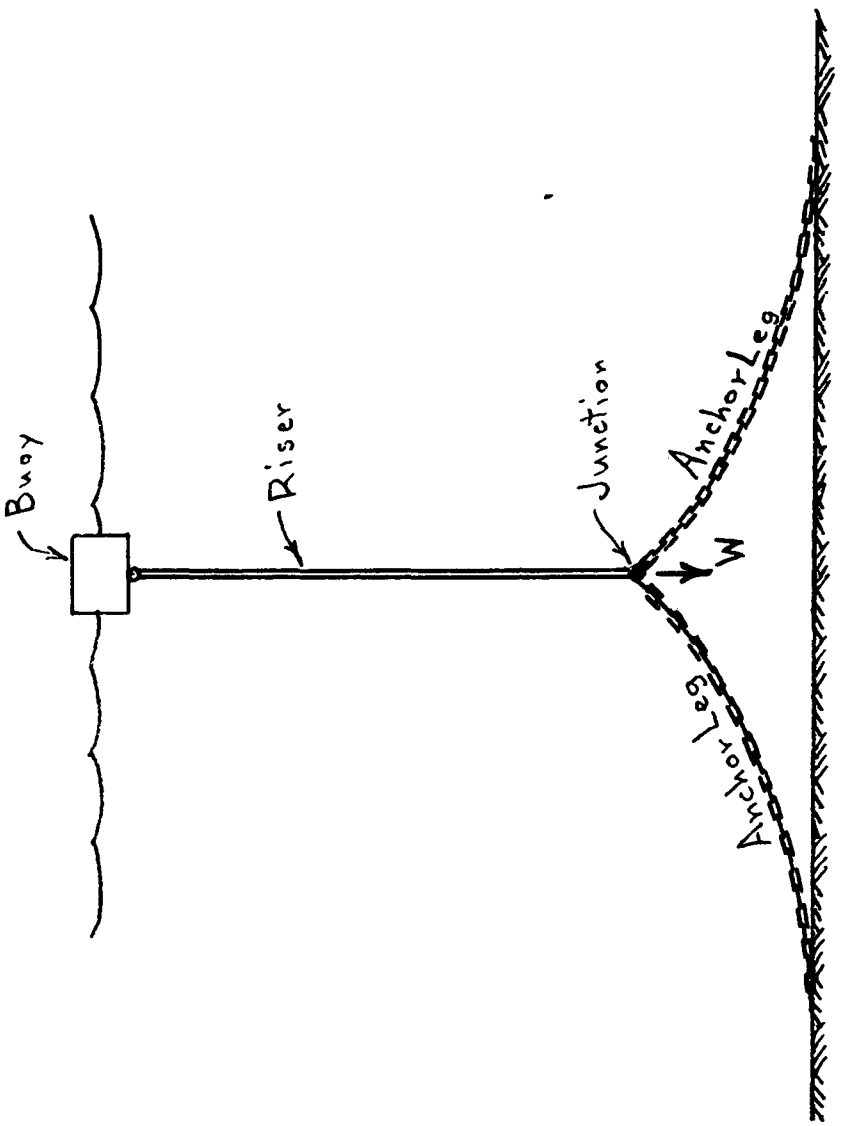

Figure 14. Elevation view of undeflected catenary and single anchor leg mooring.

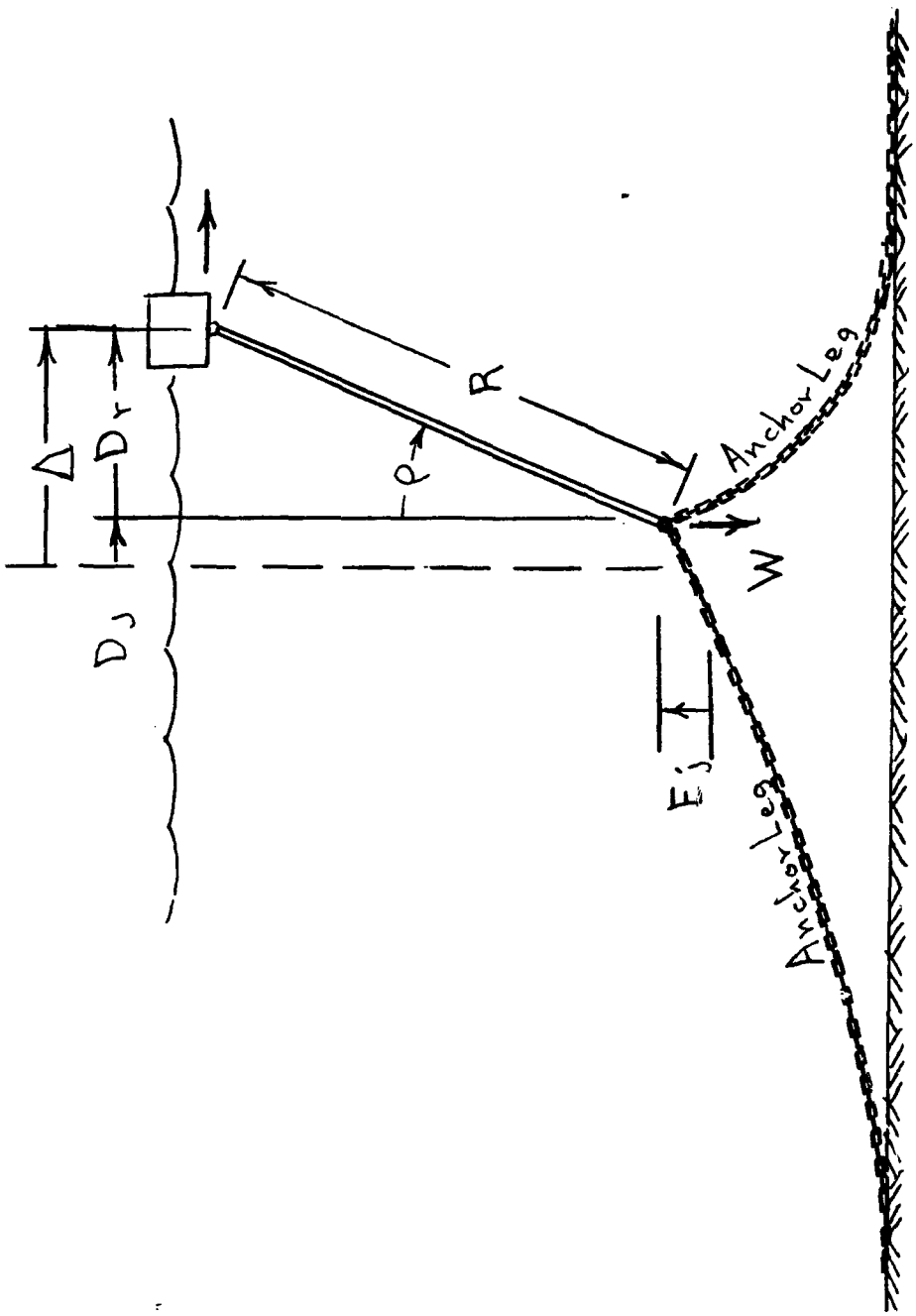

Figure 15. Catenary and single anchor leg mooring with deflected buoy, showing deflection and elevation of catenary junction point.

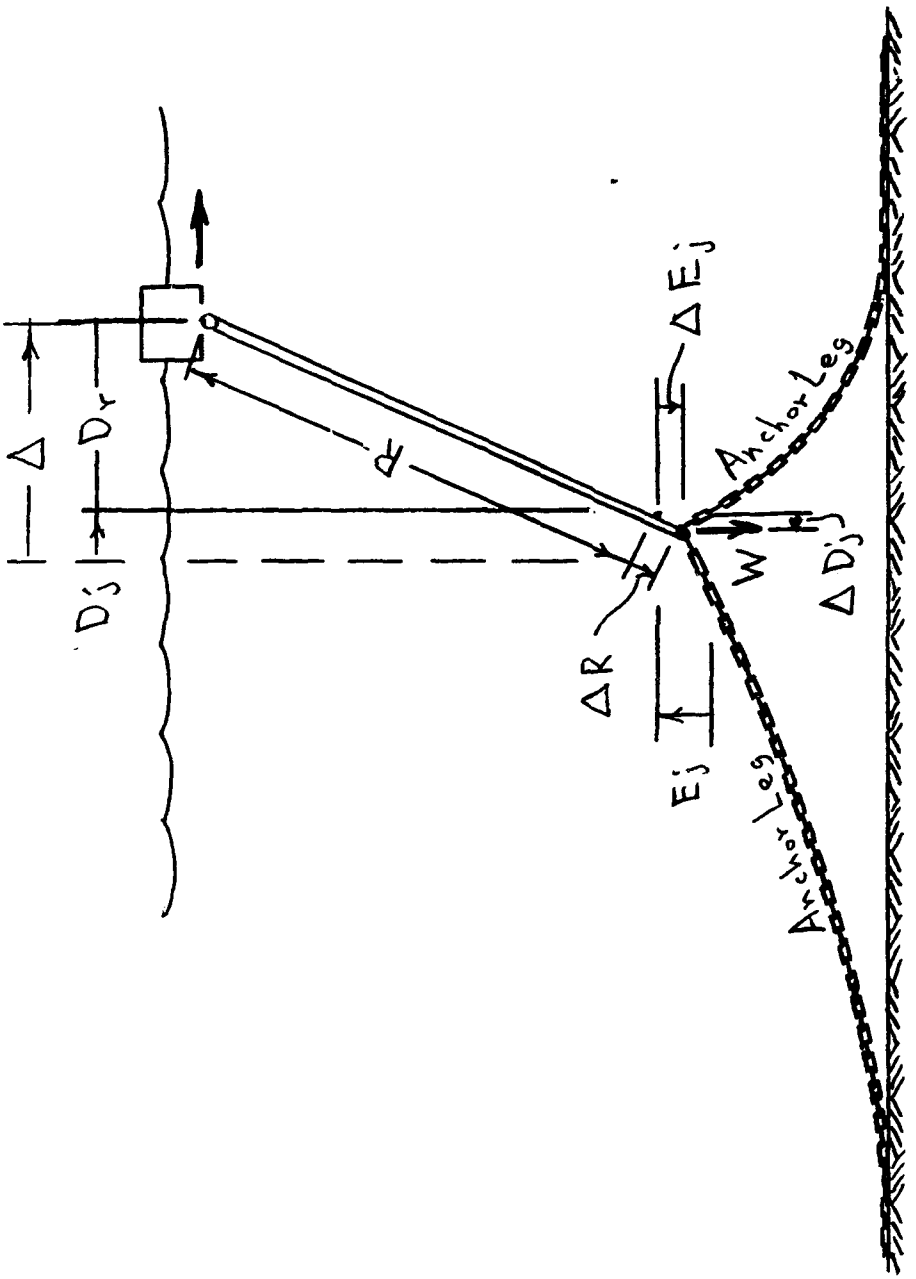

Figure 16. Catenary and single anchor leg mooring with deflected buoy and stretched riser, showing regression and depression of catenary junction point.

APPENDIX C

Description of the CASALM Computer Program

The CASALM Computer Program is written in Microsoft Visual Basic 3.

C-1 Visual Basic Language Files

The uncomplied program consists of five principal modules. These modules are described in detail in this memorandum. The Attached Flow Charts illustrate the execution of these modules. These principal modules are :

CASALM.BAS	: Sets
CASALM_F.BAS	: Calculates the horizontal force on the CASALM corresponding to an input buoy deflection.
CASALM_D.BAS	: Calculates the CASALM buoy deflection which results from an input horizontal force.
Jnctn_F.BAS	: Sums the horizontal and vertical catenary anchor leg forces on a junction.
SegmtCat.BAS	: Solves the force-deflection characteristics for a three-segment catenary anchor leg.

A number of other modules are used in calculating and displaying various output values:

CASALM.MAK	: A listing of the various modules used in generating the program (by Visual Basic)
CASALM_1.FRM	: A collection of various subroutines and also description of the various display screens (by Visual Basic)
TablCalc.BAS	: Calculates and displays ??
CASALMNT.FRM	: Displays notes on the CASALM Program
Cat_Grid.FRM	: Displays the initial (undelfected junction) parameters for the catenary anchor legs
DataPlot.FRM	: Calculates and displays a graph and a table of force vs CASALM deflection.
EnrgPlot.FRM	: Calculates and displays a graph and a table of firce vs energy.
Dynamic.FRM	: Calculates the dynamic response of the CASALM using an approximation technique.
File_Man.FRM	: Manages the data file save and retrieve functions on the menu.

The complete text of these files are given in Appendix D, which is bound with this Appendix C. The original files are included on the CASALM Mooring Analysis Computer Program distribution disk, which accompanies the primary report.

Table C-1 lists the Program Logic Markings which are used throughout these files to indicate Subroutines, GoTo statements Next statements, If statements, and other features.

C-2 CASALM Program General Outline

Figure C-1 shows the general outline of the CASALM program. At the start of the program, input data is provided and then checked for completeness and accuracy. The program then branches depending upon if Buoy Force **Fb** or Buoy Displacement **Db** was input.

If **Fb** is input, the program determines the buoy deflection, using the subroutine CASALM_F(Fb, Db). It then displays the resulting buoy deflection.

If **Db** is input, the program determines the buoy force which produces that deflection, using the subroutine CASALM_F(Db, Fb), and then it displays the result.

C-3 CASALM_F Subroutine

Figure C-2 shows the logic of the CASALM_F(Db, Fb) subroutine, which uses an input value Db for buoy displacement.

The subroutine sets a trial value for junction deflection and uses this together with Db to calculate the riser deflection Dr, riser angle Rho, and resulting junction elevation JncElv. It then sets a trial value for riser length.

Based on these values, the subroutine determines the Junction forces exerted by the catenary anchor legs for the particular junction elevation and junction deflection, calling on the subroutine Jnctn_F(Dj, Fhj, Fvj). With the resulting forces, the CASALM_F subroutine recalculates the riser length and checks this new value for agreement with the trial value. If the riser lengths don't agree, then the trial value is adjusted and the junction forces are recalculated.

If the trial and calculated Riser Lengths agree (within a set tolerances), then the riser angle, junction elevation, and riser deflection are recalcuated. The sum of the junction deflection Dj and the resulting riser deflection Dr are then checked against the input buoy deflection. If these don't agree, then the junction deflection is adjusted, and the calculation process is begun again.

If the deflection values agree, the CASALM_F subroutine is completed.

C-4 CASALM_D Subroutine

Figure C-3 shows the logic of the CASALM_D(Fb, Db) Subroutine, which uses an input value Fb for the Buoy Force. The subroutine converges on the corresponding junction elevation, though successive trials bound by upper and lower junction elevation limits.

The initial lower limit is the junction elevation in the undeflected position. The initial upper limit is based on the riser angle calculated with the horizontal input force applied at the top of the riser and the sum of the vertical anchor leg forces at the initial junction elevation and the junction weight applied vertically at the bottom of the riser. The final riser angle and thus the junction elevation will be less than this limiting value, because the vertical anchor leg forces increase as the junction elevation increases. A trial junction elevation is then set between these limiting values.

With the trial junction elevation established, a trial junction deflection is then set. This value is initially very small. The sums of horizontal and vertical forces are then determined for the trial junction elevation and deflection, using the JForce subroutine. The resulting sum of horizontal forces on the junction is then checked against the input buoy force. If agreement is not achieved, the trial junction deflection is adjusted, and the junction forces are recalculated.

When the sum of horizontal forces on the junction agrees with the applied buoy force (within a tolerance band), the subroutine then determines the new riser angle and the resulting junction elevation. The trial junction elevation is compared with the resulting junction elevation. If necessary, the trial junction elevation is adjusted, and the calculations are repeated.

The CASALM Subroutine is satisfied when both the junction elevation and junction deflection trial and resulting values agree within set tolerances.

C-5 Junction Force Solution, Jnct_F

Figure C-4 is a flow chart illustrating the Jnctn_F(Dj) Subroutine. This solution scheme is essentially that which is used for the Catenary Anchor Leg Mooring (CALM) at a fixed water depth. In this case, that water depth is the junction elevation, which is varied in sequential passes trough this subroutine.

The subroutine first sets the summation values to zero. It then indexes through the catenary anchor legs, from I = 1 to AnMax, the total number of anchor legs. For each anchor leg the subroutine determines its angle and then its top deflection based on that angle and the input top deflection.

If the particular anchor leg top is not deflected by the junction deflection (within a small tolerance band) , then the corresponding horizontal force is taken as that at the non-deflected junction position. This eliminates the need for calculating anchor leg forces in some cases.

If the particular anchor leg top is deflected in the negative direction beyond its slack position, then the horizontal force in that leg is zero and the vertical force is equal to the suspended weight of anchor leg at the present junction elevation.

Otherwise, the SegmCat subroutine is called upon to calculate the horizontal and vertical forces at the top of the particular anchor leg.

After determining the horizontal and vertical forces for the particular anchor leg, the Jnctn_F subroutine adds these to the sum of previous values. It also checks the horizontal force to determine if it is greater or less than the previous maximum or minimum value respectively, and then it adjusts the maximum or minimum value if necessary.

After all anchor legs have been analyzed, the Jnctn_F subroutine is satisfied.

C-6 Solving the Catenary Anchor Leg, SegmtCat

The SegmtCat subroutine calculates the force-deflection characteristics of a three-segment catenary anchor leg with weights at the connections between segments. The catenary anchor leg solution is a complex process, involving several steps. The subroutine can accept an input value for either the horizontal force Ht, the tension force at the top of the leg Tt, or the deflection at the top of the leg. As input, only one of these values is defined. The subroutine then calculates the other two parameters as output. As employed in the CASALM program, SegmtCat only handles top deflection as input, and thus the other two options have not been extensively verified.

Figure C-5 shows how the SegmtCat subroutine deals with the various possible input data situations.

The subroutine calculates the vertical force corresponding to the slack position (no catenary top deflection) at the defined junction elevation, based on the weights of sinkers and lengths of segments lifted off the sea floor accounting for segment stretch. This sets a minimum vertical force VfMin. The subroutine calculates a maximum tension force Tfmax corresponding to the strength of the weakest component. These values are then used to calculate a pseudo maximum horizontal force HfMax which serves as an upper bound for subsequent solutions.

The subroutine then checks for the validity of the input value. If a non-zero value for Hf is input then this is the governing input and other input values are ignored. If Hf is not defined, but a non-zero value for Tf is input then this is the governing input and any input for Dt is ignored. Otherwise a non-zero value for Dt is the governing input. If all input values are zero, then the slack case is assumed.

The subroutine seeks a solution which satisfies an input value for the top deflection, Dt. The basic solution scheme is to assume a trial value for Hf and to adjust this value until the desired value of Dt is achieved.

The values of Hf and Dh corresponding to that position in which the catenary anchor leg is tangent at its anchor leg are determined. In this position, the top vertical force is known to

equal the sum of weights of all of the segments and sinkers. The initial trial value for Hf is then calculated based on linear interpolation to that known condition

HfTrial = Dt * HfTan / DhTan

With a trial value Hf for the applied horizontal force, a trial vertical force is then assumed. That trial force is determined by linear interpolation between the ...

VfTrial = Hf * (VfTan - VfMin) / HfTan + VfMin

With a trial value for Vf the program then proceeds to solve the Multi-Segment Catenary. That routine is shown in Figure C-6. The segments are numbered sequentially from the bottom or sea floor end. Not all segments need be defined, and if a segment is not defined, the program skips over the solution pertaining to that particular segment.

If the upper segment 3 is defined, the program determines if there is a vertical force Vf3b at the bottom of that segment. If Vf3b is less than or equal to zero, then segment 3 is tangent to the sea floor, and the program proceeds to sum the vertical projected segment lengths.

If Vf3b is greater than zero, then there is uplift on the sinker 2 between segment 3 and segment 2, and the program solves the uplift case for the upper segment to determine the vertical projected segment length Y23. The program adds the upper sinker weight to Vf3b in order to determine the vertical force Vf2t at the top of segment 2.

In like manner, the program determines if segment 2 is defined, and then proceeds to solve for Vf2b and Y12. It then adds the weight of the lower sinker to determine the vertical force Vf1t on the top of the lower segment 1.

And then in like manner, the program determines if segment 1 is defined and then proceeds to solve for its vertically projected height Y01.

The vertical projected segment heights are then summed and compared with the junction elevation Y. If the values do not agree (within a tolerance band), then the trial value for Vft is adjusted, and the procedure is repeated.

When vertical projected segment length convergence is achieved on the junction elevation Y, the subroutine then proceeds to solve for the horizontal projection of the lifted segment lengths. This procedure is illustrated in Figure C-7.

If segment 3 is defined and is tangent, then it is only necessary to determine the horizontal projected length of that segment before proceeding to check for the resulting horizontal deflection. If segment 3 has a vertical bottom force, then the horizontal projected length of that segment is calculated.

In like manner, the program determines and calculates the horizontal length properties of segment 2 and then of segment 1.

The horizontal projected lengths of the segments are summed, the initial sum of horizontal projected lengths for the anchor leg is subtracted, and this result is compared with the trial horizontal deflection. If the values do not agree (within a tolerance band), the trial value of Hf is adjusted, and the Multi-Segment Catenary Solution procedure (top of Figure 6) is begun again.

Full convergence is achieved when the vertical projected segment lengths agree with the junction elevation and the horizontal projected segment lengths agree with the horizontal deflection Dt of the top of the catenary anchor leg. When this is achieved, the subroutine proceeds to calculate other parameters of interest. The subroutine is then satisfied, and the program returns to the Jnct_F subroutine.

flowchrt.mem:August 18, 1997

Table C-1 Programming Conventions

```
Sub Name ()   '<<<<<<<<<<<<<<<<<<<<<<<<<<<< NAME
'  Date
'  Program Name
...
End Sub       '>>>>>>>>>>>>>>>>>>>>>>>>>>>> NAME

' ___________________SECTION NAME_____________

Rem : _____________________________ Major Division

' --------------------------- minor division

Rem : Explanation

                'variable or step description

                                    'FUNCTION()

                                  'SUBROUTINE()

REPEAT#:            ''''''''''''''''''''''''''''''''''''''''''/-#-\
...
  GoTp REPEAT#      '''''''''''''''''''''''''/|#|\

  GoTo CONTINUE#    '......................\|#|/
...
CONTINUE#:    ':::::::::::::::::::::::::::\_#_/

For I         '==========================\=I=/
...
Next I        '++++++++++++++++++++++++++/+I+\

If (  ) Then    '??????????????????????????if?
...
ElseIf (  )     'eeeeeeeeeeeeeeeeeeee?else_if?
...
End If          'xxxxxxxxxxxxxxxxxxxx?end_if?
```

CASALM Solution

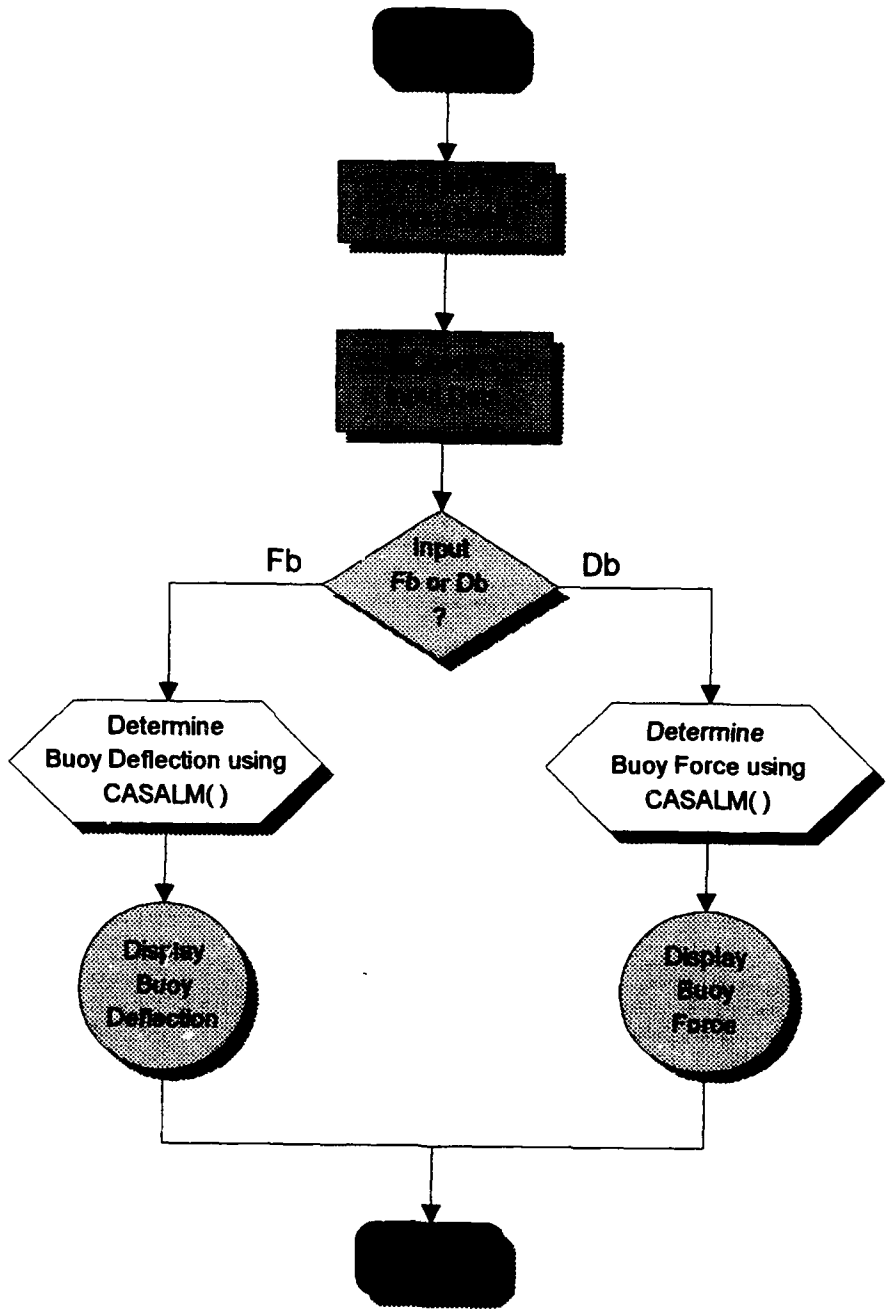

Figure C-1 General Flow of CASALM Computer Program

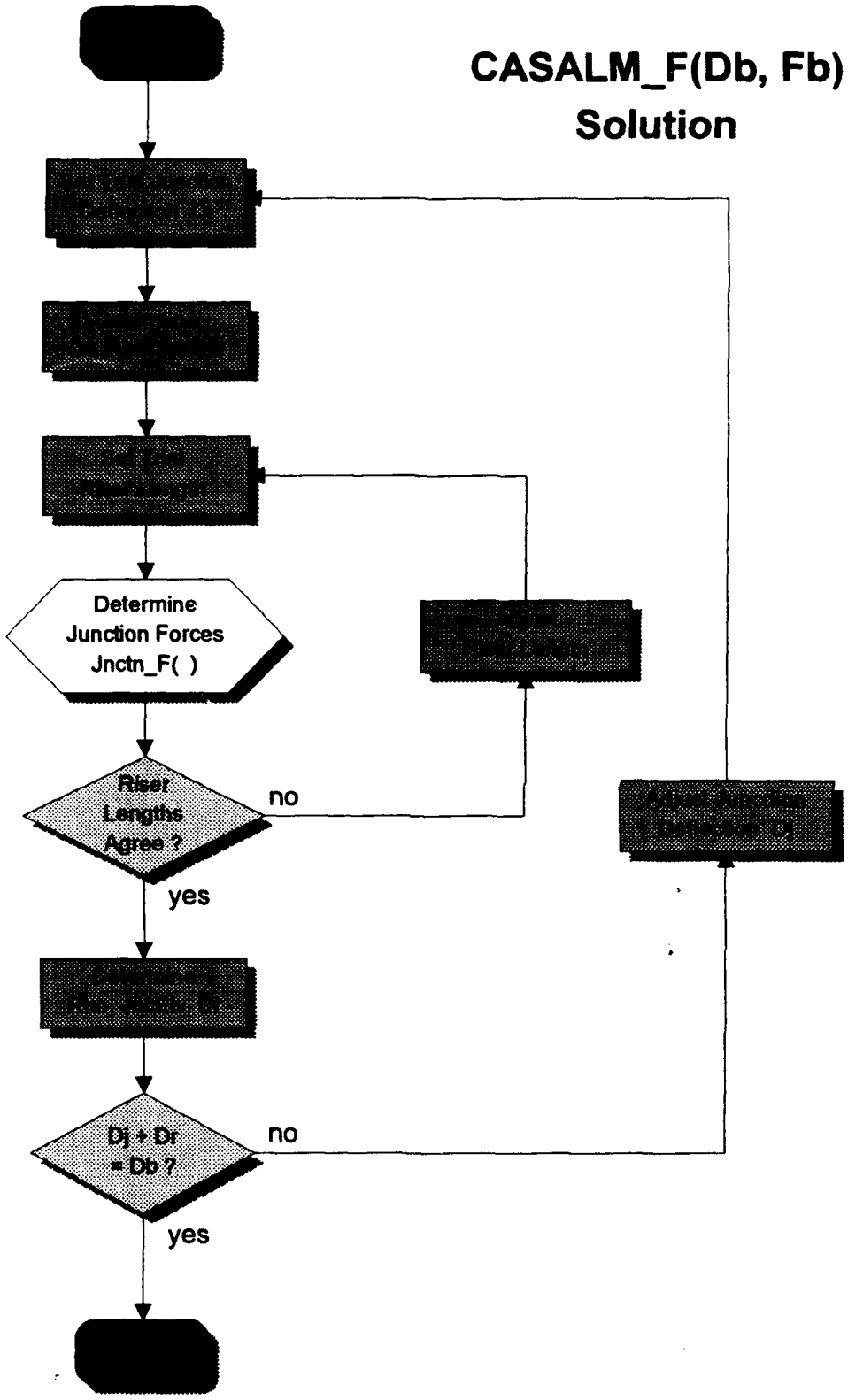

Figure C-2 Logic of the CASALM_F(Db, Fb) Subroutine

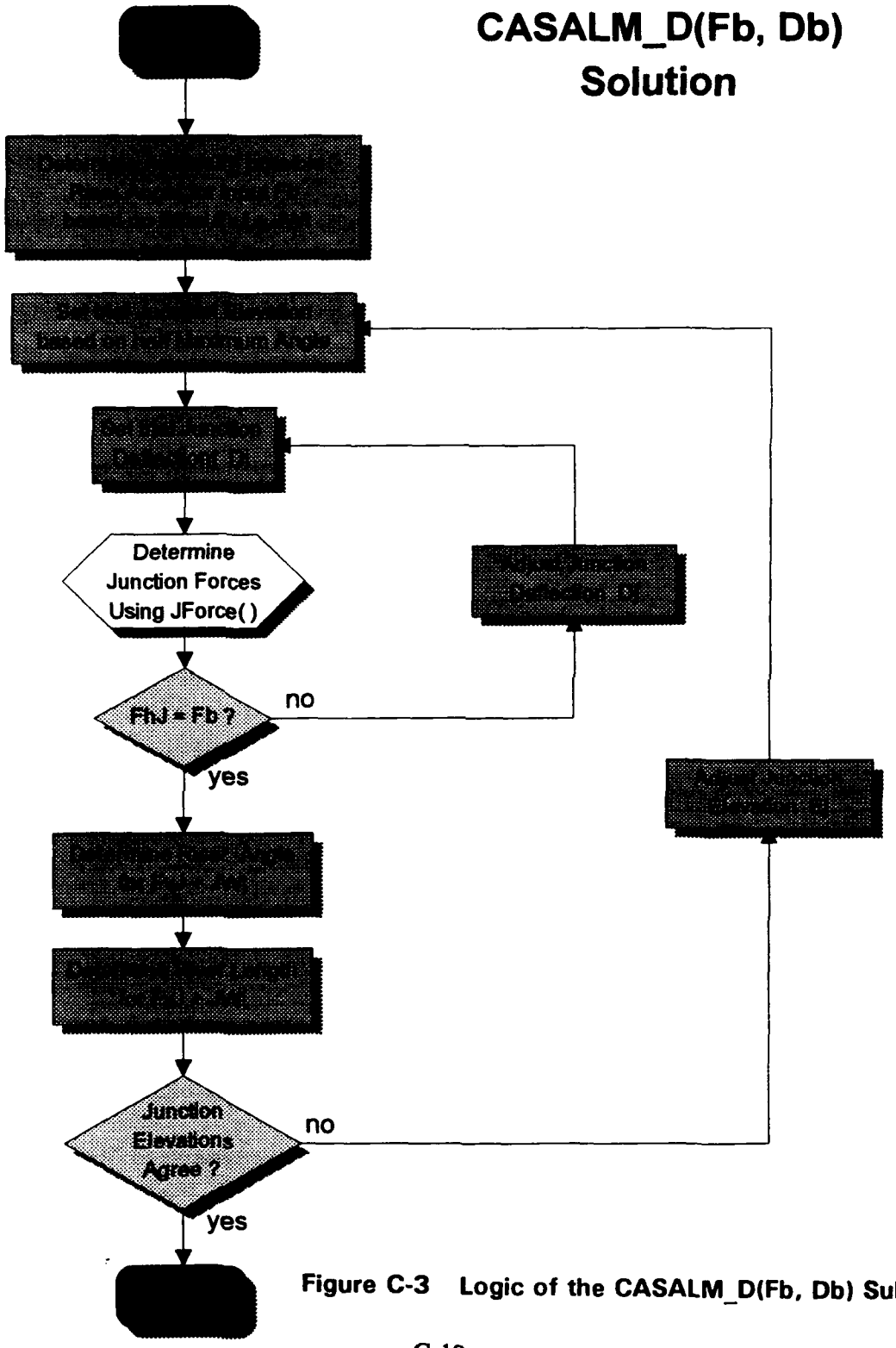

Figure C-3 Logic of the CASALM_D(Fb, Db) Subroutine

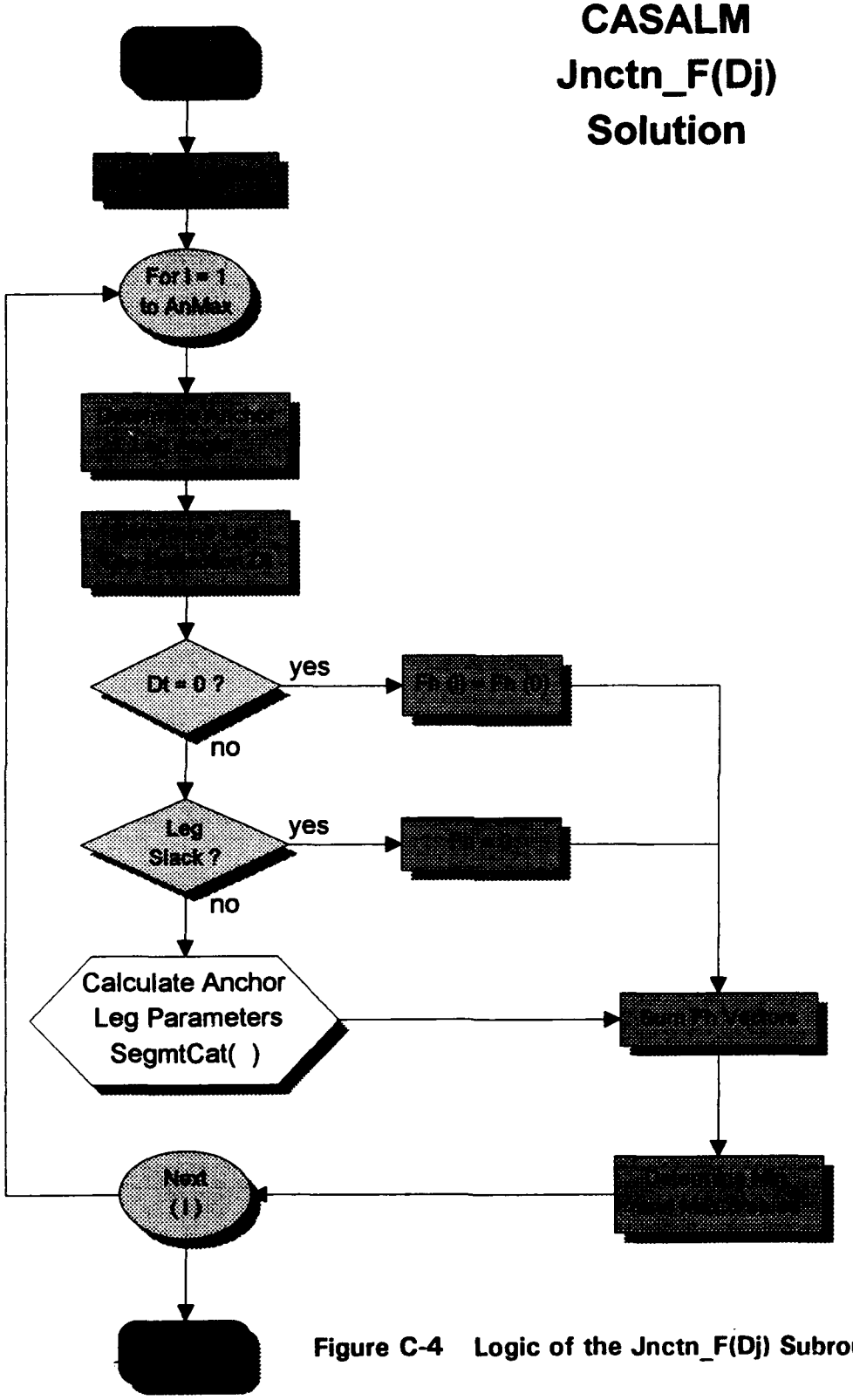

Figure C-4 Logic of the Jnctn_F(Dj) Subroutine

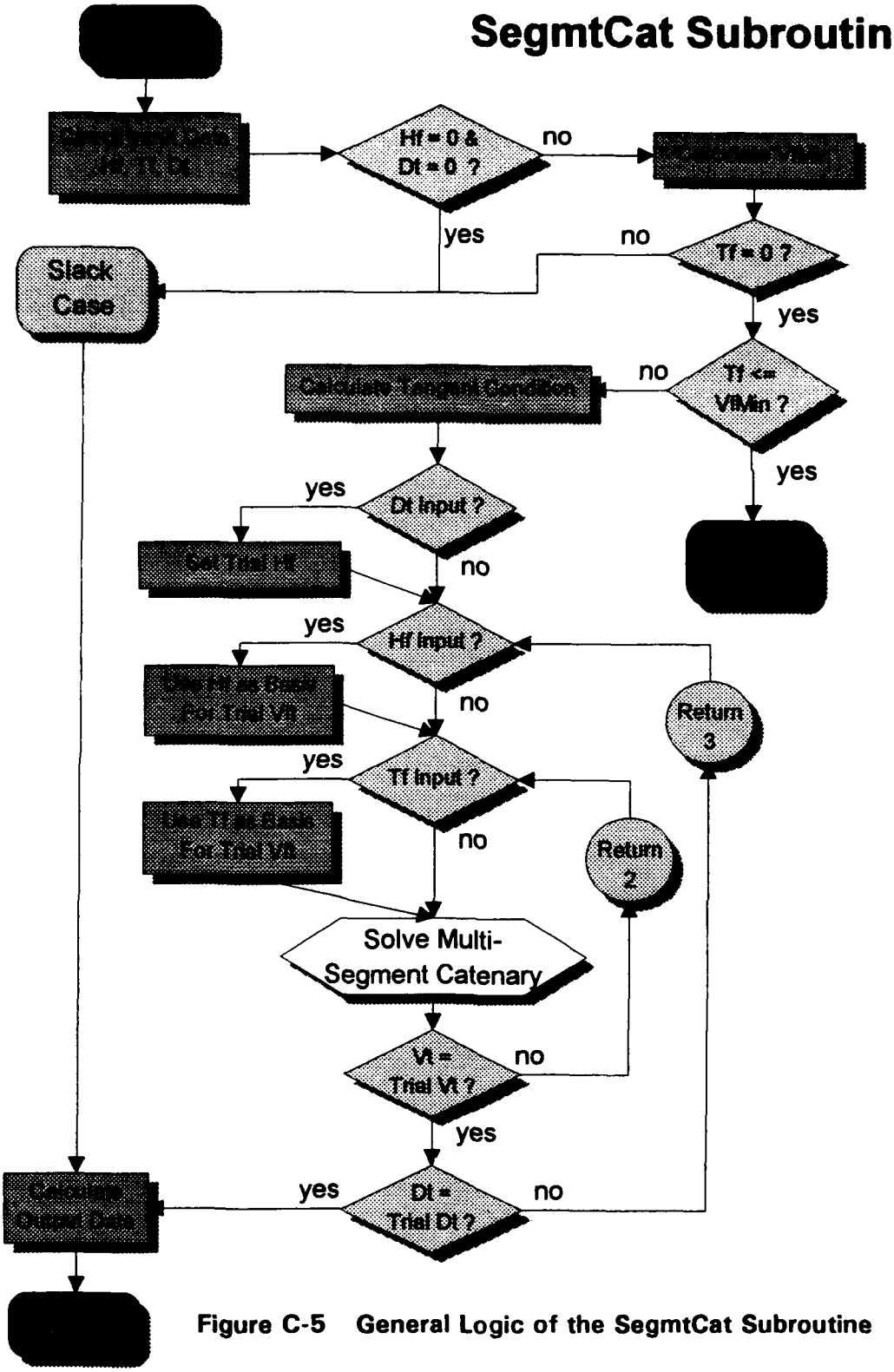

Figure C-5 General Logic of the SegmtCat Subroutine

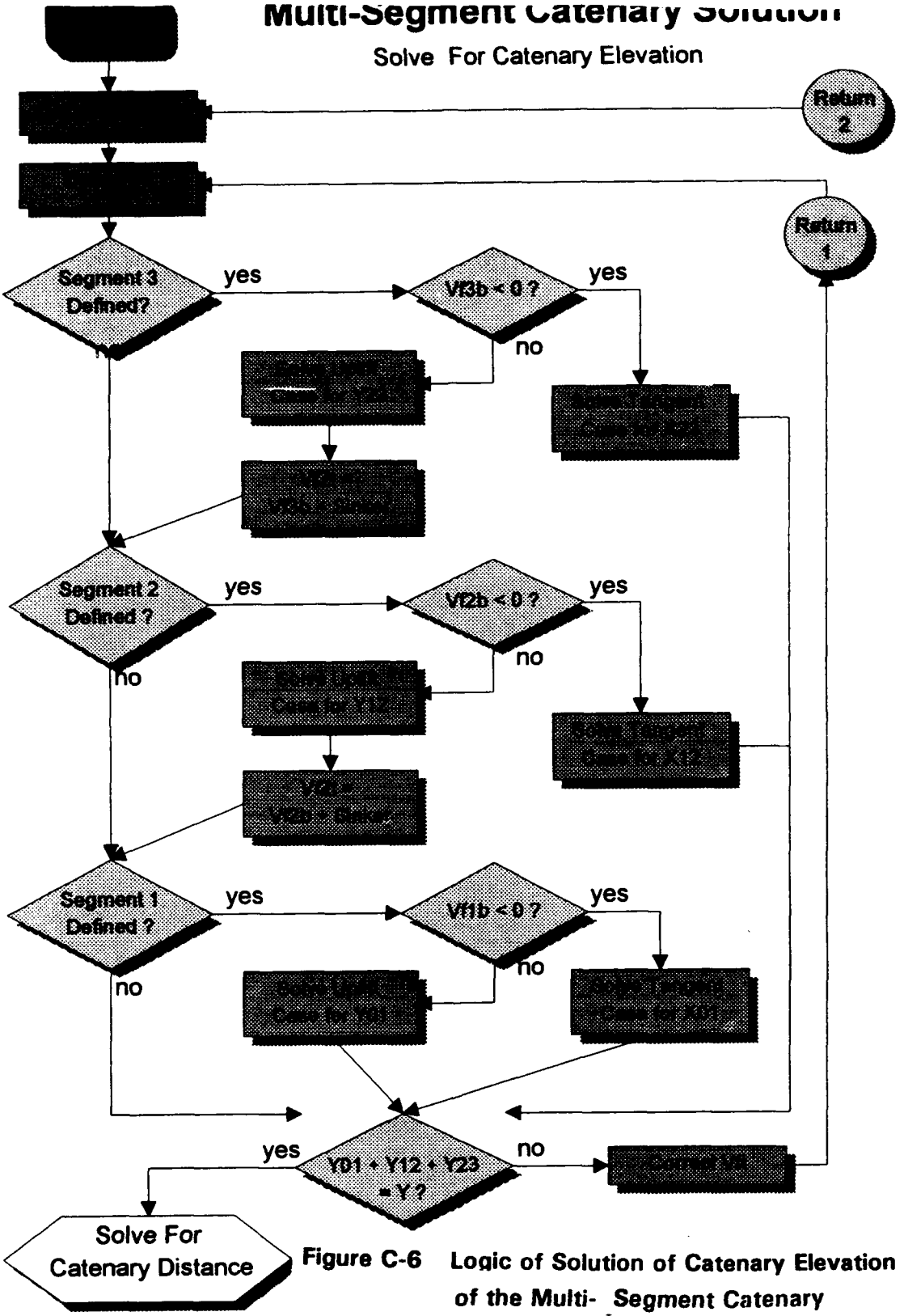

Figure C-6 **Logic of Solution of Catenary Elevation of the Multi- Segment Catenary (Within SegmtCat Subroutine)**

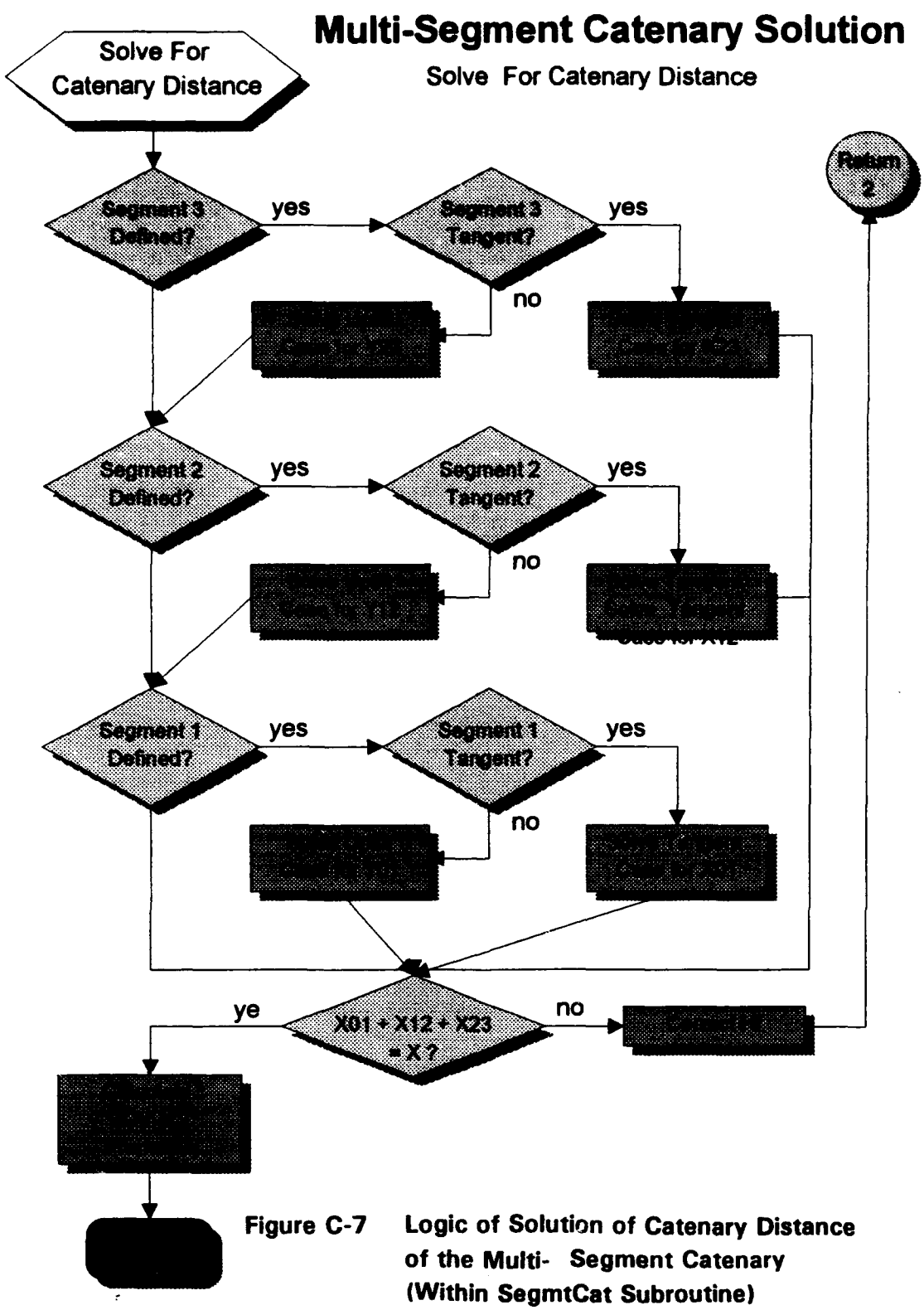

Figure C-7 Logic of Solution of Catenary Distance of the Multi- Segment Catenary (Within SegmtCat Subroutine)

APPENDIX D

Source Program for the CASALM Computer Program

The source program for the CASALM computer program may be found in Appendix A on the same disc as the CASALM Computer Program file. This is in a format that can be printed by most word processing software. The hardcopy output is 200 pages.

Two hardcopy documents were provided with the original and copy No. 1 of the final report. However, these were bound separately.

APPENDIX E

Mooring Line Technology

E-1 Introduction

This Appendix provides design and performance information for various types of tension members which might be used as mooring lines in a deep water mooring system. Emphasis is given to synthetic fiber rope mooring lines because performance data and other information is not widely known and well documented for these ropes. Such information for wire rope and chain information is better known and can be obtained from other sources, and thus, that information is only summarized in this report.

Strength is obviously the most important criteria for any such mooring system. For the MOB in deep water, mooring component design forces may need to be as high as 2,000 kip (900 tonne). Large ranges of cyclic mooring force may be experienced, especially in storm conditions.

Weight is another important criteria in the selection of tension members for deep water lines, both to minimize the pretension which is required to support the long length of mooring line and to reduce the weights of material which must be transported and handled during installation. The light weight of high strength synthetic fiber rope is attractive when compared to that of wire rope and chain. Synthetic fiber ropes with a wide range of elastic properties are available.

The elasticity of the tension member is yet another important criteria. Although chain mooring systems achieve most of their restoring force from the catenary effect, the elasticity of the chain itself can be an important consideration, especially in long lengths and under high tensions. Because of its light weight, which produces almost no catenary effect, the elasticity of synthetic fiber rope is the principal source of its restoring force in a mooring system.

The final design of a deep water mooring system should be done with a comprehensive mooring system analysis computer program, capable of accurately modeling tension member elasticity as well as unit weight, strength, geometry, component length, and pretension, in order to determine that combination of these important parameters which gives optimum or at least satisfactory performance.

This Appendix provides data on typical strengths, unit weights, and elastic moduli of the types of tension members which might be used in deep water moorings. But for final design, the actual data for particular candidate tension members should be obtained from the manufacturers. This is especially so for synthetic fiber ropes, because these important properties can be tailored by varying lay length and other design and manufacturing parameters.

E-2 Chain

In very deep water, the suspended weight of chain is so great that supporting the chain's own weight consumes a large portion or all of its working strength. Thus chain is not a good candidate for use as the riser leg portion of a deep water mooring.

Chain can effectively be utilized in the ground legs of the CASALM. Here, the catenary effect of its weight may benefit the system's response characteristics. The total weight of the long lengths of chain that might be required in deep water moorings is also an important consideration. Long lengths of large chain are difficult and costly to transport. Special or heavy lift equipment may be required to handle heavy chain during installation.

Chain specifications are determined by classification society (or similar organization) standards. These set strength, material and quality requirements. Each classification society has its own codes, but many are the same or at least equivalent products. Some chain types likely to be considered for the CASALM system are Gr 3, Gr 4, ORQ, RQ4, R3, R4 and NVK4-RIG. Stud link anchor chain is the most common for mooring applications, but studless chain is relatively new and is being used for this service.

Studless anchor chain may be substituted for stud link chain. For the same weight, the chain size will be 4% larger with about a 9% increase in strength. For the same size, the strength is the same. Besides size, studless chain is designated by type, with the same codes as stud chain (Gr 3, ORQ, etc.). Studless chain has a lower modulus (greater elasticity) and a longer fatigue life than stud chain.

Strength, modulus and weight data for three grades of 4 in. (100 mm) chain are provided in the following table. The suspended submerged weight of 10,000 ft (3,000 m) of Grade 3 chain constitutes over 90% of its strength, and that of Grade 4 chain constitutes about 67% of its strength.

Representative Property Values for 4" Stud Link Chain

Chain Grade 4 in. (100 mm)	Min. Strength kips	Elasticity Modulus lb/in/in x 10^6	Weight- lbs(mass)/ft
Grade 3 Stud	1,586	18.2	147
ORQ Stud	1,707	19.6	147
Grade 4 Stud	2,217	25.4	147
Gr 4 Studless	2,217	21.6	135

Source: Ramnäs Anchor Chain Catalog, 1996 & Ramnäs Bulletin 1995-04-26

Strength and weight data for other chain sizes may be calculated from the following formulae:

LOAD (kips) = $c \times d^2 \times (9.9 - 0.018 \times d)$
where d is chain size in mm, c is given in the following table.

MASS (lbs/ft) = $0.0147 \times d^2$ (mass equation for stud link chain)
MASS (lbs/ft) = $0.0135 \times d^2$ (mass equation for studless link chain)

	Grade 3		ORQ		Grade 4		Studless	
	Proof Load	Break Load	Proof Load	Break Load	Proof Load	Break Load	Proof Load	Break Load
c	0.0137	0.0196	0.014	0.0211	0.0216	0.0274	0.0233	0.030
From: Scan Ramnas Catalog No. 1996 04 5								

Chain may be used as connector segments on the ends of wire or synthetic fiber rope. Here chain provides chafe resistance against other system components and against the sea floor. It also provides a convenient means of grasping the other tension member during handling and of adjusting the end position during final assembly in order to achieve the desired overall length and pretension.

E-3 Wire Rope

Wire rope may be used in both the riser leg and the ground leg of a deep water mooring. However, as with chain, the suspended weight of chain in the riser leg is a concern. In 10,000 ft (3,000 m) water depth, the suspended weight of a typical 4 in. (100 mm) wire rope is 30 kip (14 tonne), about 20% of its strength. This weight can be compensated for with submerged buoys or other flotation means placed along the length of the wire. However, the use of such flotation devices greatly complicates the installation process and increases material costs.

The catenary effect of wire rope may be useful in ground legs.

Wire rope is subject to corrosion. This corrosion effect may not be severe in deep water, but it must be reckoned with near the surface. Special jackets, anodes or impressed current may be required if the mooring is to have a long service life.

Typical strength, modulus and weight data for 4.0 in. (100 mm) diameter wire rope that might be used for the CASALM computer program are provided in the table below.

Representative Values of 4 in. (100 m) Wire Rope

Rope Type / Size - in. Dia	Min. Strength - kips	Elasticity - lb/in/in x 10^6	Weight - lbs(mass)/ft x 10^6
6 x 37 EIP IWRC Bright 4.0 in. dia.	1,440	121	29.4
6 x 37 EIP IWRC Galv. 4.0 in. dia.	1,300	121	29.4

E-4 Synthetic Fiber Rope

E-4.1 Introduction

High strength synthetic fiber ropes can presently be manufactured in relatively long lengths. Rope of 3,300 kip (1,500 tonne) have recently been tested successful. Production of lengths of this rope 5000 ft (1500 m) long is considered feasible. If there is sufficient need, the equipment for accomplishing the final assembly of such large ropes could be mounted on a barge, enabling extremely long lengths of rope to be made on site.

The fiber ropes that are likely to be used are not expected to be effected by the marine environment. Corrosion is not a concern with the rope, although it can be a consideration in the choice of terminations. Hydrolysis is generally not a concern.

Several studies indicate that polyester and aramid fiber ropes can be expected to have better cyclic load fatigue life than wire rope, even if such wire rope is protected against corrosion.

E-4.2 Fiber Materials

In this discussion, fiber materials are divided into two groups; conventional fibers and high strength / high modulus fibers. These are listed below along with representative properties for the better grades of fibers produced for use in ropes.

Conventional Fiber Rope Materials				
Material	Specific Gravity	Relative Modulus[1]	Specific Strength (N/tex)[2]	Notes
Nylon (Polyamide)	1.14	0.4	0.84	Wet strength reduction 10%. Wet condition may significantly reduce abrasion resistance. Moderate creep may occur.
Polyester	1.38	1.0	0.84	Good wet abrasion resistance for marine finish fibers. Very low creep
Polypropylene	0.92	0.9	0.73	Lower strength. Subject to creep. Floats in water.

High Strength, High Modulus Fiber Rope Materials				
Material	Specific Gravity	Relative Modulus[1]	Strength (N/tex)[2]	Notes
Aramid, HM (Kevlar 29)	1.44	2.7	2.03	Sensitive to axial compression and internal fiber degradation under cyclic loading. No creep.
Aramid, VHM (Kevlar 49)	1.44	4.0	2.08	Same as Kevlar 29 with higher modulus.
HMPE (Spectra 900, Dynema)	0.97	3.4	2.65	Low melting point. Moderate to high creep. Floats in water
HMPE (Spectra 1000)	0.97	3.6	3.1	Same as Spectra 900, except stronger and less tendency to creep
LCAP (Vectran)	1.41	2.5	2.0	Virtually no creep.

[1] A relative value with polyester as a base of 1 is presented. The modulus is a measure of the elasticity under load.

[2] The data is for strength in Newtons divided by the linear density (tex). Use this value to compare the strength of one fiber to another. As bundles of tiny filaments, textile fiber yarns do not have a true diameter; therefore, the usual units of strength, such as psi, are not applicable. The size of filament yarn is normally measured by linear density. (tex = weight in grams of 1000 meters of filament yarn).

E-4.3 Fiber Rope Materials for Deep Water Moorings

Aramid, polyester, and HMPE fibers are all attractive candidates for making high performance fiber ropes for use in deep water moorings.

Aramid - High Modulus (Kevlar 29, Twaron)

Aramid fiber has been widely used in smaller ropes and has also been successfully used in some large diameter ropes. Aramid provides a high strength to weight ratio. It has extremely low creep characteristics. Aramid fiber rope is a good candidate for use as the riser of the CASALM in deep water.

Axial compression fatigue has been found to be a major problem in some large aramid fiber ropes in some cyclic fatigue applications, especially where the rope is allowed to flex or to relax to a relatively low tension. This problem with fatigue is generally related to the method by which the rope is terminated and to the manner in which it is handled. Special attention should be given to termination design and application.

Aramid - Very High Modulus (Kevlar 49)

This aramid fiber is very similar to Kevlar 29, except it has a significantly higher elastic modulus. It otherwise has essentially the same strength and weight properties. It is more expensive than the high modulus form of aramid, and thus it should only be considered where stiffness is a very desirable property.

Because of its very high modulus, the rope-making efficiency of this form of aramid as not as good, and breaking strength may be less unless extra attention is given to component tensions during rope design and manufacturing. Also, the propensity to axial compression fatigue may be greater because of the higher modulus.

Polyester

Large polyester fiber rope has about half the strength of aramid fiber ropes of the same size and unit weight. The elastic modulus of polyester rope is about one-fourth that of high modulus aramid rope. This lower modulus may be very beneficial in the anchor legs of a deep water mooring

The best grades of polyester fiber, treated for marine service, are very resistant to internal abrasion and thus have excellent cyclic fatigue life. Polyester fibers do not suffer from the axial compression fatigue which is sometimes a problem in aramid ropes. Creep is very low once the rope length is stabilized by the first few loadings.

On a strength basis, polyester fiber ropes are about one-half the cost of aramid and about one-third that of HMPE.

Very large polyester ropes may be adversely affected by heat buildup under high rates of cyclic loading if a wide load range is involved (as might occur in a 100 year storm). This may require consideration in the design if this fiber is to be used.

HMPE - Spectra, Dyneema

HMPE stands for high modulus polyethylene. Ropes made of this high modulus fiber material are slightly stronger than aramid fiber ropes of the same size. Because HMPE has a specific gravity less than 1, these ropes are much lighter than polyester and aramid ropes, and they will float in water.

This is a fairly rugged fiber, and would be expected to perform well under cyclic loading. HMPE ropes may be a candidate for the CASALM riser.

HMPE fiber is subject to creep under moderate to high working loads. Creep of HMPE fiber ropes does not affect strength until considerable elongation has taken place (perhaps 10% to 15% creep). However, a change in rope length and modulus due to creep may adversely affect system performance and may not be acceptable. Creep considerations may also make it unattractive for applications where relatively high working loads are expected and a long life is required.

Presently, HMPE is the most costly of the fibers that are under consideration. In addition, the availability may be limited, at least in the near term.

E-4.4 Other Synthetic Fibers

The fiber rope materials discussed below are not considered to be favorable candidates for use in deep water moorings.

Nylon

Nylon is adversely affected by water, especially in the absence of a good quality marine finish. Nylon fiber generally looses about 10% of its strength when wet. The wet nylon fiber also swells and contracts. The fiber strength loss combined with the fiber swelling can cause as much as a 20% decrease in strength in wet nylon ropes. Because these wet affects occur within the fiber, the degradation persists even after the rope appears to become dry again.

Water also reduces the abrasion resistance of the nylon fiber. This significantly reduces the cyclic loading life of nylon rope, such that the service life of a nylon rope is generally much less than that of a polyester rope in the same service. This also reduces the wet nylon rope's resistance against external abrasion.

The elastic modulus of nylon rope is about half that of polyester rope. The greater elasticity of nylon makes it desirable in some applications. Nylon tends to creep at moderate sustained loads.

Polypropylene

Polypropylene rope is not as strong as polyester or nylon rope. Polypropylene and polyester have similar elastic moduli. Polypropylene rope floats on water.

Polypropylene creeps more than nylon and much more than polyester. Of the two, polyester would normally be the preferred choice.

New higher strength versions of polypropylene fiber are now being offered in rope. Polypropylene fiber is also sometimes blended with polyester fiber to produce a form of rope which has many properties similar to that of regular polyester rope, but at lesser cost and with lighter weight. Thus, polypropylene in these special forms might be attractive in ropes for deep water moorings from a cost standpoint.

LCAP - Vectran

LCAP stands for Liquid Crystal Aromatic Polyester. This fiber material has generally good properties for ropes in deep water moorings. It is similar in performance to high modulus aramid. However, LCAP is relatively new, is in short supply, and is much more expensive than the other materials discussed here. Thus ,it does not appear to be an attractive candidate for deep water mooring ropes at this time.

E-4.5 Fiber Rope Constructions

Fiber ropes are manufactured in a variety of different constructions, referring to the forms in which the fiber yarns are assembled into strands and these strands are then assembled into the rope. The traditional twisted (laid) and braided (plaited) rope constructions used for general purpose working ropes are not generally suitable for use in large, high performance ropes for deep water moorings. These traditional constructions are relatively inefficient; only about 40% of the potential fiber strength is converted into rope strength. In addition, the fiber component crossover points cause considerable inter-fiber abrasion which results in significant strength reduction in cyclic load service over time. These deficiencies are especially important in large ropes made of high modulus fibers (as distinct from conventional fibers).

The rope constructions which are recommended here can achieve fiber conversion strength efficiencies of 65% to 75%. This higher strength efficiency results in a smaller, lighter, less expensive rope for a given strength One feature of these more efficient rope structures is that the yarns, and also in some forms the strands, are more parallel to the rope axis, which increases strength, increases elastic modulus, and reduces internal fiber abrasion.

Parallel Strand - Refer to Figure E-1. This rope consisting of strands (sometimes called subropes) which are parallel to the rope axis and are held together by a braided or extruded jacket. Half of the strands are right lay and half are left lay, producing a rope which is virtually torque free.

Parallel strand ropes can presently be manufactured in sizes up to 10 in. (250mm) diameter, in a continuous length of 4,250 ft (1,300 m). A polyester parallel strand rope of this size would have a break strength of about 3,300 kip (1,500 tonne). A 7 in. (180 m) diameter parallel strand rope would have a strength of about 1,800 kip (900 tonne) in polyester and 2,600 kip (1,300 tonne) in aramid. Larger aramid ropes are feasible, but the strength and other performance qualities of such a rope have not been verified..

The individual twisted-yarn strands of such parallel strand ropes are made on widely available conventional rope making machines. The assembly of these strands into the parallel strand construction and then the braiding or extruding of the jacket takes specialized machinery, but this is not excessively complex or expensive. Thus, it may be feasible to make even larger parallel strand ropes.

Also, parallel strand rope making equipment might be mounted on a barge to assemble the rope from individual strands made up in advance and shipped to the site on large reels. By this technique, very large ropes of very long length could be made at or near the mooring installation site

Figure E-1

PARALLEL STRAND ROPE CONSTRUCTION

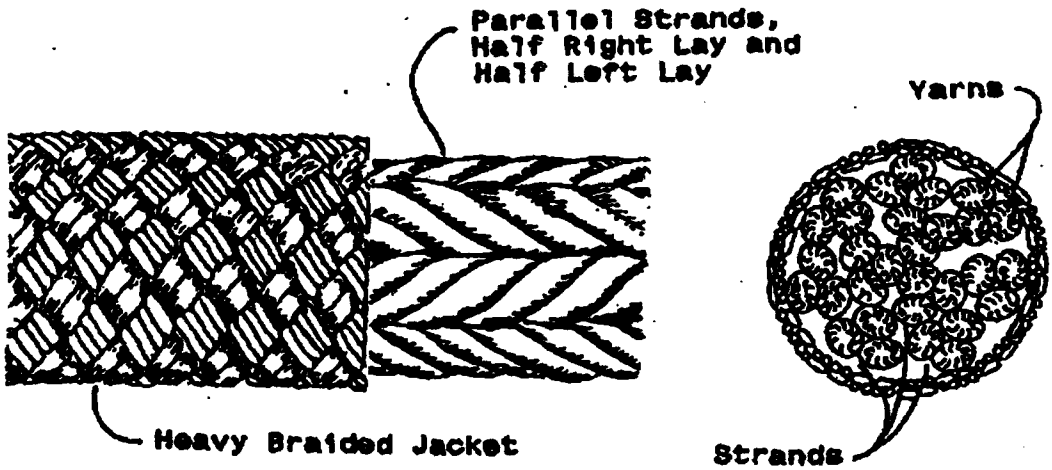

Helical Strand Rope Construction - Refer to Figures E-2 & E-3. These ropes are made on planetary strander in the same manner as wire rope. This is sometimes referred to as wire rope construction. Typical helical strand constructions are 7-strand (6 strands around a center strand), 19-strand (12 around 6 around 1) and 37-strand (18 around 12 around 6 around 1).

Large polyester ropes with 3,300 kip (1500 tonne) break strength have been tested. Similar strengths in aramid ropes are feasible and very large sizes have been tested.

The continuous length of such helical strand rope is limited by the size of the closing strander.

Torque balance and torque resistance can be important considerations with helical strand rope. The direction in which the strands are laid to form the rope is opposite to the direction in which the which the yarns are twisted when forming these strands. If done properly, this minimizes the tendency for the rope to twist when tension is applied. This is especially important when all of the strands are laid in the same direction. The 37-strand construction can be nearly torque balanced if the inner two layers are laid in the opposite direction to that of outer strand layer.

Helical strand ropes can be severely we torque is introduced into the rope from an external source. This can result for examp hen a helical strand fiber rope is coupled in series with a wire rope which has different torque-tension characteristics.

The most common construction for polyester rope is the 7-strand; this has been extensively tested. Large aramid ropes have been tested in all three types A braided or extruded jacket is sometimes necessary to hold the rope together when it is not under tension.

Figure E-2

HELICAL 7 - STRAND ROPE CONSTRUCTION

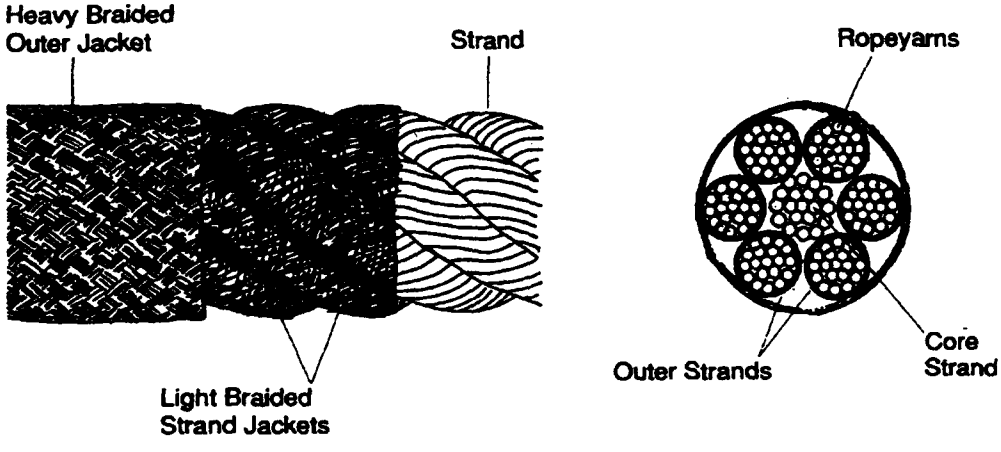

Figure E-3

HELICAL 37-STRAND CONSTRUCTION

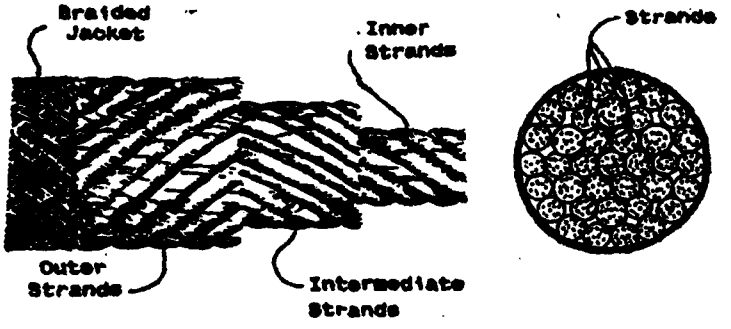

Parallel Yarn Construction - Refer to Figure E-3. This rope construction is formed by bundling a large bundle of individual fiber yarns together in parallel. In some versions, smaller bundles of yarn are prepared with a small amount of twist (half left hand and half right hand twist) and these are laid in parallel; this is distinct from the parallel strand construction in that the degree of twist in the sub-bundles is very low. An extruded (most common) or braided jacket is required to h... the yarns together.

The parallel strand construction is usually preferred to the parallel yarn construction. Although very similar, the parallel strand construction is more flexible, less likely to compress the fibers and easier to terminate.

Figure E-4

PARALLEL FIBER ROPE CONSTRUCTION

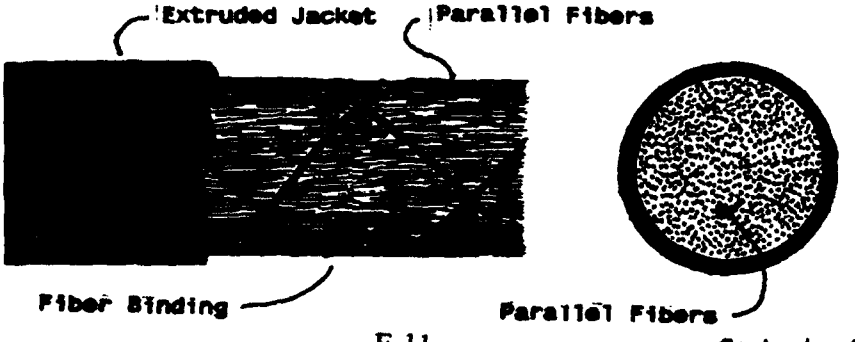

E-4.6 Fiber Rope Properties

The properties of representative sizes of parallel strand ropes of different materials are provided in the following tables. These data represent minimum strengths that are expected to be met by a number of maunfactures using normal production processes; higher strengths may be possible.

Typical High Performance Fiber Rope Properties

Aramid Rope, Parallel Strand (Kevlar 29)				
Diameter Inch (mm)	Dry Weight lb/ft	Weight in Water lb/ft	Break Strength kip	Modulus lb/in/in x 10^6
3.0 (76)	3.2	0.9	650	16.3
3.5 (90)	4.3	1.2	890	22.3
4.0 (100)	5.7	1.6	1,160	29.0
4.5 (115)	7.2	2	1,470	36.7
5.0 (130)	8.8	2.5	1,800	45.0
6.0 (152)	12.0	3.1	2,600	65.0

HMPE Rope, Parallel Strand (Spectra 900)				
Diameter Inch (mm)	Dry Weight lb/ft	Weight in Water lb/ft	Break Strength kip	Modulus lb/in/in x 10^6
3.0 (76)	2.3	-0.14	671	20.1
3.5 (90)	3.2	-0.19	914	27.4
4.0 (100)	4.1	-0.25	1,193	35.8
4.5 (115)	5.2	-0.31	1,510	45.3
5.0 (127)	6.5	-0.39	1,865	56
6.0 (152)	9.4	-0.50	2,600	74.3

Note: The polyester jackets normally used with these ropes would increase the weight in water.

Polyester Rope, Parallel Strand				
Diameter Inch (mm)	Dry Weight lb/ft	Weight in Water lb/ft	Break Strength lbsx10^3	Modulus lb/in/in x 10^6
3.0 (76)	3.1	0.8	448	5
4.0 (100)	5.4	1.4	719	8
6.0 (150)	12.2	3.2	1,390	16
7.0 (180)	16.7	4.3	1,800	21
10.0 (250)	34.0	8.8	3,200	40

E-4.7 Fiber Rope Terminations

Eye Splice - Parallel Strand Rope - The eye splice termination is well suited to the parallel strand rope construction. The jacket is removed from the rope, the individual strands are forming through a thimble or around a spool to form an eye, and then each individual strand is spliced back into itself, using an adaptation of the splicing technique for three strand rope.

Eye Splice - Helical Stand Rope - The seven strand rope is spliced using an adaptation of wire rope splicing techniques. Wire rope splicing techniques can also be used on polyester 18 and 36 strand ropes. However, problems with axial compression fatigue have beer experiences when such splicing techniques were applied to large 36 strand aramid fiber ropes.

Divided Socket Potted Termination - A special divided socket potted socket technique was developed by Tension Technology International and Tension Member Technology, under contract to the Navy, to increase the strength efficiency of large aramid rope terminations. This potted socket will also minimize these problems with axial compression fatigue in large aramid ropes. Further testing may be necessary to determine the actual strength efficiency of this potted socket termination on very large ropes.

Barrel and Spike - Parallel Fiber Rope - The parallel fiber type of rope construction is usually terminated by spreading the fibers on the periphery of a tapered barrel and then securing them by wedging with a tapered spike. This barrel and spike termination develops full strength in small rope sizes. But strength efficiency falls off, and abrasion or fatigue problems occur when this technology is scaled up to very large ropes.

Divided Socket Potted Termination - Parallel Fiber Ropes - The divided potted socket termination is suitable for larger parallel fiber ropes.

Splicing Parallel Fiber Ropes - Such ropes are sometimes terminated by arranging groups of fibers in strand-like bundles and then either splicing these like conventional rope or braiding these over the existing parallel fiber rope.

Termination Hardware - Spools or thimbles are placed in the rope eye to connected with other hardware, such as shackles, links, or pad eyes. The termination hardware should be designed to avoid abrasion and other problems, especially during cyclic loading. The termination hardware must be secured in the eye to avoid problems during handling operations.

E-5 Discussion

Parallel strand or parallel yarn constructions of aramid or HMPE fibers provide the highest elastic moduli and also the highest strength (size for size). These rope constructions are essentially torque free, and they are relatively torque tolerant.

Polyester ropes have relatively low elastic moduli, which can be beneficial for system response.

The torque balance and torque resistance characteristics of helical strand rope construction must be considered in any deep water mooring application. If a non-torque balanced rope is used in an installation where both ends are not secured against roptation, then the rope will rotate when tension is applied and will loose a substantial portion of its strength. This can occure for example if such a rope is installed and then left attached to a buoy which is free to rotate prior to attachment to the moored vessel.

If a torque free or balanced fiber rope is used in series with a wire rope which has different torque characteristics, then the wire rope will probably cause that fiber to rotate and loose strength. Also, if a long length of helical strand rope is highly tensioned in a mooring and then retrieved, it must be handled very carefully in order to avoid kinking or other torque related problems.

Chain is too heavy for use as the riser section of a mooring in deep water. The suspended weight of wire rope is also a concern in very deep water. Chain or wire rope may be used as the ground leg of a mooring, where the weight provides a catenary effect and where abrasion resistance is a concern.

E-6 REFERENCES, FIBER ROPE

Bolt, H.M., et al, "Anchor Chain - New Data, New Design Lines and Practical Details", OTC 7707, Offshore Technology Conference, Houston, TX, May 1995

Bridon American, Wire Rope Products Brochure, unnumbered, Wilkes-Barre, PA, undated.

Bridon Marine, Data Sheet, "Viking 7 Polyester Braided Rope", Ref. No. QMGR: 1895 Rev. 0, Charlton, England, July 1995

Casey, N.F., "The Fatigue Endurance of Wire Ropes for Mooring Offshore Structures", OIPEEC Round Table Conference, Delft, Holland, September 1993

Del Vecchio, C.J., "High Efficiency Polyester Fibre Ropes for Deep Water Moorings", Deep Oil Technology Conference, Rio de Janario, Brazil, November 1995

Dercksen, A., "On the Analysis of Mooring Systems Using Synthetic Ropes", Offshore Technology Conference, Houston, TX, May 1994

Flory, J.F., et al, "Fiber Ropes for Ocean Engineering in the 21st Century", Civil Engineering in the Oceans Conference, College Station, TX, November 1992

Flory, et al, "Improvement in Potted Socket Terminations", Oceans '95 Conference, San Diego, CA, October 1995

Hearle, J.W.S., et al, "Modelling Axial Compression Fatigue in Fibre Ropes", International Offshore and Polar Engineering Conference, the Hague, the Netherlands, June 1995

Knoff, Warren F., "Prediction of Long Term Strength Retention of Kevlar Aramid Fibers in Aqueous Environments", Oceans '94 Conference, Washington, D.C., September 1994

Koralek, A.S., 'Performance of a Lightweight Aramid Mooring line", Offshore Technology Conference, Houston, TX, May 1987

Leech, C.M., et al, "modeling Tension and Torque Properties of Fibre Ropes and Splices", International Offshore and Polar Engineering Conference", Singapore, 1993

Marlow Ropes, Brochure, "High Technology Ropes", No. RD1:7, Hailsham, England, dated February 1985; Brochure, "Superline Steelite", Version 3.2, Hailasham, England, dated September 1995

Overington, M.S., et al, "Modelling Heat Buildup in Large Polyester Ropes", International Offshore and Polar Engineering Conference", Los Angeles, CA, May 1996

Potts, A.E., et al, "Factors Influencing the Endurance of Steel Wire Ropes for Mooring Offshore Structures", Offshore Technology Conference, Houston, TX, May 1988

Riewald, P.G., "Performance Analysis of an Aramid Mooring Line", Offshore Technology Conference, Houston, TX, May 1986

Scana Ramnäs, Anchor Chain Catalog No. 1996 04 5, Ramnäs, Sweden, 1996

United Ropeworks (USA), Brochure, "Marine Products", No. 122-5/87, Montgomeryville, PA, dated 1987; Brochure, "Phillystran Polyester", No. 140-9/91, dated 1991.

Waters, D., et al, "Developments in Fatigue Assessments of Large Diameter Wire Ropes Used in Offshore Moorings", Offshore Technology Conference, Houston TX, May 1985

Wilde, B., et al, "Conceptual Design and Comparison of Aramid and Polyester Taut Leg Spread Moorings for Deep Water Applications", Offshore Technology Conference, Houston TX, May 1996

Zimerman, Z., et al, "Axial Corrosion Fatigue of Wire Rope", Offshore Technology Conference, Houston TX, May 1985

E-7 Sources: Materials, Large Wire & Fiber Ropes and Chains

E-7.1 High Performance Fibers

Akzo Nobel Fibers ..... Twaron aramid, polyester
P.O. Box 9300
Arnhem 6800 SB
the Netherlands

Allied Fibers Technical Center ..... Spectra HMPE, polyester
P.O. Box 31
Petersburg, VA 23803

DSM Research ..... Dynema HMPE
P.O. Box 18
6180 MD Gellen
the Netherlands

duPont Advanced Fibers Systems ..... Kevlar aramid, polyester
P.O. Box 27001
Richmond, VA 23261

Hoechst Celanese ..... Vectran LCAP, polyester
P.O. Box 32414
Charlotte, NC 28232

E-7.2 Large High Performance Synthetic Fiber Ropes

American Group, Samson Division
2090 Thornton
Ferndale, WA 98248

Cortland Cable Co.
P.O. Box 330
Cortland, NY 13045

Jacques - De Regt
P.O. Box 49
2900 AA Capelle a/d Ijssel
the Netherlands

Le Lis N.V.
Baantje 12
9220 Hamme
Belgium

Marlow Ropes, Ltd (Bridon is now part of Marlow Ropes)
Diplocks Way
Hailsham, East Sussex BN27 3JS
England

United Ropeworks
151 Commerce Dr.
Montgomeryville, PA 18936

Vermeire N.V.
Industriepark "Zwaarveld" 19
9220 Hamme,
Belgium

Whitehill Manufacturing Co.
P.O. Box 356
Lima, PA 19037

E-7.3 Large Wire Ropes

Bridon American Corporation
P.O. Box 6000
Wilkes-Barre, PA 18773

Wire Rope Corporation of America
P.O. Box 288
St. Joseph, MO 64502

E-7.4 Chain

Scana Rammäs AB
S-730 60 Rammäs
Sweeden

Hamanaka International, Inc.
1980 Post Oak Blvd, Suite 1000
Houston TX 77056

APPENDIX F

Anchoring Technology

F-1 Introduction

Mooring a very large vessel, such as the MOB, in water as deep as 10,000 ft (3,000 m) will require anchors with high uplift capacity. Installation of such anchors in very deep water will require special means for deploying, locating and setting of anchors. Some of the candidate mooring system designs also require relatively accurate control of the length of each mooring leg.

The following anchoring types that may meet the requirements of deep water mooring systems are review in this Appendix.

- Suction Pile Anchors
- Slender Driven Piles
- Plate Anchors
  - Embedded by Pile Driver
  - Embedded by Suction Device
- Traditional Drag Embedment Anchors
- High Uplift Drag Embedment Anchors
- Drilled Piles

Installation methods for these anchors are discussed. Cost has not been considered in this study, except in a very general way.

The first three anchor types listed are those most likely to be used in a deep water mooring system. All are technically feasible. Selection of the particular anchor type for a particular deep water mooring would be based on site analysis, installation considerations, availability of equipment, logistics and cost.

The analysis for the anchors and conclusions drawn assume the sedimentary bottom soils generally found in very deep water. Some information is provided in this report to show how candidate anchors may vary with soil conditions.

This report is not intended to provide specific design information. Some referenced papers provide more detailed information on design of anchors relative to soil characteristics, effects of cyclic loading, configurations, strength, other design parameters and installation.

The organizations listed in Section F-9 were interviewed as part of this investigation. Commercial literature from those organizations has been relied upon for experience, background and product description. Mention of these firms and inclusion of their product data in this report does not imply endorsement of the product or agreement with the correctness of the data.

F-2 Suction Pile Anchors

F-2.1 Design and Installation

Suction piles are typically large metal or concrete cylinders, closed at the top (during installation at least) and open on the bottom end. Refer to Figure F-1 (from MATech literature, undated).

The suction pile is lowered from the surface to the sea floor and set on the bottom in an upright position. Weight of the pile forces the bottom of the cylinder into the sea floor, forming a seal against external pressure. The interior of the pile is then evacuated with a suction pump. As the interior of the pile is evaluated, the external water pressure forces the pile into the sea floor.

For deep water installations, the pump is attached to the cylinder. An umbilical from the surface powers the pump that evacuates the cylinder. The umbilical may preferable be separate from the strength member used for lowering the pile. The pump is usually recovered to the surface after installation of the pile. In some designs, the top of the cylinder is removed along with the pump.

Very high horizontal and vertical holding power can be achieved when the suction pile is properly designed and embedded to a suitable depth (Colliat 1995: Colliat 1996, Larsen 1989; Senpere 1982)

Suction piles achieve vertical holding capacity both from friction between the exterior cylinder surface and the soil and from the combined mass of the pile and entrained soil/water. (Sparrevik, 1996). Horizontal holding capacity comes from the compressive and shear strength of the soil as the horizontal mooring force tends to attempt to pull the pile through the soil.

The mooring leg is usually attached to the side of the pile (as opposed to the top) to optimize lateral holding capacity. In soft soils, the mooring line connection point should be well below the pile top in order to reduce the overturning moment. Much of the theory for predicting the performance of suction piles comes from the work done on long slender piles, accommodating for differences in how the areas associated with diameter and length are distributed.

F-2.2 Suction Anchor Performance

A typical suction anchor for a rating of 650 to 900 kip (300 to 400 tonne) horizontal holding capacity may be 15 ft (4.5 m) diameter and 36 ft (11 m) long. It may weigh up to 90 kip (40 tonnes). The 10 : 1 design holding capacity to weight ratio for this example is typical.

Anchor capacity ratings quoted by designers are generally based on scale model testing and various theories on soil mechanics plus a design factor. Full scale testing of suction piles has been limited mostly to validating the rated holding capacity of the anchors rather than determining actual breakout loads. The data reported by Sparreuk is the most significant (Sparreuki 1996). Some uplift was

involved in these tests, but data on this is limited due to concentration on horizontal holding capacity. Some reported test data do not indicate the true limit of anchor capacity; rather, they were proof loadings that verified the rated (design) holding capacity in the horizontal direction. Other methods of analysis for load carrying capacity have been proposed (Fines, 1991), including consideration for cyclic loading (Clukey, 1995).

Rated horizontal holding capacities on some typical suction pile anchors that have been deployed are provided in Table F-1 below (from MATech Engineering literature, undated).

Diameter metre (ft)	Length metre (ft)	Design Holding Capacity metric tons
3.7 (12)	10 (32.8)	200
3.8 (12.5)	8.8 (29.8)	230
4.5 (14.7)	6.2 (20.3)	300

Table F-1
Typical Dimensions and Capacities of Suction Anchors

F-2.3 Installation and Recovery

Suction piles are lowered to the sea floor with a strength member. Not counting the weight of the lowering lines and rigging, the weight deployed over the side would be about 40 tonnes per anchor for anchors in the 400 tonne holding capacity range.

A power, control and instrumentation umbilical is also required. This is used to power and control the pump on the pile and to monitor any instrumentation.

The mooring leg associated with each anchor would most likely be lowered at the same time. Therefore, the weight will be higher than for the anchor alone.

It is imperative that the initial penetration of the pile occurs when the pile is vertical within 10° or less (Sparrevik). Some extra complexity is involved to maintain this vertical condition and to achieve correct angular orientation so that the mooring leg attachment (most likely on the side of the cylinder) is towards the center of the overall mooring. All operations to achieve the installation objectives in very deep water are feasible; however, the long lengths of lifting line, positioning line and umbilical require equipment capable of dealing with the significant length and volume of line involved.

Suction piles would be instrumented to show depth of penetration and inclination. An ROV would most likely be used to monitor the operation and perhaps to perform disconnect/reconnect functions.

Methods have been developed to relieve soil plugs that may develop inside the cylinder and to perform evacuation with forceful pulses to increase penetration forces in hard soils.

The pump (and sometimes the top of the pile) and umbilical is expected to be recovered to the surface with the strength member that was used to lower the pile.

Vessel and equipment requirements for installation depend on the mode of operation and are discussed in the section of this report on installation. The vessels that are selected to handle the CASALM junction weight and the ground legs of the system are also expected to be adequate for the operational requirements of the suction pile anchors, the umbilicals and the power/control facilities.

Suction piles can be easily recovered by pumping water into the top of the pile. This releases the suction and forces out the soil plug. Connection facilities for ROV operations must be provided to connect recovery related equipment. Recovery loads would be equal to the weight of the pile and lifting line.

F-2.4 Sources

Most major offshore construction contractors should be able to build and install suction anchor piles. Suction piles have been designed by users or by engineers/contractors working on a specific offshore oil or marine project. Some examples are described in the references (Colliat, 1995 & 1996; Fines, 1991; Sparrevik, 1996). The design and operational procedures should, however, come from persons or organizations experienced in this field.

Following are brief descriptions of several experienced firms. More detailed information on suppliers is included found in Section F-9.

Suction Pile Technology is a joint venture of Noorhoek Diving and Volker Stevin Offshore both of the Netherlands. They hold a license from Shell for their patents on suction anchors. They offer engineering and installation services related to suction pile anchors.

MENCK of Germany (also see Section F3.6) may offer to supply the design, the piles, pumping equipment and on-site engineering support as a commercial service. As of May, 1996, this action was under consideration but not finalized.

Because of the simplicity of construction, either in steel or concrete, suction piles can be fabricated near the use site. The installation equipment could be a package supplied by a contractor or service such as MENCK or Suction Pile Technology.

F-2.5 Conclusions

Suction piles appear a very attractive candidate for anchoring very large vessels where there is a sufficient thickness of deep sea sedimentary soils. The advantages are:

The simplest to embed (relative to other types of anchors)

Least likely to have water depth limitations

Good holding capacity in horizontal and vertical directions

Lowering weight is not prohibitive; lower than other options

Easy to recover.

Suction piles may not be suited where the sea bottom is very hard.

F-3 Slender Driven Piles

F-3.1 Description

Slender piles have been driven in water as deep as 3,500 ft (1,200 m). An installation is planned at 5,400 ft (1,650 m). Commercial operator MENCK feels that 6,600 ft (2,000 m) water depth is reasonable. IHC Hydrohammer feels comfortable with that water depth and is actively investigating 10,000 (3000 m) water depth operations. The above observations are based on discussions with these organizations. Thus , the objective of installation in 10,000 ft (3,000 m) water depth appears to be technically feasible in the foreseeable future.

Figures F-2 and F-3 show typical pile driving hammers that are used to install underwater piles. The underwater hydraulic hammer is placed on the end of the pile before it is lowered. The energy to operate the hammer may come from an underwater electro/hydraulic power unit mounted on the hammer and driven by electrical power from the surface or from a hydraulic power supply on the surface which provides hydraulic fluid to the hammer at high pressure. In either case, an umbilical is required.

F-3.2 Performance

The holding capacity of a driven piles in the vertical direction depends on the soil and the length of pile. For the large horizontal forces that are expected, large top diameters will be required; 7 ft (2 m) diameter piles are feasible.). The mooring leg connection could be made up to 65 ft (20 m) below the seabed. Side plates are commonly attached near the pile top to increase area and thus holding capacity in the horizontal direction. Various configurations could easily provide lateral holding capacity in excess of a 500 tonnes design load. For high lateral load resistance a large wall thickness may be required over some of the length to resist bending; this will add to the weight.

F-3.3 Installation and Retrieval

A crane barge with about a 200 ton lifting capacity and a large amount of available deck space would normally be required to install large piles in deep water. A modified semi-submersible drilling rig has been used to deploy and drive large piles and this is a feasible option. The MOB itself could be configured to execute deployment of the anchors and mooring legs.

Some instrumentation and/or ROV surveillance would most likely be required to assure that the pile did not buckle and was driven to the proper depth.

Installation times of 12 to 15 hours per pile could be expected. This is influenced by water depth, as lowering time and retrieval of the hammer may take one to two hours each way if a crane barge is used and probably longer if the drilling derrick of a semisubmersible is used.

Slender drive piles can not be retrieved. This should not be a concern in very deep water, especially if the tops are below the sea floor. A means of disconnecting the mooring lines should be provided if the seabed is to be left clear.

F-3.4 Sources

Information on suppliers will be found in Section F-9, under 'Pile Drivers'. In general, these firms supply the hammers and support equipment with some operating personnel, and they may also design the piles. The piles themselves are usually fabricated on site by the project contractor.

F-3.5 Conclusions

Slender driven piles are a reasonable candidate for deep water mooring systems. The principal advantages are :

Proven performance in a variety of soils

Sufficient capacity in horizontal and vertical directions

Water depths of 6,500 ft (2,000 m) appear feasible and studies for 10,000 ft (3,000 m) are underway.

Vessels to meet installation requirements are available.

Disadvantages and unknown factors include:

Unproven driver operation in very deep water beyond 2000 meters.

Mobilization of vessels and equipment may involve long lead times and long transit times.

Extensive support equipment requirements.

Costly due to vessel time and installation equipment.

F-4 Plate Anchors

F-4.1 Description

Plate anchors are flat surfaces that are driven on edge into the sea floor.

The mooring line is attached to an offset bracket on the plate. After reaching the desired depth of penetration, the anchor is set by pulling on the mooring line in the vertical direction. This causes the plate to rotate into a position where the flat surface can bear effectively on the soil, perpendicular to

the general direction of pull of the mooring line. Plates (keys) which are retracted during driving but which then open as the anchor is set in order to present greater area to engage the soil, are used to induce this rotation in very soft soils.

The setting operation causes the anchors to raise from the driven penetration depth. Allowance must be made for this rise effect when determining the depth of initial penetration, and generally this rise is assumed to be twice the anchor length (Forest, 1995).

F-4.2 Performance

Plate anchors can be made large enough to resist virtually any required horizontal or vertical mooring forces. To achieve 550 kip (250 tonnes) ultimate load in typical soil conditions, a plate anchor may require 60 ft^2 (5.5 m^2) of surface area (design factor of 2 was assumed). Such an anchor may have two plates that are 7.5 x 4 ft (2.3 x 1.2 m) separated by a 4 foot (1.2 m) web; the weight might be about 7 kip (4 tonnes) after all structural requirements are met. The ratio of design holding capacity to anchor weight is, therefore about 60 : 1.

Methods for anchor performance prediction are given in the references (Forest, 1995).

F-4.3 Installation and Recovery

Plate anchors may be driven either by pile driving hammers or by the suction anchor technique. These methods have been described above.

Plate anchors have been installed by pile driving hammers in relatively shallow water. It should be possible to adapt this technology to deep water mooring system installations.

The plate anchors will most likely cost less than the slender pile, require a smaller pile driver and be easier to handle (less weight and a more compact driver/anchor assembly than with a long pile). The additional operation of setting the plate anchor by pulling vertically on it after it has been driven poses an extra operation compared to driving of slender piles.

The plate anchor must be installed so that the offset mooring line connection is on the side of the anchor facing the center of the mooring pattern. A means of achieving and verifying this orientation will be necessary.

It is probably feasible to adapt the suction pile concept for the purpose of embedding a plate anchor. A suction device may be much easier to operate in deep water than a pile driver. However, research for this report did not reveal any attempts to utilize the suction anchor technique for installing plate anchors.

The following items are of concern and would need to be addressed:

How to embed a plate anchor with the mooring line attached as it appears that it would be in the way of the suction device.

Effects of disturbing the soil around the anchor as the suction pile is removed after embedding the plate anchor.

The magnitude of the driving force relative to the combined resistance of the anchor and the suction device is presently unknown.

Proper orientation of the plate anchor.

Plate anchors would not be recovered. Since they will be buried below the mudline, they should not cause concern. A means of disconnecting the mooring line should be provided if the bottom is to be left clear.

F-4.4 Sources

Plate anchors are generally designed by users or their contractors for specific projects. The design parameters are well defined, however (refer to: Forest, 1995). Experienced personnel should be used in establishing design and procedures.

There are no suppliers that provide a line of standard plate anchors. Section F-9 lists suppliers of underwater pile drivers and of suction anchor installation equipment.

F-4.5 Conclusion

Plate anchors installed by a pile driver are an attractive choice for use in deep water. The advantages are:

Performance is predictable if the soil conditions are known.

The anchor is suitable for the soils anticipated in very deep water.

Anchor weight will be the lowest of all those considered; however, the weight of the pile driver must be considered for installation.

Embedment in deep water is within the state of the art for pile driver operation or the technology can be reasonably assumed to be able to operate at these depths in the future.

F-5 Traditional Drag Embedment Anchors

F-5.1 Description

Drag embedment anchors have a large fluke area that provides high holding capacity in a wide variety of soils. Resistance to movement is primarily in the horizontal direction in line with the mooring forces. Advanced designs provide very high holding power relative to anchor weight. By

far, the market for high holding capacity drag embedment anchors is presently dominated by the Vryhof Stevpris Mk 5 anchor and the Bruce FFTS Mk 4 anchor. Refer to Figures F-4, F-5 and F-6.

These anchors depend on penetration into the soil on the sea floor which is achieved by dragging the anchor until it is buried (set). Dragging is usually done by the mooring line itself and the tension must be applied nearly tangent to the sea floor to achieve suitable depth of penetration. The anchor may drag further over time and penetrate deeper into the soil if mooring forces are cyclic and/or exceed the initial installation forces.

F-5.2 Performance

Drag embedment anchors are well developed and proven by use. They can achieve very high horizontal holding capacity, well within the range necessary for deep water mooring systems. The most advanced deigns for anchors give maximum holding capacities that are safely rated at 20 to 40 times the anchor weight but this ratio could be as high as 30 to 60 as suggested by some anchor suppliers (van den Haak, 1990).

Anchor holding capacity is plotted against anchor weight for various types of soil in Figures F-5 and F-7. Stevpris anchors weighing as much as 140 kip (65 tonne) have been built. The maximum holding capacity determined by the holding power graph should be divided by at least 1.5 to arrive at the design capacity.

The vertical uplift capacity of advanced drag embedment anchors can be quite high in soft soils of adequate depth and may meet CASALM requirements. In some cases with sand or hard soils, however, uplift capacity may be insufficient for the optimum CASALM design. This deficiency could be offset by using very large anchors, by modifying the anchors for greater uplift capacity (while sacrificing some horizontal capacity), by utilizing longer mooring legs or by adding weights into the mooring legs; however, these approaches would result in more difficult handling and installation operations. An anchor modified for higher uplift capacity is shown in Figure F-7.

To set properly, the initial horizontal angle at the sea floor should not exceed 5°. Most advanced anchor designs are not recommended for operational pulling angles higher than 5° in sand or very dense soils. But values up to 20° have been found acceptable in soft soils if the anchors are known to be well buried. A working value of 10° (including design factor) is accepted by API for soft soils with adequate penetration (see API reference in Section F-8).

For example, a 65 kip (30 tonne) anchor at 25 to 1 holding capacity ratio has a maximum horizontal capacity of 1,600 kip (750 tonne). At a design factor of 1.5, the rated horizontal capacity becomes 1,100 kip (500 tonne). If a 5° uplift angle is assumed, there would be 100 kip (45 tonne) of vertical rated capacity. However, at 20°, the rated uplift capacity would be 375 kip (170 tonne).

Another design approach that has been verified to some extent is to assume that the anchor will have a maximum vertical capacity equal to about 1.4 to 2 times the installation load applied tangent to the

sea floor. For the 1.4 factor and a design factor of 1.5, the vertical design load becomes approximately 0.9 times the installation load. If the installation load is 250 tonnes, the design uplift capacity would be 225 tonnes. Consequently, to achieve high uplift capacity, very high installation forces will be required, but these may be feasible with the tensioner system described in Section F5-3 below.

The claims of high uplift capacity for advanced embedment anchors as made by some anchor suppliers for well buried anchors (as is possible with soft soils) are supported by anecdotal data from actual mooring situations by noting the very high breakout loads often encountered during anchor recovery. Typically, a vertical pull is applied to the anchor via the mooring line to extract the anchor; these loads have been observed to approach or exceed the highest mooring load observed during service.

F-5.3 Installation and Recovery

Lowering the anchors and the mooring chains to the sea floor and positioning them accurately in deep water can be done with current technology. A pendant line would be required for both the anchor and for the end of the mooring leg, thus necessitating two anchor handling vessels.

Once on the sea floor, the anchors will need to be set. For a three anchor mooring arrangement this can be done by utilizing devices similar to Vryhof's Stevtensioner or the 'Bruce ' Tensioner. Refer to Figures F-8 and F-9. These ratcheting devices drag the anchors from the center of the pattern with a pull near to tangent to the sea floor until they all set at equal tensions. The tensioner is operated by a single vertical pulling line from the anchor handling vessel. Some development work would most likely be required to assure reliability during installation and over the long term (as the tensioner will become a permanent part of the mooring system). Bruce seems to have more experience in this area. The very high horizontal installation forces required for high uplift capacity described in Section F-5.2 is provided by this tensioner system.

If the tensioner system is used, the mooring legs will require significant amounts of chain in their length as it is required to reset the ratchet for each tensioning cycle.

If more than three anchors are required, setting of the anchors becomes more complicated in order to tension all legs equally. The handling of the large number of pendant lines and operation of the tensioner may be troublesome in deep water.

The drag distance of anchors may be excessive relative to the small tolerance on mooring leg length in the CASALM system. Advanced technology anchors set quickly with little drag in soft soils, especially if they are properly seated on the sea floor prior to dragging. However, optimum anchor setting conditions cannot be universally guaranteed. An ROV would be used to observe the anchor as it begins to bury; if an anchor starts well, it would be expected to bury quickly and effectively in soft soils.

Recovery of drag embedment anchors is possible by pulling on the crown (back) of the anchor. A pendant line with facilities to allow for ROV attachment of a pendant line would be required. Breakout forces can be very large.

F-5.4 Sources

Vryhof Ankers of the Netherlands and Bruce Anchor of the United Kingdom are the best known producers of drag embedment anchors. Refer to Section F-9. Other firms fabricate similar anchors.

F-5.5 Conclusion

Traditional drag embedment anchors may be technically feasible for use in deep water moorings, but they are unlikely to be prime candidates. The drawbacks are :

Complicated installation, especially if four or more anchors are required due to the necessity for simultaneous tensioning of the anchors to embed them,

Dragging of the anchors to embed them making mooring leg length control difficult,

Requirement for large amounts of chain in the mooring legs which may restrict system optimization; for example, this may limit the utilization of synthetic or wire rope.

Mobilization of extra anchor handling vessels and equipment compared to other anchoring concepts,

High breakout forces for anchor recovery.

F-6 High Uplift Capacity Drag Embedment Anchors

F-6.1 Description

Specially configured drag embedment anchors have recently been developed that have high vertical uplift capacity. They embed in the normal way by dragging with the mooring line as it is nearly tangent with the sea floor. In one approach, the anchor is outfitted with a 'trip line' that, after setting of the anchor, alters the direction of mooring line pull on the anchor to optimize the resistance to vertical uplift. Figure F-10 shows an anchor whose arm is 'triggered' after embedment; the arm rotates to provide greater uplift capcity.

Current developments indicate that the 'trip line' and the associated extra operation may have been eliminated in this type of anchor.

F-6.2 Performance

Tests by Vryhof predict that high vertical capacity anchors can achieve a vertical holding power of 2 times the installation load in soft to moderate soils while Bruce claims a value of 3 to 1. In sand or firm soils this factor may be 1.4. Using the holding capacity factor of 2 cited above and a design factor of 1.5, the anchor would be expected to hold 1.33 times the installation load. To hold 500 tonnes, the installation load would need to be 376 tonnes when pulling nearly tangent to the sea floor. In this example, it would be expected that the horizontal holding capacity would be at least 500 tonnes also once soil solidification has taken place..

F-6.3 Installation and Recovery

Installation would be virtually the same as that for traditional drag embedment anchors as described in F-5.3. The tensioner described in Section F-5 would be utilized. After embedment of the anchor, there may be an extra step to pull on the 'trip line' to release the anchor into the operating mode. Recovery may be possible if very high break-out forces can be tolerated. A high strength line from the surface will be required.

F-6.4 Sources

Both Vryhof Ankers and Bruce Anchors are developing high uplift anchors. Refer to Section A F-9 for data on these firms.

F-6.5 Conclusion

The maximum uplift angle for the CASALM system will be a predictable value. Unless the vertical uplift angle is very high, perhaps over 20° it would appear that a traditional drag embedment anchor would serve the application just as well. The possible benefit of a lighter weight anchor is probably not sufficient to recommend this anchor over the traditional embedment anchor for soft and deep soils. Also, these anchors are still under development.

F-7 Drilled Piles

F-7.1 Description

Piles can be set into holes that have been drilled in advance. This is essentially the same as installing casing into a hole drilled for an oil well. Grouting is normally required around the pile.

F-7.2 Performance

Drilled piles should perform similar to slender driven piles. Large top diameters, with the mooring line secured well below the top of the pile is possible and would be expected. With such an arrangement and with grouting, these piles could offer the highest holding capacity. They would resist bending better than slender piles. It is possible that this may be necessary in some very hard soils if the CASALM load requirements are very high.

F-7.3 Installation

A dynamically positioned drilling vessel and related equipment to drill piles into very deep water and grout them in place would be necessary. Support vessels will be needed. Mobilization of equipment would most likely take considerable time unless dedicated beforehand.

F-7.4 Sources

Offshore oil drilling contractors would be engaged to bore the holes for the piles. They would install and grout the piles. The design of the piles would most likely be done by an engineering or drilling contractor with expertise in this area.

F-7.5 Conclusion

It is unlikely that the soil requirements for CASALM would require the extra cost and complexity to warrant drilled piles. However, this is an option that would utilize existing technology.

SUCTION-EMPLACED PILES

To prove the feasibility and to control the process, extensive full-scale tests were conducted. The successful experiments showed once and for all the simplicity of the suction emplacement and the low investment required for installation. From operational experience it has been established that suction piles can be installed from different types of offshore vessels, crane barges, work boats and such-like and even from the after deck of a supply boat.

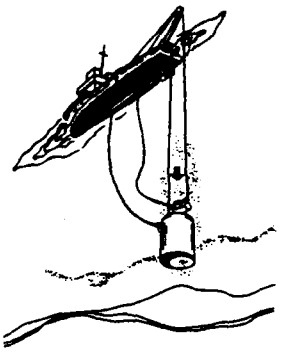

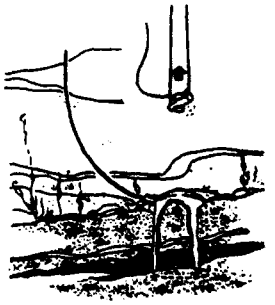

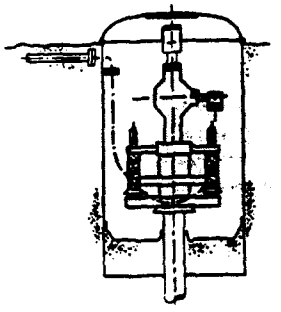

A P P L I C A T I O N S

Harbour Estuary Rotterdam:

3 anchor piles, Harbour Estuary Rotterdam
Use: fixed single line mooring systems
Holding capacity under 60 degrees with the horizontal: 2 MN (200 ton)
Dimensions: dia 3.7 m, length 10 m
Soil condition: medium dense sand with interlayered clayey seams

5 anchor piles,
BMK, Nieuwe Waterweg Estuary, Holland
Use: mooring systems of work barges
Lateral holding capacity: 2 MN
Dimensions: dia 3.7 m, length 10 m
Soil condition: varying from clay and peat to medium dense sand

4 anchor piles, Rotterdam, Waalhaven
Use: fixed single line mooring systems
Holding capacity under 60 degrees with the horizontal: 1.5 MN (150 ton)
Dimensions: dia 3.7 m, length 8.9 m
Soil condition: soft to medium clay

1 anchor pile, Amsterdam, Y-haven
Use: fixed single line mooring system
Holding capacity, dimensions and soil condition similar to the foregoing application

2 anchor piles,
Zaandam, Wim Thomassenhaven
Use: fixed single line mooring systems
Lateral holding capacity: 500 kN
Dimensions: dia 3.3 m, length 4.75 m
Soil condition: soft to medium clay

Offshore:

12 anchor piles,
Danbor, Gorm field, North Sea
Use: permanent mooring of 2 storage tankers with single buoys
Lateral holding capacity: 2 MN
Dimensions: dia 3.8 m, length 9 m
Soil condition: medium to very dense sand

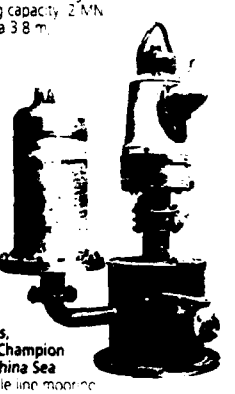

5 anchor piles,
Brunei Shell, Champion field, South China Sea
Use: fixed single line mooring systems to moor drilling tenders and work barges
Lateral holding capacities: 1 up to 3 MN, depending on seabed condition
Dimensions: dia 4.5 m, length 6.2 m
Soil condition: varying from soft clayey soils to dense sand

Figure F-1
Typical Suction Pile Anchor
(Figure from MaTech literature)

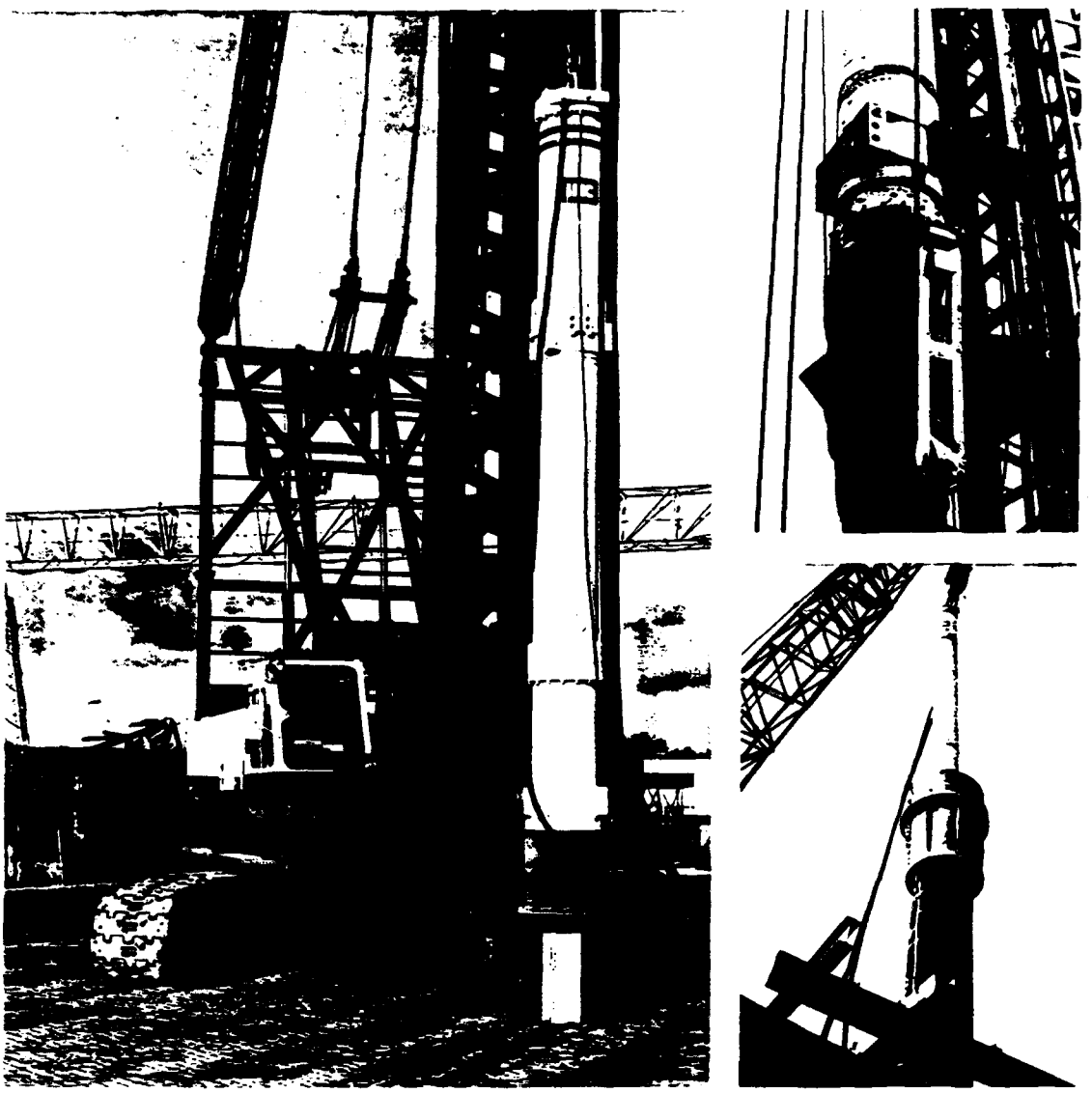

Figure F-2
Underwater Pile Driver
(Figure from IHC Hydrohammer literature)

MENCK

Underwater Girdle Power Pack

Is there any major offshore contractor without a MENCK hammer? Around 90 % of all piles driven offshore under water have been installed with MHU hammers. With this experience in hydraulic underwater pile driving technology, our new deep water hammer system was successfully tested in 1000 m water depth.
Today it represents the most advanced Hammer-Power Pack combination and is designed to work in 2000 m water depths.

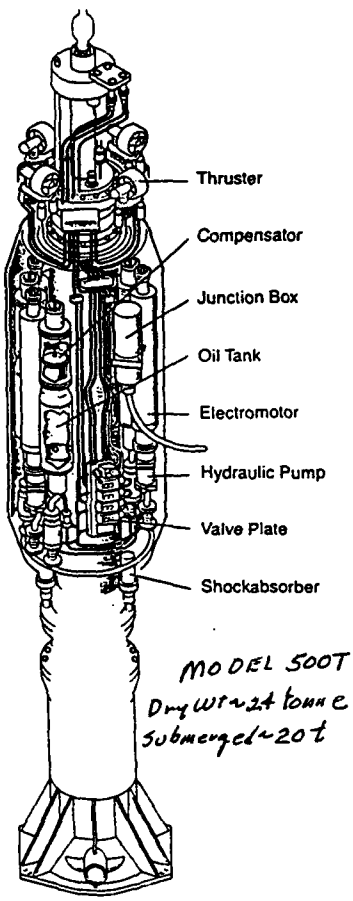

The Underwater Girdle Power Pack (UW-GPP) wrapped around the MHU hammer offers a number of advantages for deep water installations.

The advantages include:

Very light Hammer-Power Pack unit for fast and precise positioning in very deep water.

Virtually no environmental contamination hazards exist during storage, handling and operation. There is no air and water pollution with hydraulic hammers. The risk of oil spills is reduced to the minimum. The small total quantity of hydraulic oil is stored within the hammer-UW-GPP unit in well protected single tanks.

Proven components are used for the hammer and Underwater Girdle Power Pack (UW-GPP).

Minimal energy losses in the hammer, due to contained air circulation in the hammer housing.

Low energy transfer losses between barge and hammer. The high voltage power required for the motors is transferred through the power cores in the one umbilical with minimum losses. This compares very favourably with the high losses associated with long hydraulic hoses for pressure and return lines.

Only one operating line has to be handled: the power umbilical. Handling is further simplified by reeling the continuous length on a winch. This power umbilical includes all necessary lines: power cores, electric conductors for control and monitoring of hammer and UW-GPP, air hose for supply of air to the hammer.

All underwater equipment is handled as one compact unit. The hammer and UW-GPP being fully integrated. Easy uprighting on board and good control during stabbing on the pile as well as during driving.

Hammer can position itself towards the pile with the aid of (optional) thrusters, after having been brought near the pile with the aid of barge and crane movements. This will become increasingly important in deeper water due to the time delay associated with long lifting lines.

UW-GPP can easily be separated from the hammer and used for other applications such as:

— surface Power Pack for hammer or other equipment.
— fully separated UW-GPP for the operation of hydraulic hammers.
— hydraulic power plant for other functions, e.g. driving of jet pumps.

MENCK GMBH
WERNER-VON-SIEMENS-STRASSE 2
D-2086 ELLERAU
WEST GERMANY
TELEPHONE: (0) 41 06 - 70 02-0
TELEX 213294 MENK D
TELEFAX: (0) 41 06 - 7 48 12

Figure F-3
Underwater Pile Driver
(From MENK literature)

vryhof ankers

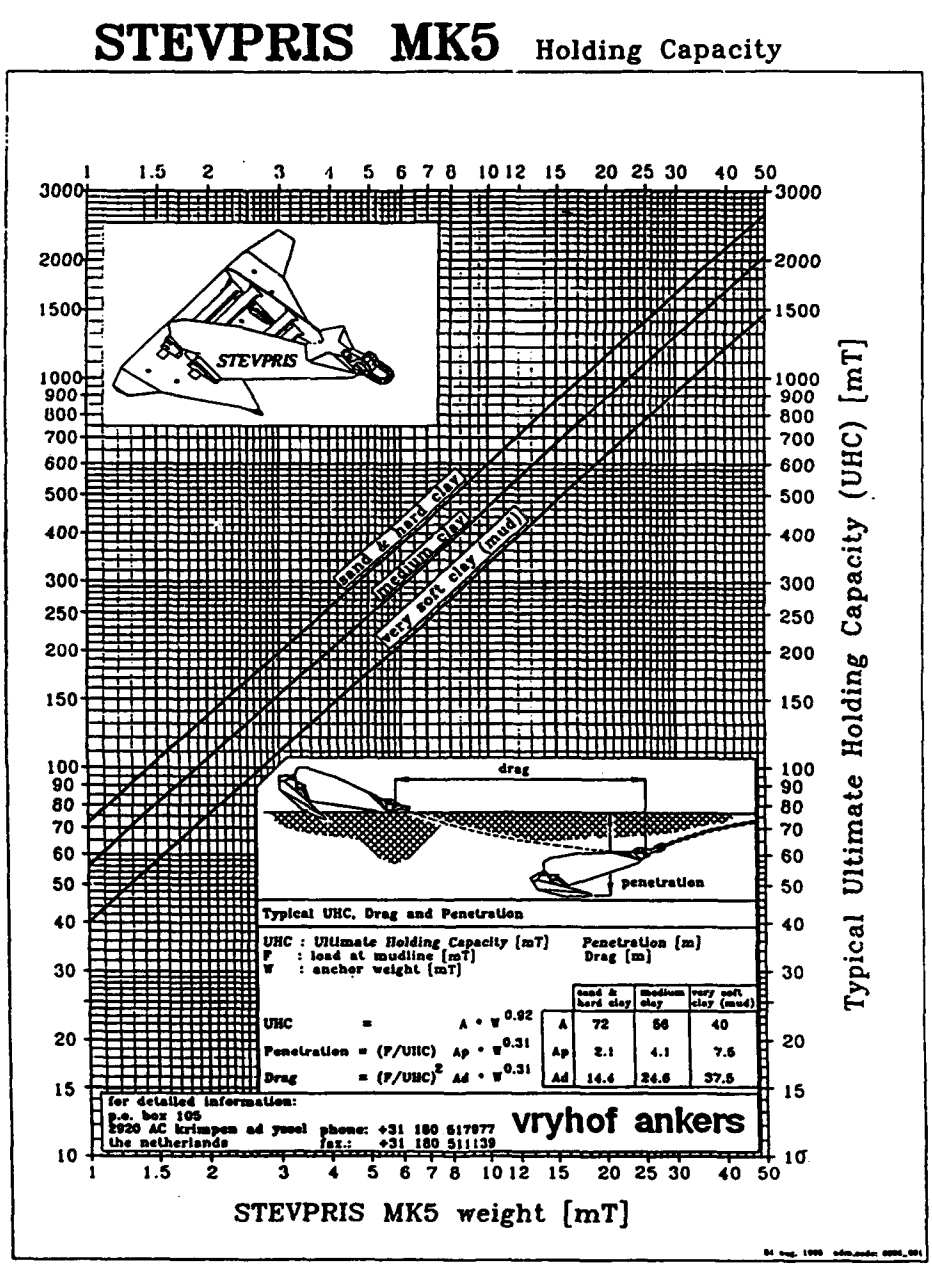

Figure F-4
'Vryhof' High Hold Drag Embedment Anchor
(From Vryhof literature)

BRUCE FFTS MK 4 ANCHOR

PATENTED

THE LATEST DEVELOPMENT IN ANCHOR TECHNOLOGY FROM BRUCE ANCHOR LIMITED

- ★ Superior holding performance in *all seabeds.*
- ★ Complete self-righting ability, even if it lands upside down.
- ★ Choice of fluke angles for optimum performance in hard and soft bottoms.
- ★ Simplified fluke angle adjustment by moving two plain pins, no welding required.
- ★ Disassembly into two parts for easier, lower cost shipping.
- ★ Approved by L.R.S., D.N.V. and R.I.N.A. as a general purpose high holding power anchor.

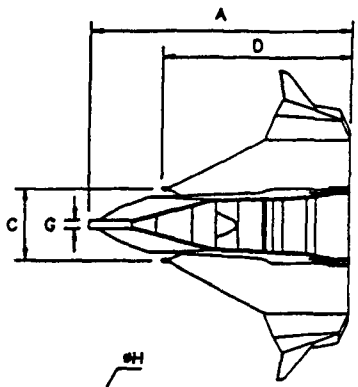

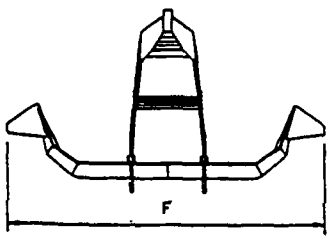

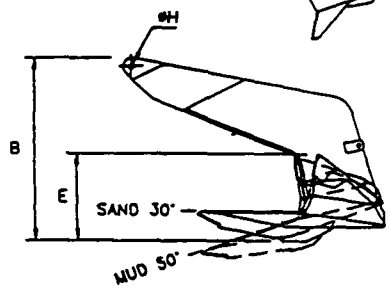

The table gives nominal dimensions of certain sizes but since the anchors are fabricated from steel plate they can be supplied in any size to suit customer requirements, from 250kg up to 60,000kg.

Weight kg	NOMINAL DIMENSIONS (in mm)							
	A	B	C	D	E	F	G max.	H min.
500	1827	1280	500	1303	606	2188	58	44
1500	2648	1854	723	1888	878	3172	65	53
3000	3409	2388	931	2431	1131	4085	95	75
5000	4029	2822	1100	2873	1336	4828	115	87
9000	4846	3394	1324	3456	1607	5806	157	117
12000	5437	3808	1486	3878	1803	6514	157	117
15000	5728	4012	1566	4085	1900	6864	157	117
20000	6319	4426	1726	4507	2095	7571	180	155
30000	7225	5060	1974	5153	2396	8656	180	155
40000	8034	5627	2195	5730	2664	9626	210	180

In the interest of continuous product improvement rights are reserved to change specifications and recommendations without notice

Figure F-5
Bruce' High Hold Drag Embedment Anchor
(From Bruce Anchor literature)

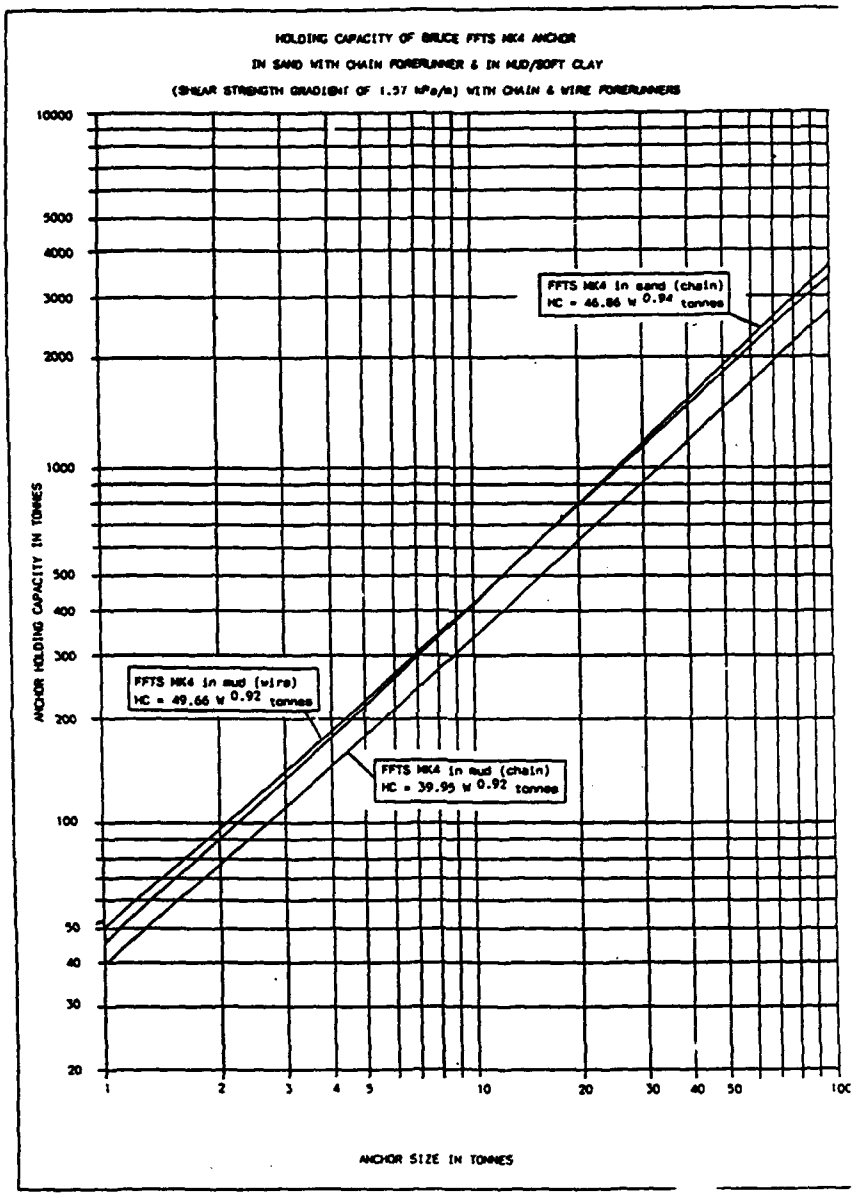

Figure F-6
'Bruce FFTS Mk4' Anchor Capacity Chart
(From Bruce Anchor Literature)

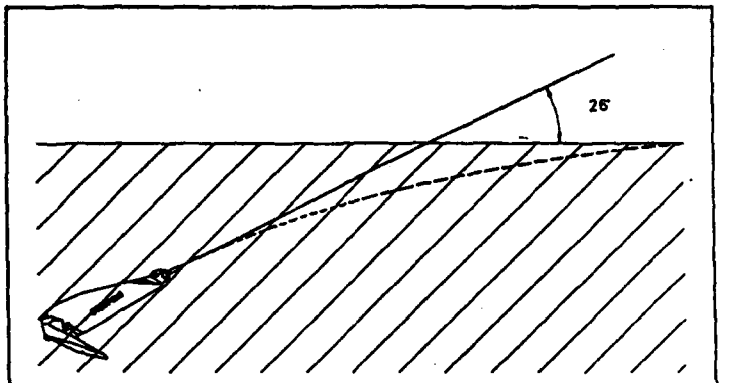

Fig. 12, Standard Stevpris anchor used for uplift loading

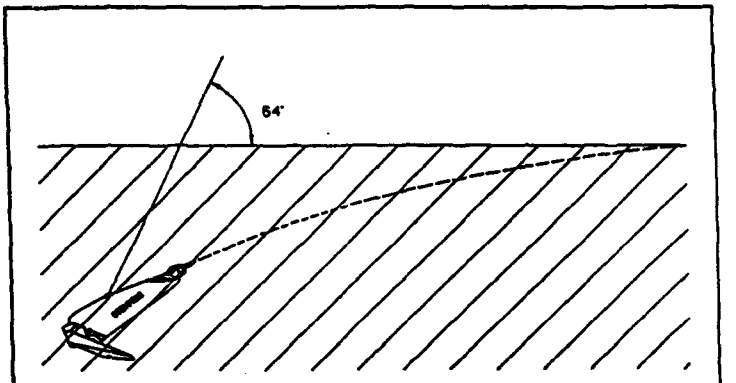

Fig. 13, Modified STEVPRIS anchor allowing for uplift loading.

Figure F-7
Modification to Standard Anchor
Increased Vertical Capacity
(From Vryhof literature)

STEVTENSIONER

FOR A SIMULTANEOUS TENSIONING OF DIAMETRICALLY OPPOSED ANCHORS AND ANCHOR PILES

FOR PROJECTS OF ANY SIZE, IN ANY WATER DEPTH - EVEN IN TYPHOON AREAS AND HEAVY TIDAL CURRENTS

As one of the latest inventions by Vryhof Ankers, the Stevtensioner is scoring a considerable impact as the paramount economiser in offshore mooring. It is implemented in a wide variety of projects to prove its unique capabilities. The results are beyond all expectations. Stevtensioner is a breakthrough in mooring technology.

Vryhof Ankers in the Netherlands leads the way in anchor design and -manufacture, while also widely contributing to innovation in this field with inventions such as the Stevtensioner and anchor handling tools.

Stevtensioner generates
- a saving in pulling forces
- a saving in chain lengths
- reduction in plant and equipment
- reduction in system complexity
- rapid, economical pretensioning and refitting

Multiplication by 2^5-3

You can put aside expensive equipment and complex systems now that the Stevtensioner is available to multiply the vertical pulling forces produced by the winches of supply vessels or crane barges. The horizontal load for the object to be (pre)tensioned is therefore 2^5-3 times higher than the initial vertical load.

Stevtensioner is used for
- simultaneous tensioning of mooring legs fitted with drag anchors
- pretensioning of anchor pile chains
- permanent tensioning of mooring systems - the Vryhof device is then left in this vertical position - with the anchor legs in very short catenary position
- demolition of jetties, harbour moles, quays and offshore structures

Saving chain lengths

Instead of exerting extreme tensions on the buoy, it is preferable to use a system with one single vertical buoy chain to be connected with a 3-point mooring system. A configuration such as this will reduce the vertical load on the buoy from 1250 tons to 256 tons, saving costly investments in chain and buoy.

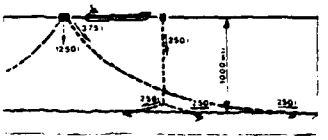

Principle

Fig. 1
- two chains, A – B, are connected to their anchors, 1 – 2, and to the Stevtensioner, T
- chain A is fixed to the tensioner whereas chain B can slide through
- chain B will slide through, till both chains produce more resistance than the vertical section of chain B
- at this point chain B locks automatically in the Stevtensioner.

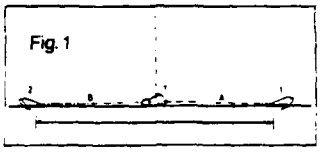

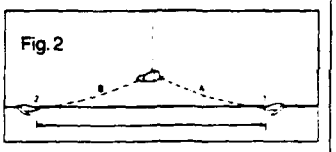

Fig. 2
With the two chains locked, the Stevtensioner is heaved some 20-30 m. The base of the triangle, C, decreases and the anchor penetrates the soil, creating holding power.

The Stevtensioner is heaved to the maximum and the lowered. Chain B slides further through the tensioner and the procedure per fig. 2 starts anew, decreasing the base and making the anchors penetrate, creating holding power.

Again and again the yo-yoing sequence is repeated till the required load is recorded. Usually this is achieved in 4-7 steps.

Finally chain A is released and the Stevtensioner brought back on board the vessel.

Building up the tension by yo-yoing

... vertical forces applied
---- horizontal forces applied

Note:
- When heaving the Stevtensioner the horizontal forces will increase.
- At point A the anchors start penetrating as a consequence of heaving the Stevtensioner.
- At point B either the maximum height of heaving the Stevtensioner or the maximum capacity of the winch is reached. The forces are reduced to zero by lowering the tensioner.
- The anchors automatically enter a short soaking period.
- At point C the Stevtensioner slides along the chain increasing the horizontal forces and stretching the chain.

At each 'A' of a yo-yo action the anchors penetrate the soil further.

In the beginning the vertical forces are higher than the horizontal ones because of the relatively high influence of the chain weight. When the horizontal forces increase, this influence is reduced and finally the vertical force will be approx. 33-40% of the horizontal one.

Figure F-8
'Vryhof' Opposed Anchor Tensioner
(Vryhof 'Stevtensioner' literature)

ANCHOR SYSTEM PRE-TENSIONING OPERATION

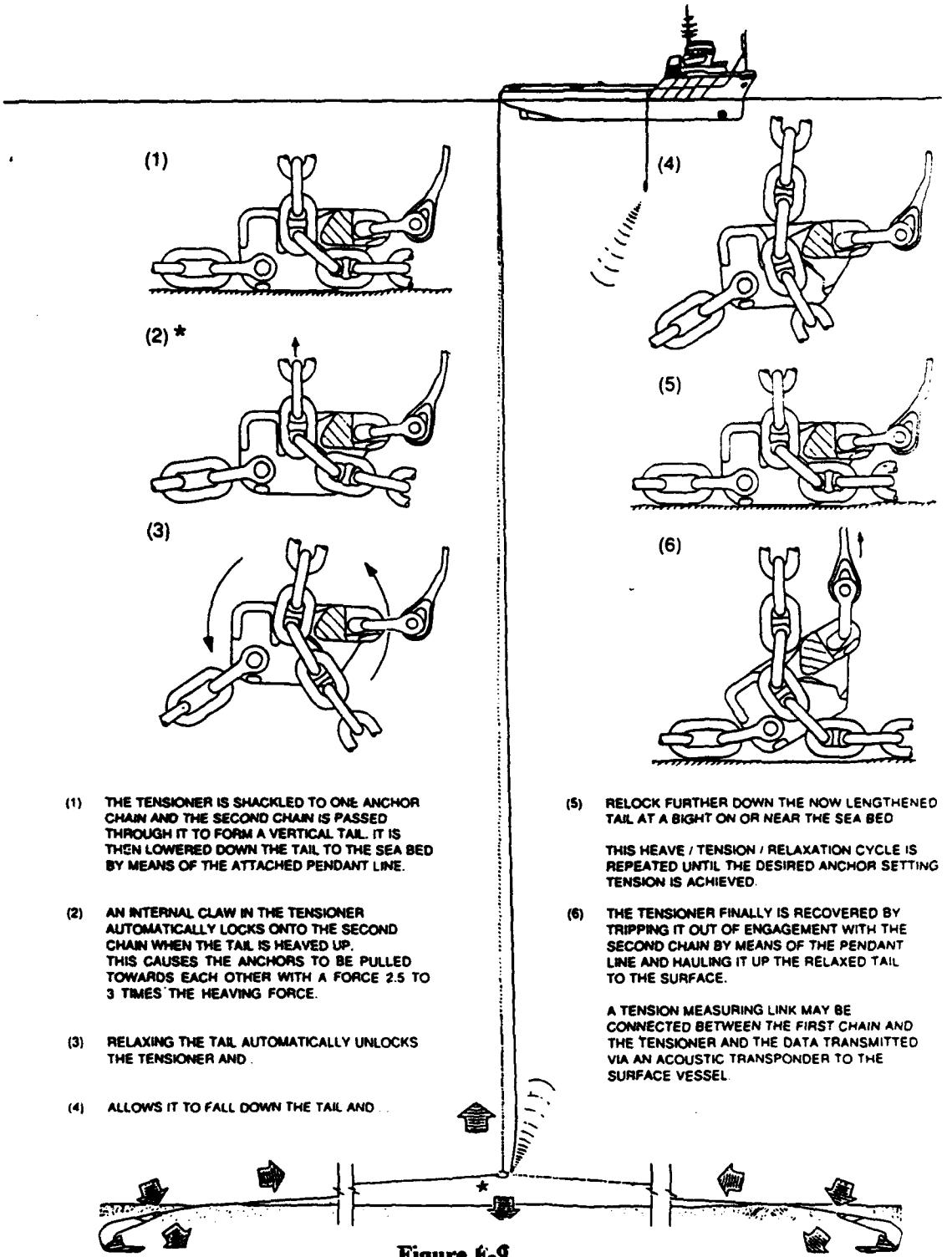

(1) THE TENSIONER IS SHACKLED TO ONE ANCHOR CHAIN AND THE SECOND CHAIN IS PASSED THROUGH IT TO FORM A VERTICAL TAIL. IT IS THEN LOWERED DOWN THE TAIL TO THE SEA BED BY MEANS OF THE ATTACHED PENDANT LINE.

(2) AN INTERNAL CLAW IN THE TENSIONER AUTOMATICALLY LOCKS ONTO THE SECOND CHAIN WHEN THE TAIL IS HEAVED UP. THIS CAUSES THE ANCHORS TO BE PULLED TOWARDS EACH OTHER WITH A FORCE 2.5 TO 3 TIMES THE HEAVING FORCE.

(3) RELAXING THE TAIL AUTOMATICALLY UNLOCKS THE TENSIONER AND

(4) ALLOWS IT TO FALL DOWN THE TAIL AND

(5) RELOCK FURTHER DOWN THE NOW LENGTHENED TAIL AT A BIGHT ON OR NEAR THE SEA BED

THIS HEAVE / TENSION / RELAXATION CYCLE IS REPEATED UNTIL THE DESIRED ANCHOR SETTING TENSION IS ACHIEVED.

(6) THE TENSIONER FINALLY IS RECOVERED BY TRIPPING IT OUT OF ENGAGEMENT WITH THE SECOND CHAIN BY MEANS OF THE PENDANT LINE AND HAULING IT UP THE RELAXED TAIL TO THE SURFACE.

A TENSION MEASURING LINK MAY BE CONNECTED BETWEEN THE FIRST CHAIN AND THE TENSIONER AND THE DATA TRANSMITTED VIA AN ACOUSTIC TRANSPONDER TO THE SURFACE VESSEL.

Figure F-9
Operation of 'Bruce' Opposed Anchor Tensioner
(From Bruce Anchor literature)

STATE OF THE ART ANCHOR TECHNOLOGY, THE BRUCE DENLA OFFERS HIGH UPLIFT CAPACITY WITH LOW INSTALLATION COSTS COMPARED WITH CONVENTIONAL ANCHORS OR PILES. MASSIVE COST SAVINGS CAN BE MADE IN HARDWARE THROUGH USING SHORTER MOORING LINES IN HIGH UPLIFT, TAUT MOORING SYSTEMS.

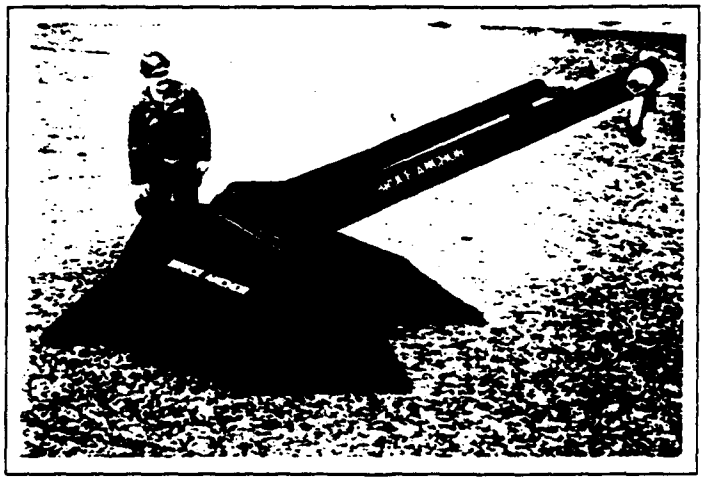

- Holding capacity in excess of 100 times anchors weight.
- Same capacity at any uplift angle from 0 to 90°
- Low installation loads.
- Installation possible by anchor handling vessel using conventional methods.
- Control of anchor trajectory allows installation to specified position
- Reduced installation time and costs.
- Suitable for exploration rigs as well as permanent applications.
- Low recovery loads possible using rear fluke pendant line.
- Fabricated structure can be tailored to particular applications.
- Taut mooring system designs become possible and affordable.

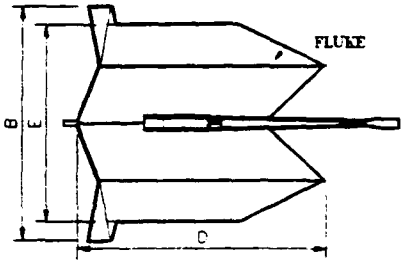

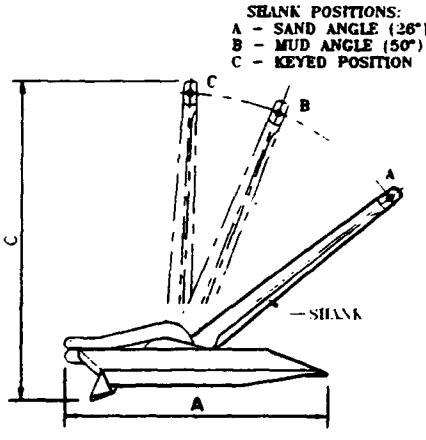

TYPICAL DENLA DIMENSIONS (mm):

DENLA SIZE (kg)	LEADING DIMENSIONS A	B	C	D	E
1000	2808	2541	3700	2650	2128
5000	4802	4345	6327	4531	3639
10000	6050	5474	7971	5709	4585
15000	6925	6267	9125	6535	5248

IN THE INTEREST OF CONTINUOUS PRODUCT IMPROVEMENT, RIGHTS ARE RESERVED TO CHANGE SPECIFICATIONS AND DIMENSIONS WITHOUT NOTICE

Figure F-10
High Uplift Anchor
Note extra arm for 'trigger'
(From Bruce Anchor Literature)

F-8 References, Anchors

American Petroleum Institute (API), Draft Recommended Practice 2SK, First Edition, "Recommended Practice for Design and Analysis of Station Keeping Systems for Floating Structures", Washington, D.C. (June, 1995)

Clukey, E. C., et al, "The Response of Suction Caissons in Normally Consolidated Clays to Cyclic TLP Loading Conditions", OTC 7796, Offshore Technology Conference, Houston, TX (1995)

Colliat, J. L., "Design and Installation of Suction Anchor Piles at a Soft Clay Site in the Gulf of Guinea", OTC 8150, Offshore Technology Conference, Houston, TX (1996)

Colliat, J. L., et al, "Caisson Foundations as Alternate Anchors for Permanent Mooring of a Process Barge Offshore Congo", OTC 7797, Offshore Technology Conference, Houston, TX (1996)

Cuckson, J., "The Suction Pile Finds Its Place", Offshore Engineer, April 1981

Degankamp, G., "Use of Drag Embedment Anchors in Mooring Systems for FPSO's", Commercial Publication by Vryhof Anchors, B. V., Krimpen ad Yssel, the Netherlands. (October 1995)

Forest, J., et al, "Design Guide of Pile-Driven Plate Anchors", Naval Facilities Service Center, Technical Report No. TR-2039-OCN, Port Huneme, CA. (March 1995)

Fines, et al, "Snorre TLP Tethers and Foundation", OTC 6623, Offshore Technology Conference, Houston, TX (1991)

Larsen, P., "Suction Anchors as an Anchoring System for Floating Offshore Constructions", OTC 6029, Offshore Technology Conference, Houston, TX (1989)

MATech Engineering, "Suction Emplaced Piles" Commercial Data Sheet, Maassluis, the Netherlands. (Undated)

MENCK, "Offshore Hydraulic Pile Driving Hammers", Commercial Data Sheet, Ellerau, Germany. (1990)

NCEL, "Drag Embedment Anchors for Navy Moorings", Technical Data Sheet No. 83-08R, Port Hueneme, CA (1987)

Senpere, D., et al, "Suction Pile Anchors - a Proven Alternative to Driving or Drilling", OTC 4206, Offshore Technology Conference, Houston, TX (1982)

Sparrevik, P., "Suction Anchor Piles, State of the Art", Mooring and Anchoring Conference, Aberdeen, Scotland, June 1996

Taylor, R. J., "Interaction of Anchors with Soil and Anchor Design", NCEL Technical Note No. N-

1267, Port Hueneme, CA. (1982)

Taylor, R. J., "Performance of Conventional Anchors", OTC 4048, Offshore Technology Conference, Houston, TX (1981)

van den Haak, R., "Anchor Manual", Commercial Publication by Vryhof Ankers, B. V., Krimpen ad Yssel, the Netherlands. (1990)

van den Haak, R., "Criteria for A Good Anchor Design", a paper presented to: Norske Sivilingeniorers Forening. (November 1988)